ILLINOIS STATE WATER SURVEY

at the

University of Illinois
Urbana, Illinois

RAINFALL EVALUATION STUDIES

by

Floyd A. Huff and Paul T. Schickedanz

FINAL REPORT - PART II

DESCRIPTION OF INDIVIDUAL STUDIES

Principal Investigator: Floyd A. Huff

National Science Foundation
Atmospheric Sciences Section
NSF GA-1360

April 1970

CONTENTS

CONTENTS (Cont'd)

CONTENTS (Cont'd)

CONTENTS (Cont'd)

CONTENTS (Cont'd)

CONTENTS (Cont'd)

ILLUSTRATIONS

TABLES

INTRODUCTION

The basic purpose of Part II of this Final Report under NSF-1360 is to provide a detailed description of various studies carried out under this grant with respect to data used, analytical procedures employed, results of analyses, and conclusions. It serves as a single source of all findings obtained from the various studies undertaken. As reported in Part I, several papers have been published in professional journals to summarize results of certain studies, and other papers are in preparation for publication in the interest of widespread dissemination of the material. However, Part II will serve as the only source of information for those studies, such as the Illinois precipitation climatology, considered to be primarily of localized interest in weather modification applications. Other minor studies of interest and potential use in precipitation modification experiments are also included in Part II.

DEFINITION OF TERMS USED FREQUENTLY IN REPORT

A storm is defined as a precipitation period separated from preceding and succeeding precipitation on the sampling area by 6 hours or more. This definition has been found most suitable for separating storms resulting from different synoptic causes on the various raingage networks.

Winter refers to the 3-month period, December-February. Spring includes March, April, and May. Summer incorporates June, July, and August. September, October, and November constitute Fall.

The growing season or warm season as used in this report includes the 5-month period, May-September. The cold season or water supply replenishment season encompasses the 7 months from October through April.

RAINGAGE NETWORKS USED IN RESEARCH

Data from 5 dense raingage networks operated in Illinois by the State Water Survey were employed in various phases of the research under NSF-1360. A description of these networks is provided in Part I of this Final Report. The network locations are shown in Fig. 1, and the sampling patterns in the two networks used most frequently in the research are illustrated in Fig. 2.

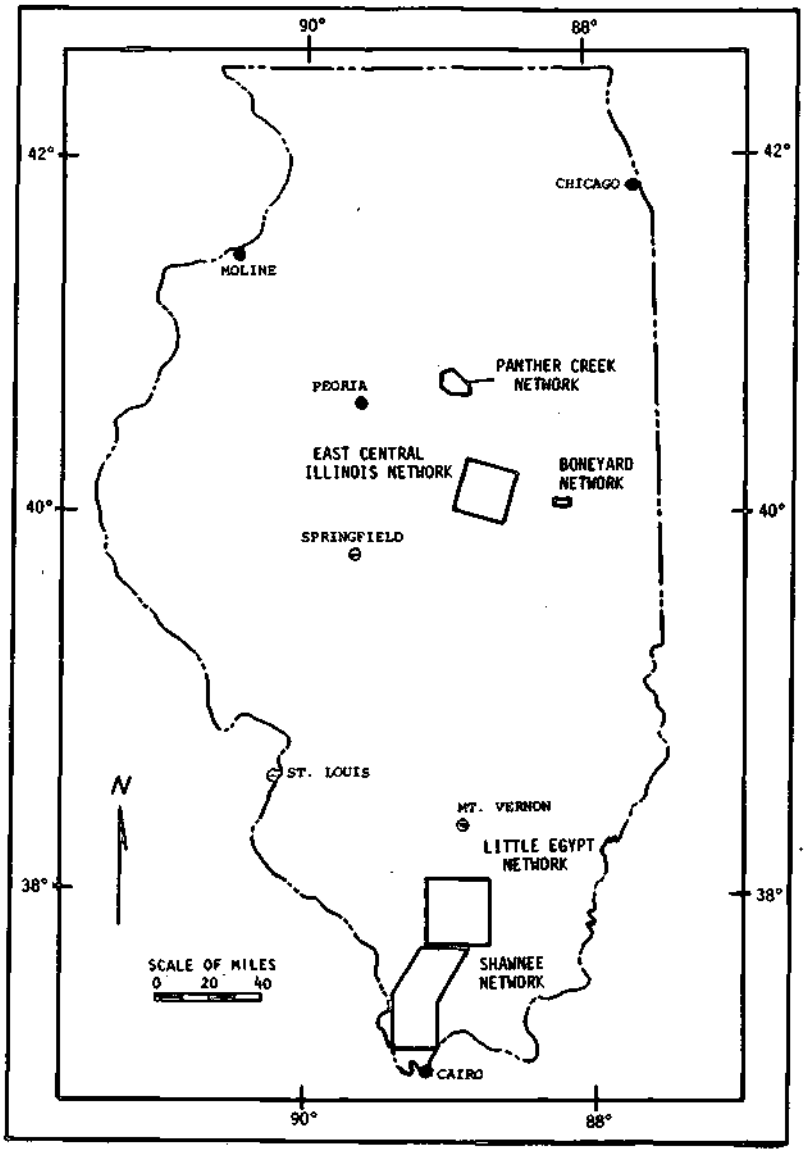

Figure 1. Raingage networks used in research.

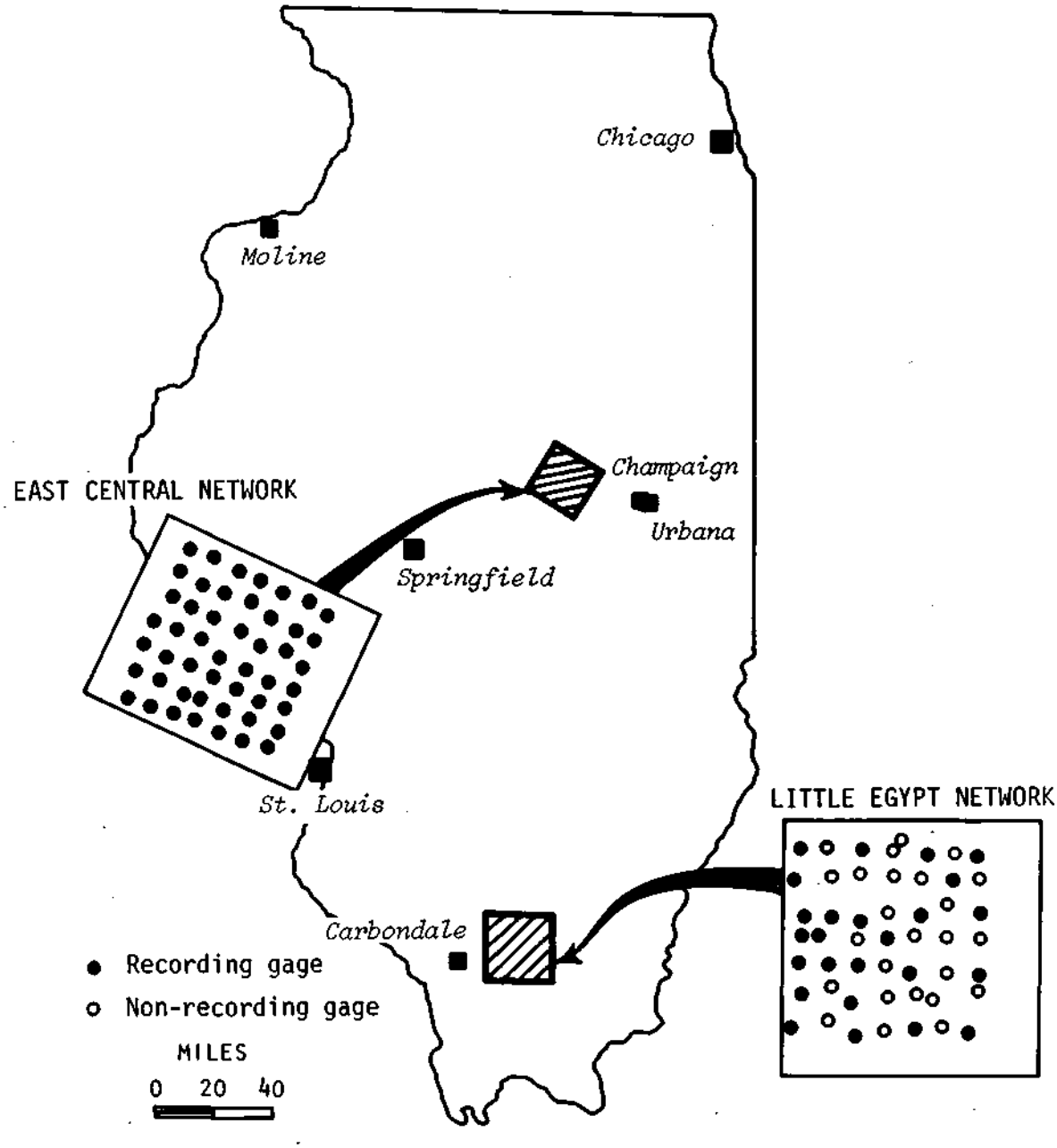

Figure 2. Sampling patterns in two major networks.

MESOSCALE SPATIAL VARIABILITY IN MIDWESTERN PRECIPITATION

Introduction

The existence of relatively large spatial and temporal variability in precipitation, particularly in thunderstorms and rainshowers, is generally recognized among meteorologists and hydrologists. However, data to define this variability in quantitative terms have been inadequate, especially with respect to small areas and various types of storm conditions. Operation of several concentrated raingage networks in central and southern Illinois in recent years has provided a unique set of data to 1) determine the mesoscale spatial variability of natural precipitation in a typical midwestern climate and 2) provide quantitative measures of the effects of several meteorological variables upon the spatial distribution of precipitation. Results presented here should be generally applicable to other areas of similar precipitation climate and topography.

In hydrometeorology, specific knowledge of precipitation variability is pertinent in establishing watershed raingaging facilities and in interpreting rainfall-runoff relationships. In weather modification studies, natural variability must be considered in both the planning and verification of field experiments. Failure to do so may lead to poorly-designed sampling programs and invalid interpretation of experimental results. Knowledge of the spatial variability of natural precipitation is especially pertinent in cloud seeding experiments involving target-control comparisons. It is helpful in the selection of experimental areas, in the determination of sampling procedures, in the establishment of precipitation measurement networks, and in the statistical interpretation of the seeding results. As pointed out by McDonald (1956), precipitation variability above all else has stood in the way of efforts to secure an immediate answer to the question of the efficacy of cloud seeding.

Data Used in Study

Data from four of the networks shown in Fig. 1 were used in the study. A 12-yr sample from the East Central Illinois Network during 1955-1966 provided 1178 storms in which the areal mean rainfall exceeded 0.01 inch, the basic requirement for inclusion in the variability study. The Boneyard Network of 10 gages in 10 mi^2 sampled 1066 storms in the 1954-1964 period that were included in the study. The Little Egypt Network of 49 gages in 550 mi^2 provided 964 storms in the 1958-1966 period. The Panther Creek Network yielded data for 724 storms in a 7-yr operational period (1954-1960).

All networks are located in relatively flat terrain which is characteristic of the major midwestern agricultural regions. The two larger networks have areas approximately equal to that of the average county in Illinois. The East Central Illinois Network is located in the heart of the midwestern hybrid corn

and soybean region, in which crop yields and farm income are very high in years of favorable weather. Consequently, it is a region in which the economic benefits from successful weather modification could be outstanding under some circumstances.

Analytical Procedures

The spatial relative variability was obtained by the simple method presented by Conrad and Pollak (1950), in which it is defined by:

$$V = 100(AD/M) \quad (1)$$

where V is the relative variability in percent, M is the mean of the sample, and AD is the average deviation from the mean. Investigation was made of storm, monthly, seasonal, and extended period variability relations. For storms that did not have measurable rainfall at some gages in the network, a second calculation of relative variability was made after eliminating the zero or trace observations. This provides a more useful variability measure for some applications.

In the storm studies, correlation analyses were used to determine the degree of relationship between storm relative variability (V), areal mean precipitation (P), maximum network precipitation (P_m), and storm duration (D), when the storms were grouped by synoptic weather type, precipitation type, and season. Simple and multiple correlation coefficients were determined with the data expressed in both linear and logarithmic terms. From these correlation analyses and graphical plottings of the data, decisions were made on the regression analyses to be performed with respect to data transformation and independent variables. In the monthly and longer studies, relations were developed between V, total precipitation (P_t), and area (A).

Storm Variability

In the study of individual storms, correlation analyses produced higher coefficients with logarithmic transformations than with the linear variables, as indicated by graphical plots of the data in preliminary studies. The differences are illustrated in Table 1 in which linear and logarithmic computations of correlation coefficients (r) and coefficients of determination (r^2) are shown for V, P, and D in summer storms on the East Central Illinois Network.

Table 1 is typical of the results obtained with the data grouped according to season, precipitation type, and synoptic weather type. As indicated in Table 1, only a small improvement in the relationships was found when V was related to both P and D as opposed to P alone. This is due to a relatively strong correlation between P and D; as mean rainfall increases, the storm duration also tends to increase. Consequently, it was decided to develop regression equations relating the logarithms of V and P.

Table 1. Correlation between V, P, and D in summer storms on East Central Illinois Network.

	r			r^2(%)		
Transformation	V-P	V-D	V-P ,D	V-P	V-D	V-P,D
Linear	-0.60	-0.54	0.64	36	29	41
Logarithmic	-0.76	-0.73	0.30	58	53	64

Regression equations were developed with the data grouped according to season, precipitation type, and synoptic weather type. Further analyses indicated that the seasonal grouping was strongly related to the frequency distribution of precipitation types in the four seasons. Therefore, the precipitation type classification was selected for further study.

Precipitation type relations. The data were grouped according to the four major types, thunderstorms (TRW), rainshowers (RW), steady rain (R), and snow (S). Other types were too few to be included in the study. Where more than one precipitation type prevailed during a storm, the storm was assigned to the type which was responsible for the major portion of the storm precipitation. If this could not be determined, the storm was omitted from the study. The data from all four networks were combined to obtain regression equations (2) through (9). Eqs. (2) through (5) show relations based upon all sampling points for TRW, RW, R, and S, respectively. Eqs. (6) through (9) are similar equations based upon the use of only those network gages with measurable storm precipitation.

$$V_2 = 9.92\ P^{-0.43}\ A^{0.17} \tag{2}$$

$$V_3 = 8.88\ P^{-0.44}\ A^{0.15} \tag{3}$$

$$V_4 = 7.17\ P^{-0.45}\ A^{0.12} \tag{4}$$

$$V_5 = 8.73\ P^{-0.41}\ A^{0.08} \tag{5}$$

$$V_6 = 9.49\ P^{-0.35}\ A^{0.17} \tag{6}$$

$$V_7 = 8.38\ P^{-0.36}\ A^{0.16} \tag{7}$$

$$V_8 = 6.77\ P^{-0.37}\ A^{0.13} \tag{8}$$

$$V_9 = 9.68\ P^{-0.34}\ A^{0.07} \qquad (9)$$

In Table 2, Eqs. (2) to (9) have been solved for selected values of P and an area of 500 mi^2 to illustrate the effects of precipitation type and storm magnitude upon spatial variability. Table 3 illustrates the effect of increasing sampling area on V. Before discussing these tables further, it should be emphasized that snow measurements are subject to relatively large sampling errors, especially with unshielded gages in strong winds and low-density snow. Consequently, the values of V are probably larger than the true values in nature, and the snow relations should be considered only approximations for comparison purposes. Snow values have been omitted for P greater than 0.50 inch because of the small number of cases above this level.

The primary importance of Eqs. (2) to (9) is to replace qualitative knowledge with quantitative information on the changes in spatial variability as storm magnitude (mean rainfall) and size of sampling area increase and the characteristics of the storm precipitation vary. Qualitatively, the general trend for the relative variability to decrease with increasing mean rainfall and to be greater with unstable types of precipitation (TRW, RW) as opposed to stable types (R, S) is well known. Now it is possible to define these two trends in quantitative terms for a typical midwestern region, as illustrated in Table 2. For example, this table shows the average relative variability decreasing by a factor of approximately two when the mean rainfall on 500 mi^2 increases from 0.10 inch to 0.50 inch and by a factor of nearly four when the mean is increased further to 2 inches. Similarly, the relatively large differences between the spatial variability of precipitation types is portrayed in Table 2. The larger ratio with heavy storms apparently results from a trend for the stable type of precipitation to approach uniformity slightly faster than the unstable type as P increases.

Table 2. Precipitation type comparisons of average storm relative variability on 500 mi^2.

Precipitation type	Relative variability (%) for given mean precipitation (in)				
	0.10	0.25	0.50	1.00	2.00
			All gages		
TRW	77	51	39	28	21
RW	62	42	31	23	17
R	43	28	21	15	11
S	37	26	19	--	--
TRW/R	1.79	1.86	1.86	1.87	1.91
			Only gages with measurable amounts		
TRW	61	45	35	28	21
RW	52	37	29	23	17
R	36	26	20	15	11
S	33	24	19	--	--
TRW/R	1.69	1.73	1.75	1.87	1.91

Table 3 illustrates quantitatively the effect of increasing sampling area on the average spatial variability through the use of regression values for a 0.50-inch storm. The table indicates that TRW variability increases approximately 30% as the area increases from 10 to 50 mi^2, after which the rate of change decelerates and is approximately double the 10-mi^2 value at 500 mi^2. The R-increase with area is considerably slower, with the 500-mi^2 variability about 60% greater than the 10-mi^2 value.

Table 3. Effect of area on relative variability in 0.50-inch storm.

Precipitation type	Relative variability (%) for given area (mi^2)			
	10	50	100	500
TRW	20	26	29	39
R	13	16	17	21
TRW/R	1.54	1.63	1.71	1.86

The previous discussions have been limited to average relative variability, since this is a convenient statistic for comparing the effects of storm magnitude, sampling area, and precipitation type on spatial variance. Analyses of the Illinois network data showed the spatial variability to be an unstable precipitation parameter with large differences frequently observed between storms of similar magnitude and precipitation type. This is illustrated quantitatively in Table 4 which shows the upper and lower 10% ranges about the average relative variability in thunderstorms and steady rain on the East Central Illinois Network of 400 mi^2. The direct application of spatial variability as an evaluation parameter in weather modification experiments does not appear feasible in view of its great interstorm variance.

Table 4. Range of relative variability in TRW and R on 400 mi^2.

	Relative variability (%) for given mean precipitation (in)				
	0.10	0.25	0.50	1.00	2.00
			TRW		
Upper 10%	135	95	72	55	42
Average	74	50	37	27	20
Lower 10%	27	19	14	11	8
			R		
Upper 10%	90	60	45	33	24
Average	41	27	20	15	11
Lower 10%	16	11	8	6	4

Seasonal effects. In the preceding analyses, no distinction was made between the variability of specific precipitation types between seasons. All data were grouped to obtain a large sample to establish the overall differential effects of precipitation type on spatial variability throughout the year. It would be desirable to separate each precipitation type by season also, since it seems likely that for a given precipitation type stronger rainfall gradients exist in warm season storms than in cold season precipitation. Thunderstorms are too infrequent in winter in Illinois to provide an adequate sample for comparisons despite the relatively long records on the sampling networks. Snow, of course, is absent in summer. Consequently, a comparison could be undertaken only for RW and R.

Seasonal comparisons of RW and R were made on the East Central Illinois Network of 400 mi^2 for which the longest record (12 yr) was available. On this area, results indicated that the average rainfall gradient, as measured by the relative variability, was approximately twice as large in summer as in winter for a given mean precipitation, and was about 60% greater in summer than in spring or fall. Other considerations being equal, it is apparent that precipitation modification effects could be evaluated statistically with a substantially shorter sampling period in the cold season, when the major replenishment of water supply takes place in the Midwest, than in the crop-growing season when agriculture would benefit most by successful cloud seeding.

Synoptic type relations. The data were grouped according to six basic storm types to obtain a quantitative measure of their differential effect on spatial variability. Data from the four networks were then combined and a regression equation obtained for each type. Relative variability was related to mean precipitation and area, similar to the procedure followed in the precipitation type analyses. The results are illustrated in Table 5 through the use of equation values for 500 mi^2. Low centers and occluded fronts were combined, because the few cases of occluded fronts appeared similar in V characteristics to the low center storms. Storm types were obtained from synoptic maps published by the U. S. Weather Bureau.

Table 5. Synoptic storm type comparisons of relative variability on 500 mi^2.

	Average relative variability (%) for given mean precipitation (in)				
Storm type	0.10	0.25	0.50	1.00	2.00
Air Mass	83	60	47	37	29
Cold Fronts	61	44	34	27	21
Warm Fronts	63	43	33	24	18
Static Fronts	76	53	41	31	24
Low Centers - Occluded Fronts	43	30	23	17	13
Squall Lines	80	51	37	26	19
Air Mass/ Low Center	1.93	2.00	2.04	2.18	2.23

Unfortunately, the regression curves from which Table 5 was constructed did not produce parallel curves for all types, so that a simple statement of the relative effects of each type cannot be made. Throughout the range of P, however, the highest relative variability was found with air mass storms and the lowest with low centers. Air mass storms, in general, are more scattered spatially than frontal storms, encompass less area on the average than frontal storms, but are frequently characterized by steep rainfall gradients since they are usually associated with unstable precipitation types (TRW, RW). Thus, the spatial variability tends to be considerably greater in these storms. Conversely, low centers are more likely to be associated with widespread precipitation of relatively long duration over a given sampling area than the other storm types of Table 5. Therefore, spatial variability tends to minimize in such storms. The air mass average variability is approximately twice that of low center storms.

Stationary frontal storms rank next to air mass storms in high variability over most of the P-range of Table 5. Although these storms are often of relatively long duration, they are frequently associated with intense thunderstorms and rainshowers with steep rainfall gradients. Differences in spatial variability between cold frontal and warm frontal storms appear insignificant. Since high spatial variability intensifies the problem of rain modification evaluation, it is obvious from Table 5 that the seeding of air mass instability showers, such as done on Project Whitetop (Decker and Schickedanz, 1965), presents an unusually difficult evaluation problem when surface rainfall is the primary verification tool.

The results in Table 5, which are based upon data for all seasons and all precipitation types combined, provide a quantitative measure of the average effects of synoptic types on spatial variability on an annual basis. The relatively large ratios of air mass/low center variability result partly from the predominant occurrence of air mass storms in the warm season and with TRW or RW, whereas low centers are distributed more uniformly with respect to precipitation type and season. Therefore, an analysis was made of the above ratio for TRW, which also restricted the comparison largely to the warm season. When this was done, the ratio ranged from 1.7 to 1.8, compared with the 1.9 to 2.2 range in Table 5. A similar analysis performed on the cold front/low center ratio showed insignificant differences from the values of Table 5, since the strong seasonal and precipitation type bias is not present with these storms.

Extended Period Variability

For some purposes, knowledge of the relative variability on a given area over periods of a month, season, or years is of more interest than storm variability. One example is the establishment of sampling requirements for long-term weather modification experiments.

Monthly relative variability relations were investigated first through use of the 12-yr sample from the East Central Illinois Network. This network was subdivided to provide data for areas of 50, 100, 200, and 400 mi^2. Months were grouped by the four standard seasons (winter, spring, summer, fall). This division was made because of the differences in precipitation characteristics between seasons. Regression equations were then developed for each group of

months by relating the relative variability to total monthly precipitation (P_t) and sampling area (A). The four equations for winter, spring, summer, and fall are:

$$V_w = 6.63\ P_t^{-0.23}\ A^{0.13} \quad (10)$$

$$V_{sp} = 6.97\ P_t^{-0.30}\ A^{0.16} \quad (11)$$

$$V_{su} = 13.06\ P_t^{-0.52}\ A^{0.15} \quad (12)$$

$$V_f = 7.51\ P_t^{-0.26}\ A^{0.14} \quad (13)$$

The spring and fall equations yield nearly identical variabilities for a given P_t and A.

The effects of total precipitation, area, and season on the monthly spatial variability are illustrated in Tables 6 and 7. Table 6 shows a decrease of 2% in winter variability as the monthly average precipitation doubles, whereas a doubling of the monthly precipitation in summer produces a much more pronounced decrease in spatial variability. The summer-winter difference maximizes at low precipitation values. At 1-inch, the summer variability is approximately twice the winter value, but with 4-inch monthly totals, it is only about 45% greater. This is related to the spotty showers of small areal extent which usually characterize the summer rainfall in much below normal months.

Table 6. Average monthly relative variability on 400 mi^2.

	Variability (%) for given monthly mean precipitation (in)				
Season	0.5	1.0	2.0	4.0	8.0
Winter	17	15	13	11	9
Spring-Fall	22	18	15	12	10
Summer	46	32	22	16	11

The area effect is illustrated in Table 7 for a monthly precipitation of 4 inches in winter and summer. The relative variability increases slowly with area. In summer, it increases approximately 2% for each doubling of the area, and in winter the change is only 1% as the area doubles.

Table 7. Variation of monthly relative variability with area for a 4-inch precipitation.

	Variability (%) for given area (mi^2)			
Season	50	100	200	400
Winter	8	9	10	11
Summer	11	13	14	16

Next, the relative variability was calculated for total precipitation for periods of 3, 6, 12, 24, and 60 months on the 400 mi^2 to ascertain the length of sampling period required to minimize the relative variability to a constant value. The 3-month and 6-month variabilities were calculated starting at each month of the year to determine the seasonal effect. The variability decreased from an average of 9 to 11% for 3-month periods (depending upon the starting month) to 7 to 8% for 6-month totals, 6% for 12 months, and 5% for 24 months. When the time period integration exceeded 24 months, the average relative variability decreased to a constant value of 4% on the 400 mi^2.

Thus, it was clearly demonstrated that the relative variability becomes minor when precipitation is summed over a period of several years in an area of relatively homogeneous precipitation climate. This finding does not imply that some points or small areas within the larger sampling area cannot show significant departures from the areal mean. Such occurrences have been shown in an earlier paper by Huff (1966). The results do, however, imply that the average departure from the mean of a large number of measurements within the sampling area will be relatively small.

Summary and Conclusions

Data from four dense raingage networks in Illinois were analyzed to obtain quantitative measures of the mesoscale spatial variability for storm, monthly, and extended period precipitation in a typical midwestern climate. Results should provide useful knowledge for climatologists, hydrometeorologists, and those atmospheric scientists concerned with weather modification.

The spatial relative variability of storm precipitation was found to be related exponentially to mean precipitation. The relation was not significantly improved by adding other variables, such as storm duration and maximum storm precipitation. The relative variability tends to increase with increasing area and was substantially greater with unstable types of precipitation (RW, TRW) than with steady types (R, S). Grouped by synoptic storm type, the highest relative variability was obtained with air mass storms and the lowest with low center passages. The relative variability, although a useful parameter to evaluate the general effects of various meteorological factors upon storm spatial variability, displays large differences between storms of similar

precipitation volume, precipitation type, and synoptic storm type; because of its interstorm instability, it is not a desirable parameter in itself for the evaluation of weather modification experiments.

Monthly precipitation variability showed little difference between fall, winter, and spring months, but large differences between cold season months and summer, when precipitation totals were light. Determination of average relative variability for extended periods of 3 to 60 months indicated that the variability minimizes to a constant after time periods of 24 months are integrated into the calculation. The average spatial variability becomes minor when precipitation is summed for several years over an area of relatively homogeneous precipitation climate.

CLIMATOLOGICAL ASSESSMENT OF NATURAL PRECIPITATION CHARACTERISTICS FOR USE IN WEATHER MODIFICATION

SECTION 1 - CLIMATOLOGICAL CHARACTERISTICS OF STORM PRECIPITATION

Introduction

A substantial deficiency exists in our understanding of the natural distribution of precipitation. As a result, both the planning and evaluation of cloud seeding experiments for the modification of surface precipitation have been made more difficult, and an urgent need created for accumulating the necessary knowledge to define the natural distribution adequately. Furthermore, understanding of the natural distribution will provide a useful tool for evaluating expected benefits from cloud seeding in a given climatic region when the capabilities of weather modification become better defined and operational skills improved.

Presently, however, the natural distributions can be used to obtain first estimates of potential future benefits under various assumed capabilities, as will be illustrated later. From such calculations, considerable information can be obtained relative to the feasibility and/or desirability of incorporating seeding-induced precipitation into the design of future water supply systems and in evaluating future requirements for irrigation as an agricultural water supplement.

Extensive analyses of Illinois precipitation data were undertaken to define the natural distributions and to develop techniques for using the acquired knowledge in weather modification applications in Illinois and other areas with similar humid, continental climates. As one part of this research, a study was made of the climatological characteristics of storm precipitation through use of data from a 12-yr operation of the East Central Illinois Network (Fig. 2). The effects of storm intensity and duration, precipitation type,

synoptic weather type, season, and departure from climatic averages were investigated. Frequency distributions of both rainfall depth and number of storms were developed for various data classifications, and application of these distributions in weather modification illustrated. Through relating areal to point distributions, a technique was devised for use in deriving precipitation distribution relations for other climatic areas lacking dense network data.

There is no intent here to provide a unique plan for (1) evaluating all the potential benefits of cloud seeding or (2) designing and verifying weather modification experiments. However, it is the strong conviction of the Principal Investigator that natural distribution studies provide essential background knowledge and a useful meteorological tool for evaluating the potential benefits of cloud seeding in implementing agricultural and urban water supply needs, and in developing optimum scientific application of cloud seeding in any given climatic region. The primary purpose of this study then, is to show how natural distributions were developed for one region, illustrate a few potential applications in weather modification, and, hopefully, stimulate others to undertake similar background studies for their region of interest.

Data from 1344 storms on the sampling area of 400 mi^2 provided the primary input to the study. The storm definition used in the Illinois research resulted in most storm days having a single storm period, so that findings of this study should provide reasonable approximations of daily precipitation distribution characteristics. The network data were supplemented by long-term daily precipitation data on point rainfall from the climatic network of the U. S. Weather Bureau in Illinois which includes an area of 56,000 mi^2. A total of 57 stations with complete records for the 50-yr period, 1906-1955, were employed to maintain consistency with previous climatological studies performed for the state.

Analytical Procedures

All storms were used in which measurable rainfall was recorded at one or more gages on the network. Then, for each grouping or stratification of storms, the network mean precipitation for all qualifying storms was ranked from high to low. These ranked data were then plotted on probability paper and smooth curves drawn through the plotted points. This provided families of cumulative frequency curves, such as shown in Fig. 3a, in which cumulative percent of total annual precipitation is related to the magnitude of the areal mean precipitation in storms stratified by storm duration. Similar cumulative distributions were determined between cumulative percent of total number of storms and areal mean precipitation, such as illustrated in Fig. 3b. From these two sets of curves, a third set was constructed relating cumulative percent of total precipitation to cumulative percent of the total number of storms (Fig. 4). The foregoing procedure was later repeated after eliminating all storms in which the network mean was less than 0.01 inch.

These three types of curves were used to define the distribution characteristics of areal mean rainfall. Based on the dense sampling network and 12 consecutive years of data, the results presented in this report are considered reliable estimates of the climatological characteristics of

precipitation within the limits defined in each analysis. Obviously, there are statistical limitations in the data treatment as will be brought out later.

The foregoing analytical procedure was followed for various groupings of the data. These included groupings for (1) all storms combined, (2) seasons, (3) precipitation type, (4) synoptic weather type, (5) storm duration, and (6) wet and dry periods. Also, several combinations of the above groupings, such as sub-grouping of precipitation types by storm duration, were investigated.

Precipitation type classifications were thunderstorms, rainshowers, continuous or intermittent rain, snow, and combinations of the foregoing basic types. Synoptic weather types included the various types of fronts, low center passages, air mass storms, and squall lines. When occasionally more than one synoptic type contributed to the storm precipitation, the storm was assigned to the type that the analysts indicated was the major contributor. Synoptic weather maps and weather observer records were used in the precipitation type and synoptic weather type classifying. The data groupings and analyses were dictated both by available climatological knowledge from other Illinois studies and from the size of the data sample. In regions with distinctly different precipitation climates, the investigator should vary the data treatment to fit best the climatological characteristics of his region.

Since dense network data are relatively scarce, undertaking similar studies in other areas would be greatly facilitated if point rainfall records could be used to estimate precipitation characteristics on mesoscale areas in which weather modification might be undertaken. Consequently, 3 point records in the Illinois sampling network were selected and subjected to the same analyses used for the areal study to (1) determine point-areal relationships, and (2) evaluate the applicability of point rainfall statistics for characterizing areal precipitation.

Frequently, daily precipitation is used in the evaluation of cloud seeding experiments. The results of the Illinois storm study were believed to be nearly equivalent to those that would be obtained from using daily totals. After verification of this hypothesis from the network data and evaluation of the network point-areal relationship, long-term point rainfall records from the Illinois climatic network of the U. S. Weather Bureau were employed to obtain a statewide climatological pattern of the distribution characteristics of daily rainfall. These patterns can then be used as a guide in weather modification activities in any portion of the state. Similar patterns could be determined for other states from their climatic records.

Effects of Storm Duration, Precipitation Type, and Synoptic Type on Distribution Characteristics

The most significant differences were found between the climatological distribution curves when the data were grouped by storm duration. Variations in the distribution characteristics between the several synoptic types resulted primarily from the tendency for some types to have a larger percentage of their storms with either relatively long or short durations. For instance,

air mass storms are usually of short duration compared to low center and warm front storms. Similarly, no strong trend was found for large differences between precipitation types. However, these findings could differ substantially in other climatic regions.

Table 8 shows how the climatological distribution of storm mean precipitation is related to storm duration. For example, reading horizontally in the upper portion of the table it is seen that with durations of 3 hr or less on the network, 28% of the total precipitation, on the average, will result from a network mean exceeding 0.50 inch, whereas this percentage increases gradually to 95% with durations in excess of 24 hours. Reading vertically in the upper portion of Table 8 an estimate of the distribution of storm mean rainfall in each duration category is obtained. Thus, for storms with durations of 3 hr or less, 80% of the rainfall, on the average, results from network means exceeding 0.10 inch compared with 7% in storms exceeding 1 inch. The lower part of Table 8 shows how storm duration affects the relation between storm mean rainfall and the frequency distribution of storm occurrences. This table stresses the importance of the storm duration factor in the establishment of the distribution characteristics of storm precipitation in this climatic region.

Table 8. Average 12-yr distribution of network storm precipitation grouped by storm duration.

Network mean storm precipitation (in) exceeded	Cumulative percent of total precipitation for given duration (hrs) ≤3	3.1-6.0	6.1-12.0	12.1-24.0	24.1-48.0	All storms combined
1.00	7	22	29	54	80	41
0.50	28	52	61	85	95	70
0.25	52	79	87	96	99	86
0.10	80	93	96	99	>99	95
	Cumulative percent of total storm occurrences for given duration (hrs)					
1.00	<1	4	8	26	53	7
0.50	2	15	26	56	78	19
0.25	9	34	52	80	89	33
0.10	26	60	80	95	96	50

A further investigation was made of differences in distribution characteristics when the data were grouped according to (1) storm duration and precipitation type, and (2) duration and synoptic weather type. Erratic trends resulted. These may be primarily the result of sampling problems resulting from the much smaller number of cases in each class interval with the double grouping and/or the interdependence of the parameters used. In any case, it

appeared undesirable to pursue this approach further, and additional study was confined to the single grouping by storm duration which appeared to separate the distributions in a most significant manner.

Areal Distribution Characteristics

In the final analyses of areal distribution characteristics, relationships were developed for grouping of storms by duration using (1) all storms in which measurable precipitation was recorded on the network, (2) only storms in which the areal mean precipitation was 0.01 inch or more, and (3) air mass storms with durations of 3 hr or less. These air mass storms occur largely in the warm season and are primarily of the afternoon type that result from diurnal heating effects. The air mass category was selected for separate attention because (1) two major weather modification projects in Arizona (Battan, 1966) and Missouri (Braham, 1966) were concerned with nonfrontal convective rainfall, (2) considerable effort is being devoted presently to convective cloud research in the extensive weather modification program of the Bureau of Reclamation (U. S. Department of Interior, 1968), and (3) air mass storms contribute significantly to warm-season precipitation in Illinois and their relative importance appears to increase during dry periods, as will be discussed later. Although the Arizona and Missouri experiments did not indicate increases from cloud seeding, Battan (1966) lists others who claim success in seeding convective clouds and concludes that "additional research is needed to resolve the conflicting views on the physics of convective precipitation and on the efficacy of various cloud seeding techniques."

Average annual distributions based upon the complete 12-yr sample are shown in Figs. 3-4 for storms grouped by duration. The sample size was inadequate for constructing a curve for the few storm durations exceeding 48 hr. Interpretation of these figures was discussed in conjunction with Table 8. Fig. 4 provides a measure of the distribution of total precipitation with respect to the frequency of storm occurrences. All durations exceeding 12 hr are incorporated into a single curve since differences between them were slight.

The 3 sets of curves provide quantitative estimates of the average distribution characteristics that may be used for guidance in weather modification, hydrological design, and other problems in which such climatological information is useful. The effects of storm duration on the distributions are clearly evident from the curves and earlier discussions. Fig. 4 illustrates well the climatological trend for a large percentage of the total precipitation to occur in a small percentage of the storm occurrences. For example, the curves indicate that 50% of the total precipitation occurring in storms with durations of 3 hr or less is recorded in 9% of the storm occurrences in an average year.

Point-Areal Relations

In the investigation of the relation between point and areal storm distributions, three gages on the 400 mi^2 were selected for the study. One gage (No. 25) was located in the center of the network, another (No. 29) on

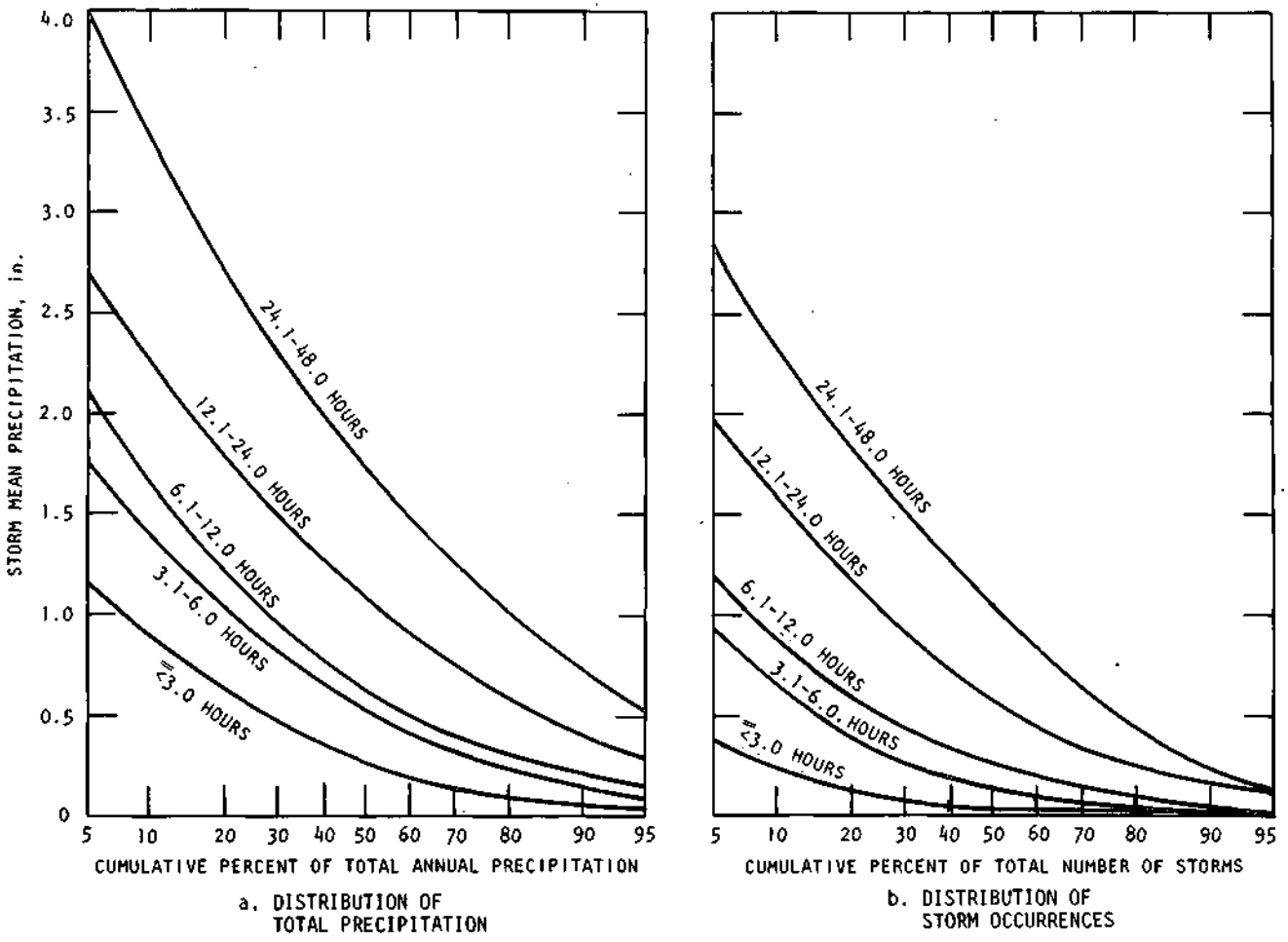

Figure 3. Average annual distributions grouped by storm duration.

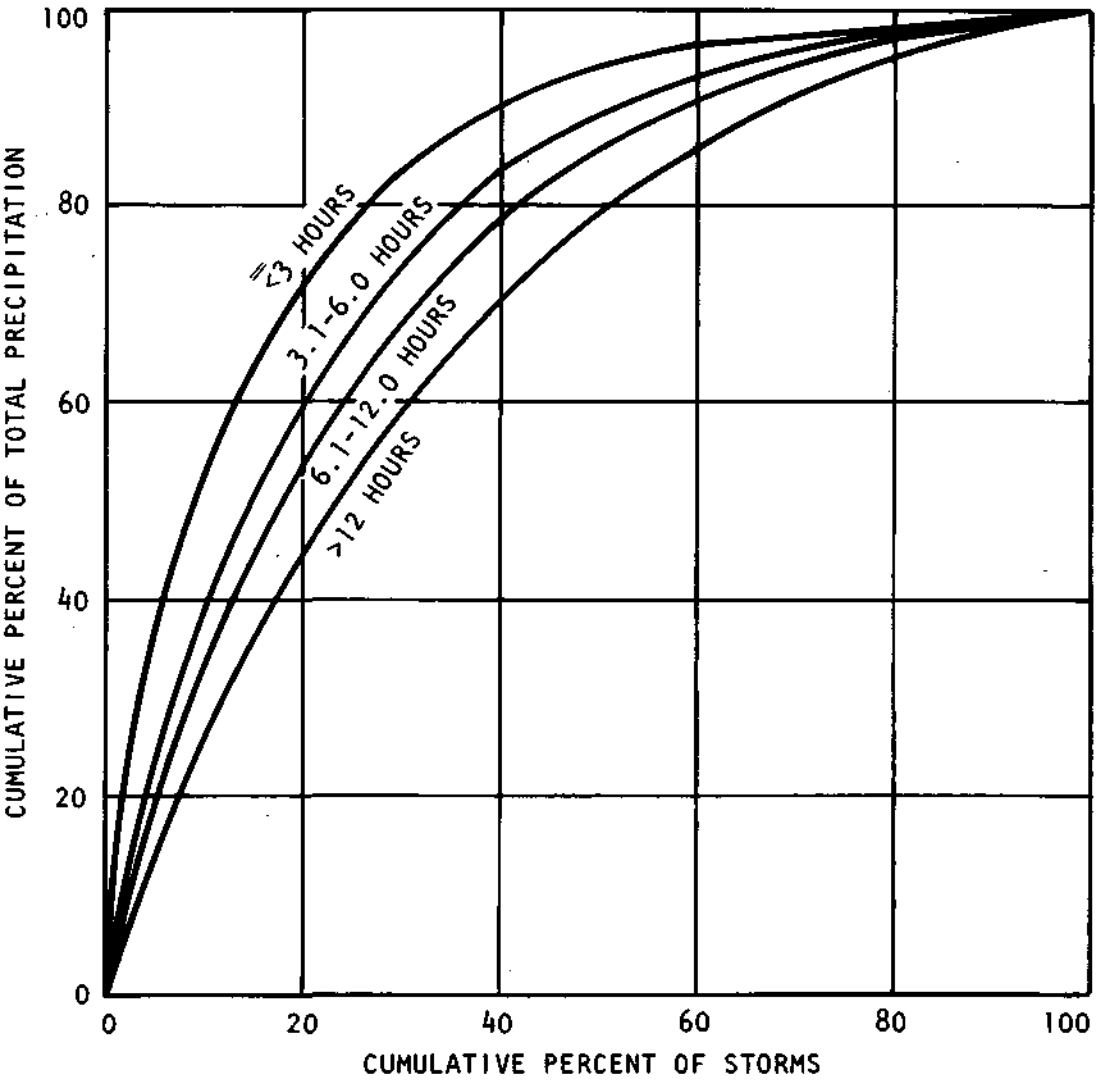

Figure 4. Relation between distributions of total precipitation and storm occurrences.

the western edge in a region of relatively heavy precipitation during the 12-yr sampling period, and the third (No. 21) on the eastern edge in a region of relatively light average precipitation with respect to the network. Analysis procedures were the same as used in the areal studies, and the same types of curves were developed. Sub-areas of 50, 100, and 200 mi^2 also were selected within the 400 mi^2 to provide information on other areas.

The results of the point-areal investigation are illustrated in Table 9 which shows comparisons of the average annual percent of storm occurrences for various intervals of mean precipitation on areas ranging from a point to 400 mi^2. The point values are for the central gage (No. 25). Also, equivalent point values are shown at the network center for daily precipitation, based upon the statewide pattern constructed from long-term climatological records of the U. S. Weather Bureau.

Considering the sampling limitations and sources of observation errors in a study of this type, Table 9 indicates that differences in the distribution characteristics are small for areas up to 400 mi^2, and that the distributions of point precipitation for storms and daily amounts are very similar. Similar conclusions were reached after examining seasonally stratified data. Consequently, it appears that point precipitation data from climatological stations may be used to obtain estimates of precipitation distribution characteristics for areas up to several hundred square miles.

Table 9. Relation between storm precipitation distributions on selected areas.

Areal mean precipitation (in)	Percent of total number of storms for given area (mi^2)					USWB daily point
	Gage 25	50	100	200	400	
≤ 0.10	38	45	46	46	47	38
0.11-0.50	37	34	34	33	34	40
0.51-1.00	15	13	12	13	12	14
> 1.00	10	8	8	8	7	8
	Percent of total precipitation for given area (mi^2)					
≤ 0.10	4	5	6	6	5	5
0.11-0.50	24	25	25	25	25	29
0.51-1.00	28	29	28	28	29	30
> 1.00	44	41	41	41	41	36

Fig. 5 illustrates the application of daily point precipitation records from climatological stations to obtain estimates of precipitation distribution characteristics. This figure shows the average percentage of total annual

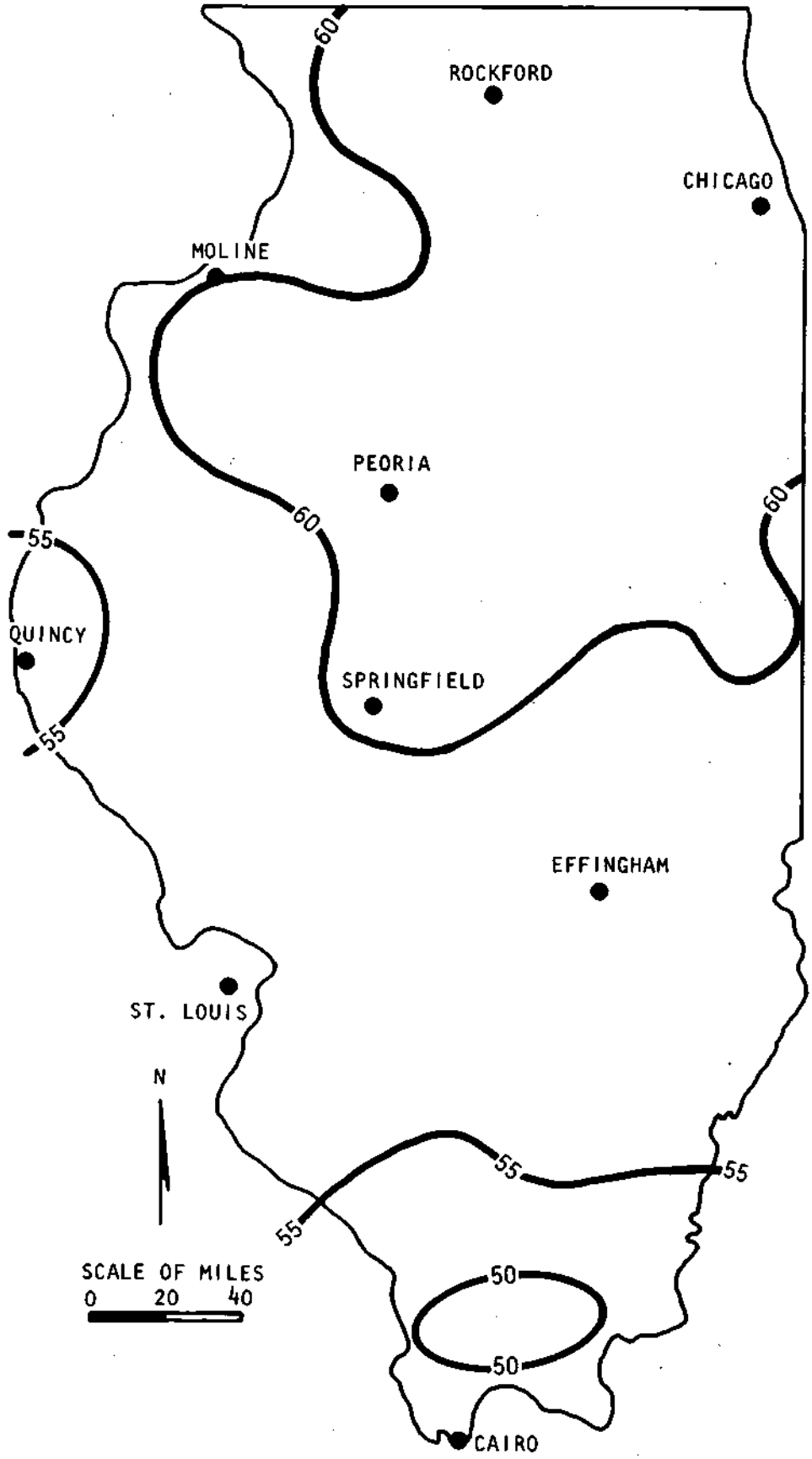

Figure 5. Average annual percentage of total precipitation from daily amounts of 0.11-1.00 inch.

precipitation from daily amounts in the range from 0.11 to 1.00 inches, a range of storm intensities in which seeding increases appear feasible. Fig. 5 is based upon 57 long-term stations distributed throughout the state. The pattern is quite flat with a slight decrease in percentages from north to south.

The point distribution patterns could be defined further by using data from recording gage stations in state climatic networks. Distributions could then be derived for storms of various duration similar to those presented earlier in the network studies. With this basic background information, quantitative estimates of the benefits of precipitation modification under known or hypothesized seeding conditions could be evaluated.

SECTION 2 - POTENTIAL APPLICATION OF CLIMATOLOGICAL CHARACTERISTICS IN PRECIPITATION MODIFICATION

In this highly controversial field, the validity of the assumptions and results presented in the author's illustrations in the following paragraphs are certain to be challenged. However, it is emphasized that natural distribution relations may be used with any hypothesis one wishes to apply with respect to his specific evaluation of weather modification capabilities and forecasting skill (if this is pertinent to his assessment). The author's examples, in which upper cutoffs in rain intensity are used, could only be accomplished by a continuous seeding program on all rain-producing clouds. Presently, this would be exceedingly difficult (if not impossible), and the results therefore represent seeding benefits with optimum operational efficiency under the assumed capabilities. However, as will be shown later, this type of calculation has provided certain valuable information relative to the possible future use of weather modification in Illinois. Furthermore, the primary purpose of the illustrations is to demonstrate to the reader how natural precipitation distributions may be applied as a useful tool in weather modification. As indicated earlier, the natural distributions will become increasingly more useful as scientific knowledge increases in this relatively crude science of weather modification.

Approach to Climatological Application in Midwest

Seeding increases in naturally heavy storms may not be feasible or desirable. Furthermore, relatively large percentage increases in very light storms would not produce significant added amounts for agricultural or water supply purposes, especially during dry periods when evaporation and infiltration are high and runoff is usually insignificant. As a first approximation to illustrate use of the climatological distributions described in Section 1, the author has assumed that seeding of Midwestern storms which produce 0.10 inch or less naturally would not significantly help the agricultural or water supply needs, and that storms capable of producing over one inch of precipitation

are too efficient naturally for substantial increases to result from seeding. In fact, the main desire here would probably be to overseed in wet periods to reduce surface damages.

The two major beneficiaries from successful precipitation modification would be agriculture and water supply (municipal and industrial). In the Midwest, the growing season from May through September encompasses the period of principle agricultural needs in years of deficient rainfall. Similarly, the major contribution to water supplies is during the period from October through April when evapotranspiration is at a minimum. Consequently, an investigation was made of the characteristics of the precipitation distribution during these two periods.

Average relations were developed for the 12-yr sampling period on the network. Also, separate relations were developed for the 3 wettest and 3 driest seasons to evaluate their differences from the average distributions. Cloud seeding is most likely to be undertaken in dry periods, so that the dry-season relations are especially pertinent from the standpoint of precipitation modification. A separate analysis of air mass storms was performed for the growing season. During the 12-yr period there were 675 warm-season storms; 29% were air mass storms and these contributed 17% of the total rainfall.

Table 10 shows comparisons between the two seasons for average, wet, and dry conditions. Only small differences exist in the average distribution of total precipitation (P_t) between the warm and cold seasons; consequently, the annual distribution discussed earlier (Table 8 and Fig. 3) does not depart much from the seasonal distributions. With respect to the average distribution of storm occurrences (N_t), appreciable differences exist because warm season storms have heavier mean rainfall for a given percentage of the cases. The average number of cold season storms was 20% greater than the warm season. However, the warm season averaged 17.15 inches per year compared with 15.54 in the cold season. Thus, fewer storms produce more rainfall in the May-September period, and result in the trends discussed above.

Analyses indicate that air mass storms become relatively more important in dry periods. In the 3 driest years, air mass storms accounted for 26% of the total precipitation compared with an average of 17% for the 12-yr sampling period and only 7% in the 3 wettest years.

Surprisingly, average rainfall from air mass storms in the 3 dry years was considerably greater than the average for the 12-yr sampling period, averaging 3.36 inches per year compared with 2.85 inches or 18% above the 12-yr average. Also, the frequency of air mass storms was near average. Only moderate drought conditions existed in these dry years, however. The growing season rainfall ranged from 69% to 81% of the average, whereas it is only 30% to 50% of the climatic average under severe drought conditions (Huff and Changnon, 1963). Consequently, air mass shower developments were probably helped in the 3 dry years by the climatic combination of below-average frontal activity, above-average maximum temperatures favoring the development of thermal instability, and the absence of an extremely dry atmosphere.

Table 10. Distribution of network mean precipitation in average, wet, and dry years.

Cumulative percent P_t*, N_t*	Network mean precipitation (in) equalled or exceeded					
	Average		Dry		Wet	
	P_t	N_t	P_t	N_t	P_t	N_t
			May - September			
10	2.20	1.00	2.20	0.82	2.83	1.75
25	1.41	0.47	1.40	0.40	1.86	0.62
50	0.85	0.16	0.83	0.13	1.12	0.20
75	0.43	0.06	0.41	0.05	0.60	0.07
90	0.20	0.02	0.18	0.02	0.27	0.02
			October - April			
10	2.16	0.81	1.91	0.75	2.18	0.93
25	1.40	0.38	1.28	0.33	1.48	0.41
50	0.80	0.11	0.72	0.09	0.87	0.11
75	0.39	0.05	0.32	0.04	0.41	0.05
90	0.15	0.03	0.11	0.02	0.16	0.03

* P_t - Total precipitation, N_t - Number of storms with mean > 0.01 in.

Other factors being equal, the dry years experienced in the 12-yr sampling period appear to have been relatively favorable for air mass seeding from the standpoint of frequency and quantity of showers. Here, we are only concerned with measuring the potential, based upon climatological analyses of natural data. The actual likelihood that any increase could come from seeding such dry-year air mass storms must await the decision of further cloud physics research.

Use of Natural Precipitation Distributions in Evaluating Cloud Seeding

In the Illinois study, nomograms were developed from the precipitation distributions to facilitate the calculation of potential benefits of cloud seeding during the agricultural and water-supply seasons under several assumed weather modification capabilities. The first of these nomograms is illustrated in Fig. 6 which shows the effects of 20% increases from hypothetical seeding on total May-September rainfall on the 400 mi^2 area for (1) all storms combined under dry-year conditions, (2) all storms combined in an average year, (3) air mass storms in dry periods, and (4) air mass storms in an average year. In view of the 3-yr sample and small percentage of total rainfall from air mass storms, the air mass dry-year nomogram should be used only as a first approximation of typical dry conditions.

The use of the nomogram can be explained best by an example. Assume a continuous seeding operation on the target and that cloud seeding is capable of producing an average increase of 20% in all storms in which the areal mean rainfall produced naturally is 0.5 inch or less, but that seeding storms of greater intensity (over 0.5 inch) will have no effect (positive or negative) upon the natural rainfall. The abscissa shows the upper limit of areal mean rainfall for a given assumption, and the ordinate shows the percentage increase in total seasonal rainfall resulting from the defined capability. Thus, in a typical dry-year the curves indicate a realized rainfall increase of 6.4% compared to 5.9% in an average year. From a practical standpoint, this difference is insignificant, considering the sources of errors involved in the observation and analyses of rainfall data even under optimum conditions which are closely met in these network studies. The foregoing example provides an estimate of maximum benefits under the assumed seeding capability. In practice, forecasting limitations and operational problems would make it extremely difficult to recognize and seed every storm. Thus, if one assumes only 80% of the natural storms are seeded, the realized increase in the example lowers from 6% to 5%.

Fig. 6 can be used also to determine potential seeding benefits within specific ranges of storm mean rainfall. For example, assume that only storms in which the mean rainfall is greater than 0.10 and less than 1 inch are affected by seeding. Then simply subtracting the calculated increases at these two levels produces an estimate of the maximum benefit. Also, the effects of other assumed seeding increases, such as 10% or 30%, can be obtained by multiplying the nomogram answer by the ratio of the desired percentage to 20. Similarly, the nomogram can be used to calculate the potential effects of selective seeding. For example, one could determine the results of seeding only 20% of the storms in any mean rainfall range and for any assumed percentage increase in these seeded storms. If one believes all storm intensities are significantly affected by seeding, the 1-inch cutoff in Fig. 6 can be extended to include all storms.

If one considers certain storm types affected beneficially by seeding and others detrimentally, then quantitative precipitation forecasting skill would have a major effect on the benefits and disbenefits of seeding natural storms. Until this skill is better defined and seeding technology substantially advanced from its present status, one can only use the climatological distributions developed here for estimating weather modification potential under various assumed capabilities.

It was shown earlier that storm duration has a pronounced effect upon the mean rainfall distribution curves (see Fig. 3). Therefore, nomograms were constructed to permit consideration of this factor in estimating potential cloud seeding benefits in Illinois during the agricultural and water-supply seasons. These curves are shown in Fig. 7 for average conditions and duration classifications which appeared most desirable from the various analyses performed in this study. As shown earlier, percentage differences between dry and average seasons were insignificantly small, so only one set of nomograms is presented for each season based on use of all storm data. Since most of the air mass storms had durations of 3 hr or less, separate duration curves could not be determined reliably. Also, such storms were too infrequent in the cold season to be treated separately.

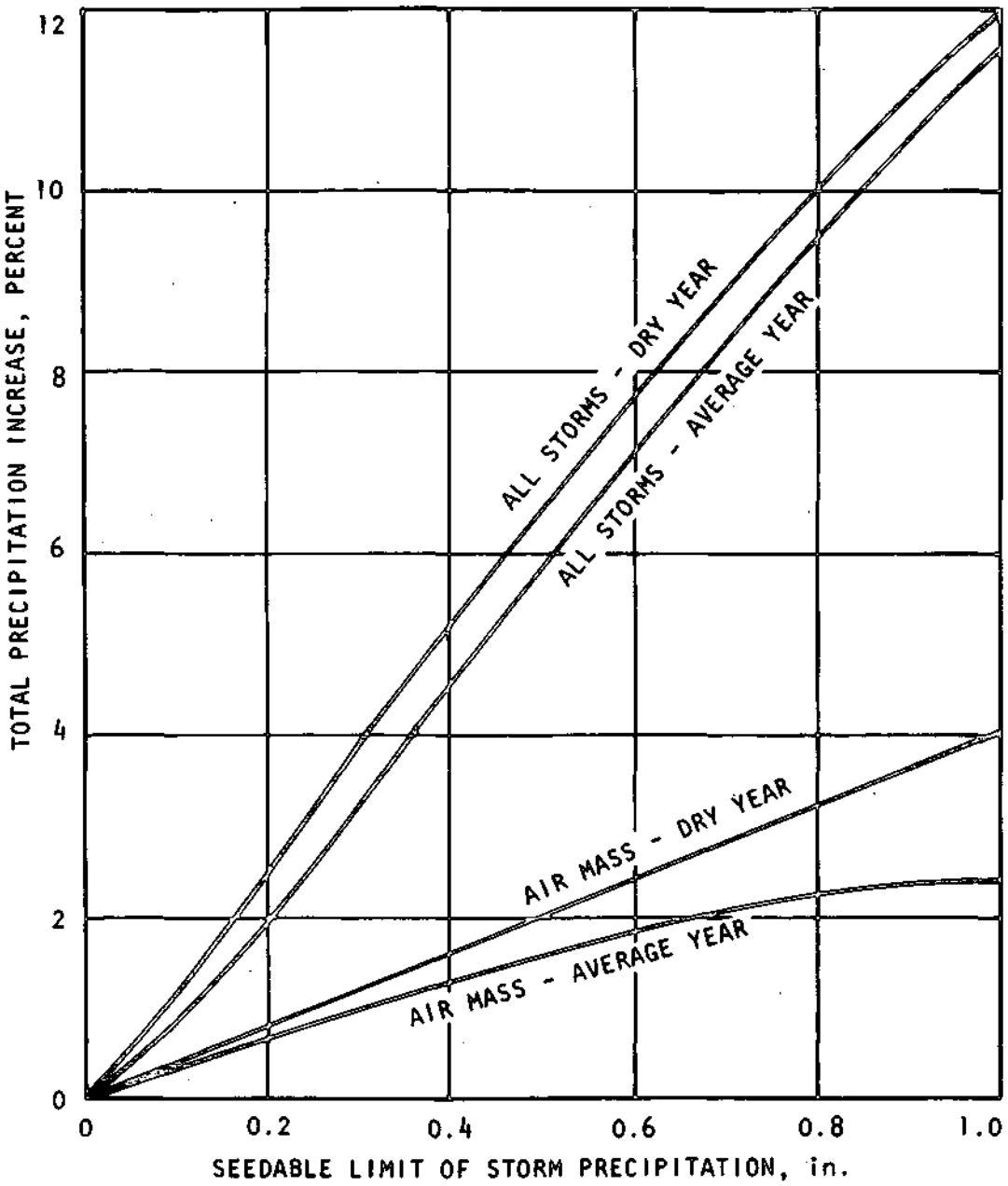

Figure 6. Effects of 20% seeding-induced increases on total May-September rainfall.

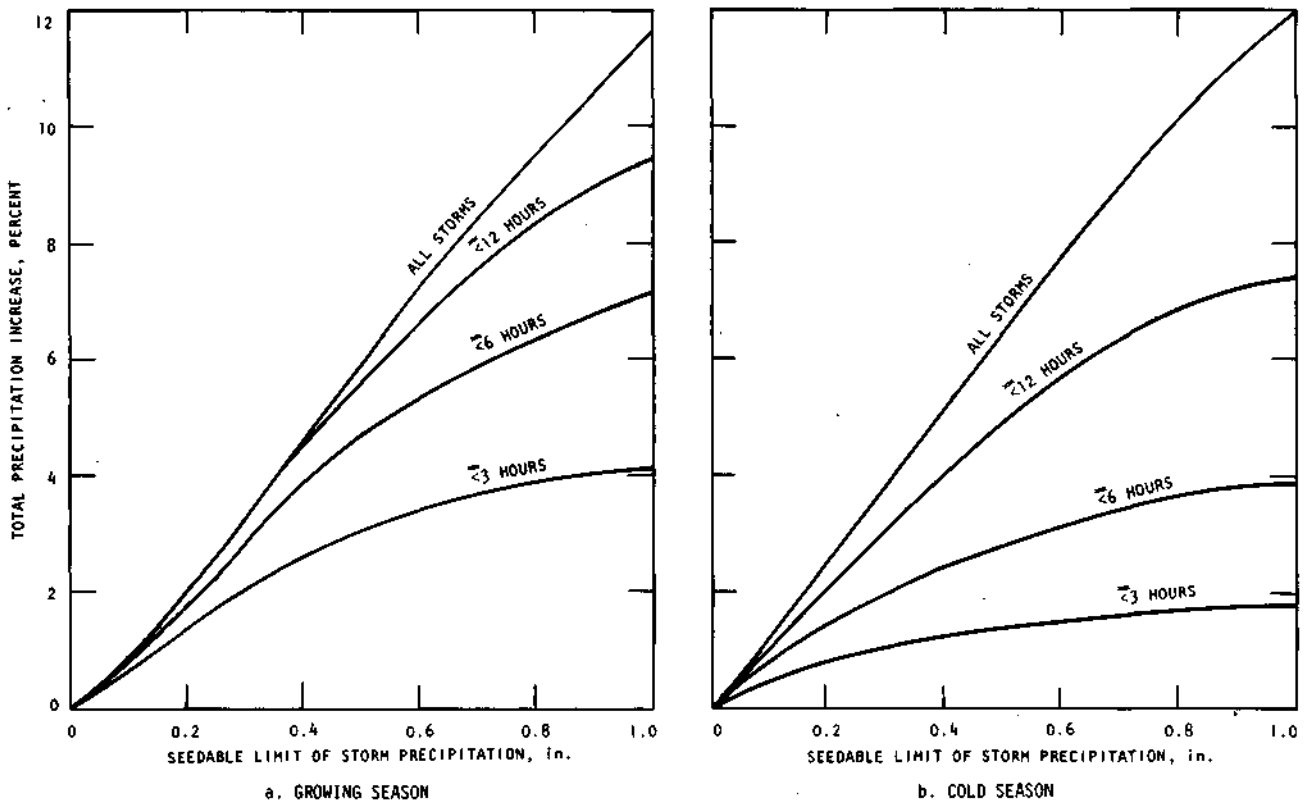

Figure 7. Effects of 20% seeding-induced increases in storms of selected duration on total seasonal precipitation.

Fig. 7 shows that the realized surface increases in seasonal precipitation are relatively small, especially in the October-April period, unless storms of relatively long duration can be successfully seeded. This results from the strong trend for precipitation to increase with increasing storm duration, and this trend is more pronounced in the colder part of the year when large-scale systems and steady types of precipitation are prevalent. Results obtained from three point rainfall curves within the network (described earlier) agreed quite closely with the areal mean values of Fig. 7, further indicating the utility of point data in natural distribution studies when networks are unavailable.

The final report of the Panel on Weather Modification and Climate of the National Academy of Sciences (MacDonald, 1966) stated that considerable statistical evidence had been found that increases of 10% to 20% can be induced by cloud seeding under favorable conditions. Figs. 6-7 show that it would be difficult to achieve seasonal increases of this magnitude in the Midwest by seeding on days with natural rainfall unless (1) seeding intensifies heavy rainstorms (> 1.0 inch mean) and/or (2) very large percentage increases are produced in storms of light to moderate intensity. Soil erosion, reservoir silting, and flooding may result in more damage than benefits from stimulation of heavy storms, especially storms of short duration that deposit their water with high rates of rainfall.

Fig. 6 indicates that seeding of warm-season, air mass storms cannot substantially increase the growing season rainfall by itself; therefore, both frontal and non-frontal storms must be seeded under Midwestern climatic conditions to achieve substantial aid for the farmer. Assuming a 20% seeding increase from all air mass storms which naturally produce areal means of 1 inch or less, the total May-September increase in a typical year would be 2% to 4% according to Fig. 6.

Seeding of Non-Precipitating Clouds

Another possibility for added precipitation which cannot be directly evaluated from natural rainfall data is that seeding might yield substantial rainfall on days with clouds that would not normally precipitate on the target area. The statistics on natural rainfall distributions do not provide a direct answer to the potential results of this attack. Indirectly, however, some conception of the problems involved can be discerned.

First, assume that only air mass conditions are to be seeded (Fig. 6), and that an average increase of 20% can be achieved from seeding those storms which produce 1 inch or less naturally. The resulting increase in a typical dry-year is 4%. In the sampling network used here, 26% of the May-September rainfall in an average dry-year comes from air mass storms. Then, if a 25% increase in the number of air mass rain-producing storms could be achieved, and these had a mean rainfall distribution similar to the natural distribution, the total May-September rainfall would be increased approximately 10% as a result of the additional rainfall from precipitating clouds (4%) and the induced precipitators (6%). The same result could be obtained by causing a rainfall increase of 50% in natural storms producing means of 1 inch or less (Fig. 6).

The above assumptions were made only for the sake of illustration, and their feasibility is a problem for the cloud physicists. Network rainfall statistics (Changnon, 1963) and Illinois cloud climatology (Changnon and Huff, 1957) indicate that in an average summer there are 3 to 4 times as many hours with cumulus clouds as there are hours with rainfall.

Summary and Conclusions

Storm data from a 12-yr operation of a network of 49 recording raingages in 400 mi^2 in central Illinois were used to determine the precipitation distribution characteristics on areas ranging from a point to 400 mi^2, and to demonstrate the use of derived distribution relations in evaluating the potential effects of cloud seeding on such areas. Distributions were defined by relating magnitude of storm precipitation to both cumulative percent of total precipitation and cumulative percent of total number of storms per season and year. Stratifications of the data according to storm intensity and duration, precipitation type, synoptic weather type, and relative wetness or dryness of seasonal and annual precipitation were tested to evaluate their influences upon the distribution characteristics.

Seasonally and annually the most significant differences between distribution curves were found when the data were grouped by storm duration. Variations between synoptic weather types resulted primarily from the tendency for some types to have a larger percentage of their storms with relatively long or short durations. Similarly, no strong trend was found for large differences between distribution curves for precipitation type. Air mass storms were found to become increasingly important in dry periods, accounting for 26% of the growing season rainfall in the 3 driest years, compared with 17% for the 12-yr sampling period and 7% in the 3 wettest years.

From the precipitation distributions, nomograms were developed to facilitate the calculation of potential benefits from cloud seeding under various seeding capabilities during the growing season (May-September) and the water-supply replenishment season (October-April).

Investigation of the relationship between the distributions of point and areal mean rainfall and between storm and daily precipitation were made through use of the network data and long-term Weather Bureau climatic stations in Illinois. Results indicated that for areas up to several hundred square miles daily point rainfall totals can be used to obtain a reasonable estimate of the precipitation distribution characteristics, and, consequently, aid in the evaluation of potential seeding benefits.

A general conclusion from this study is that cloud seeding must produce large increases in rainfall under favorable circumstances and/or initiate substantial rainfall from non-precipitating clouds, if substantial contributions are to be made to the agricultural industry and municipal water supplies under Illinois climatic conditions.

EFFECTS OF NATURAL RAINFALL VARIABILITY IN EVALUATING CLOUD SEEDING EXPERIMENTS

Introduction

In an earlier study, Huff (1966) used data from dense raingage networks in Illinois to investigate the effect of natural rainfall variability upon verification of cloud seeding experiments in midwestern, warm season rainfall on areas of county size or less. Hypothetical seeding experiments were made on network data for periods of 1 to 5 months during May to September and for durations of 1 to 10 years. Both target-control and single-area randomized experiments were investigated. A simple grouping of the data into air mass storms and all storms combined was used in the study.

Results indicated that the background interference from natural rainfall variability is substantial in warm season precipitation, and clearly illustrated the pitfalls in evaluating the effects of cloud seeding from short-term experiments. However, a number of questions were raised as a result of this earlier study. These included the comparable effects of natural rainfall in other seasons, the influence of areal mean rainfall (storm magnitude) in seeding evaluations, and the effect of storm duration in verifying modification effects. Consequently, the earlier study was considerably expanded in an effort to answer the foregoing questions, the results of which are summarized here.

In the expanded study, data were used for the 10-yr period, 1955-1964, primarily from the East Central Illinois Network of 49 recording raingages in 400 square miles (Fig. 2). For comparative purposes, certain analyses were performed on data from the Little Egypt Network of 49 raingages in 550 mi^2.

Analytical Procedures

The data sample consisted of all storms which produced measurable rainfall at any network gage. The average network precipitation was the basic measure of storm precipitation used in the study.

Two basic types of natural precipitation comparisons were used in the variability studies. In the first, the precipitation data were grouped by a randomized sampling procedure into hypothetically seeded and unseeded storms following the procedure of Battan and Kassander (1960) in the Arizona seeding experiments. From a chronological listing of the storms, the first storm in the series was designated as either a seeded or unseeded storm by random selection. The second storm was then placed automatically in the opposite group. Succeeding pairs of storms were grouped in a similar manner throughout each storm group analyzed. The randomizing procedure was accomplished on a IBM-7094 computer, and the randomizing repeated 100 times on each storm group to provide a probability distribution of differences between hypothetically seeded and unseeded storms.

In the second set of comparison tests, the effects of natural rainfall variability on the familiar target-control type of seeding evaluation was investigated. Primary emphasis was placed upon the randomized, cross-over type of seeding described by Gabriel (1967). This seeding technique tends to minimize any natural rainfall pattern differences that may be present in the selected target and control areas. Again, a computer program was utilized in the randomizing procedure and the randomizing repeated 100 times for each data group to provide a probability distribution of the hypothetical seeding effects.

Single Area Sampling

First, the Arizona sampling method was applied to all storms combined on an annual and seasonal basis for each of two 5-yr periods, 1955-1959 and 1960-1964, and for the 10-yr period, 1955-1964. Several weather modification experiments have had durations of approximately 5 years, and the 1960-1964 period coincides with cloud seeding experiments in the neighboring state of Missouri (Braham, 1965). The 10-yr period should provide useful information for evaluating the desirability of undertaking exceptionally long-term experiments to minimize background interference from natural precipitation variability.

For each data group, the storms were divided into two groups of hypothetically seeded and unseeded storms, and comparisons made by summing the 5-yr or 10-yr total rainfall in each. As indicated earlier, this hypothetical randomized seeding experiment was repeated 100 times to obtain an estimate of the frequency distribution of the natural precipitation differences between two sets of data drawn from the same population.

The type of distribution curves resulting from the hypothetical seeding experiments are illustrated in Fig. 8 through use of annual and summer storm data recorded in the 1960-1964 period. An excellent data fit was usually obtained on logarithmic probability paper when the various data groups were plotted in this manner. Results of the single-area sampling study are summarized in Tables 11 to 15, which have been derived from curves similar to those in Fig. 8 for various stratifications of the data in the 5-yr period, 1960-1964, and the 10-yr period, 1955-1964. The number of storms in each data group is indicated at the bottom of each table. The 1955-1959 distributions have been omitted in most cases since they lead to the same conclusions as the 1960-1964 data.

Seasonal and annual comparisons. Table 11 shows the frequency distribution of the hypothetical seeded to unseeded ratio resulting from natural precipitation variability on a seasonal and annual basis. All recorded storm data were used in obtaining these relations.

Interpretation of Table 11 and the following tables is illustrated by reference to the annual column for 1960-1964. Here, it is indicated that if seeding had been carried out in this area on every precipitation day in

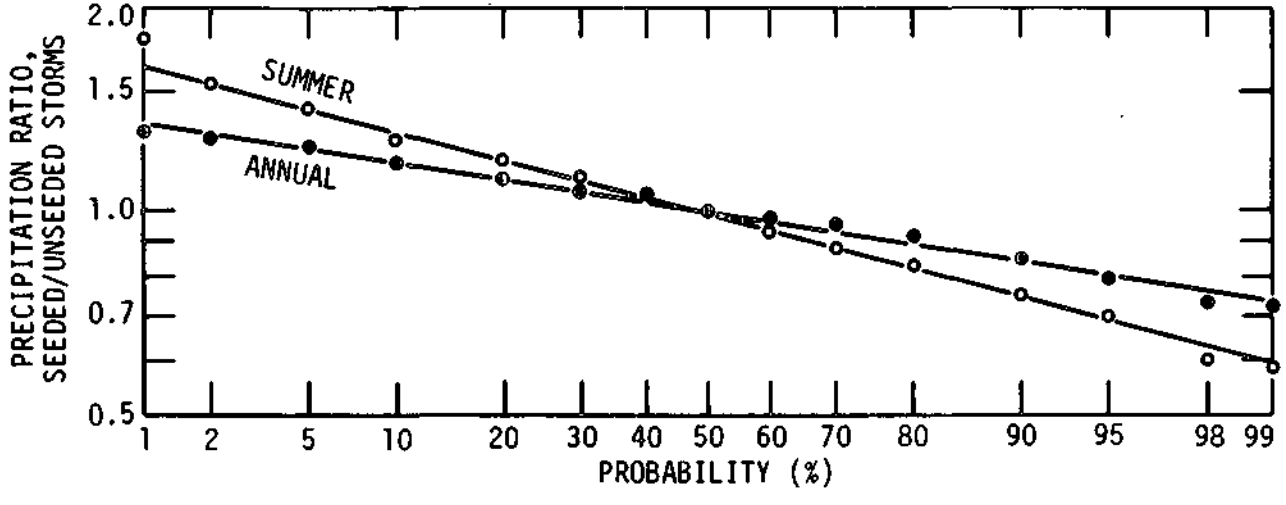

Figure 8. Distribution of differences between hypothetically seeded and unseeded storms on East Central Illinois Network.

1960-1964 (or a similar 5-yr period), there is a 5-percent probability that an apparent increase of 23% (ratio = 1.23), due entirely to natural precipitation variability, would have occurred in the sample of seeded storms. Similarly, employing this type of randomized experiment, an 11% apparent increase can be expected to occur in 20% of such 5-yr experiments. If seeding is confined to the summer months, Table 11 indicates there is a 5-percent chance of a 40% or greater apparent increase in the seeded storm sample and a 20-percent probability of an 18% or greater increase produced by natural variability.

Comparison of the two periods in Table 11 shows that the background interference from natural rainfall variability decreases substantially as the sampling period is lengthened from 5 to 10 years. For example, the range between the 5% to 95% probability values decreases from 1.23-0.81 to 1.17-0.87 for annual experiments, from 1.40-0.69 to 1.33-0.78 in summer rainfall, and from 1.50-0.66 to 1.42-0.67 in winter precipitation. However, even after 10 years the background interference from natural precipitation variability remains substantial on either an annual or seasonal basis. Thus, the 1955-1964 data indicate a 5% probability of an apparent increase of 17% from natural causes if all storms during the 10-yr period had been seeded, and this apparent increase ranges from 33% to 49% if seeding had been restricted to a particular season.

The much larger storm sample in the annual group compared with the seasonal groups results in a significantly lower degree of background interference from natural causes in annual probability distributions. For example, the 5% probability shows an apparent increase of 23% annually compared with 40% for summer in the 1960-1964 sample. Table 11 clearly illustrates the difficulty confronting the experimenter who is endeavoring to verify the possible increase of a few percent in the natural precipitation from cloud seeding, when the single-area randomized experimental technique is employed under midwestern climatic conditions.

An interesting statistic from Table 11 is that the natural variability interference is greater in winter than in summer, although the spatial relative variability in midwestern storms is much greater, on the average, in summer storms in which thunderstorms and rainshowers usually prevail (Huff and Shipp, 1968). The greater interstorm relative variability in winter is related to the difference in mean precipitation characteristics. Other studies of Illinois data have shown that, on the average, summer storms have areal mean rainfall approximately twice that of winter storms, although winter storms normally last longer and display less spatial variability. Also, the smaller number of winter storms may be a contributing factor. Regardless of the cause, seasonal difference in interstorm variability is a factor which should be considered in the design of weather modification experiments.

Mean precipitation effect. Tables 12 and 13 have been included to provide quantitative information on the effect of storm magnitude in the verification of single-area randomized seeding experiments. Here, hypothetical seeding has been performed on storms with mean precipitation of 0.01-0.10 inch and 0.11-1.00 inch. The latter group is one in which seeding-induced increases

Table 11. Distribution of seeded to unseeded ratio in all storms combined.

Prob. (%)	Annual	Winter	Spring	Summer	Fall
			1960 - 1964		
1	1.37	1.78	1.78	1.57	1.89
5	1.23	1.50	1.50	1.40	1.58
10	1.19	1.37	1.37	1.30	1.44
20	1.11	1.22	1.21	1.18	1.29
30	1.07	1.13	1.07	1.10	1.18
40	1.03	1.06	1.03	1.04	1.10
50	1.00	1.00	0.98	0.99	1.03
60	0.97	0.93	0.92	0.93	0.96
70	0.94	0.86	0.86	0.88	0.90
80	0.90	0.80	0.78	0.82	0.83
90	0.85	0.72	0.70	0.75	0.74
95	0.81	0.66	0.64	0.69	0.67
99	0.74	0.55	0.54	0.60	0.56
N	634	124	206	179	128
			1955 - 1964		
1	1.23	1.67	1.57	1.49	1.74
5	1.17	1.42	1.39	1.33	1.49
10	1.12	1.31	1.30	1.26	1.37
20	1.09	1.18	1.19	1.18	1.25
30	1.06	1.09	1.12	1.11	1.17
40	1.03	1.03	1.07	1.06	1.09
50	1.00	0.98	1.01	1.01	1.02
60	0.98	0.92	0.97	0.97	0.97
70	0.96	0.87	0.93	0.93	0.91
80	0.94	0.81	0.87	0.88	0.85
90	0.90	0.73	0.80	0.83	0.77
95	0.87	0.67	0.75	0.78	0.71
99	0.82	0.57	0.66	0.70	0.61
N	1144	205	334	367	238

may be most effective. Unless the seeding-induced increase in lesser storms is very great, the contribution to surface water would be insignificant. The precipitation-producing processes in storms producing over one inch of rainfall are likely to be too efficient to be significantly affected by seeding, and could in fact cause more damage than benefit if they were intensified further.

Except for winter, Table 12 based on 1960-1964 data shows a substantial decrease in background interference with the heavier storm means of 0.11 to 1.00 inch. Table 13 for the 10-yr period shows trends similar to those in Table 12. Except for the summer and annual periods of 1955-1964, there were too few storms with means over one inch to derive a probability distribution. In these two cases, the probability distributions did not depart significantly from those for 0.11 to 1.00 inch. The additional interference from natural variability when storms with trace amounts are included in the verification program is shown by comparing Table 11, which contains all storms, with Tables 12 and 13. The foregoing statistics show that verification of seeding effects is somewhat easier if interest is primarily in moderate to heavy storms as opposed to light storms, and they provide quantitative estimates of the differential effects.

Storm duration effect. Table 14 provides quantitative information on the effects of natural variability when storms are grouped according to storm duration. In preparing this table, all storms in each period and each storm duration were used in the hypothetical seeding experiments. In general, an overall trend is indicated for the background interference to decrease with increasing storm duration, but this trend is not consistent between durations. For example, the 5-percent probability in the 1960-1964 analysis decreases from 1.52 to 1.43 as duration increases from less than 3 hours to 3.1 to 6.0 hours, then increases to 1.48 for 6.1 to 12.0 hours, and decreases substantially to 1.40 in storms with durations exceeding 12 hours. Comparison with the "annual" column of Table 11 shows that the duration stratification through separation of the total sample into smaller groups has created a greater degree of variability in all duration classes than was present when all storms were treated as a single sample.

This leads to the obvious conclusion that duration grouping is undesirable in seeding experiments, especially in relatively short-term experiments, unless primary emphasis is being placed on seeding storms within a certain duration range. For example, in an aircraft seeding program it might be economically unfeasible or physically impossible to seed continuously in long-duration storms, such as those exceeding 6 or 12 hours. Also, future research may show seeding is ineffective in such widespread storms. Table 14 then provides quantitative estimates of the natural variability effect which can be used in planning seeding experiments that are restricted with respect to storm duration.

Air mass storms. Table 15 summarizes the results of hypothetical seeding experiments with nonfrontal air mass storms. The air mass category was selected for special attention, because some investigators have suggested that nonfrontal convective rainfall offers the greatest opportunity for effective seeding. Furthermore, outstanding cloud seeding experiments in Arizona during the period 1957-1964 (Battan and Kassander, 1960) and in Missouri during 1960-1964 (Braham, 1966) concentrated on the treatment of convective storms.

Table 12. Effect of storm mean precipitation on distribution of seeded to unseeded ratio during 1960-1964.

Prob. (%)	Ratio equalled or exceeded for given period				
	Annual	Winter	Spring	Summer	Fall
			Mean = 0.01" - 0.10"		
1	1.28	1.46	1.66	1.62	1.71
5	1.20	1.30	1.43	1.41	1.47
10	1.14	1.22	1.33	1.31	1.33
20	1.10	1.13	1.22	1.20	1.20
30	1.06	1.08	1.13	1.12	1.11
40	1.03	1.04	1.07	1.07	1.04
50	1.00	1.00	1.01	1.01	0.98
60	0.98	0.95	0.96	0.96	0.92
70	0.96	0.91	0.91	0.90	0.86
80	0.93	0.86	0.85	0.83	0.80
90	0.89	0.80	0.78	0.77	0.72
95	0.85	0.76	0.72	0.72	0.66
99	0.80	0.68	0.62	0.62	0.56
N	268	71	85	62	50
			Mean = 0.11" - 1.00"		
1	1.22	1.74	1.36	1.33	1.47
5	1.15	1.50	1.24	1.23	1.30
10	1.11	1.39	1.18	1.17	1.22
20	1.07	1.27	1.11	1.10	1.14
30	1.04	1.18	1.07	1.05	1.08
40	1.02	1.10	1.03	1.01	1.03
50	1.00	1.05	1.00	0.98	0.99
60	0.98	1.00	0.96	0.95	0.95
70	0.96	0.94	0.93	0.91	0.90
80	0.93	0.88	0.89	0.88	0.86
90	0.90	0.80	0.84	0.83	0.80
95	0.87	0.74	0.80	0.78	0.75
99	0.83	0.64	0.74	0.72	0.67
N	247	39	86	72	50

Table 13. Effect of storm mean precipitation on distribution of seeded to unseeded ratio during 1955-1964.

Prob. (%)	Ratio equalled or exceeded for given period				
	Annual	Winter	Spring	Summer	Fall
			Mean = 0.01" - 0.10"		
1	1.23	1.53	1.40	1.33	1.53
5	1.17	1.35	1.27	1.22	1.35
10	1.13	1.27	1.20	1.17	1.26
20	1.09	1.15	1.12	1.10	1.14
30	1.05	1.09	1.08	1.07	1.09
40	1.03	1.03	1.03	1.03	1.03
50	1.00	0.98	0.99	1.00	0.98
60	0.98	0.93	0.95	0.97	0.93
70	0.96	0.88	0.91	0.93	0.88
80	0.94	0.82	0.87	0.89	0.82
90	0.90	0.76	0.82	0.85	0.76
95	0.87	0.70	0.77	0.81	0.70
99	0.82	0.62	0.70	0.74	0.62
N	462	111	129	128	94
			Mean = 0.11" - 1.00"		
1	1.15	1.55	1.27	1.31	1.37
5	1.10	1.35	1.19	1.21	1.25
10	1.08	1.25	1.15	1.17	1.20
20	1.05	1.15	1.10	1.10	1.12
30	1.03	1.08	1.05	1.07	1.07
40	1.01	1.02	1.02	1.03	1.02
50	1.00	0.97	1.00	1.00	0.97
60	0.98	0.92	0.98	0.98	0.92
70	0.96	0.87	0.95	0.95	0.87
80	0.94	0.82	0.92	0.92	0.82
90	0.92	0.75	0.89	0.88	0.75
95	0.90	0.70	0.86	0.84	0.70
99	0.87	0.61	0.80	0.78	0.61
N	458	69	150	144	95

Table 14. Effect of storm duration on distribution of seeded to unseeded ratio for all storms combined.

Prob.	Ratio for given storm durations (hours)			
(%)	≤ 3	3.1-6.0	6.1-12.0	12.1-24.0
	1960 - 1964			
1	1.79	1.66	1.69	1.60
5	1.52	1.43	1.48	1.40
10	1.40	1.31	1.36	1.30
20	1.37	1.20	1.22	1.20
30	1.18	1.12	1.14	1.12
40	1.10	1.05	1.08	1.06
50	1.03	1.00	1.02	1.01
60	0.97	0.94	0.97	0.96
70	0.91	0.88	0.91	0.92
80	0.85	0.83	0.85	0.86
90	0.76	0.75	0.77	0.80
95	0.70	0.69	0.71	0.74
99	0.59.	0.59	0.61	0.65
N	310	132	98	82
	1955 - 1964			
1	1.46	1.53	1.34	1.36
5	1.30	1.36	1.22	1.25
10	1.21	1.28	1.17	1.19
20	1.14	1.19	1.10	1.12
30	1.08	1.12	1.05	1.08
40	1.04	1.07	1.01	1.04
50	1.00	1.02	0.98	1.01
60	0.96	0.98	0.94	0.98
70	0.91	0.94	0.91	0.95
80	0.87	0.89	0.88	0.91
90	0.81	0.83	0.83	0.86
95	0.76	0.77	0.78	0.82
99	0.68	0.68	0.72	0.75
N	582	218	170	138

Spring, fall, and winter distributions have been omitted in Table 15 because of the small number of air mass storms during these seasons in the sampling network. Also, over 70% of the air mass storms had durations less than 3 hours, and over 50% had areal means less than 0.05 inch. Consequently, duration groupings were not used, and only two mean rainfall groups were investigated. Data for the 5-yr period, 1955-1959, have been included in this table to show differences in the probability distributions derived from two separate periods of equal length. In this case, the interstorm natural variability was considerably greater in the 1960-1964 period. Table 15 shows the expected decreasing effect of natural variability with increasing length of sampling period. Comparison of Table 15 with Table 11 provides quantitative measures of the difference in natural variability effect when only air mass storms are seeded as opposed to seeding of all storms.

Cross-Over Target-Control Sampling

Employing 1960-1964 data, hypothetical seeding was performed on the East Central Illinois Network through use of randomized cross-over target-control sampling. For this purpose, the sampling network was divided into two areas comprising the southwestern and northeastern halves. These contiguous target-control areas provide estimates of the minimum background interference from natural precipitation variability that may be expected in the verification of midwestern cloud seeding experiments. Under these sampling conditions, not only do the target and control frequently come under the influence of the same mesoscale system, but are closely related in time and space within the mesosystem.

Only very small climatic differences in precipitation exist within the network. Long-term records of the U. S. Weather Bureau indicate a normal decrease of approximately one percent in annual precipitation from the southwestern to northeastern halves of the sampling network, with a 2-3% average increase in the growing season (May-September). For the 5-yr sampling period, the dense network data showed an average decrease of approximately 3% for the growing season and 1% for the annual precipitation. During individual years, however, the differences between the two halves of the network were sometimes substantial. Differences ranged from -15 to +21% in the five individual growing seasons.

Annual and seasonal comparisons. The effect of length of sampling period in the cross-over target-control method of verification is illustrated in Table 16. Here, probability distributions are shown for consecutive periods of 1, 2, 3, and 5 years, and these are based upon the use of all storms in which the network mean precipitation equalled or exceeded 0.01 inch. Under the conditions of this hypothetical experiment, it was found that the background level of interference was relatively low compared to the single-area type of verification discussed earlier and summarized in Tables 11 to 15. Furthermore, the natural variability effect decreased only slightly when the sampling period was increased from 1 to 5 years. Examination of the other individual years showed the highest variability effect in 1963 when the ratio had a range of 1.09-0.89 from the 5 to 95% levels. This would indicate that under seeding

Table 15. Distribution of seeded to unseeded ratio in air mass storms.

Prob. (%)	Annual, all storms			Summer, all storms		
	Ratio for given period					
	1955-59	1960-64	1955-64	1955-59	1960-64	1955-64
1	2.62	3.05	2.46	2.50	3.02	2.37
5	1.98	2.08	1.78	1.88	2.20	1.84
10	1.68	1.81	1.55	1.63	1.85	1.61
20	1.39	1.46	1.33	1.37	1.51	1.38
30	1.21	1.23	1.21	1.19	1.30	1.23
40	1.08	1.08	1.11	1.07	1.15	1.11
50	0.97	0.96	1.02	0.96	1.02	1.01
60	0.87	0.84	0.96	0.87	0.90	0.93
70	0.77	0.74	0.89	0.77	0.79	0.85
80	0.68	0.63	0.82	0.68	0.68	0.76
90	0.56	0.50	0.73	0.57	0.56	0.65
95	0.48	0.43	0.67	0.49	0.47	0.57
99	0.36	0.28	0.57	0.37	0.34	0.45
N	118	85	203	87	66	153
	Annual, mean ≧ 0.01"			Summer, mean ≧ 0.01"		
1	2.58	2.87	1.98	2.80	3.05	2.02
5	1.98	2.11	1.59	2.10	2.25	1.65
10	1.72	1.80	1.43	1.80	1.90	1.48
20	1.45	1.47	1.23	1.50	1.57	1.30
30	1.28	1.27	1.12	1.31	1.36	1.18
40	1.15	1.12	1.03	1.18	1.20	1.09
50	1.04	1.00	0.95	1.05	1.07	1.01
60	0.95	0.89	0.87	0.95	0.95	0.93
70	0.86	0.79	0.80	0.85	0.84	0.86
80	0.75	0.68	0.73	0.75	0.73	0.78
90	0.64	0.56	0.63	0.63	0.60	0.68
95	0.55	0.47	0.56	0.54	0.51	0.61
99	0.43	0.35	0.45	0.40	0.37	0.49
N	91	62	153	64	49	113

Table 15 (cont'd). Distribution of seeded to unseeded ratio in air mass storms.

Annual, mean = 0.11"-1.00"

Prob. (%)	Ratio for given period		
	1955-59	1960-64	1955-64
1	1.73	1.84	1.62
5	1.48	1.55	1.42
10	1.35	1.42	1.31
20	1.21	1.28	1.20
30	1.12	1.18	1.12
40	1.06	1.10	1.06
50	1.00	1.03	1.00
60	0.94	0.97	0.95
70	0.88	0.90	0.90
80	0.82	0.84	0.85
90	0.74	0.75	0.78
95	0.67	0.68	0.72
99	0.57	0.57	0.63
N	38	26	64

Table 16. Time distribution of seeded to unseeded ratios in randomized cross-over target-control experiments on East Central Illinois Network for storm mean precipitation ≧ 0.01 inch.

Prob. (%)	Ratio for given period			
	1960	1960-61	1960-62	1960-64
1	1.09	1.08	1.07	1.07
5	1.07	1.06	1.05	1.04
10	1.05	1.04	1.04	1.03
20	1.03	1.03	1.02	1.02
30	1.02	1.01	1.01	1.01
40	1.01	1.00	1.00	1.01
50	1.00	1.00	1.00	1.00
60	0.99	0.99	0.99	1.00
70	0.98	0.98	0.99	0.99
80	0.97	0.97	0.98	0.98
90	0.96	0.96	0.97	0.97
95	0.94	0.95	0.96	0.96
99	0.92	0.93	0.94	0.94
N	105	216	316	513

experiments in which all types of storms are seeded little is to be gained with extension of the experiment beyond 1 to 2 years with this type of verification procedure, if target and control have very similar precipitation climates.

Table 17 provides quantitative estimates of the natural variability effects when seeding is conducted on a seasonal basis. In addition to the conventional seasons, the May-September and October-April periods have been included. A point of interest in this table is that the greatest background interference occurs in summer and in the growing season and minimizes in winter and during the October-April period. This is directly opposite of the findings with the single-area verification technique. With the cross-over target-control method, in which all storms are seeded and target and control interchanged, the effect of interstorm variability (time variability) in storm mean rainfall has been minimized. With the target-control verification, the background interference is governed primarily by the spatial extent and intensity of storm rainfall. As a result, the maximum effect is greatest in summer when storms are frequently of small areal extent, and large differences in intensity occur within short distances.

Table 17. Seasonal distribution of seeded to unseeded ratios in randomized cross-over target-control experiments on East Central Illinois Network for storm mean precipitation ≧ 0.01 inch.

Prob.	Ratio for given period					
(%)	Winter	Spring	Summer	Fall	May-September	October-April
1	1.06	1.07	1.12	1.08	1.08	1.04
5	1.04	1.05	1.09	1.05	1.07	1.02
10	1.03	1.03	1.07	1.03	1.05	1.01
20	1.02	1.02	1.04	1.02	1.03	1.01-
30	1.01	1.01	1.02	1.01	1.02	1.00+
40	1.00+	1.00+	1.01	1.01-	1.01	1.00+
50	1.00	1.00	1.00	1.00	1.00	1.00
60	1.00-	0.99	0.99	0.99	0.99	1.00-
70	0.99	0.98	0.98	0.98	0.98	0.99
80	0.98	0.97	0.96	0.97	0.97	0.98
90	0.97	0.96	0.94	0.96	0.96	0.98-
95	0.96	0.95	0.92	0.95	0.95	0.97
99	0.95	0.94	0.90	0.94	0.93	0.96
N	102	159	140	112	234	279

Mean precipitation effect. Hypothetical seeding experiments with the single-area technique indicated decreasing interference from natural precipitation variability with increasing storm mean rainfall. That is, stratification of experimental data according to storm intensity might be helpful in the verification

of cloud seeding effects. Similar experiments with the target-control method indicate that there is no advantage in this type of stratification. In fact, the subgrouping through decreasing the number of samples in each analytical unit could have a deleterious effect, as illustrated in Table 18. Here, storms in which the mean precipitation was in the range from 0.11 to 1.00 inch have been separated from the sample used in Tables 16 and 17 which included all storms with measurable precipitation. The major difference is between the summer distributions where an appreciable increase in the natural variability effect is indicated for the group of 0.11 to 1.00 inch. In general, however, there is little difference between the seasonal and annual distributions in Tables 16-18. Again, it appears that the appreciable effect of mean precipitation found with the single-area sampling was related to the interstorm variability which has been minimized in the target-control method.

Table 18. Seasonal distribution of seeded to unseeded ratios in randomized cross-over target-control experiments on East Central Illinois Network for storm mean precipitation = 0.11 to 1.00 inch.

Prob.	Ratio for given period						
(%)	Winter	Spring	Summer	Fall	May-Sept.	Oct.-Apr.	Annual
1	1.08	1.08	1.17	1.09	1.10	1.03	1.06
5	1.06	1.06	1.11	1.07	1.07	1.02	1.04
10	1.04	1.05	1.09	1.05	1.05	1.01	1.03
20	1.02	1.03	1.06	1.03	1.04	1.01-	1.02
30	1.01	1.02	1.03	1.01	1.02	1.00+	1.01+
40	1.00+	1.01-	1.01	1.00+	1.01	1.00+	1.01
50	1.00	1.00	1.00	1.00	1.00	1.00	1.00
60	1.00-	1.00-	0.98	0.99	0.99	0.99	0.99
70	0.99	0.99	0.96	0.98	0.98	0.98+	0.98+
80	0.98	0.98	0.94	0.97	0.96	0.98	0.98
90	0.97	0.97	0.91	0.96	0.95	0.97+	0.97+
95	0.96	0.96	0.88	0.94	0.93	0.97	0.97
99	0.95	0.94	0.84	0.92	0.91	0.96	0.96
N	40	86	72	49	121	126	247

Storm duration effect. The effect of storm duration on the distribution of hypothetical seeded to unseeded ratios is illustrated in Table 19 through use of all storms during 1960-1964 in which areal means equalled or exceeded 0.01 inch. The duration effect in the target-control verification technique is even weaker than in the single-area method discussed in conjunction with Table 14. An appreciable decrease in the natural variability effect is indicated in Table 19 when storm durations exceed 12 hours. For shorter durations, however, the ratio trends are inconsistent and differences do not appear to be significant. The ratios for durations of 12.1 to 24.0 hours in Table 19 are nearly identical with those obtained for all storms combined in Table 16.

Table 19. Effect of storm duration on distribution of seeded to unseeded ratios in randomized cross-over target-control experiments on East Central Illinois Network.

1960-1961

Prob. (%)	Ratio for given duration (hours) ≤ 3.0	3.1-6.0	6.1-12.0	12.1-24.0
1	1.12	1.15	1.11	1.07
5	1.09	1.11	1.08	1.05
10	1.07	1.09	1.06	1.04
20	1.05	1.05	1.04	1.03
30	1.03	1.03	1.02	1.02
40	1.01	1.01	1.01	1.01
50	1.00	1.00	1.00	1.00
60	0.99	0.98	0.98	1.00-
70	0.98	0.97	0.97	0.99
80	0.96	0.95	0.96	0.98
90	0.94	0.93	0.94	0.97
95	0.92	0.90	0.92	0.96
99	0.90	0.87	0.89	0.94
N	206	117	96	80

Air mass storms. In Table 20, quantitative estimates are provided for the natural variability effect in air mass storms when the cross-over target-control verification is used. Estimates are provided only for the May-September period for two mean rainfall groups for the reasons stated in the single-area sampling discussions. Here, the separation of mean rainfalls of 0.11 inch to 1.00 inch from the combined storm group has practically no effect upon the seeded to unseeded ratios. Comparison of Table 20 with Table 16 provides a quantitative measure of the increasing background interference from natural rainfall variability in the separate verification of air mass storm seeding effects.

As pointed out earlier, the coinciding target-control areas used in the foregoing hypothetical experiments provide optimum conditions for minimizing the effect of natural variability in the verification of cloud seeding experiments. Because of the contamination problem, coinciding target-control areas would not be acceptable in field experiments. The results presented in Table 16 to 20 should be interpreted as the lowest level of background interference from natural precipitation variability to be expected when seeding is carried out on areas of county size or smaller.

Table 20. Distribution of seeded to unseeded ratios in randomized cross-over target-control experiments on East Central Illinois Network for air mass storms during May-September 1960-1964.

Prob. (%)	Ratio for given storm mean (in) ≥ 0.01	0.11-1.00
1	1.32	1.34
5	1.23	1.24
10	1.18	1.18
20	1.12	1.12
30	1.08	1.08
40	1.04	1.04
50	1.01	1.01
60	0.98	0.98
70	0.95	0.95
80	0.92	0.92
90	0.88	0.87
95	0.83	0.83
99	0.78	0.77
N	52	28

Distance effect on target-control experiments. In an effort to obtain information on the maximum interference from precipitation variability, hypothetical target-control experiments were made with the randomized cross-over design between the East Central Illinois and Little Egypt Networks (Fig. 2). These networks are located approximately 125 miles apart and would not normally be used as target-control areas. However, they do provide an opportunity for estimating the maximum effect that might occur. Since they are not located closely in time or space, major differences in precipitation characteristics may occur from one network to the other as storms pass through them. Normal summer rainfall is nearly identical in the two areas, but the winter normal precipitation is approximately 60% greater in the Little Egypt Network.

Table 21 shows the distribution of hypothetical seeded to unseeded ratios for winter and summer 1960-1964 between the two networks. Only storms having means of 0.01 or greater on both networks were used. This insured the use of only those synoptic situations capable of producing precipitation in both target and control areas, a condition most likely to be present under target-control seeding experiments. Only relatively small differences are indicated between the two seasons in Table 21 despite the climatic differences in winter. This suggests that the cross-over design has been effective in minimizing the climatic effect.

Of most interest is the comparison of Table 21 with the winter and summer distributions in Table 17. As expected, the values in Table 17, reflecting optimum conditions for minimizing the natural variability effect, show much

smaller background interference than do the ratios in Table 21, which provide an estimate of the maximum effect to be expected from natural precipitation variability in target-control experiments utilizing a randomized cross-over design.

Table 21. Distribution of seeded to unseeded ratios in cross-over target-control comparisons between East Central Illinois and Little Egypt networks, 1960-1964, storm means ≧ 0.01 inch.

Prob. (%)	Ratio for given season	
	Winter	Summer
1	1.60	1.66
5	1.40	1.44
10	1.29	1.34
20	1.19	1.22
30	1.11	1.15
40	1.05	1.08
50	0.99	1.02
60	0.93	0.97
70	0.88	0.92
80	0.83	0.87
90	0.76	0.79
95	0.70	0.73
99	0.60	0.64
N	65	76

Comparison of Tables 11 and 21 brings out another interesting feature. With the wide separation of target and control in Table 21, the target-control ratios are approaching the single-area ratios for winter and summer, and are much closer to the single-area values than to the optimum target-control ratios in Table 16.

Effects of Synoptic Storm and Precipitation Types

Other stratifications of the storm data were made according to precipitation type and synoptic storm type. With the single-area sampling (Arizona method), both types of stratification increased the background interference from natural variability in all groups from that obtained with all storms combined. That is, any advantage that may have accrued from the stratifications was more than offset by the deleterious effect of the smaller storm sample in the individual groups resulting from the stratifications.

In the cross-over target-control sampling tests, the effect of the stratifications was pronounced only in the case of air mass storms which were discussed previously. With this synoptic storm type, the natural variability factor is much larger than with frontal storms or low pressure centers, both of which showed variability effects similar to those obtained with all storms combined. Also, stratification of the target-control data according to precipitation type did not cause significant deviations from the relations obtained with all storms combined in Tables 16 and 17. In general, the results of both the single-area and target-control analyses indicate that stratification of the data according to synoptic storm or precipitation type is undesirable from the standpoint of statistical evaluation.

Fixed Target-Control Sampling

In past weather modification efforts, particularly those in which commercial cloud seeders were involved, fixed target and control areas were sometimes used. In the earlier study (Huff, 1966), evaluation of the natural variability effects with this method was made for the summer and growing season (May-September). In the present study, similar analyses were accomplished for the water supply replenishment period, October to April.

In the first hypothetical seeding experiment, the southwestern part of the East Central Illinois Network was used as the control and the northeastern part as the target. Results are shown for the water supply replenishment season, October-April, in Table 22, along with May-September results from the earlier study. Differences in seasonal precipitation are shown for each year, 2-yr moving totals, 5-yr moving totals, and for the 10-yr sampling period. This table indicates that substantial differences may exist between target and control due to natural variability for sampling periods of 1 to 2 years, but differences reduce to a small percentage for 5-yr periods. For the October-April period, differences were found to be generally small after a sampling period of 2 years was incorporated into the experiments. A similar hypothetical experiment performed on the southwestern and northeastern parts of the Little Egypt Network in southern Illinois for the 10-yr period, 1958-1967, gave very similar results. Again, the hypothetical experiments are indicative of minimum differences to be expected under midwestern climatic conditions, since the target and control are side by side. More detailed information on natural variability effects with increasing distance between target and control is contained in the earlier paper (Huff, 1966).

Summary and Conclusions

The primary purpose of this study was to provide quantitative data on natural precipitation variability which, in turn, may be utilized in the planning and design of cloud seeding experiments to establish the capability of producing rainfall increases during the crop growing season and/or those months during which water supply replenishment normally maximizes. The study was restricted to areas of county size or smaller for which network precipitation data were

Table 22. NE-SW percentage differences in seasonal precipitation on East Central Illinois Network.

Period	Difference (%) May-Sept.	Oct.-April
Number	Single Season	
1	-9	-1
2	+1	+1
3	+1	0
4	-1	0
5	+1	0
6	-10	+3
7	-10	+7
8	+15	+2
9	-4	-1
10	-5	-1
Median	5	1
	2-year moving totals	
1	-4	0
2	+1	0
3	-1	0
4	-1	0
5	-5	+2
6	-10	+6
7	0	0
8	+7	0
9	-5	-1
Median	4	0
	5-year moving totals	
1	-2	0
2	-2	+1
3	-5	+2
4	-2	+2
5	-2	+2
6	-3	+2
Median	2	2
10-Year	-3	0

available for accurate definition of the natural rainfall variability. For efficient agricultural application in periods of light to moderate drought, seeding capability on areas of this size must eventually be determined. Furthermore, many municipal water supplies are obtained from areas of this size or smaller.

Precipitation data from two dense raingage networks in Illinois were used to evaluate the effects of natural precipitation variability upon the verification of cloud seeding experiments. The effects of storm duration, areal mean precipitation, and storm types upon the background interference created by natural precipitation variability were investigated. This was done for both randomized sampling of a single area and target-control types of experiments to determine whether the influence of natural rainfall variability can be lowered significantly through various stratifications of the data.

Comparison of the effects of natural precipitation variability on the single-area and cross-over, target-control types of experiments indicates that the variability interference is appreciably less with the target-control experiments, as predicted by statistical theory, provided that the target and control are close together. As the distance increases, the superiority of the target-control method decreases. In the Illinois study, the superiority was relatively small when target and control were separated by 125 miles, the distance between the two dense raingage networks.

However, when tests of the natural variability effect on cross-over, target-control experiments were made on adjacent target and control areas (SW and NE halves of raingage network), the superiority of this method over the single-area randomizing was very substantial. For example, in the hypothetical seeding of all summer storms during the 5-yr period, 1960-1964, analyses indicated a 10% chance of an apparent increase of 30% due entirely to natural rainfall variability. With the cross-over, target-control tests, only an apparent increase of 7% was indicated at the 10-percent probability level. For year-around hypothetical seeding tests, the corresponding apparent increases were 19% and 3%, respectively. With adjacent target and control areas the contamination problem is acute, and some separation would undoubtedly be necessary under operational conditions. The results provided from the two networks used here provide estimates of the minimum and maximum effects of natural precipitation variability in target-control experiments.

Investigation of the effects of stratifying the precipitation data according to areal mean precipitation indicated some advantage in the single-area experiments and no significant advantage in the cross-over, target-control tests. Storm duration stratification was found to have a small effect on verification of seeding effects with both techniques. Seasonal stratification of data had a moderate influence.

In general, it was found that the data stratifications by decreasing the test sample size increased the natural variability effect and, therefore, intensified the problem of verifying seeding effects by statistical analyses. This was particularly true with the single-area technique in which interstorm variability is a stronger factor than in the cross-over, target-control method.

SPATIAL CORRELATIONS OF STORM, MONTHLY, AND SEASONAL PRECIPITATION

Introduction

The problem of accurately representing the spatial distribution of precipitation frequently arises in hydrologic investigations, weather modification experiments, and agricultural research. Until recent years, there was a great deficiency in the number of dense raingage networks with adequate length of records from which sampling requirements could be determined satisfactorily under various meteorological conditions. Limited studies performed in the past were concentrated primarily on relating sampling error to mean rainfall and size of sampling area to obtain estimates of gage density requirements.

In the Midwest, Light (1947) used a 38-storm sample from a network of 500 raingages on 8000 mi^2 in Ohio to evaluate effects on sampling error in the range from 500 to 8000 mi^2. However, he did not define the effect of storm rainfall amounts. Linsley and Kohler (1951) used a 68-storm sample from an Ohio network to derive an empirical equation relating sampling error to areal mean rainfall and number of gages on a fixed area of 220 mi^2. Huff and Neill (1957) used a sample of 300 storms from several dense networks in Illinois to obtain error relationships for areas of 25 to 400 mi^2 and rainfall amounts up to 5 inches in warm season storms. McGuinness (1963) used data from 81 storms collected on a dense network of 64 gages in an Ohio watershed of 7.16 mi^2 to obtain relations between sampling error, mean rainfall, and gage density. He further combined his results with those of previous investigators to construct a nomogram for estimating sampling errors in midwestern storms with gage density ranging from 0.1 to 1000 mi^2 per gage.

More recently, Hershfield (1967) used data from 15 heavy rainstorms on each of 23 densely gaged networks operated by the U. S. Department of Agriculture to investigate raingage spacing needs through use of spatial correlation patterns. From these patterns, based upon sampling periods of 3 to 7 years, he concluded that optimum gage spacing varies considerably depending upon the climatic regime, and that within a given sampling network the correlation between gages decreases faster in some directions than others, depending upon storm movement, topography, and other factors.

This section of the Final Report describes and summarizes the findings from an extensive investigation of sampling requirements in the establishment of precipitation measurement networks. The basic analytical approach involved the use of statistical correlation techniques. Data from three dense networks of raingages in Illinois were used to provide a range of measurements including 1-min and 10-min average rainfall rates, total storm rainfall, monthly precipitation, and seasonal precipitation. In the storm studies, analyses were made of the effects of season, synoptic weather type, precipitation type, storm intensity and duration, storm movement, number of rain cells, wind flow, and other factors in developing the correlation relationships.

Data and Analytical Procedures

Data for the 5-yr period, 1960-1964, from the East Central Illinois Network (ECIN) and the Little Egypt Network (LEN) in southern Illinois (Fig. 2) were used in the total storm analysis. As in all other studies, a storm was defined as a precipitation period separated from preceding and succeeding precipitation by 6 hours or more.

For the monthly and seasonal analyses, data from the entire 13-yr period of record, 1955-1967, on ECIN, and the complete 10-yr record, 1958-1967, on LEN were used to obtain the maximum possible sample size for analysis. In addition, 3142 minutes of data from 29 storms during 1952-1953 on the Goose Creek Network (GCN) of 100 mi^2 in central Illinois (Fig. 10c) were used to obtain correlation patterns for 1-min rainfall amounts, the best available estimate of instantaneous rainfall rates, and for investigating average 10-min rates. This special network, installed for radar-rainfall research, contained 50 recording gages with 12.6-inch orifices and 6-hr gears which permitted reading of 1-min amounts (Huff and Neill, 1956).

Initially, data from ECIN were used to evaluate the effect of data transformations on spatial correlation patterns. Evaluated were several transformations frequently used to normalize precipitation data, including the square root, fourth root, and logarithm of the precipitation. The effect of the transformations was inconsistent among the various data stratifications. No marked superiority was obtained in the spatial correlations with respect to pattern consistency and correlation decay with distance. Consequently, all correlation analyses presented in this paper were restricted to untransformed data.

In each network, rows of gages along the western and northern borders were used to obtain correlation coefficients in W-E and N-S directions. Also, correlation coefficients were calculated about the central gage in each network, in a NW-SE direction from the NW corner of each network, and in a SW-NE direction from the SW corner. These combinations were then used to determine directional effects upon spatial correlation which could result from topographical or climatic factors. For each directional analysis and each data stratification, isocorrelation maps were drawn. From these maps, the variation of correlation coefficient with distance was obtained through interpolation.

Total storm data were divided into the usual two seasonal groups, May-September and October-April. Next, within these two seasonal groups, the data were separated into three basic synoptic storm types through use of published synoptic weather maps of the U. S. Weather Bureau. Types included frontal storms, low center passages, and air mass storms. Analyses did not show substantial differences in the patterns associated with the various frontal types and squall lines, so all were combined in the frontal storm group.

Synoptic Storm Patterns

Fig. 9 shows correlation patterns about the central gage on ECIN in May-September storms associated with air mass instability, low center passages,

and fronts. These patterns were derived from 195 frontal storms, 73 air mass storms, and 28 low center passages. The differences in correlation are striking, especially between air mass storms and low centers. With low centers, the correlation coefficient exceeds 0.90 over the entire 400 mi^2, whereas in air mass storms it decreases to less than 0.60 at the southern edge of the network, 9 to 10 miles from the central gage. The correlation patterns indicate a general SW-NE orientation, although this tendency is less pronounced with air mass storms. Storms move most frequently across the network from SW or WSW (Huff, 1967a), and the correlation patterns are, of course, responsive to this climatological characteristic.

Rain Type and Rainfall Rate Patterns

The difference in correlation patterns between rainfall types is illustrated in Fig. 10 which shows isocorrelation maps about the central gage for May-September storms in which (10a) thunderstorms or rainshowers dominated and (10b) in which steady rain produced the surface precipitation. The two maps are quite comparable to those for fronts and low centers in Fig. 9. This is reasonable since most frontal storms occur with the TRW-RW combination, whereas steady rain is more likely to be associated with low center passages in the May-September period.

Fig. 10 also shows the average correlation pattern of 1-min rainfall rates about the most central gage on GCN. Most of these storms consisted of thunderstorms and rainshowers, and occurred during the warm season. Although not a completely representative climatological sample, these storms do provide a first approximation of the correlation decay with distance in the spatial distribution of instantaneous rainfall rates.

The general effects of various meteorological factors on the correlation decay with distance in storms are illustrated in Table 23 through the use of May-September data from ECIN. In this table, correlation coefficients are shown about the network's central gage. At the bottom of Table 23, relations are shown for the ungrouped storm data, and for 1-min and 10-min rainfall rates from the GCN data for comparison with grouped storm relations.

Storm Duration Effects

The storm duration relations in Table 23 are interesting. Correlation decay decreases with increasing duration with storms lasting up to 12 hours, then the trend reverses. Since this same behavior was observed in the ECIN October-April storms and on LEN, the reversal appears to be real rather than a sampling vagary present in this particular sample of storms. A possible explanation is that the long duration storms are usually associated with extensive synoptic storm systems, and storm movements across the network are more likely to shift during these lengthy storm periods as the weather system approaches and passes.

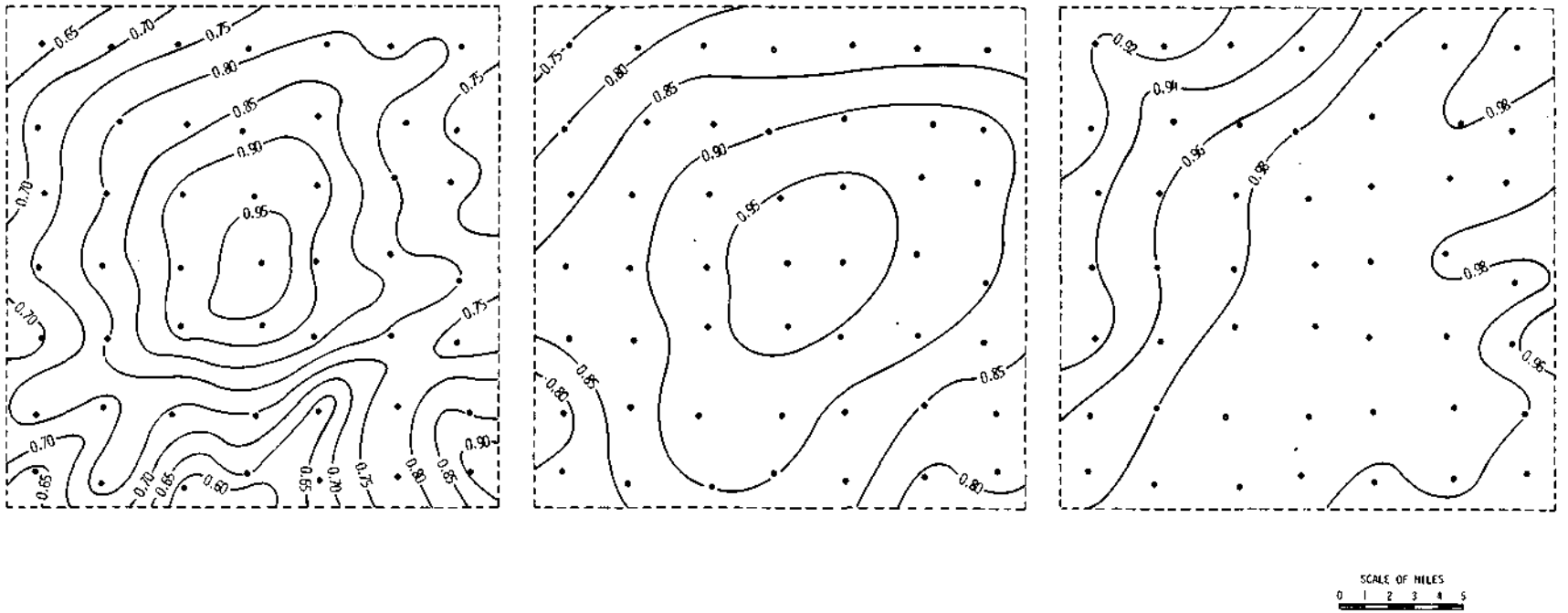

a. Air-mass storms

b. Frontal storms

c. Low centers

Figure 9. Correlation patterns of synoptic types in May-September storms on East Central Illinois Network.

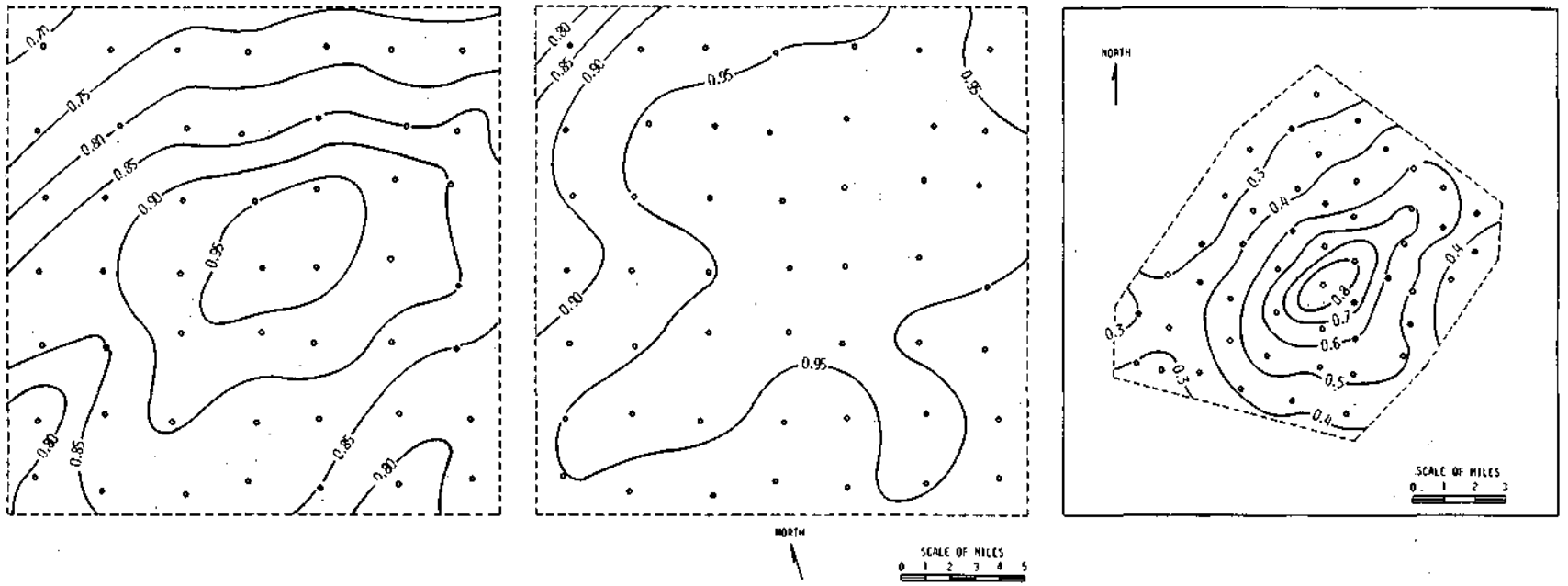

a. Thunderstorms and rainshowers b. Steady rain c. 1-minute rainfall rates

Figure 10. Correlation patterns associated with precipitation types and rain rates in warm season storms on East Central Illinois and Goose Creek Networks.

Table 23. Variation of correlation coefficient with distance about central gage in East Central Illinois and Goose Creek Networks during May-September storms.

		Average correlation coefficient for given distance (mi)					
Group	N	1	2	4	6	8	10
TRW-RW	249	0.98	0.96	0.92	0.88	0.85	0.82
R	33	0.99	0.98	0.96	0.94	0.93	0.92
Fronts	195	0.98	0.96	0.94	0.91	0.88	0.86
Low centers	28	1.00-	0.99+	0.99	0.98	0.97	0.96
Air mass storms	73	0.97	0.94	0.87	0.79	0.76	0.74
≤ 3 hr	184	0.96	0.91	0.82	0.75	0.70	0.65
3.1-6.0 hr	61	0.97	0.95	0.90	0.86	0.81	0.76
6.1-12.0 hr	29	0.98	0.96	0.93	0.91	0.89	0.87
12.1-24.0 hr	19	0.97	0.95	0.82	0.72	0.69	0.66
0.01-0.10 in	111	0.96	0.93	0.90	0.88	0.87	0.82
0.11-0.25 in	53	0.46	0.22	0.05	-0.02	-0.06	-0.10
0.26-0.50 in	33	0.86	0.69	0.32	0.11	0.06	0.03
0.51-1.00 in	36	0.84	0.68	0.38	0.22	0.12	0.06
> 1.00 in	19	0.96	0.93	0.88	0.82	0.77	0.71
Ungrouped storms	296	0.98	0.96	0.93	0.89	0.86	0.84
1-min rain rate (Goose Creek)	3142	0.77	0.60	0.40	0.31	----	----
10-min rain rate	2829	0.76	0.61	0.44	0.38	----	----

Mean Rainfall Relations

The mean rainfall groupings in Table 23 indicate that average precipitation within a sampling area has very little effect upon point-to-point correlations. The trend of correlation is very erratic with increasing mean rainfall, and is relatively low in three of the five data groups. Erratic trends and relatively low correlation coefficients were also found during the October-April period and on LEN for both seasons.

Standard Error of Correlation Coefficients

The standard error of the correlation coefficients in Table 23 were calculated to provide a measure of the reliability of the relations presented. For ungrouped storms, the standard error increased gradually from 0.002 at 1 mile to 0.02 at 10 miles. With the TRW-RW stratification, a similar distribution was obtained. The standard error increased slightly with the relatively small sample of steady rains (R) for which it reached a maximum of 0.03 at 10 miles.

In the synoptic weather stratifications, the largest standard error occurred with air mass storms in which it increased from approximately 0.01 at 1 mile to 0.05 at 10 miles. In the duration groupings, the maxima occurred at 10 miles with values of 0.04, 0.05, 0.05, and 0.13, respectively, progressing from the shortest to longest duration groups. In general, the standard errors calculated for the various groupings were relatively small; therefore, the average relations presented in Table 23 are considered valid and representative of correlation decay in May-September storms under the climatic conditions prevailing in the sampling areas.

Directional Effects

The directional effect on storm rainfall correlations is illustrated in Table 24 through use of May-September data from ECIN. In this table, average correlation coefficients are shown for distances up to 20 miles when the correlations are calculated in each of four directions. With increasing distance, W-E correlations are consistently higher than the N-S values, and explain 10-12% more of the variance at distances of 10-15 miles. The SW-NE correlations are very close to the W-E values and the NW-SE correlations are similar to the N-S group. The slightly better correlations with the W-E and SW-NE groups reflect the more frequent movement of storms from these directions compared with the other two directional groups. Similar May-September relations were found on LEN. In the October-April period, the directional differences were even smaller than in the May-September period on both networks. Overall, this phase of the analyses indicates a slightly greater sampling density is required in the N-S and NW-SE directions to maintain an equivalent measurement error in isohyetal patterns of total storm rainfall throughout a given sampling area.

The lower part of Table 24 shows the average spacing of raingages required in W-E and N-S directions to maintain selected levels of variance explained. These statistics were calculated from the relations shown in the upper part of the table. They may be used as a guide if one wishes to maintain equivalent measurement accuracy in various directions within a sampling area.

Raingage Spacing Requirements

Table 25 provides a general summary of raingage spacing required on a grid pattern to achieve various degrees of average correlation (r) and, in turn, percentages of explained variance (r^2) under various conditions. The relations are based upon weighted averages of the correlation coefficient obtained in the directional analysis. The 1-min rainfall rate values are based upon interpolation of the correlation decay curve, since the average network spacing was 1 gage per 1.4 mile and the average correlation coefficient had decreased to approximately 0.7 at this distance from correlated points. Also, curve interpolation was involved in obtaining the values for some of the higher correlations in the other groupings because of the limiting gage spacing on the networks. A limiting distance of 20 miles has been used in the calculations because of the network sizes.

Table 24. Directional effect on correlation decay with distance in ungrouped May-September storms on East Central Illinois Network.

	Average correlation coefficient for given distance (mi)							
Direction	2	4	6	8	10	12	15	20
W-E	0.96	0.93	0.90	0.88	0.86	0.84	0.81	0.77
N-S	0.96	0.91	0.87	0.83	0.79	0.76	0.74	0.72
NW-SE	0.96	0.92	0.88	0.84	0.80	0.77	0.75	0.71
SW-NE	0.94	0.91	0.89	0.87	0.85	0.83	0.79	0.73

	Spacing (mi) for given direction	
Variance explained (%)	W-E	N-S
90	2.7	2.2
80	6.0	4.5
70	12.4	7.8
60	19.6	11.3
50	20	20

Earlier discussion showed a directional bias in correlation, depending upon frequency of storm movements. However, it was assumed in preparing Table 25 that most users are interested in the average accuracy of storm measurements combining all directions. In this case, the grid pattern would be most suitable and raingage spacing could be based upon directional averages, such as used in Table 25. Directional differences in correlation in Illinois storms (Table 24) were found to be relatively small so that the averaging process is probably acceptable for most purposes.

In the October-April storms of Table 25, snow (S) has been shown only for ECIN because of (1) the different editing and analytical procedures used on LEN which consisted of both recording and non-recording gages, and (2) the relatively small sample of snow storms on this southern Illinois network. Snow is usually a stable type of precipitation in the ECIN area, and correlations of its water equivalent would be expected to be similar to those for steady-type rain (R). However, the snowfall is frequently accompanied by strong, gusty winds. As a result, the measurement accuracy is very poor with recording raingages, and this is reflected in the spacing requirements of Table 25 which are similar to those for May-September air mass storms. Thus, the ECIN snow data provide a measure of the sampling errors associated with wind-driven snows when recording gages are used for depth measurements.

The deterioration in sampling accuracy with snowfall is brought out further by the small sample of R + S mixed that occurred on ECIN. As shown in Table 25, the sampling requirements are intermediate between those of steady rain and snowfall.

As expected, Table 25 shows that a substantially greater density of raingages is needed in the warm season (May-September) than in the colder months of the year (October-April) to maintain a given level of explained variance. For example, assume one wishes to install a network with a raingage spacing that will explain 90% of the storm variance, on the average, combining all types of storms. Then, reference to the "all storms" columns shows that a gage spacing of 2 miles is needed in May-September compared with 6 miles during October-April. If the user is concerned with a similar accuracy in the measurement of air mass storms, the spacing would be 1 mile. However, if a project is concerned only with measurements during the passage of low centers, a spacing of 8-10 miles would be adequate to achieve an explained variance of 90% in Illinois storms.

Table 25. Average storm relation between raingage spacing and correlation coefficient.

May-September storms

r	r^2 (%)	All storms	TRW, RW	R + RW	R	Lows	Fronts	Air mass	1-min rates
			Spacing (mi) for given correlation						
0.95	90	2	2	3	10	10	2	1	0.2
0.90	81	5	4	7	>20	>20	5	3	0.4
0.85	72	8	7	15			9	5	0.6
0.80	64	12	10	>20			13	7	0.8
0.75	57	17	14				18	9	1.0
0.70	49	>20	>20	___	___	___	>20	13	1.2
Number of storms		629	544	33	50	62	410	157	29

October-April storms

r	r^2 (%)	All storms	TRW, RW	R, R + RW	Lows	Fronts	ECIN S	ECIN R + S
			Spacing (mi) for given correlation					
0.95	90	6	5	13	8	4	1	2
0.90	81	18	10	>20	>20	13	2	8
0.85	72	>20	15			>20	4	13
0.80	64		20				6	>20
0.75	57						11	
0.70	49	___	___	___	___	___	20	___
Number of storms		654	267	188	310	305	90	28

Wind Flow and Rainfall Orientation Effects

As part of another study, average wind flow in the lower 500 mb of the atmosphere had been determined for 1960-1964 summer storms on LEN. These data provided a convenient means for investigating whether correlation decay is influenced significantly by the wind movement in the lower atmosphere which should, of course, exert some control on storm movements across the network. This knowledge should be useful in the planning and statistical evaluation of weather modification experiments.

Results of the wind movement analysis are summarized in Table 26. Here, the average correlation coefficient (r) change with distance, based upon an average in all directions, is shown for all summer storms combined. This provides an estimate of the average correlation decay with distance for a square grid pattern of raingages. The percentage of the variance explained (r^2) by these correlation coefficients is also shown. Then, the difference in explained variance between the grid pattern and each wind movement is presented to provide an estimate of the improvement (or deterioration) obtained with wind stratification of the data from synoptic weather maps.

Table 26 shows appreciable improvement in r^2 in four of the six directions for which there were sufficient data to calculate correlation coefficients. Only wind flow from NW showed decreased correlation. The increase in correlation was greatest with SW flow with which a 30% improvement in r^2 was achieved at the greater distances. The decreases with NW winds may be related to the tendency for these storms (usually post-frontal) to be relatively small in areal extent, frequently affecting only a portion of the network. Overall, Table 26 shows variable results from wind stratification but indicates some advantage in using this procedure in weather modification experiments and other applied research since improvement was obtained in most cases.

Calculations of the standard error of differences between two correlation coefficients were made between the coefficients for all storms combined and each of the directional groups in Table 26. This was done to obtain an estimate of the strength of the relations presented in this table. The differences between the coefficients for all storms and those with SW wind flow were found to be significant at the 95-% level at all distances. The differences associated with WNW and WSW winds were significant at the 95-% level for distances up to 8 miles and 10 miles, respectively. Differences did not reach the 95-% level of significance with the other wind directions. Relatively large standard errors in correlation coefficients were obtained with S-SSW and NW winds. Thus, the results of Table 26 should be interpreted with caution, particularly for those directions with the smallest samples (S-SSW, WNW, NW).

In an effort to determine why large improvements in correlation were not obtained consistently with wind stratification, calculations were made of the frequency with which the major axis of the network rainfall was in the mean direction of the wind flow in the lower atmosphere. Only 22% of the rainfall patterns were found to have their major axis parallel (±10°) to the wind movement, whereas 30% were over 10° to the right of the wind axis, 32% over 10°

to the left, and 16% had complex patterns that provided no distinct storm orientation. With NW winds, less than 20% of the storms moved parallel to the wind axis. The common cross-wind movement of the rainfall patterns helps to explain the inconsistencies of Table 26.

Table 26. Effect of wind flow on spatial correlation in summer storms.

	Number of storms	Distance (mi) from sampling point						
		2	4	6	8	10	15	20
		All storms combined						
r	210	0.92	0.86	0.81	0.77	0.74	0.68	0.64
r^2 (%)	210	85	74	66	59	54	46	41
Mean wind flow		Difference (%) in variance explained between ungrouped and wind stratified storms						
S-SSW	17	+5	+7	+7	+12	+13	+15	+12
SW	35	+9	+16	+20	+22	+28	+30	+31
WSW	69	+7	+11	+10	+11	+10	+9	+8
W	44	+1	+2	0	0	-1	-1	+1
WNW	23	+7	+11	+13	+15	+14	+12	+9
NW	22	-4	-8	-10	-10	-10	-10	-12

The orientation of the surface rainfall pattern provides a measure of the direction of storm movement across a sampling network. Therefore, the summer storms on LEN were used to determine correlation coefficients parallel to the major axis of storms. This resulted in a substantial improvement over the wind-stratified correlations. The degree of improvement is illustrated in Table 27 which shows r and r^2 (%) for W-E oriented rainfall patterns and wind flow. The explained variance increased by 15-20% beginning at the 6-mile distance. The correlation coefficient decreased to 0.90 at 3 miles in the wind-oriented correlations compared with 6 miles for the rainfall orientation.

Summer Patterns

A further division of the growing season (May-September) was made to investigate correlation patterns in the three summer months of June through August. These months are the most important from the standpoint of Illinois crops, and are months in which very intense and frequently spotty rainstorms occur. Fig. 11 shows the relation between average correlation coefficient and distance on the two sampling networks in central and southern Illinois. The correlation decay was greater on LEN which climatically receives a larger portion of its summer rainfall from scattered air mass storms (Huff, 1966). Except for the summer months, the correlation patterns were very similar on both networks.

Table 27. Comparison between W-E wind-oriented and W-E rainfall-oriented correlation patterns.

	Number of storms	Distance (mi) from sampling point 1	2	4	6	8	10	12	15	20
		Correlation coefficent								
Wind	44	0.97	0.93	0.87	0.81	0.76	0.73	0.70	0.67	0.65
Raindfall	49	0.98	0.96	0.93	0.90	0.87	0.85	0.83	0.81	0.78
		Variance explained (%)								
Wind	44	94	86	76	66	58	53	49	45	42
Rainfall	49	96	92	87	81	76	72	69	66	61

Monthly and Seasonal Relations

For some purposes, knowledge of the spacing requirements for the measurement of monthly and seasonal precipitation is of primary interest. Table 28 shows monthly and seasonal correlation relations for May-September on LEN and ECIN, obtained through averaging of the several directional patterns which showed only small differences. The two networks were not combined because of appreciable differences at the longer distances. Ungrouped storm relations have been included in the table for comparison purposes.

Table 28. Average storm, monthly, and seasonal correlations for May-September.

	Number of cases	Average correlation coefficient at given distance (mi) 2	4	6	8	10	12	15	20
ECIN monthly	65	0.94	0.89	0.86	0.83	0.80	0.78	0.75	0.72
LEN monthly	58	0.96	0.94	0.92	0.90	0.89	0.88	0.87	0.85
ECIN seasonal	13	0.94	0.91	0.88	0.86	0.85	0.84	0.82	0.79
LEN seasonal	10	0.96	0.92	0.90	0.89	0.88	0.87	0.86	0.84
ECIN ungrouped storms	296	0.96	0.92	0.89	0.86	0.83	0.80	0.77	0.74
LEN ungrouped storms	333	0.95	0.91	0.87	0.84	0.81	0.78	0.76	0.74

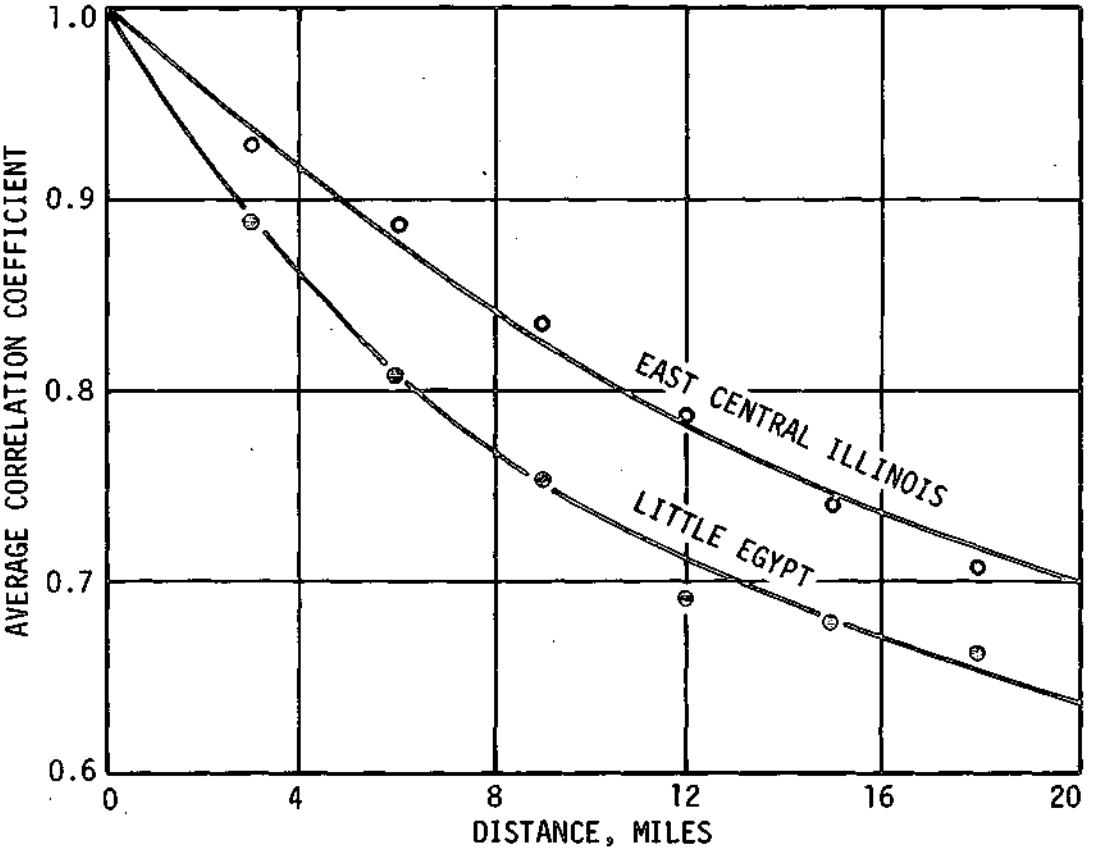

Figure 11. Comparison of summer correlations on East Central Illinois and Little Egypt Networks.

For both monthly and seasonal rainfall, the correlation decay with distance was less on LEN. Analyses of the standard error of difference between two correlation coefficients were applied to the monthly and. seasonal data of Table 28. The differences were significant at the 95-% level for the monthly correlations. However, at most of the distances, the 95-% significance level was not reached with the seasonal comparisons. These statistical calculations indicate climatic differences may exist in the monthly rainfall patterns between the two networks, at least for certain months. The decrease in correlation differences with seasonal totals suggests that, if climatic differences are sufficient to substantially influence the monthly correlation patterns, the effect maximizes in certain months.

Overall, large differences did not exist between storm, monthly, and seasonal correlation relations so that a total storm sampling network would satisfy sampling for all periods. There would be little economic benefit in differentiating between total storm, monthly, and seasonal raingage spacing requirements, especially if a relatively high degree of accuracy is desired in all three measurements.

Summary and Conclusions

Data from the three networks, which ranged in size from 100 to 550 mi^2, provided measurements ranging from 1-min rates through total storm precipitation to monthly and seasonal totals. Spatial correlation patterns were established for the data grouped according to season, precipitation type, synoptic weather type, storm intensity and duration, storm movement, and other factors. The results obtained from this study should be generally representative of the Midwest and other areas with similar precipitation climates.

Correlation decay with distance, used to indicate sampling requirements for establishing rainfall patterns, was greatest in storms associated with thunderstorms, rainshowers, and air mass storms. Conversely, minimum decay occurred with steady rain and the passage of low pressure centers. Seasonally, the correlation decay with distance in storms was much greater in the growing season, May-September, than during the October-April period when water supply replenishment normally maximizes. For 90-% explained variance, on the average, in all storms combined, a gage spacing of 2 miles is needed in the warm season compared with 6 miles in the cold season. However, if similar accuracy is required in air mass storms, the gage spacing must be decreased to 1 mile. If measurements are to be made only in low center passages, a spacing of 8-10 miles is adequate for the above accuracy level.

Spatial correlation increased, on the average, with increasing duration in storms lasting up to approximately 12 hours, after which a reversal in this trend occurred. Erratic trends were found when the storms were grouped according to network mean precipitation. General improvement in correlation occurred when the storms were grouped by wind direction and storm movement.

Directionally, slightly higher correlations were obtained in W-E and SW-NE directions compared with those made in N-S and NW-SE directions across

the networks. Large differences were not found between total storm, monthly, and seasonal correlation relations, so that a total storm sampling network should satisfy sampling needs for all of these periods. However, sampling requirements are much greater when the measurements of rainfall rate are needed. For example, with a minimum acceptance of 75-% explained variance between sampling points, a gage spacing of 0.3 mile is needed for 1-min average rates compared with 7.5 miles for total storm rainfall in warm season storms.

CORRELATION OF STORM MEAN PRECIPITATION BETWEEN ADJACENT AREAS

Introduction

As another aid in the determination of sampling requirements for weather modification experiments, analyses were made of the correlation of storm mean precipitation between contiguous and separated sampling areas. Data for the 5-yr period, 1960-1964, were used in the study.

The contiguous sampling areas were the southwestern and northeastern halves of the 400-mi^2 network (Fig. 1) described earlier in this report. The centers of these contiguous areas are approximately 14 miles apart. Several methods of stratifying the precipitation data were investigated to evaluate seasonal and meteorological effects on the degree of correlation. The analyses were restricted to storms in which the areal mean equalled or exceeded 0.01 inch on the 400-mi^2 network.

Correlation coefficients were determined between the 400-mi^2 network and the Boneyard urban network of 10 mi^2 (Fig. 1) to obtain a measure of the change in correlation of storm mean precipitation with increasing distance between areas. The centers of these networks are approximately 30 miles apart in a west-east direction, and their closest boundaries are separated by approximately 16 miles.

Analyses and Results

First, all storms in the 5-yr sample on the two adjacent areas of 200 mi^2 were correlated to obtain a measure of the relationship when all types of weather conditions and precipitation characteristics are combined. Then, the storms were divided into two seasonal groups, May-September and October-April. For each season, correlation analyses were performed for all storms combined, and for two areal means groups separated at 0.50 inch. This was done to obtain a generalized measure of the effect of precipitation volume on the correlation between the adjacent 200-mi^2 areas. Next, the May-September data were divided further into smaller groups of network means, as shown in Table 29, to explore the effect of storm rainfall volume in more detail.

Table 29. Correlation of storm mean precipitation between SW and NE parts of 400 mi^2 network, 1960-1964.

Storm means	Correlation coefficient	Variance explained (%)	Number of storms
1. All Storms ≥ 0.01 inch	0.96	92	513
2. May-September ≥ 0.01 inch	0.94	89	234
3. May-September = 0.01-0.50 inch	0.78	61	177
4. May-September > 0.50 inch	0.87	76	57
5. October-April ≥ 0.01 inch	0.99	98	279
6. October-April = 0.01-0.50 inch	0.97	94	232
7. October-April > 0.50 inch	0.96	92	47
8. May-September = 0.01-0.10 inch	0.51	26	92
9. May-September = 0.11-1.00 inch	0.79	62	121
10. May-September > 1.00 inch	0.86	74	21
May-September storm duration (hours)			
1. ≤ 3	0.88	77	127
2. 3.1 - 6.0	0.89	79	56
3. 6.1 - 12.0	0.92	85	30
4. 12.1 - 24.0	0.91	83	18
May-September rain type			
1. TRW and RW	0.93	86	178
2. R	0.99	98	24
May-September storm type			
1. Air Mass	0.88	77	53
2. Fronts	0.94	89	160
3. Low Centers	0.99	98	21

The effect of storm duration was investigated through use of the May-September storms grouped into the classes listed in Table 29. Also, the effect of rain type and synoptic storm type were investigated.

It should be remembered that the correlation analyses discussed here are concerned with areal mean precipitation, whereas in the previous section the analyses were concerned with correlation of point precipitation with increasing distance. Consequently, the effects of the data stratifications according to mean precipitation, storm duration, rain type, and synoptic storm type are not necessarily the same.

Results of the study of contiguous areas are summarized in Table 29 which shows the correlation coefficient, variance explained (%), and number of storms for each data group used in the study. Under the groupings by storm means, correlations are considerably higher in the October-April period than in the May-September period for similar data stratifications. The additional groupings for May-September indicate that the correlation between adjacent areas increases substantially with increasing mean precipitation in the sampling region. This finding is related to the greater spottiness in the rainfall distribution from light showers.

Table 29 shows a weak trend for the correlation to increase with increasing length of storm. However, the standard errors of estimate of the correlation coefficients of the longer durations (6-24 hr) are approximately equal to their difference in correlation from the shortest duration (≷ 3 hr).

Substantial differences are indicated between the two rain types and between the three synoptic storm types of Table 29. As expected, air mass storms show the weakest correlation, and low center storms have the highest correlation among synoptic types. Steady rains correlate somewhat better than the shower types (TRW, RW).

Correlation coefficients between the separated areas are shown in Table 30 for all May-September storms in each year of the 1960-1964 period. This table serves two purposes. First, it illustrates how the degree of correlation between mean rainfall on two nearby areas may vary substantially between years. Secondly, when compared with Table 29, it shows the effect of increasing distance on the correlation of storm mean rainfall.

Table 30. Correlation of storm mean precipitation between separated areas.

Year	Correlation coefficient	Variance explained (%)
1960	0.82	67
1961	0.80	64
1962	0.81	66
1963	0.64	41
1964	0.96	93
Average	0.81	66
Median	0.82	66
1960-1964 combined	0.77	60

Table 30 shows a 1960-1964 overall correlation coefficient of 0.82 and 66% of the variance explained between the separated areas. For the contiguous areas (Table 29, item 2), the equivalent numbers are 0.94 and 89%. Thus,

there was a decrease in the explained variance of 23% when the distance between areal centers increased from 14 to 30 miles.

Conclusions

The results indicate that correlation of mean storm precipitation between nearby areas is considerably better in the October-April period than in the May-September period. Stratification of precipitation according to areal mean rainfall may be desirable in the growing season period for establishing verification procedures in weather modification. However, there appears to be no significant advantage in doing so in the colder part of the year, according to the correlation analyses performed here.

Also, there appears to be little gained by grouping according to storm duration, but the results provide some support for grouping by synoptic weather and rainfall types. Air mass storms, which are frequently small in areal extent and widely variable in rainfall intensity, do not correlate as strongly between adjacent sampling areas as frontal storms and low center passages, which characteristically encompass larger areas than air mass showers.

An example of the verification problem in weather modification experiments during the growing season is brought out by the correlation comparisons between the contiguous and separated areas. The time variation in the background interference from natural rainfall variability is demonstrated also by the yearly variations in the degree of correlation between the separated areas. These yearly differences further emphasize the problem of verification in short-term experiments and the necessity for extreme caution in the interpretation of statistical data from such experiments.

NATURAL VARIATION OF POINT PRECIPITATION WITH DISTANCE

Introduction

Definition of natural rainfall gradients, along with other characteristics of the surface rainfall distribution, is useful in the planning and evaluation of rain modification experiments in which surface rainfall measurements are employed to verify the results of cloud seeding. It has been the author's experience that many users of rainfall data are aware that extreme variability may occur, but they have little factual knowledge of the actual magnitude of rainfall gradients.

Several studies have been made in recent years in Illinois to provide quantitative information on rainfall gradients in midwestern storms for those involved in weather modification and for other scientists and engineers who may have use for such data. Huff (1967b) presented relationships for rainfall gradients of total storm rainfall in warm season storms. Huff, Shipp, and

Schickedanz (1969) investigated rainfall gradients of rainfall rate in warm season rainfall through use of 1-minute rainfall amounts from a special network of raingages. This data provided a close approximation of the instantaneous pattern of rainfall rates, and, thereby, yielded considerable information on the rate structure in such storms.

The reader is referred to the above publications for details on the two studies. Here, we are concerned primarily with reporting the results of a recent study of gradients in monthly and seasonal precipitation. Along with the earlier studies, these results provide quantitative estimates of precipitation gradients in Illinois and other regions of the Midwest for time intervals ranging from one minute to several months. These studies certainly do not answer all of the questions which users may have, but they do add to our basic knowledge on the natural distribution of precipitation.

Approach Used in Monthly Analyses

The basic source of data was monthly isohyetal maps prepared from data collected during the 1955-1966 period on the 400-mi^2 network (Fig. 2). Gage 25 at the center of the network was designated as the comparison gage. A circular overlay centered at the comparison gage was placed over each map. Amounts were then read at 1-mile intervals at 8 points of the compass to obtain a representative sample about the comparison gage. Next, the 8-direction average was tabulated for each interval. A range of 10 miles about the comparison gage was provided by the network.

In the analyses, the monthly data were divided into two groups. The first included the growing season months of May through September, and the second contained the months of October through April.

For each seasonal grouping, the monthly precipitation was grouped further according to total amount at the comparison gage. At each distance interval, the difference of the 8-point average from the comparison gage was determined in both inches and percent. The comparison gage amounts were divided into monthly totals having (1) less than 2.00 inches, (2) 2.00-3.99 inches, and (3) 4.00 inches or more. The sample size was not considered adequate for a more detailed division according to monthly precipitation. The above groupings provide estimates for months with relatively light, moderate, and heavy precipitation in the experimental area.

Results of Monthly Analyses

Results of the monthly analyses are summarized in Figs. 12-13. In these figures, the solid curves show the average difference from the comparison gage in percent with increasing distance. The extreme gradients (dashed lines) are defined by the upper 95% confidence band (2 standard deviations). Because differences were small and exhibited an erratic trend, the October-April curves for monthly precipitation of less than 2.00 inches and 2.00-3.99 inches have been combined. Examination of U. S. Weather Bureau monthly normals for 1931-1960

indicate maximum climatic differences of less than 5% in monthly precipitation in the 10-mile radius about the comparison gage. Maximum differences occur at 8-10 miles. Because of the small climatic differences, no effort has been made to correct the curves for climatic variation across the network.

Fig. 12 shows relations for the growing season months of May through September when thunderstorms and rainshowers produce most of the precipitation. Consequently, spatial relative variability is relatively large but tends to decrease with increasing precipitation (Huff and Shipp, 1968). This is reflected in the curves which show a general trend for the percentage differences to decrease as the monthly total at Gage 25 increases.

However, Fig. 13 for the months of October through April shows the opposite trend. Reference to data for individual months showed that this trend results primarily from the dominance of steady-type precipitation in the late fall and winter months which contribute a majority of the samples in the light precipitation group (less than 2 inches). Conversely, the months with relatively heavy precipitation (4 inches or more) result primarily from unstable types of precipitation (TRW, RW) whether they occur in fall, winter, or early spring. Therefore, spatial relative variability tends to be large. Although heavy precipitation shows larger differences in the cold season months than in the growing season, it only contributes 17% of the total October-April cases compared with 30% of the May-September months.

The major difference in the monthly precipitation gradients between the growing and cold seasons is with the relatively light amounts (less than 2 inches). Here, the growing season exhibits substantially larger gradients. From the extreme gradient curves it is apparent that total monthly precipitation does not exert a strong control on the variation of point rainfall with distance from a sampling point. Furthermore, correlation analyses indicated relatively low correlation between the variation of precipitation with distance (D) and both monthly precipitation (P) and distance between points (M). Simple and multiple correlation coefficients are shown in Table 31.

Table 31. Correlation coefficients between D, P, and M in monthly precipitation.

Season	D - P	D - M	D - P,M
May - September	0.44	0.23	0.53
October - April	0.61	0.17	0.63

The multiple correlation coefficients indicate only 28% of the variance explained by P and M in the growing season months and 40% in the cold season. A major cause of the low correlation is that the monthly precipitation gradients are determined by the areal storm patterns, particularly the heavy storm patterns. Consequently, the monthly summation of these patterns can produce a relatively large range of differences with distance from a given sampling point (raingage) in specific months, although long-term means over the sampling area may be similar.

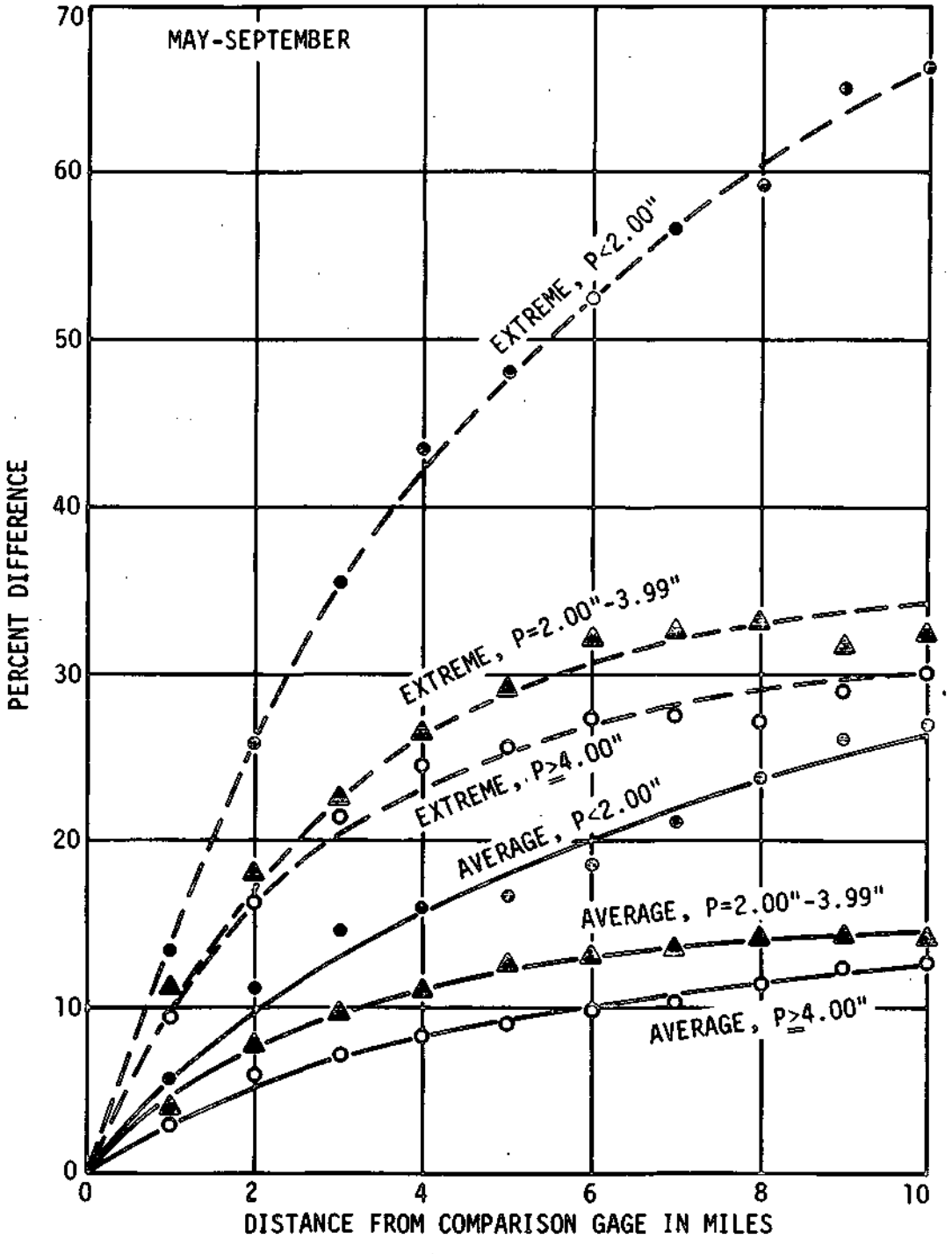

Figure 12. Variation of monthly precipitation with distance in May-September period.

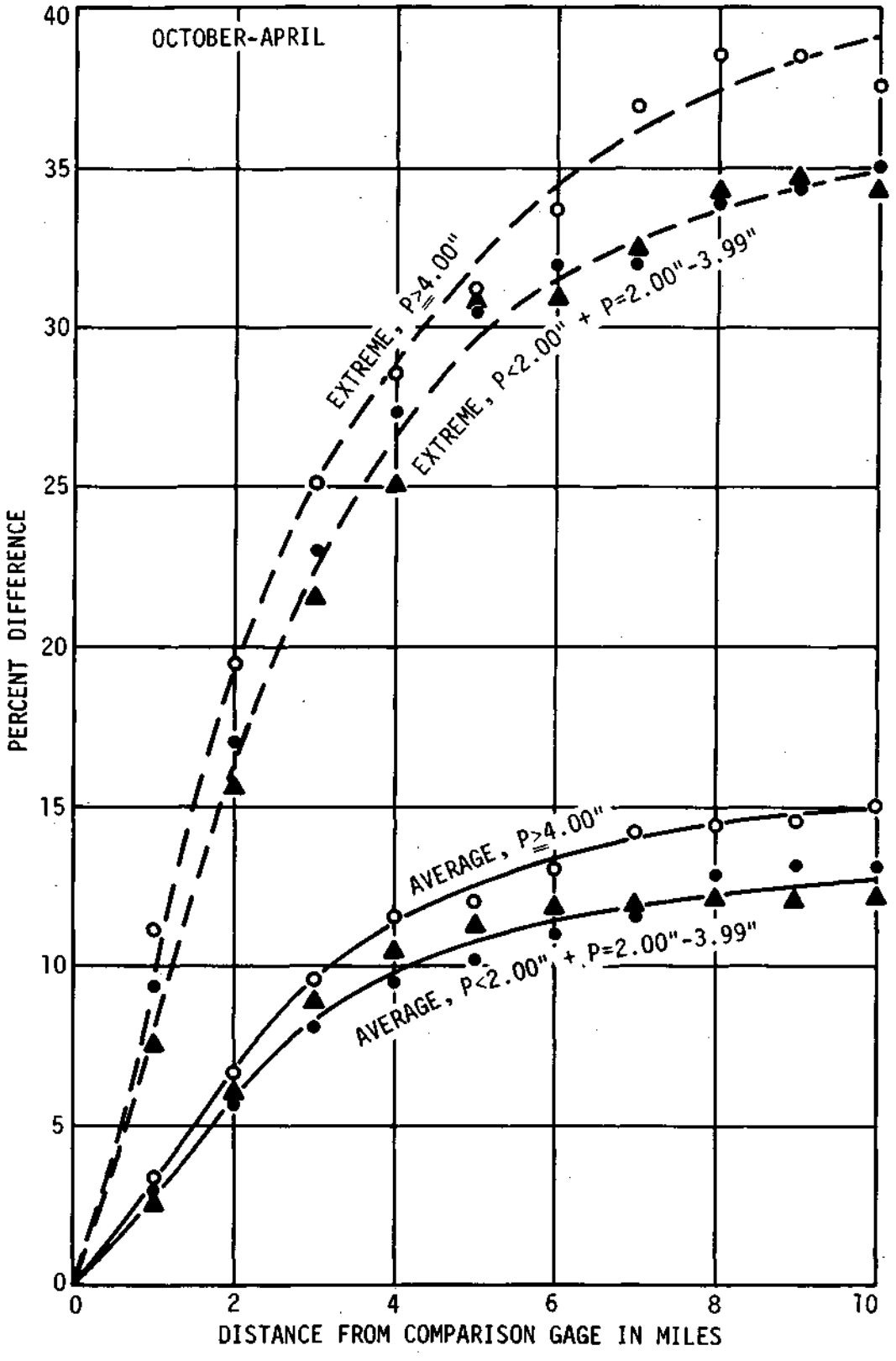

Figure 13. Variation of monthly precipitation with distance in October-April period.

Figs. 12-13 provide quantitative information on the natural variation of monthly point rainfall with distance, and, consequently, provide guidance for establishing sampling networks for various purposes in Illinois and areas of similar climate and topography. The necessity for dense networks to determine small changes in precipitation with distance in specific months is apparent from these curves. For example, they indicate that the average monthly difference during the growing season reached 10% at a distance of approximately 2 miles for monthly totals less than 2 inches at the comparison gage and at 3 miles for amounts of 2.00-3.99 inches. However, the extreme gradient curves indicate that the difference with all monthly amounts may occasionally exceed 10% at ranges of 1 to 2 miles from a raingage.

Seasonal Analyses

Seasonal totals for the 5-month growing season, May-September, were used to obtain a measure of the point rainfall gradient on a seasonal basis. Results are summarized in Fig. 14. All data were combined, since there were 12 complete samples with equivalent gage density, and plotting of the data indicated an erratic trend between seasonal total precipitation and variation with distance. As expected, the percentage variation in precipitation with distance from the comparison gage decreased substantially from that in monthly precipitation. In the 12-yr period sampled, the average percentage variation with increasing distance remained essentially constant after reaching a value of 6% at 3 miles. However, the extreme gradient curve shows the typical increasing variation with distance.

For comparison purposes, Tables 32 and 33 obtained from the earlier studies of storm rainfall gradients (Huff, 1967b) and rainfall rate gradients (Huff, Shipp, and Schickedanz, 1969) are presented. Used in conjunction with Figs. 12 and 13, they provide information on the natural variation of rainfall with distance, on the average, as the time integration increases from one minute to a 5-month season. For example, the average percentage difference in point rainfall rates 2 miles apart with a moderate summer rate of 0.50 inch/hour is 63% (Table 32). With a moderate monthly rainfall of 3.50 inches in the May-September period, the average difference at 2 miles is only 8% (Fig. 12). The seasonal curve for May-September (Fig. 14) shows a 2-mile average difference of 5%.

Table 32. Average variation of 1-minute rainfall rates with distance.

Starting point rate (inches/hour)	Average difference (%) for given distance (miles)				
	1	2	3	4	6
0.1	64	74	78	81	87
0.2	61	69	74	78	82
0.5	56	63	67	71	75
1.0	52	58	62	65	69
2.0	49	54	57	60	64
5.0	45	49	52	55	58

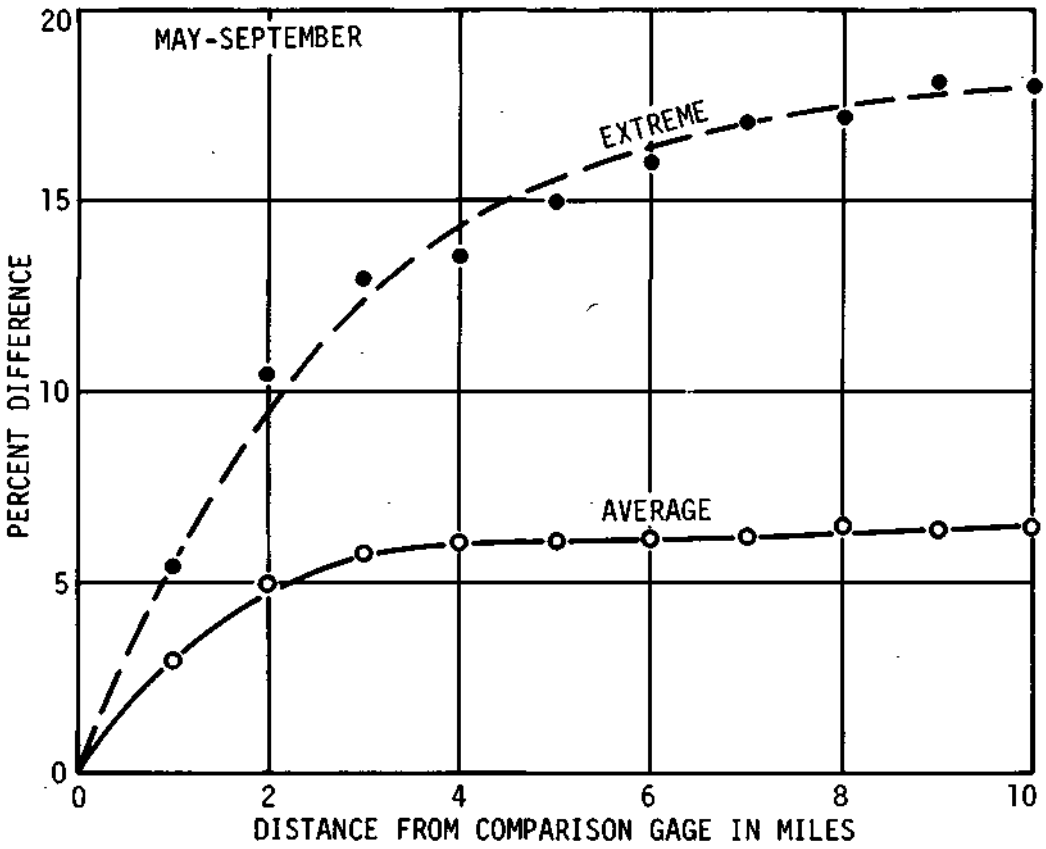

Figure 14. Variation of seasonal precipitation with distance.

Table 33. Average variation of storm rainfall with distance in warm season storms.

Starting point rainfall (inches)	Average difference (%) for given distance (miles)				
	1	2	3	4	6
0.10	60	81	92	100	>100
0.25	28	40	46	52	57
0.50	19	25	30	32	36
1.00	13	18	20	22	26
2.00	10	14	16	18	21

Conclusions

The development of monthly and seasonal relationships for estimating precipitation gradients in the Midwest, along with the results of earlier studies of total storm rainfall and 1-minute rainfall rate gradients, provide background knowledge of natural spatial variations that should be useful in the establishment of weather modification verification programs. This knowledge should also be of interest to climatologists, hydrologists, agriculturists, and others concerned with the establishment of rainfall measurement networks.

Extremely dense raingage networks would be required to measure accurately the spatial distribution of instantaneous rainfall rates. The operation, data collection, and data reduction would be extremely difficult with an adequate network of gages extending over hundreds or thousands of square miles as would be required in most weather modification projects. Unless radar can be adapted to the measurement of rainfall rates, the rate parameter is not too promising as an evaluator of weather modification effects through quantitative comparisons of rainfall intensity patterns or point intensities in seeded and non-seeded situations. Areal comparisons are treated in another section of this report.

The problem lessens gradually as time integration increases, and the background interference from natural variations becomes relatively small with seasonal rainfall. Therefore, comparison of seasonal patterns and point rainfall difference on a seasonal basis should be useful in the verification of seeding-induced effects.

TIME DISTRIBUTION MODELS OF STORM RAINFALL

Previous Research

Huff (1967a) used data from 261 storms on the 400-mi^2 network in east central Illinois (Fig. 2) to derive time distribution relations. The time

distributions were expressed as cumulative percentages of storm rainfall and storm duration to enable valid comparisons between storms and to simplify analyses and presentation of data. Relations were developed for point rainfall and for areal mean rainfall on areas of 50 to 400 mi^2. Rainfall distributions were grouped according to whether the heaviest rainfall occurred in the first, second, third, or fourth quarter of a storm.

Other analyses showed storm duration and storm mean rainfall explaining only a small portion of the variance between storms, when the time distributions were classified by quartile and expressed as percentages of total storm duration and rainfall. Part of the effects of duration and mean rainfall are absorbed in the quartile groupings, which showed a trend for the longer, heavier storms to dominate the fourth quartile grouping, whereas short duration storms accounted for a major portion of the first and second quartile groups. As a result of these analyses, it was considered more logical, as a first approximation, to determine average rainfall distributions for point and areal mean rainfall by quartile group only.

Areal groupings showed only small changes in the time distribution with increasing size of sampling area from 50 to 400 mi^2. Thus, an average relationship for areas of 50 to 400 mi^2 combined was determined, and specific area distributions expressed as departures from the average in presenting the results.

The time distributions were expressed in probability terms because of the great variability in the characteristics of the distribution from storm to storm. Numerous factors contribute to the storm variance, but no single parameter dictates the characteristics of the distribution. Among the factors are the stage of development of the storm, the size and complexity of the storm system, rainfall type, synoptic storm type, location of the sampling area with respect to the storm center, and the movement of the storm system across the sampling region. Probability distributions allow selection of a time distribution most appropriate for a particular application.

In the study discussed above, smoothed time distributions were obtained from 30-minute rainfall totals throughout each storm. Furthermore, the relations were based upon heavy storms in which areal mean rainfall exceeded 0.50 inch and/or point amounts of 1 inch or more were recorded in the sampling area. Thus, the applicability of the results to storms of lesser intensity and to those in which the rainfall was accumulated over shorter intervals of time was questionable.

The foregoing questions were clarified considerably in a later study of the time distributions characteristics of 1-minute rainfall amounts in a 50-storm sample. This sample was comprised primarily of warm season storms and contained storms varying in intensity from light to moderate to heavy (Huff, Shipp, and Schickedanz, 1969). Following the same procedure used in the 1967 study, excellent agreement was found between the time distribution properties of 1-minute rainfall and total storm rainfall.

Therefore, it was concluded that the results of the earlier study of 261 storms is applicable, as a first approximation, for deriving the time distribution

characteristics of all types of storms in which unstable types of rain predominate. The large sample of 261 storms provides a more reliable determination of model time distributions with various probabilities of occurrence.

Time Distribution Models

Statistical models of time distributions for each quartile are shown in Figs. 15 to 18 for areas of 50 to 400 mi^2 combined. These are considered typical of midwestern, warm season storms or cold season storms in which unstable rainfall types are the major rain producers. Combining all areas, 33%, 33%, 23%, and 11%, respectively, of the storms were classified as first, second, third, and fourth quartile storms. No distinct trend in quartile types was found with increasing area, although there was considerable fluctuation between areas. The statistical models are smooth curves reflecting the average rainfall distribution with time and, therefore, do not exhibit the burst characteristics of a mass rainfall curve. Probability levels from 10% to 90% are shown, but the 50% level (median) has been stressed by a heavier line, since it is probably the most useful statistic from the standpoint of most users of rainfall data.

Interpretation of the curves can be illustrated by referring to the first quartile distributions in Fig. 15. The 10% curve is typical of storms in which the rainfall is concentrated in an unusually short portion of a storm. It indicates a chance of 1 in 10 that a first quartile storm will have at least 89% of its rainfall in the first quarter of the storm period and over 95% in the first one-half of the storm. The 50% curve shows 63% and 86% of the rainfall at 25% and 50% of the storm period. The 90% curve reflects an unusually uniform distribution for first quartile storms. It may be interpreted as the distribution that will occur in 10% or less of the storms. Thus, this curve shows that in 10% of the storms, 39% or less of the rain will occur in the first quarter of the storm and 57% in the first one-half of the storm.

The curves at the various probability levels reveal characteristics of certain storm types. For example, the 10% probability curve of first quartile storms discussed above is most frequently associated with relatively short duration storms, such as the passage of an intense, prefrontal squall line in which light rain falls from the middle cloud deck system for substantial periods following the major rain bursts. Similarly, the distribution at the 90% level is most likely to be associated with longer duration storms, in which the rain is more evenly distributed during the storm period, and is often dominated by a series of rainshowers or a combination of showers and steady rain.

In the fourth quartile storms, the distribution at the 10% level is common to the passage of a large-scale weather system with warm frontal rainfall at the start of the storm and more intense cold frontal rainfall near the end. The 90% distribution may be associated with the approach and passage of a low pressure center through or near the sampling region, when light rainfall may precede the center passage for several hours and the rainfall intensity maximizes as the center passes.

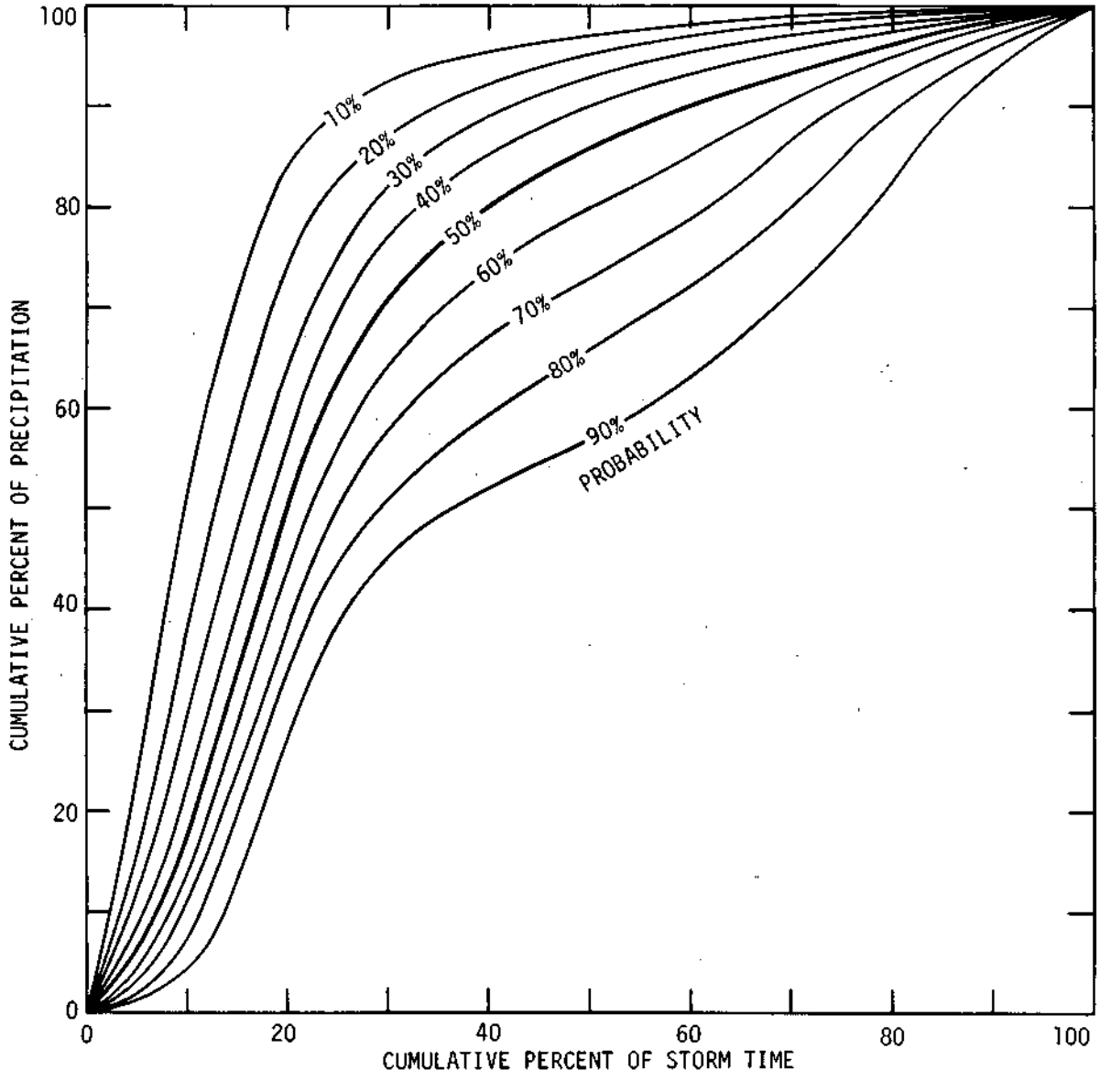

Figure 15. Time distribution of first-quartile storms.

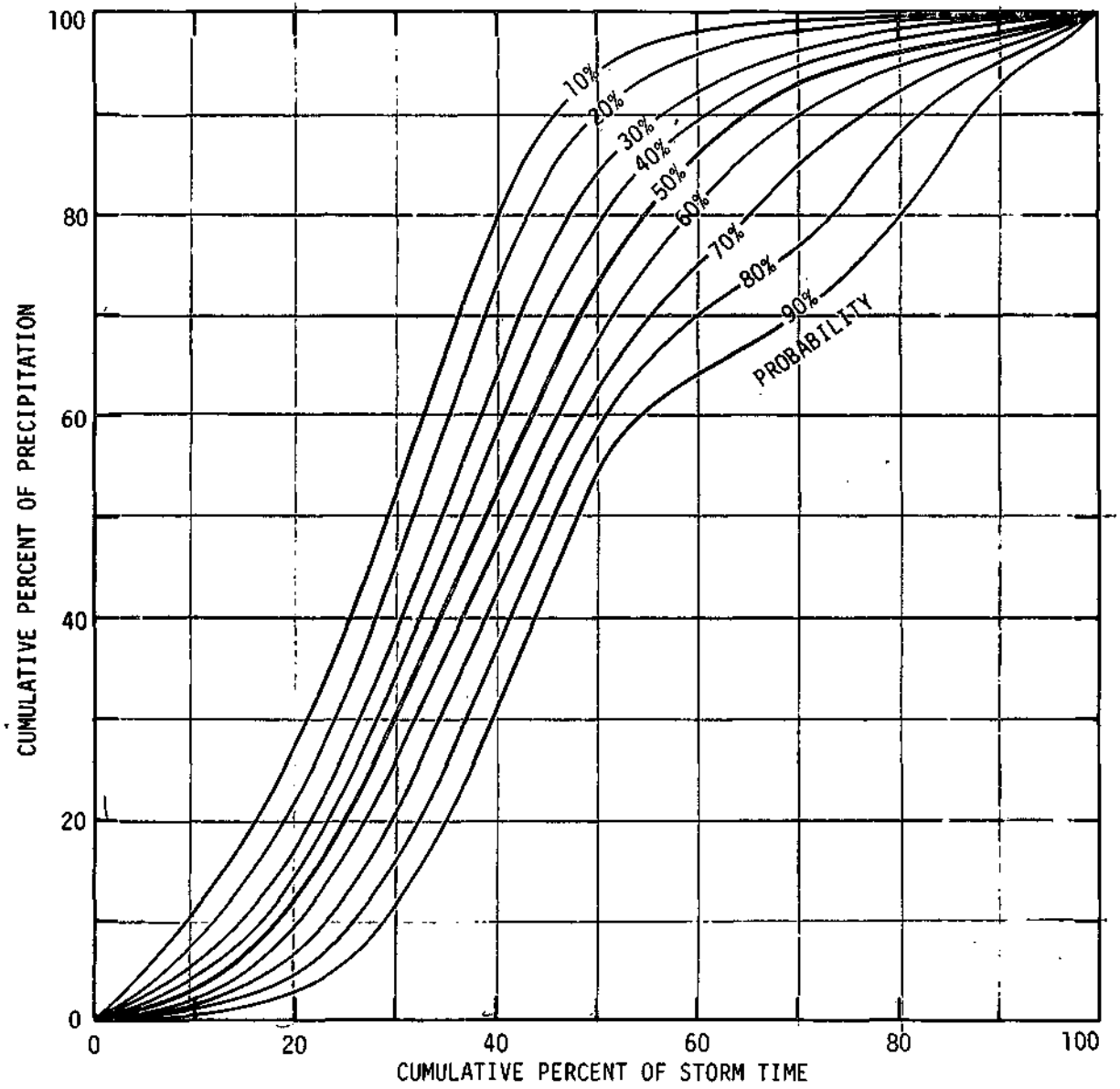

Figure 16. Tine distribution of second-quartile storms.

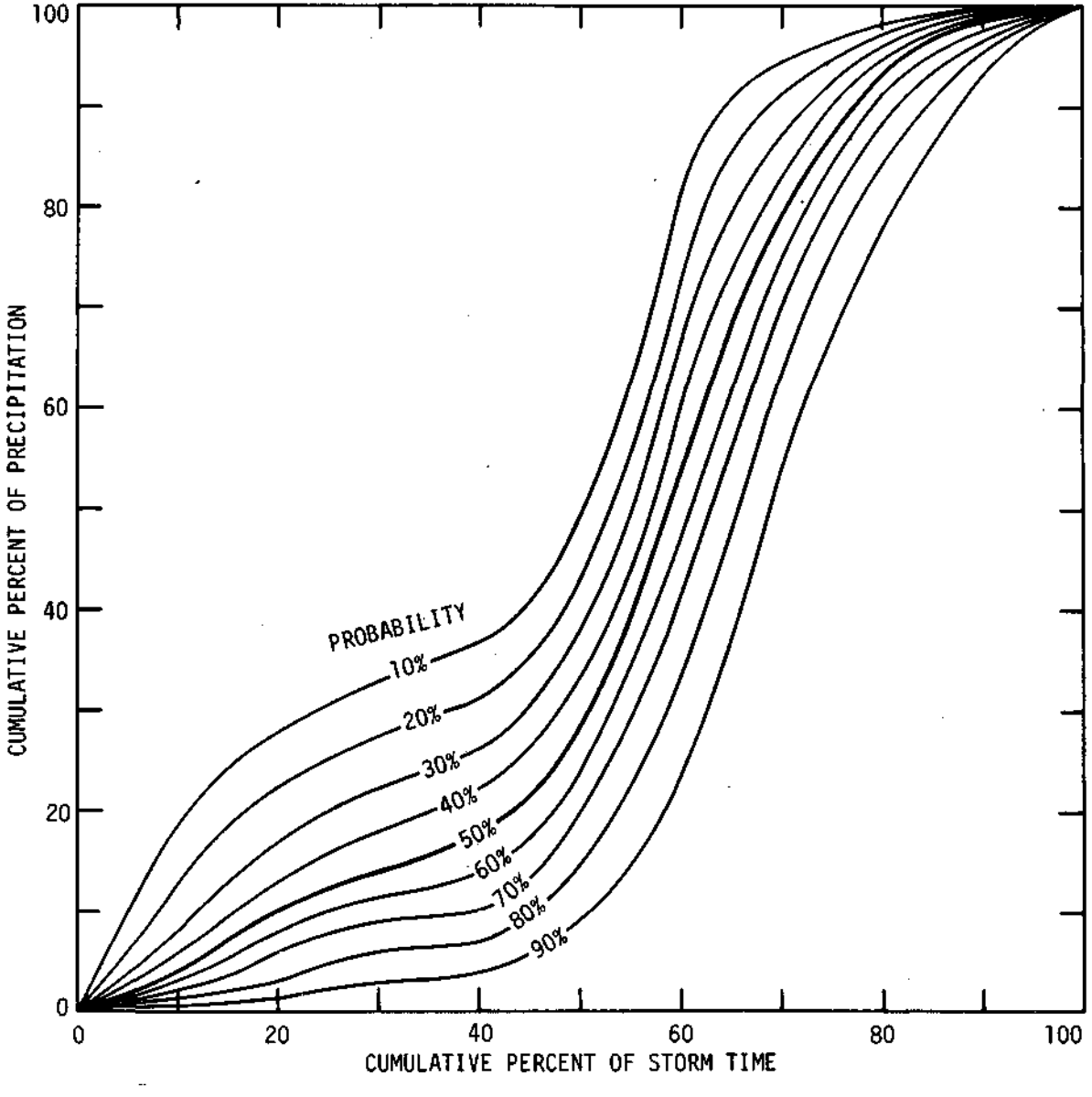

Figure 17. Time distribution of third-quartile storms.

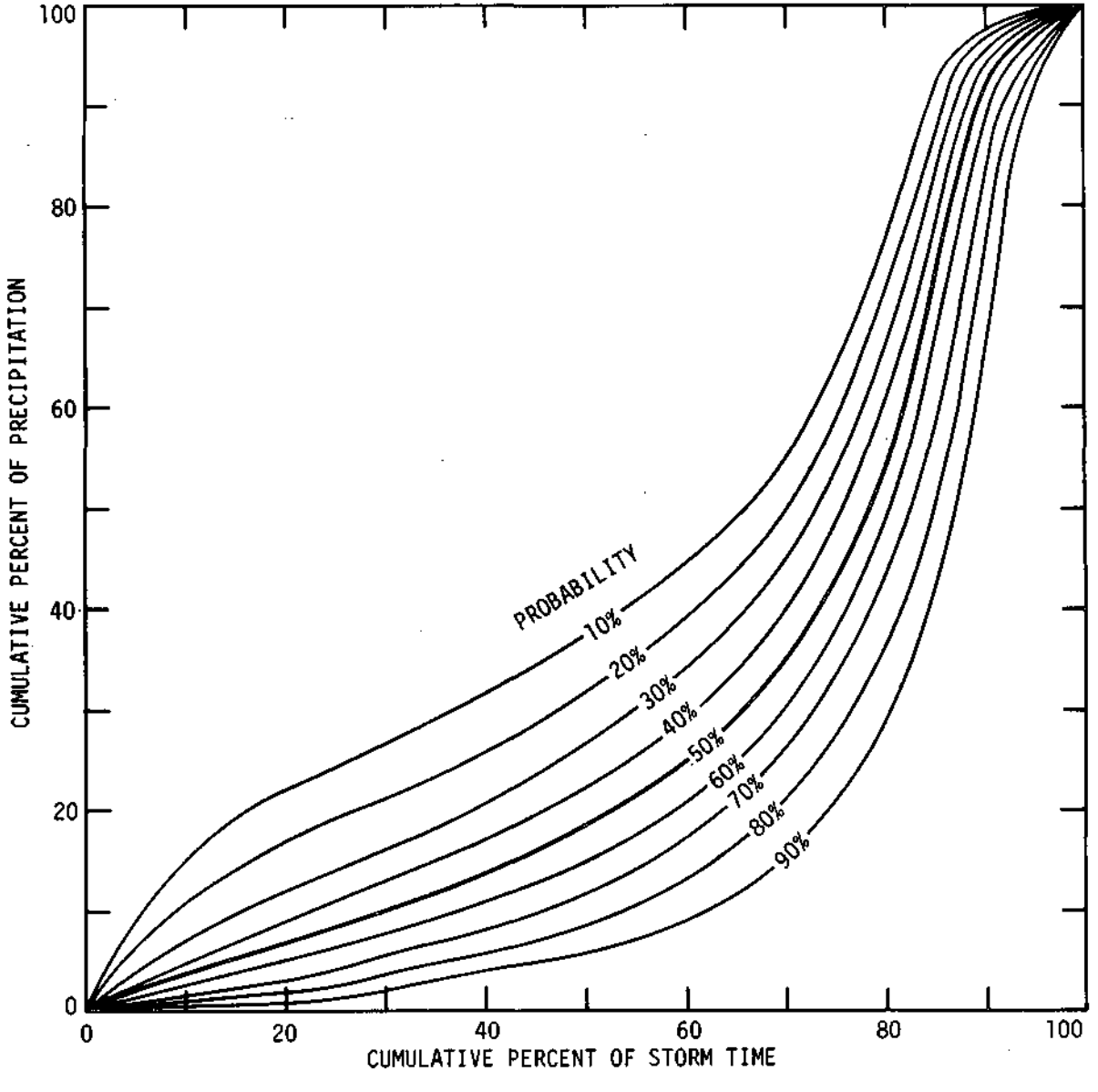

Figure 18. Time distribution of fourth-quartile storms.

In concluding the discussion of time distribution characteristics, it is emphasized that the relations presented here are empirically derived. They are not submitted as exact mathematical relationships, but rather as first approximations of a hydrometeorlogical parameter for which quantitative knowledge is sparse.

Figs. 19 and 20 provide additional information on the time characteristics of storm rainfall. Fig. 19 shows median quartile curves for point rainfall and Fig. 20 shows how the first quartile point curve differs from that for the largest area studied (400 mi). The point curve indicates larger percentages of the total rainfall at the start of storms. This tendency appears logical for rain on smaller areas. If one assumes a storm of given intensity and areal extent moving across two areas of appreciably different size, the smaller area will receive a larger percentage of its areal mean rainfall in the early part of the rain period, particularly if the storm is smaller than the network in areal extent. Table 34 illustrates the differences between the average curve for 50 to 400 mi^2 and specific areas in first quartile storms.

Table 34. Differences between average curve and specific areas for 50% probability level in first-quartile storms.

Area (mi^2)	Difference (%) for given cumulative percent of storm duration								
	10	20	30	40	50	60	70	80	90
Point	-9	-1	+5	+6	+6	+6	+5	+4	+3
10	-11	-3	+2	+1	+3	+2	+2	+2	+1
50	-2	+3	+3	+2	+2	+2	+1	0	0
100	-2	-3	0	0	0	0	0	0	0
200	-2	-3	-2	-1	-1	0	0	0	0
400	+6	+4	-1	-2	-2	-1	-1	0	0

Conclusions

The time distribution characteristics of storm rainfall in midwestern warm season storms have been defined quantitatively in considerable detail by the statistical models presented in this study. Application of these models as a verification tool in weather modification experiments does not appear promising at this time because of the large variability in storm time distributions that results from multiple causes. That is, the interference level of natural variability is too great for the detection of modest changes resulting from cloud seeding within a reasonable length of time.

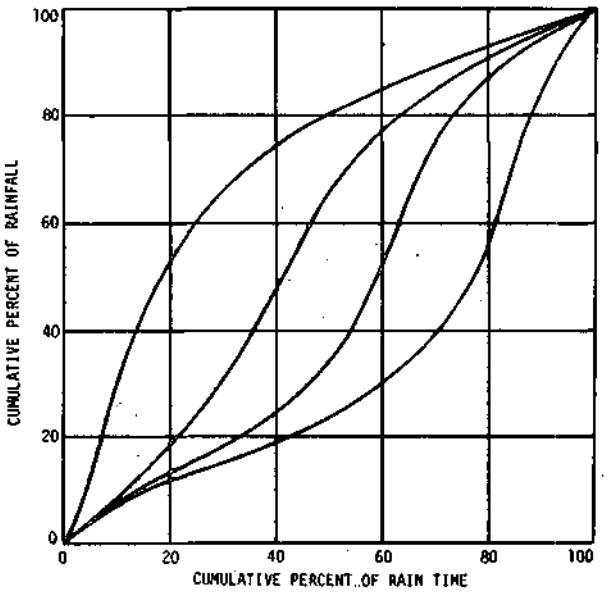

Figure 19. Median quartile curves of point rainfall.

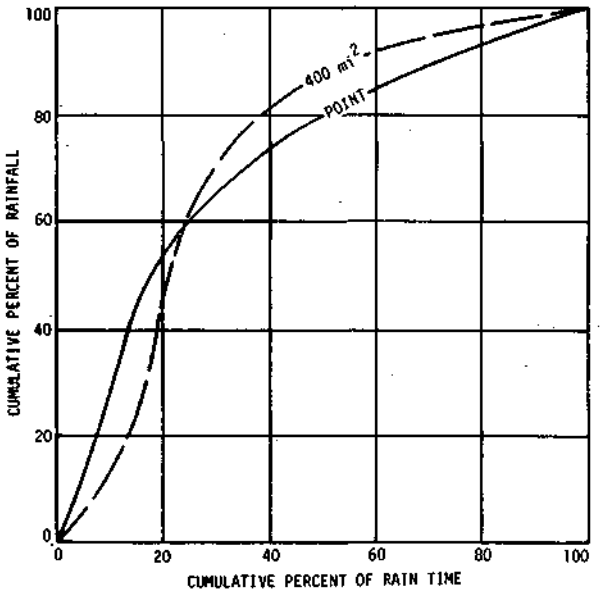

Figure 20. Differences between point and 400 mi^2 curves.

USE OF DIURNAL RAINFALL PROPERTIES IN EVALUATING SEEDING EXPERIMENTS

Climatologically, the diurnal distribution of rainfall is characterized by maxima and minima in the hourly distribution of rainfall in areas of similar precipitation climate. The distribution of maxima and minima may vary somewhat between seasons in a given area. For example, Illinois studies have been made of the diurnal distribution, based on records from 30 stations in the 10-yr period, 1948-1957. These studies have shown that the distribution of hourly mean rainfall is characterized by a well-defined winter maximum occurring during the night. In most areas of the state, a winter minimum occurs in late forenoon or early afternoon. In summer a well-defined minimum is found near noon in all sections. The primary maximum in summer occurs during the late afternoon or evening in the southern part of the state and during early morning in the northern part.

If the diurnal distribution for a given region and season remained relatively stable from year to year and cloud seeding substantially altered the magnitude and/or time sequence of the maxima and minima, then the diurnal distribution could serve as a valuable tool in the verification of weather modification experiments. Cloud seeding is frequently performed in late forenoon and afternoon to attack developing cumulus in summer when agricultural requirements for water maximize. This seeding, if effective, would very likely affect the intensity and, perhaps, the time distribution of the afternoon maxima.

A limited investigation was made of the applicability of diurnal rainfall distributions in the evaluations of weather modification experiments. For this purpose, data from two hypothetical cloud seeding targets were used. These were the two dense networks in central and southern Illinois (ECI and LEN) which include areas of 400 and 550 mi^2. ECI is typical of the precipitation climate of the North Central Section (Fig. 19), whereas LEN is within the Southeast climatic section, as defined by Huff and Neill (1959). All recording gages in each network were used to obtain average distributions of mean hourly rainfall during summer for the 5-yr period, 1960-1964. These distributions were then compared with the 10-yr sectional distributions obtained in the earlier study (1948-1957) described above.

Fig. 21 shows the diurnal distributions obtained in the 1948-1957 and 1960-1964 analyses. Normalization of the curves was achieved by expressing each hourly amount as a percentage of the mean for all hours of the day. This was done merely to facilitate interpretation of the relations. Some smoothing of the curves in each case was obtained by using 3-hourly moving averages.

A much greater fluctuation in mean rainfall between hours is shown in the network curves, especially in the North Central Section. However, the network curves are derived from a shorter sampling period and averaging is over a very small area compared with the climatic sections. Otherwise, there is considerable similarity between the time sequences of maxima and minima on comparable curves. The major maximum and minimum on ECI correspond closely in time with those in the North Central Section. The ECI afternoon maximum is quite pronounced, whereas

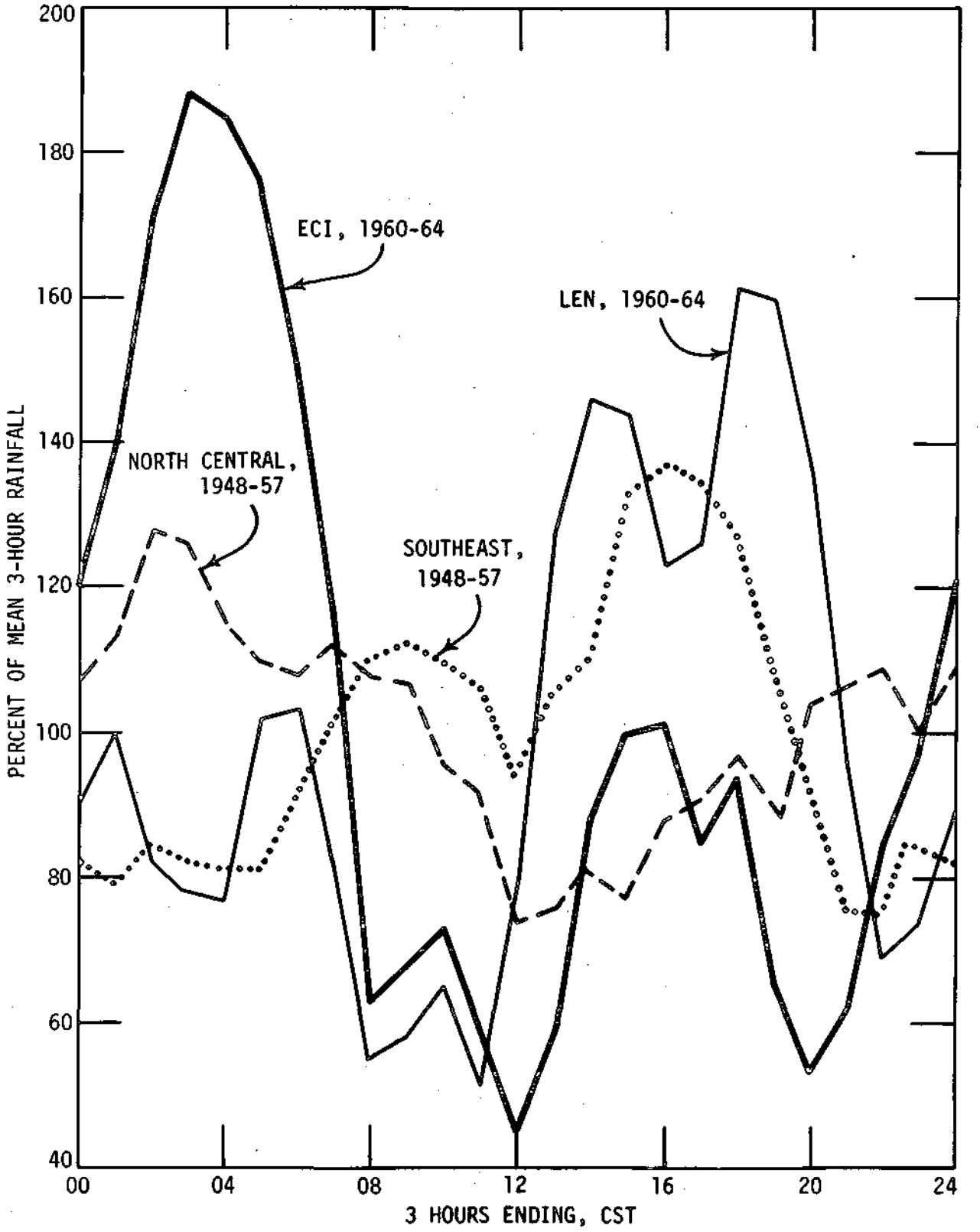

Figure 21. Comparison of diurnal distributions between climatic sections for two sampling periods.

the climatological average shows little evidence of a secondary maximum. The major maximum on LEN corresponds quite well with the Southeast major peak; otherwise, there is considerable difference in the occurrence of peaks and valleys in the diurnal distribution. Overall, Fig. 21 indicates substantial differences between the network and climatic section curves, but the variations appear to be no greater than has been observed with other precipitation parameters.

Of primary interest in weather modification experiments, however, would be the stability of two or more samples of diurnal distributions drawn from the same storm population. For example, samples from seeded and non-seeded days during an experiment are used to verify seeding effects. The problem of natural variability between such samples is treated in the section of this report dealing with downwind effects from the Project Whitetop experiments. Consequently, those results will not be repeated here.

The overall conclusion from the diurnal studies is that natural variability is a major problem in verifying cloud seeding effects through use of diurnal rainfall distributions. However, it is also concluded that natural variability is no more of a problem than it is with other rainfall parameters that are or could be used in verifying seeding effects. Therefore, it is recommended that statistical evaluation of seeding effects on diurnal distributions serve as one of several tools used in evaluating changes in surface precipitation produced by cloud seeding.

SEQUENTIAL VARIABILITY AND LAG CORRELATIONS OF STORM PRECIPITATION

Sequential Variability

Interstorm variability of areal mean precipitation was investigated through calculations of sequential variability (Conrad and Pollack, 1950). As employed in this study, the sequential variability (D) was obtained by dividing the summation of consecutive differences in storm mean rainfall by N - 1, where N is the number of storms in the sample. D takes account of both the magnitude and sequence of the sample mean precipitation (P) in characterizing the time variability. Therefore, it was considered preferable to the standard deviation or average deviation of P, which are more commonly used measures of time variability that evaluate only the magnitude of the items in a time series.

Dividing D by P and multiplying by 100 provides a measure of the time relative variability (V_d) which is useful for comparing D among various storm samples. In the Illinois study, this variability measure was used to compare the interstorm variability between seasons and years.

Data for the period January 1960 through April 1965 from the East Central Illinois Network (Fig. 2) were used in the study. The storm data were grouped into the two seasons, May-September and October-April, used throughout this report. Also, the same storm definition was used.

Results of the D study are summarized in Table 35 for each season in each of the 5 years. V_d had a slightly smaller median and yearly range of values in October to April than in May to September. However, the difference is not considered large enough to attach climatic significance to it. The major conclusion apparent from Table 35 is that interstorm variability is relatively large in all seasons.

Table 35. Sequential variability of storm precipitation.

Year	Number of storms	D (in)	P (in)	Vd (%)
		May-September		
1960	68	0.35	0.26	135
1961	49	0.59	0.46	128
1962	50	0.46	0.36	128
1963	40	0.35	0.30	117
1964	46	0.39	0.33	118
Median	49	0.39	0.33	128
		October-April		
1960	53	0.37	0.30	123
1961	66	0.33	0.25	132
1962	65	0.25	0.20	125
1963	63	0.38	0.30	127
1964	52	0.41	0.33	124
Median	63	0.37	0.30	125

Lag Correlations

The presence of time trends in storm mean precipitation was investigated through calculation of lag correlations for lags of 1 to 30 storms in the 1960-1965 sample. The data were again divided into the two seasons, May-September and October-April, for this investigation. Results are summarized in Fig. 22 which shows graphically the correlation patterns for each season in each of the five sampling periods.

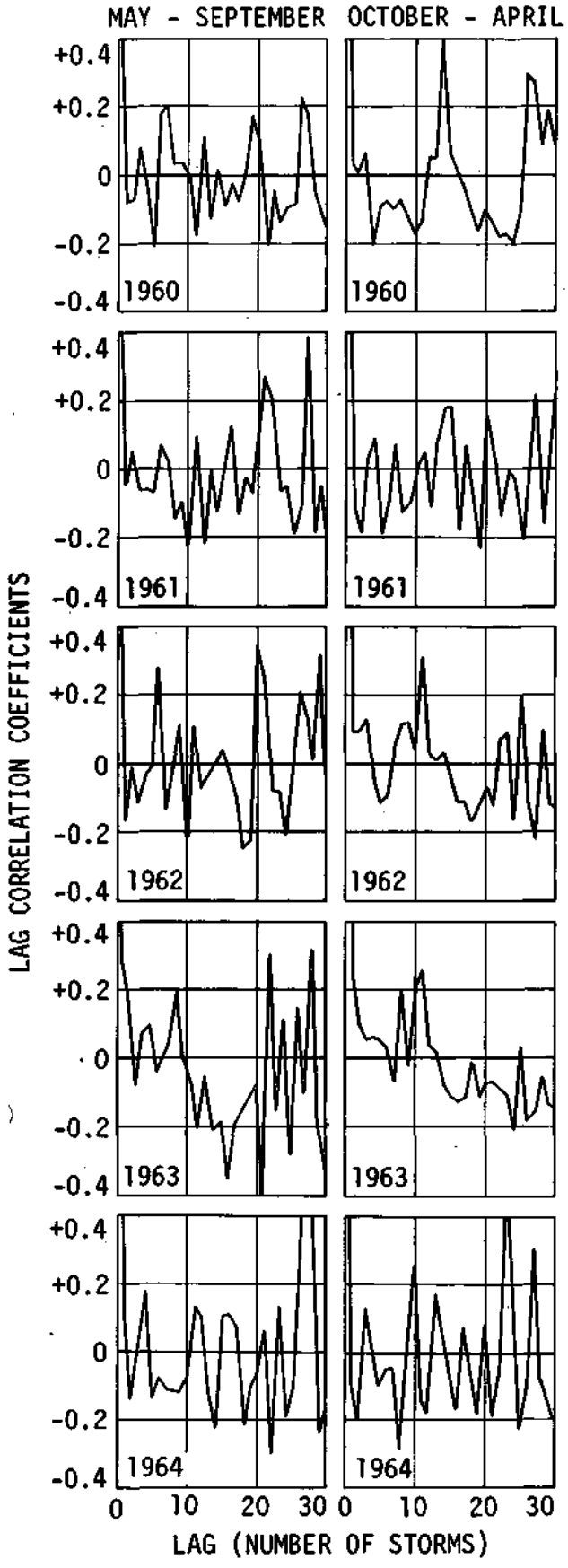

Figure 22. Lag correlations of storm precipitation grouped by season.

Examination of Fig. 22 shows a consistent trend for a positive peak in the correlation between storm separations of 26 to 28 in the May-September period, and a less pronounced trend at the same separation in the October-April storms. This corresponds approximately to a time lag of 25 to 30 storm days with the storm definition used here. Several weak trends in correlation can be discerned, but may merely reflect the vagaries of storm sampling over a 5-yr period.

Primarily, the graphs in Fig. 22 stress the lack of correlation between consecutive storms. A rapid drop in correlation to values in the range of 0.0 to 0.2 with a 1-storm lag occurred in all years except 1963 in both seasons. However, in 1963 the 1-storm lag correlations were less than 0.3, and thus, explain less than 10% of the variance.

Even within storms the lag correlation decreases rapidly. In an earlier study (Huff, Shipp, and Schickedanz, 1969), the lag correlation coefficients of 1-minute point and areal mean rainfall on 100 mi^2 were found to approach zero at an average lag of 15 minutes in warm season storms.

Conclusions

The large sequential variability and the lack of correlation between consecutive storms further support the conclusions of the previous section regarding the limited use of time distribution parameters as verification tools in precipitation modification experiments.

SAMPLING ERRORS IN MEASUREMENT OF MEAN PRECIPITATION

Introduction

The accurate measurement of mean precipitation is important in weather modification applications and other fields, such as hydrology, and agricultural research. Evaluation of sampling requirements under various meteorological conditions has been hampered greatly in the past by the lack of dense raingage networks to provide suitable data for this purpose. Several investigators have made limited studies in which sampling error was related to storm mean rainfall and size of sampling area to obtain estimates of gage density requirements. Among these were Light (1947), Linsley and Kohler (1951), Huff and Neill (1957), and McGuinness (1963).

This paper summarizes results of a study extending the earlier work of Huff and Neill (1957) in Illinois. In the present study, the effects of season, precipitation type, synoptic weather type, and storm duration on the sampling error of storm mean rainfall estimates have been investigated, in addition to the usual parameters, mean precipitation and size of sampling area. Also, the

study has been extended to include rainfall rate, monthly, and seasonal relations. The results should be considered representative only for the Midwest and other areas of similar climates. For example, the results are not transposable to the arid climates of southwestern United States.

Data Used

Data from the two dense networks in central and southern Illinois (Fig. 2) were used in the storm, monthly, and seasonal analyses. Data from a special network of 50 recording gages in 100 mi^2 were used in the rainfall rate analyses. These gages, operated during 1952-1953, were equipped with an enlarged orifice and 6-hour charts to permit measurement of 1-minute amounts (Huff and Neill, 1956). ECIN was subdivided also to provide data for areas of 50, 100, and 200 mi^2. The storm study was based primarily on data for the 5-yr period, 1960-1964. Data available on ECIN for the 5-yr period, 1955-1959, were used for comparison with results of the 1960-1964 storm study. The ECIN data for 1955-1966 were used in the monthly and seasonal analyses. The ECIN analyses were restricted to the warm season since the network was reduced to 25 gages from late fall to spring. LEN operated without reduction throughout the year.

Data from the Shawnee and Little Egypt combined networks (SHLEN) were available for a 3-yr period, 1965-1967. These data were used to obtain first approximations of sampling requirements for areas of the order of 1000 mi^2. This network (Fig. 1) consisted of 62 gages on 1125 mi^2, or approximately one gage per 18 mi^2.

Analytical Procedures

On LEN the data were divided into the two seasons used throughout this report; these are the major growing season (May-September) and the period of maximum water supply replenishment (October-April). The ECIN analyses had to be limited to the May-September period because winter gage density was considered inadequate for this study. Within each season, the storm data were analyzed further after stratifying by precipitation type and synoptic weather type.

Storm sampling error was related to mean precipitation, storm duration, and gage density within each grouping listed above. Since storm rainfall is not normally distributed, several data transformations were investigated to ascertain the best method of approaching normalization of the data. Transformations included logarithms, square roots, cube roots, and combinations of these transformations in the empirical regression equations used to fit the data. Transformations used were based upon earlier studies of the author and other investigators mentioned earlier.

The earlier studies of Huff and Neill (1957) and others did not include the storm duration factor. However, Huff and Shipp (1968) have shown that storm duration has a slight influence on the spatial variability beyond that explained by mean

precipitation alone; therefore, it was included since the sample was considered adequate to evaluate the duration effect.

The ECIN sample included 296 storms in the 1960-1964 period, whereas LEN had 333 storms in the May-September period and 316 during the October-April period. The ECIN had 285 storms in the May-September period, 1955-1959. Storms varied in duration from less than 1 hour to approximately 48 hours.

1960-1964 Storm Relations

Data transformation tests based upon multiple correlation analyses indicated a slight superiority for logarithms, followed by cube roots, square roots, and the logarithm-square root combination used by Huff and Neill in their earlier study. Table 36 illustrates the transformation comparisons in each season on the two networks of 400 and 550 mi^2 for all storms combined. Most of the discussions that follow will be restricted to results obtained from the general equation

$$\text{Log } E = a + b \text{ Log } P + c \text{ Log } G + d \text{ Log } T, \qquad (14)$$

where E is the average sampling error in inches, P is the areal mean precipitation in inches, G is gage density in mi^2/gage, T is storm duration in hours, and a, b, c, and d are constants. E represents the difference between the best estimate of the true mean (P), obtained from the maximum density of raingages on each network, and the sample mean precipitation (Pg) calculated from the gage amounts for a given value of G. For example, assume that the best estimate of mean rainfall in a storm on the 400 mi^2 network, as measured by all 49 gages, was 1 inch (P), whereas a reduced network of 25 gages (G = 16) indicated a mean of 0.9 inch (Pg). Then, E is equal to 1.0 - 0.9, or 0.1 inch.

Table 36. Multiple correlation coefficients for empirical equations using various data transformations.

			Multiple correlation coefficient for given transformation			
Network	Period	Season	Logarithms	Cube root	Square root	Square root logarithms
ECIN	1960-1964	May-Sept.	0.78	0.74	0.70	0.69
ECIN	1955-1959	May-Sept.	0.72	0.71	0.67	0.65
LEN	1960-1964	May-Sept.	0.76	0.72	0.67	0.65
LEN	1960-1964	Oct.-Apr.	0.69	0.69	0.65	0.64

For each season on each area, individual equations were developed. These were determined for all seasonal data combined and for the seasonal data grouped by precipitation and synoptic storm type. Table 37 shows intercepts and regression constants for each May-September equation on each sampling area during the 1960-1964 period. All available rainfall data were combined in obtaining these equations. Also, the LEN equation for October-April is shown at the bottom of the table. Standard errors for the various regression constants are included to indicate the reliability of the computed values. The standard error increases with decreasing area and is greatest on the regression constant for gage density.

Table 37. Logarithmic equation constants derived from 1960-1964 data.

Sampling area (mi^2)	Intercept	Regression constants P	G	T
		May-September		
50	-2.0040	0.66	0.57	-0.17
100	-2.9287	0.67	1.24	-0.20
200	-2.7583	0.68	0.97	-0.28
400	-2.4720	0.64	0.69	-0.23
550	-2.5587	0.68	0.73	-0.26
		October-April		
550	-2.9092	0.57	0.70	-0.17

A combined equation representing all of the sampling areas would be desirable for interpolating between the specific areas used here, and for smoothing the relations obtained from separate areas located in the same or very similar climatic and physiographic regions. Inspection of Table 37 indicated no definite trend in the May-September regression constants with increasing area. Therefore, it was decided to combine all network data into a single expression. This resulted in the following equation:

$$\text{Log } E = -1.5069 + 0.65\,P + 0.82\,G - 0.22\,T - 0.45\,A, \qquad (15)$$

where A is area and the other variables are the same as in Eq. 14. Standard errors of estimate for the regression coefficients on P, G, T, and A were relatively small with values of 0.01, 0.04, 0.04, and 0.02, respectively.

Difference obtained between the individual area and combined equations are illustrated in Table 38 for G = 50 mi^2/gage, P = 1.0 inch, and T = 6 hours. Except for the 100-mi^2 area that had disrupted a logical trend between the several individual equations, the agreement between the combined and individual equations is excellent in view of the natural spatial variability of precipitation data (Huff and Shipp, 1968). Consequently, the combined equation is recommended for use instead of the individual equations.

Table 38. Comparison between individual and combined equations in May-September storms for P = 1.0 in, T = 6 hr, and G = 50 mi^2/gage.

	Average sampling error (in) for given area (mi^2)				
Equation	50	100	200	400	550
Individual	0.07	0.11	0.06	0.03	0.03
Combined	0.09	0.07	0.05	0.04	0.03

At this point, it may be of interest to inspect the differences obtained between equations based on logarithmic and cube root transformations, since the latter was a close second choice in the equation selection. Table 39 illustrates the degree of difference, based upon individual equations for LEN in May-September storms for P = 1.0 inch and T = 6 hours. Only small differences occur with the cube root equation yielding slightly larger values. This comparison is typical of differences found for other areas and other values of P and T.

Table 39. Comparison of sampling errors on 400 mi^2 from logarithmic and cube root transformations in May-September storms for P = 1.0 in, and T = 6 hr.

Gage density (mi^2/gage)	Average sampling error (in)	
	Logarithmic	Cube root
25	0.02	0.03
50	0.03	0.04
100	0.05	0.07
200	0.09	0.11
400	0.14	0.16

Sampling errors calculated from Eq. 15 are shown in Fig. 23 for selected gage densities and storm durations on an area of 400 mi^2 (ECIN). This figure illustrates quantitatively how the sampling error increases with increasing mean rainfall and decreases with increasing sampling density and storm duration.

Eq. 15 provides estimates of the average sampling error. However, the rainfall gradient and, consequently, the sampling error of storm mean precipitation will vary greatly between storms of similar volume and duration, particularly during showery types. For example, intensity and spatial distribution of the individual storm cells comprising a storm will affect its areal pattern uniformity. As shown by Huff and Stout (1952), the location of the storm center with respect to the sampling area significantly affects the spatial variability. The direction of movement and orientation of the storm axis also influences the pattern characteristics. Precipitation type and synoptic storm type affect the sampling error. Except for mean precipitation, duration, and average intensity, it is difficult, if not impossible, to express these sampling error factors in quantitative terms. Thus, unless huge samples are available to permit grouping of the data according to all of these various factors, the sampling error with a given gage density in a particular storm cannot be defined with a high degree of accuracy.

The great amount of variability about the average sampling error is illustrated in Fig. 24. Here, sampling error (%) has been plotted against network mean rainfall (inches) for all May-September storms in the 1955-1964 period in which the areal mean was 0.01 inch or more and storm duration was 3 hours or less. Since sampling error changes slowly with storm duration, this duration grouping should contribute only a small portion of the interstorm variation shown in the graph. The sampling errors are for a gage density of 16 mi^2/gage (25 gages) on the 400-mi^2 network. The solid line represents the median and the dash lines encompass 95% of the observations. Although the absolute sampling error increases with increasing mean rainfall (Fig. 23), the percentage error decreases as shown in Fig. 24.

Fig. 24 shows the sampling error ranging from less than 1% to 60% in the 95-% envelope for a storm mean of 0.01 inch. Similarly, for a 1-inch mean the sampling error ranges from near zero to 14% with a median of 2.5%. The difficulty in defining the sampling error accurately in specific storms is emphasized by this data plot. As the gage density becomes less, the variation about the mean becomes greater. For example, a similar plot for a gage density of 50 mi^2/gage showed the 95-% envelope of sampling errors for a 1-inch mean ranging from less than 1% to nearly 40%.

Data from LEN (49 gages in 550 mi^2) were used to make comparisons between sampling requirements during the May-September and October-April periods. Showery precipitation prevails and small-scale air mass storms are frequent in the May-September period, whereas large-scale systems and steady precipitation types are much more frequent from October to April. Using the seasonal equations for 550 mi^2 (Table 37), Table 40 was constructed for comparison purposes. In this table, the ratio of the average sampling error in May-September 6-hour storms to that in similar October-April storms is shown for selected values of G and P. The average ratio ranges from 1.8 to

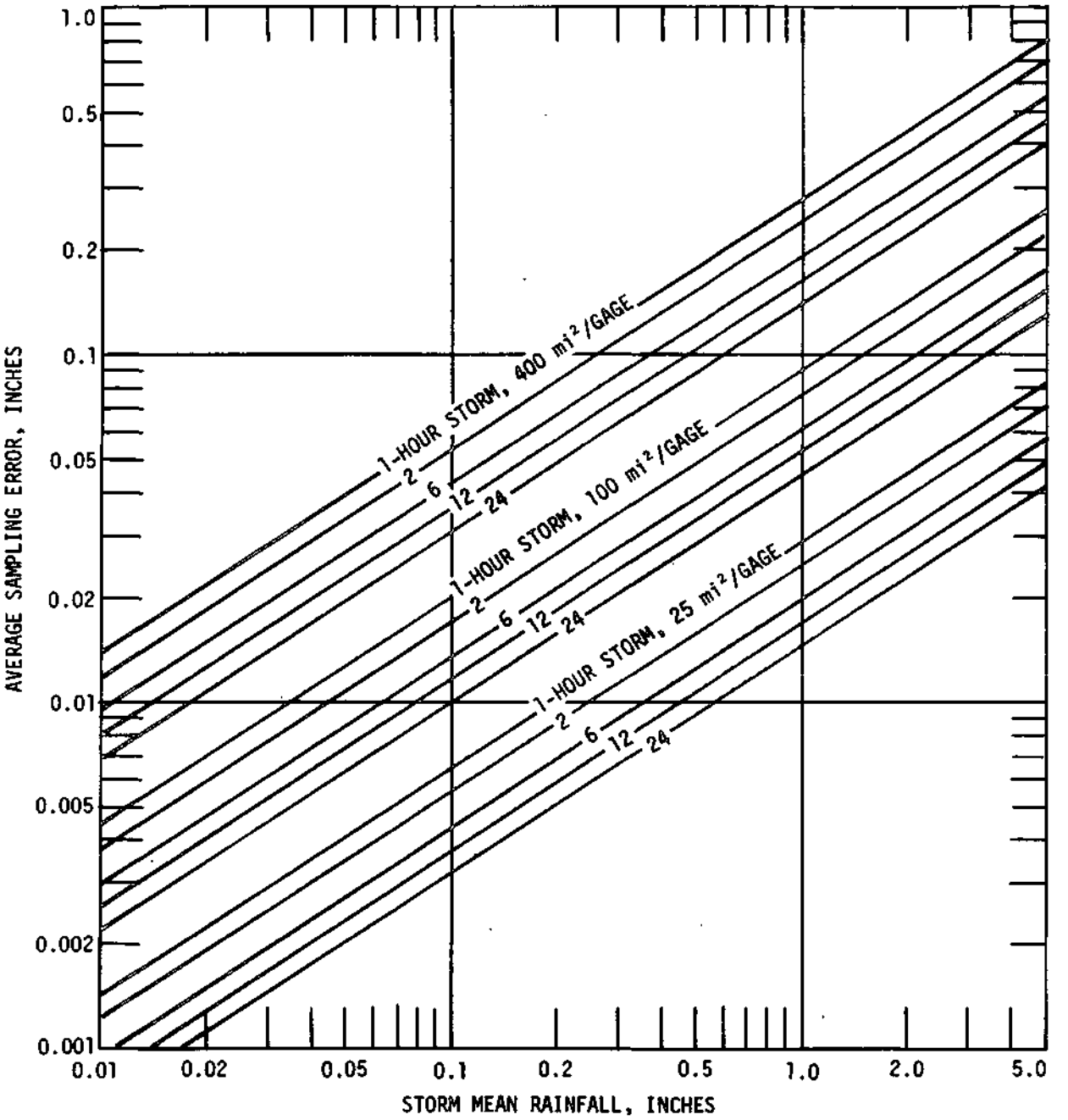

Figure 23. Sampling error relations on 400 mi

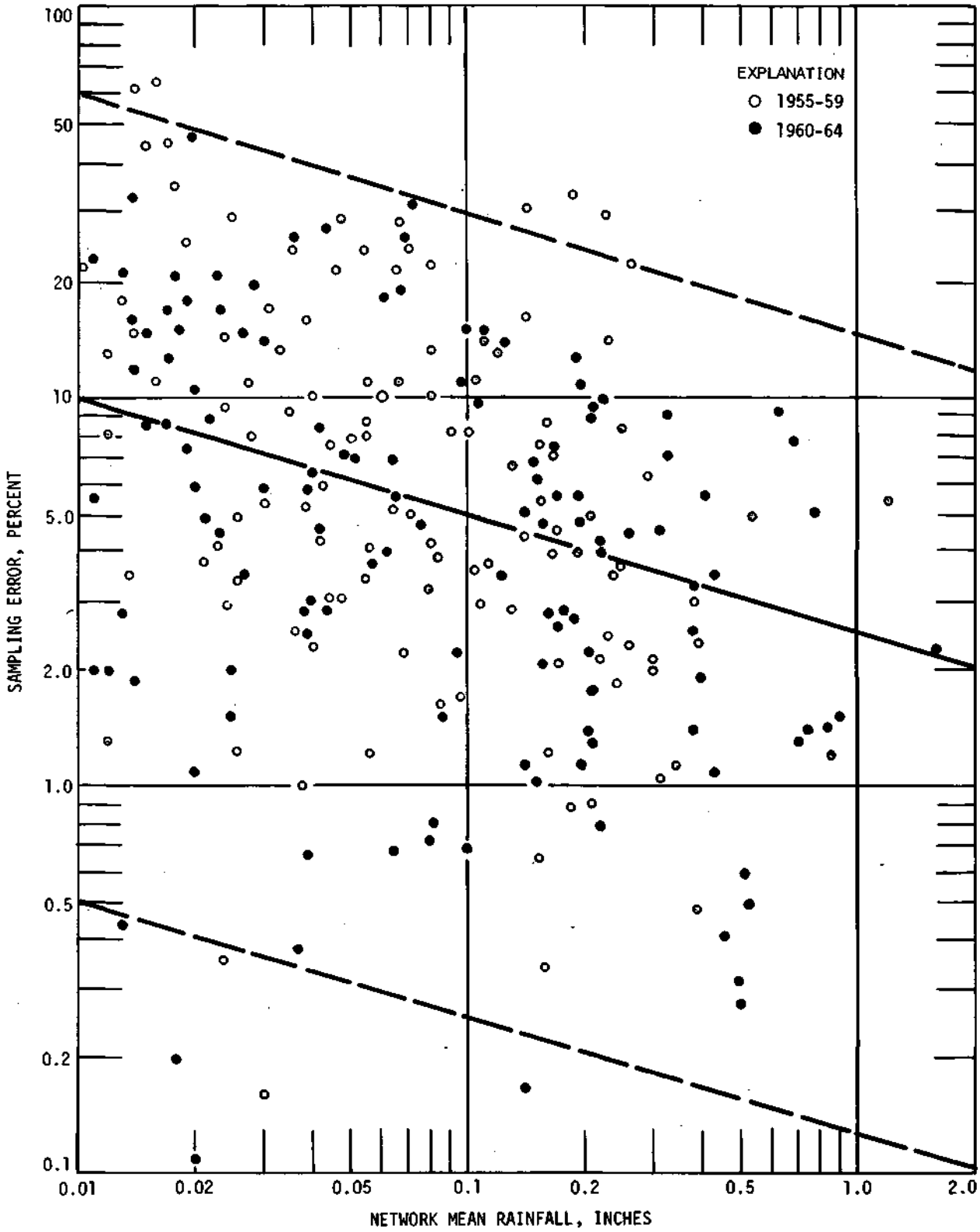

Figure 24. Sampling errors with gage density of 16 mi^2/gage in May-September storms on 400 mi^2.

2.4 with increasing P. At P = 0.50 inch, the average error for May-September is double the October-April value. Other calculations showed that the gage density must be approximately doubled to maintain the same reliability in the measurement of light rainfall amounts (0.10 inch) in changing from cold season to warm season conditions. With heavy mean rainfalls of 1 to 2 inches, the gage density must be approximately tripled.

Table 40. Comparison of average sampling errors in May-September and October-April storms on LEN.

Gage density (mi^2/gage)	Sampling error ratio, May-September to October-April, for given P (in) in 6-hr storms				
	0.10	0.25	0.50	1.00	2.00
25	2.0	1.8	1.9	2.0	2.2
50	1.5	1.7	1.9	2.2	2.3
100	1.7	2.0	2.1	2.2	2.4
200	1.8	1.9	2.1	2.0	2.5
400	1.8	2.0	2.2	2.3	2.6
Average	1.8	1.9	2.0	2.1	2.4

Next, the 1960-1964 seasonal data were subdivided by precipitation type and equations determined for each. Only those types with 30 or more observations were used in these comparative analyses. Consequently, the May-September comparisons were restricted to unstable rain types, thunderstorms (TRW) and rainshowers (RW), and steady rain (R). Typical results are illustrated in Table 41 in which seasonal comparisons are shown for LEN, P = 0.5 inch, T = 6 hours, and G varying from 25 to 400 mi^2/gage for each precipitation type and for all storms combined. The climatic network operated by ESSA in Illinois averages approximately 225 mi^2/gage. Therefore, average percentage errors for this network are closely approximated by G = 200 in Table 41.

When the gage density is 50 mi^2/gage or less, Table 41 indicates that nearly twice as many gages are needed for shower types than for steady rains to obtain the same measurement accuracy in May-September storms. In October-April storms, there appears to be little difference in the measurement accuracy among the several precipitation types until G reaches 100, after which the TRW+RW group errors become substantially larger than the others. Consequently, precipitation type need not receive serious consideration in designing a dense network for cold season operations in this climatic region.

The sampling errors for all storms combined in the May-September period are close to those for the TRW+RW group since 85% to 90% of all storms fall into this group in central and southern Illinois. The combined storm equation for October-April is not biased strongly to any type because the storm types are

more evenly distributed than in the warm season. From the results presented in Table 41, it appears that the seasonal equations for all storms combined should be satisfactory for estimating sampling requirements for most raingaging projects.

Table 41. Comparison of average sampling errors in LEN storms grouped by season and precipitation type for P = 0.5 in and T = 6 hr.

Gage density (mi^2/gage)	Average sampling error (%) for given precipitation type							
	May-September			October-April				
	TRW,RW	R	All storms combined	TRW,RW	R	R+S	S	All storms combined
25	2	2-	2	1	1-	1	1-	1
50	4	3	4	2	2-	2	1+	2
100	7	4	6	4	3	3	2	3
200	11	6	10	6	4	4	3	5
400	18	10	17	10	7	6	5	7

Synoptic storm types were investigated for their comparative effects on sampling errors. Storms were divided into the three general types used by Huff and Shipp (1968). These included frontal storms, air mass storms, and low pressure center passages. The various frontal types were not separated because differential effects were small. Results of this investigation are illustrated for LEN in Table 42 in which the format is the same as in Table 41. The largest sampling errors were found with air mass storms in both seasons, whereas those for fronts and low centers were nearly equal.

Table 42. Comparison of average sampling errors in LEN storms grouped by season and synoptic storm type for P = 0.5 in and T = 6 hr.

Gage density (mi^2/gage)	Average sampling error (%) for given storm type					
	May-September			October-April		
	Air Mass	All Fronts	Low Centers	Air Mass	All Fronts	Low Centers
25	4	2	2	2	1	1
50	5	4	3	3	2	2
100	8	6	5	5	3	3
200	12	11	9	7	5	5
400	18	18	16	11	8	8

Comparison of Successive Sampling Periods

For ECIN, a 5-yr set of data, 1955-1959, was available for the May-September period. These data were used for comparison with the 1960-1964 results to ascertain the stability and, consequently, the reliability of the 1960-1964 relations for establishing network sampling requirements. Eq. 16 is the individual equation for 400 mi^2, and Eq. 17 is for all areas combined.

$$\text{Log } E = -2.6690 + 0.66 \text{ Log } P + 0.83 \text{ Log } G - 0.05 \text{ Log } T \qquad (16)$$

$$\text{Log } E = -0.8698 + 0.68 \text{ Log } P + 0.94 \text{ Log } G - 0.01 \text{ Log } T - 0.75 \text{ Log } A \qquad (17)$$

Parameters and constants have the same interpretation as in previous equations.

Comparisons of the 1955-1959 equations with the 1960-1964 equations (Table 37, Eq. 15) show the regression coefficient of P remaining relatively constant between periods. However, a substantial change occurs in the regression coefficient on G, and the coefficients of T and A show major differences. In the 1960-1964 storms, T has considerable weight in determining sampling error (E), whereas in the 1955-1959 sample, T has very little influence. In the combined equations incorporating all areas, A has a much stronger influence on sampling error in the 1955-1959 sample than in the following 5 years.

The net effect of the equation changes is illustrated in Table 43, in which values are shown for various gage densities in 1-hour and 24-hour storms with a mean rainfall of 0.5 inch on 400 mi^2. The combined Eqs. 15 and 17 were used in the calculations. Obviously, T has practically no effect upon E in the 1955-1959 equation. Also, this equation estimates larger sampling errors for a given gage density, and the difference becomes greater with increasing storm duration.

Table 43. Comparison of effect of T-change between 1955-1959 and 1960-1964 equations for P = 0.5 in and A = 400 mi^2.

Gage density (mi^2/gage)	Sampling error (in) for given period			
	1-hour storm		24-hour storm	
	1955-1959	1960-1964	1955-1959	1960-1964
25	0.02	0.02	0.02	0.01
50	0.04-	0.03	0.04+	0.02
100	0.07	0.06	0.07-	0.03
200	0.14	0.10	0.13	0.05
400	0.26	0.18	0.25	0.09

Examination of the distribution of storm durations between the two sampling periods showed a substantial difference. A higher percentage frequency of short duration storms ($\leq$ 3 hours) occurred in 1960-1964. However, these differences do not necessarily explain why storm duration was a more important factor in determining sampling errors in the 1960-1964 storms. No satisfactory explanation has been found for this differential effect between the two periods.

In an effort to obtain an explanation of the differences in sampling error obtained from the 1955-1959 and 1960-1964 equations, calculations were made of the average storm precipitation, storm duration, and sampling error for various gage densities in the two periods. Then, the standard deviation, index of skewness, and index of kurtosis were determined for each of the three parameters.

Results are illustrated in Table 44 for a gage density of 16 mi^2/gage (25 gages) on the 400 mi^2. In this table, average precipitation ($\bar{P}$) is based upon the 49 gages comprising the network. $\bar{T}$ is the average storm duration combining all storms in each sampling period, and $\bar{E}$ is the average sampling error for all storms combined. $\bar{E}$ is defined as the difference between the 49-gage mean, the best estimate of the true mean, and the 25-gage mean.

The average storm rainfall was nearly identical for the two periods, but the average sampling error was appreciably less in the 1960-1964 period, as reflected in Eqs. 15 and 17 derived from the data. Also, the standard deviation of the average sampling error is nearly equal in both periods. The lower value of $\bar{E}$ for 1960-1964 indicates a tendency for more uniform storm rainfall patterns than in 1955-1959, since $\bar{E}$ is dependent upon the difference between the 25-gage and 49-gage means. That is, the less dense network measured the mean rainfall more accurately in 1960-1964.

Table 44. Statistical comparisons of 1955-1959 and 1960-1964 storm data for May-September on ECIN.

Parameter	Mean	Standard deviation	Index of skewness*	Index of kurtosis*
		1955-1959		
$\bar{P}$ (inches)	0.30	0.41	2.74	9.37
$\bar{T}$ (hours)	5.34	7.14	2.87	10.57
$\bar{E}$ (inches)	0.010	0.013	2.48	6.77
		1960-1964		
$\bar{P}$ (inches)	0.29	0.48	3.92	25.72
$\bar{T}$ (hours)	3.84	4.82	2.69	9.27
$\bar{E}$ (inches)	0.007	0.013	5.74	46.99

*Positively skewed and leptokurtic in all cases.

Table 44 shows much higher values of skewness and kurtosis for $\overline{E}$ and $\overline{P}$ in the 1960-1964 sample, thereby indicating substantial differences in the distribution characteristics between the two 5-yr periods. Table 44 also shows that storms tended to last longer in 1955-1959 in which the average duration was 5.3 hours compared with 3.8 hours in 1960-1964; however, skewness and kurtosis were very similar. Based solely upon the duration means, one would have expected smaller errors in the 1955-1959 period, since the sampling error tends to decrease with storm duration, other factors being equal.

The foregoing statistics indicate that basic differences existed in the areal distribution of storm rainfall between the two sampling periods. These differences were then reflected in the sampling error relationships developed from the data for each period.

The next question is what caused the differences. The major difference revealed from further analyses was that air mass storms were more frequent in the 1955-1959 period. In this period, they accounted for 33% of the storms with mean rainfall of 0.01 inch or more compared with 23% in 1960-1964. There were 82 such storms in the earlier period and 54 in 1960-1964, or approximately 50% more in 1955-1959.

As shown by Huff and Shipp (1968), the spatial relative variability is considerably greater, on the average, in air mass storms than in frontal storms, squall lines, and low center storms. In general, air mass storms are more scattered spatially and are frequently characterized by steep rainfall gradients.

During 1955-1959, the number of frontal and squall line storms with areal means of 0.01 inch or more was 143 compared with 173, a ratio of 0.83. The lower percentage of these storms in the 1955-1959 period would have tended also to produce larger sampling errors of mean rainfall than in 1960-1964. Examination of the frequency of various rainfall types showed very similar distributions in the two periods, so it is concluded that this was not a major source of the observed differences.

The foregoing comparisons of sampling errors derived from consecutive 5-yr periods illustrate the differences that may arise from natural variations in the characteristics of the rainfall distributions between such sampling periods in the same sampling area. Consequently, one must interpret sampling error relations with caution when they are based upon sampling periods of 5 years or less. The evaluations made with the 1960-1964 sample serve only as quantitative approximations, although the trends indicated by the data are believed to be reliable.

Monthly and Seasonal Rainfall Sampling

The ECIN monthly totals for May-September, 1955-1966, were used, and the network was subdivided to provide data for areas of 50, 100, 200, and 400 mi^2. As a result of tests similar to those employed in the storm study, a monthly equation combining data from all four areas was rated best for the warm season results presented here. The equation has the same interpretation as Eq. 15 in the storm studies except that P_m is monthly rainfall in Eq. 18.

$$\text{Log } E = -1.3132 + 0.72 \text{ Log } P_m + 0.73 \text{ Log } G - 0.56 \text{ Log } A. \quad (18)$$

Table 45 illustrates the magnitude of the average sampling error in percentage of monthly rainfall during the warm season for selected values of P_m, G, and A. The 95-% envelopes of sampling errors (2 standard deviations) are approximately 2.5 times the values in Table 45.

Table 45. Comparison of average sampling errors in monthly rainfall.

Gage density (mi^2/gage)	Average sampling error (%) for given areal mean rainfall (inches)						
	0.5	1.0	2.0	4.0	6.0	8.0	10.0
				50 mi^2			
25	7	6	5	4	4	3	3
50	11	9	8	7	6	5	5
				100 mi^2			
25	5	4	3	3	2	2	2
50	8	6	5	5	4	4	4
100	11	10	9	7	7	6	6
				200 mi^2			
25	3	3	2	2	2	1	1
50	5	4	4	3	3	2	2
100	9	7	6	5	5	4	4
200	15	12	10	8	7	7	6
				400 mi^2			
25	2	2	2	1	1	1	1
50	4	3	3	2	2	2	2
100	6	5	4	3	3	3	3
200	10	8	7	5	5	4	4
400	16	14	11	9	8	8	7

The 12-yr sample on ECIN was used also to obtain an estimate of the seasonal sampling errors for the total May-September rainfall. The following equation was obtained:

$$\text{Log } E = -1.3892 + 0.54 \text{ Log } P_m + 0.76 \text{ Log } G - 0.47 \text{ Log } A. \quad (19)$$

Table 46 is similar to Table 45 and shows sampling errors of seasonal rainfall for selected values of the equation parameters. Eqs. 18 and 19 provide guidance in establishing raingage networks when user interest is primarily in monthly or seasonal totals. This would occur in certain hydrologic and agricultural applications. Emphasis may be placed on these periods also in evaluating precipitation modification operations that involve municipal water supplies or agriculture.

Table 46. Comparison of average sampling errors in seasonal rainfall.

Gage density (mi^2/gage)	Average sampling error (%) for given seasonal rainfall (inches)				
	10	15	20	25	30
			50 mi^2		
25	4	3	2	2	2
50	6	5	4	3	3
			100 mi^2		
25	2	1	1	<1	<1
50	3	2	2	1	1
100	5	4	3	3	2
			200 mi^2		
25	1	1	<1	<1	<1
50	2	2	1	1	<1
100	4	3	2	2	2
200	6	5	4	3	3
			400 mi^2		
25	<1	<1	<1	<1	<1
50	2	1	<1	<1	<1
100	3	2	2	1	1
200	4	3	3	2	2
400	7	5	4	4	3

Comparison of Storm, Monthly, and Seasonal Sampling Errors

Table 47 shows a comparison of average sampling errors for storm, monthly, and seasonal rainfall on the 400-mi^2 network in the May-September period, based upon Eqs. 15, 18, and 19. Storm durations span the range of those most frequently

observed in Illinois. The rainfall values were selected to encompass light, moderate, and heavy amounts. Gage density varies from relatively dense (25 mi^2/gage) to the approximate climatic network gage density in Illinois (200 mi^2/gage). Sampling errors are expressed as percentages of the storm, monthly, or seasonal mean rainfall as measured by the 49-gage network.

Table 47. Comparison of average sampling errors in May-September rainfall on 400 mi^2 for selected time intervals.

Gage density (mi^2/gage)	Error (%) for given 1-hour rainfall (inches)			
	0.1	0.5	1.0	2.0
25	6	4	3	2
100	20	13	9	7
200	35	20	16	13
	Error (%) for given 6-hour rainfall (inches)			
	0.1	0.5	1.0	2.0
25	4	3	2	2
100	13	8	6	5
200	24	14	11	9
	Error (%) for given 24-hour rainfall (inches)			
	0.1	0.5	1.0	2.0
25	3	2	1	1
100	10	6	5	4
200	18	10	8	7
	Error (%) for given monthly rainfall (inches)			
	1.0	2.0	4.0	8.0
25	2	2	1	1
100	5	4	3	3
200	8	7	5	4
	Error (%) for given seasonal rainfall (inches)			
	10	15	20	30
25	<1	<1	<1	<1
100	3	2	2	1
200	4	3	3	2

Table 47 provides quantitative estimates of the variation of sampling error with changes in gage density, rainfall volume, and time interval included in the rainfall measurements. The expected trend for the average sampling error to decrease with increasing duration of rainfall is evident. The average error becomes small in all rainfall groups for seasonal rainfall, as shown by values less than 5% even for the climatic network density. The seasonal sampling errors with 200 mi^2/gage are equivalent to those for 25 mi^2/gage in 6-hour storms. Table 47 illustrates well how the sampling requirements decrease as the time integration of rainfall increases on a fixed sampling area.

Rainfall Rate Sampling Errors

Table 48 illustrates the magnitude of the sampling error when the time interval of measurement is reduced to 1-minute, so that a close approximation of the instantaneous rate in a storm unit is obtained. The rainfall rate values in this table were calculated from Eq. 20 which was derived from warm season storms on the 1952-1953 special network of 50 gages on 100 mi^2 (Huff, Shipp, and Schickedanz, 1969). In this equation,

$$\text{Log } E = -1.522 + 0.87 \text{ Log } R + 0.52 \text{ Log } G \qquad (20)$$

R is rainfall rate in inches/min., G is gage density in mi^2/gage, and E is the average sampling error in inches. For comparison purposes, Table 48 also includes sampling errors for a 3-hour storm, monthly, and seasonal rainfall on an area of 100 mi^2.

Storm Sampling Errors on Larger Areas

The Shawnee network, which includes over 50% of the SHLEN area in Fig. 1, differs from the other Illinois networks in that it is subject to relatively large variations in annual precipitation within its boundaries. These variations are apparently related to sudden changes in elevation between the Mississippi River Valley and the steep bluffs to the east. In fact, the network was installed to study this effect that has been noted in long-term weather records in the region. As a result of this condition, the spatial variability in SHLEN storms tends to be greater than in the flatland storms. Consequently, one would expect that a more dense network would be required in the SHLEN area to maintain a given level of sampling error.

The expected trend was found in the 3-yr sample. Table 49 shows average sampling errors for storms in the May-September period for selected gage densities and storm durations, based upon the 3-yr sample of 215 storms. The SHLEN equation obtained from this data is

$$\text{Log } E = -2.4437 + 0.71 \text{ Log } P + 0.71 \text{ Log } G - 0.11 \text{ Log } T. \qquad (21)$$

Table 48. Comparison of average sampling errors in May-September rainfall on 100 mi^2 for selected time intervals

Gage density (mi^2/gage)	Sampling error (%) for given 1-minute mean rate (in/hr)			
	0.1	0.5	1.0	5.0
25	42	33	29	23
50	59	46	42	33
100	84	66	60	46
	Sampling error (%) for given 3-hour storm rainfall (in)			
	0.1	0.5	1.0	2.0
25	10	6	4	3
50	17	10	8	6
100	30	17	13	11
	Sampling error (%) for given monthly rainfall (in)			
	1.0	2.0	4.0	8.0
25	4	3	3	2
50	6	5	5	4
100	10	9	7	6
	Sampling error (%) for given seasonal rainfall (in)			
	10	15	20	30
25	2	1	1	<1
50	3	2	2	1
100	5	4	3	2

Table 49. Average sampling errors on SHLEN in May-September storms.

Gage density (mi^2/gages)	Storm duration (hrs)	Sampling error (%) for given mean rainfall (in)			
		0.1	0.5	1.0	2.0
50	1	11	7	6	5
	6	9	6	5	4
	24	8	5	4	3
100	1	19	12	10	8
	6	15	10	8	6
	24	13	8	7	5
200	1	30	19	16	13
	6	24	16	13	11
	24	21	13	11	9
400	1	49	31	26	21
	6	41	26	21	17
	24	35	22	18	15

Summary and Conclusions

Data from dense networks of raingages in Illinois were used to investigate sampling errors in the measurement of areal mean precipitation on areas of 50 to 550 mi^2. Tests of several data transformations on storm data indicated a slight superiority for logarithms, followed closely by cube roots. Average sampling errors obtained from equations using logarithms and cube roots were only slightly different.

Storm sampling error was found to increase with increasing areal mean precipitation and to decrease with increasing sampling density (gages per unit area) and storm duration. Relatively large differences were found frequently in the sampling errors between storms of apparently similar characteristics. This emphasizes the difficulty in predicting sampling errors for specific storms with a given sampling density. The interstorm variability results from the dependency of the sampling error upon numerous factors, some of which cannot be readily expressed in mathematical terms.

Other factors being equal, air mass storms require the greatest sampling density among synoptic storm types to maintain a given error level. In the warm season, rainshowers and thunderstorms were found to require nearly twice as many gages as steady rain for a given measurement reliability. Also, the May-September sampling density requirements are two to three times those needed in the October-April period.

Considerable difference in the magnitude of storm sampling errors during the May-September period was found between consecutive 5-yr periods on the same network. Analyses indicated that the difference resulted partially, at least, from a much higher number of air mass storms in one period. Consequently, one must interpret sampling error relations with caution when they are based upon observational periods of 5 years or less.

Sampling requirements for the measurement of monthly and seasonal rainfall are less stringent than for storm precipitation. With seasonal rainfall and a relatively sparse density of 200 mi^2/gage, the average sampling error was found to be less than 5% for the enitre range of seasonal rainfalls. For a 6-hour rainfall with a mean of 0.5 inch, the average error is 14%. Thus, substantial decreases in sampling requirements occur as the time integration of rainfall increases on a fixed sampling area.

Conversely, exceptionally dense sampling networks are required for the accurate measurement of areal mean rainfall rate. Thus, for a moderate 1-minute rate of 0.5 in/hr, the average sampling error in warm season storms on a sampling area of 100 mi^2 increases from 33% with 25 mi^2/gage to 66% with 100 mi^2/gage. As pointed out in an earlier report (Huff, Shipp, and Schickedanz, 1969), if rainfall rate is to serve as a verification tool in weather modification experiments, efforts must be made to utilize a combination of radar and raingages to evaluate short-period rate properties and their changes in space and time within midwestern convective storms.

The analytical results and relations presented here may be used as a guide in the establishment of raingage networks in the Midwest and other areas of similar precipitation climate.

PRECIPITATION DETECTION ON FIXED SAMPLING AREAS

Introduction

Questions have been raised concerning the frequency and intensity of storms so small that they are undetected by the raingage networks normally used for climatological and hydrological purposes. This study attempts to answer such questions by employing data from several raingage networks of various density on fixed sampling areas of 10 to 550 mi^2. The network records range in length from 9 to 12 years.

Network Data Used

Data from the 10-gage Boneyard Network on 10 mi^2 in the urban area of Champaign-Urbana, Illinois (Fig. 25) were used to develop relations for areas of this size. The period of record used in the study was 1955-1966 during which 1233 storms were recorded.

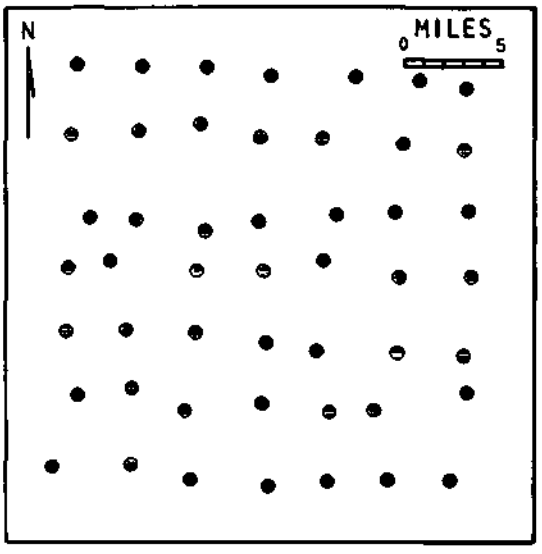

LITTLE EGYPT, 550 mi.^{2}

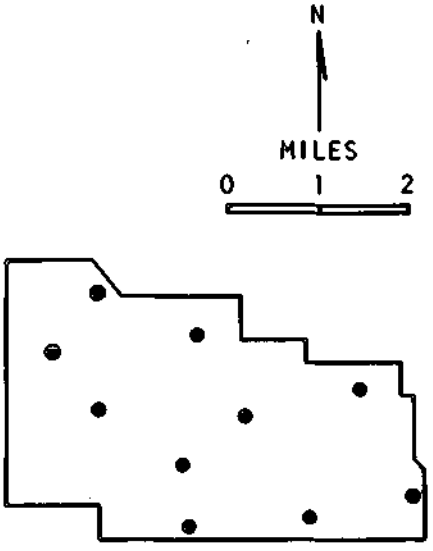

BONEYARD, 10 mi.^{2}

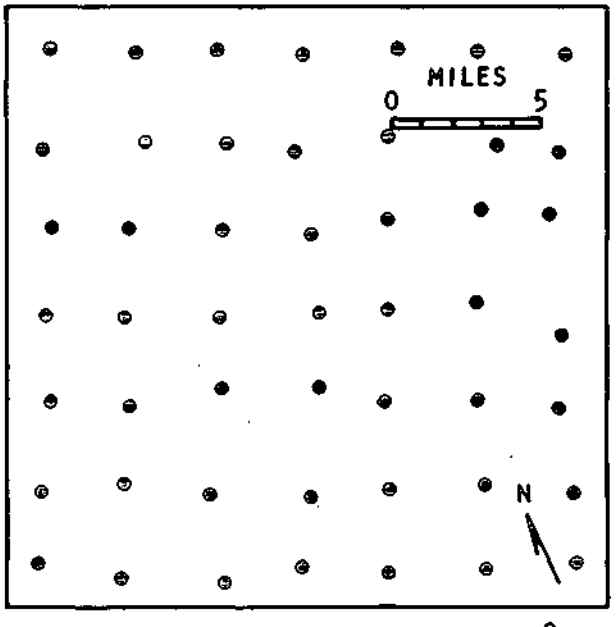

EAST-CENTRAL ILLINOIS, 400 mi.^{2}

Figure 25. Sampling networks for detection study.

Data from 1344 storms for the period, 1955-1966, on the East Central Illinois Network of 49 recording raingages in 400 mi^2 (1 gage per 8 mi^2) were used to investigate the areal extent of storms in areas of 50, 100, 200, and 400 mi^2. Square-shaped subareas of 50, 100, and 200 mi^2 were established in the central part of the network.

Data from the Little Egypt Network in southern Illinois were used to investigate the areal extent of precipitation on 550 mi^2. This 49-gage network provided approximately 1200 storms in the 9-yr period, 1958-1966.

Method of Analyses

The analyses were based upon the assumption that all precipitation areas are detected by the dense networks described above. Data from radar observations of storm dimensions, such as those of the Thunderstorm Project (Byers and Braham, 1949), indicate that very few storms, if any, would be unrecorded by these networks. If occasionally extremely small shower cells should elude all gages, they would produce network mean rainfall in the trace category.

All recorded storms were used in which one or more gages recorded 0.01 inch or more. In each storm on each network, the gage density was gradually reduced until only one gage near the center of the network remained to determine the detection capability. In selecting groups of gages for the various densities on the six networks, the spatial distribution was kept as uniform as possible. The various density of gages used on each network is shown in Table 50. For each density, a simple "yes" or "no" entry was made on a tabulation sheet. The network mean rainfall, based on all network gages, also was tabulated for later data grouping.

Table 50. Gage groups used in detection analyses.

Sampling area (mi^2)	Number of groups	Number of gages in groups
10	5	1, 2, 3, 5, 10
50	5	1, 2, 3, 5, 9
100	5	1, 2, 4, 8, 16
200	6	1, 2, 4, 8, 16, 25
400	7	1, 2, 4, 8, 16, 25, 49
550	7	1, 2, 3, 6, 12, 24, 49

The tabulated data were first subdivided according to network mean rainfall into the following groups: trace, 0.01-0.05 inch, 0.06-0.10 inch, 0.11-0.15 inch, 0.16-0.20 inch, 0.21-0.30 inch, 0.31-0.40 inch, 0.41-0.50

inch, and over 0.50 inch. Inspection of the tabulation sheets showed that all storms with network mean exceeding 0.40 inch had been detected by the minimum 1-gage density on all sampling areas. Every storm with a mean exceeding 0.20 inch was detected on all sampling areas (10-550 mi^2) by all except the minimum 1-gage network. Only three storms with means over 0.10 inch were undetected by other than the 1-gage network on the six sampling areas. Since the sample exceeded 1200 storms on two sampling areas and 1300 storms on four areas, the three undetected storms constitute an insignificant percentage of the nearly 8000 samples.

As the next step, curves were constructed from the tabulations to show the relation between cumulative percentage of detected storms and gage density for each sampling area. Separate probability curves were constructed for network mean precipitation of a trace, 0.01-0.05 inch and 0.06-0.10 inch. Since the detection capability was nearly 100% on all areas ranging from 10 to 550 mi^2 for network means exceeding 0.10 inch and more than one gage per sampling area, probability curves were not drawn for these situations. Curves were constructed for all storms combined and for storms further subdivided according to season.

Since the data analyses indicated the detection problem maximizes in summer and minimizes in winter, further discussion will be restricted to these two seasons. The annual curves merely reflected an average of the seasonal detection statistics. An example showing the summer plots for 400 mi^2 is given in Fig. 26. The number of summer storm samples ranged from 350 to 500 among the networks and the winter samples from 210 to 265.

Results of Analyses

Further examination of the individual detection curves for each sampling area showed that the results could be represented most accurately and conveniently by an exponential relation between size of sampling area and gage density for a given probability of storm detection. This has been done in Fig. 27 for detection capabilities of 80% to 99% for appropriate mean precipitation groups in summer and winter. These curves can then be used as a guide in determining sampling requirements for precipitation detection under midwestern climatic conditions. Gage density requirements for a detection capability below 80% have been omitted, since it is extremely doubtful that potential users would find a network acceptable that left 20% of the storms undetected. Only one curve is shown for winter since the number of "trace" storms was too few to derive a reliable probability curve, and only one storm with mean exceeding 0.05 inch was undetected on any of the six sampling areas.

Application of Fig. 27 can perhaps best be illustrated by an example. Assume that a cloud seeding experiment is being conducted during the summer in Illinois and that the investigators specify 99% detection of all rainstorms in a target area of 400 mi^2 as one of their verification needs. Then, referring to the family of summer "trace" curves, one finds that a density of one gage per 12 mi^2 would be required. If the user would be satisfied with detecting 90% of all storms, the gage density would lower to one gage per 20 mi^2. Now, if the user could limit his detection requirements to 99% detection of storms with

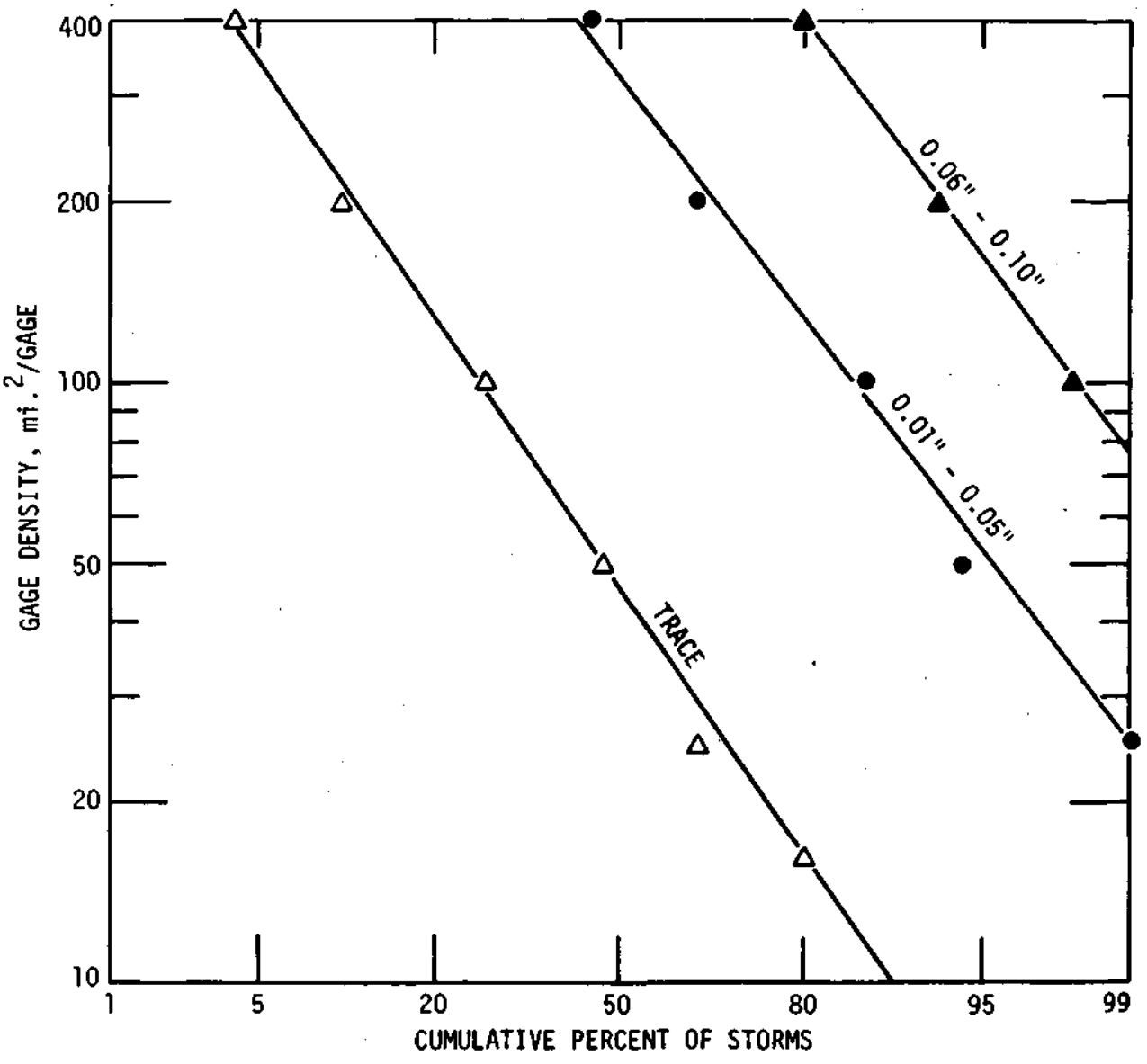

Figure 26. Summer distributions on 400 mi^2.

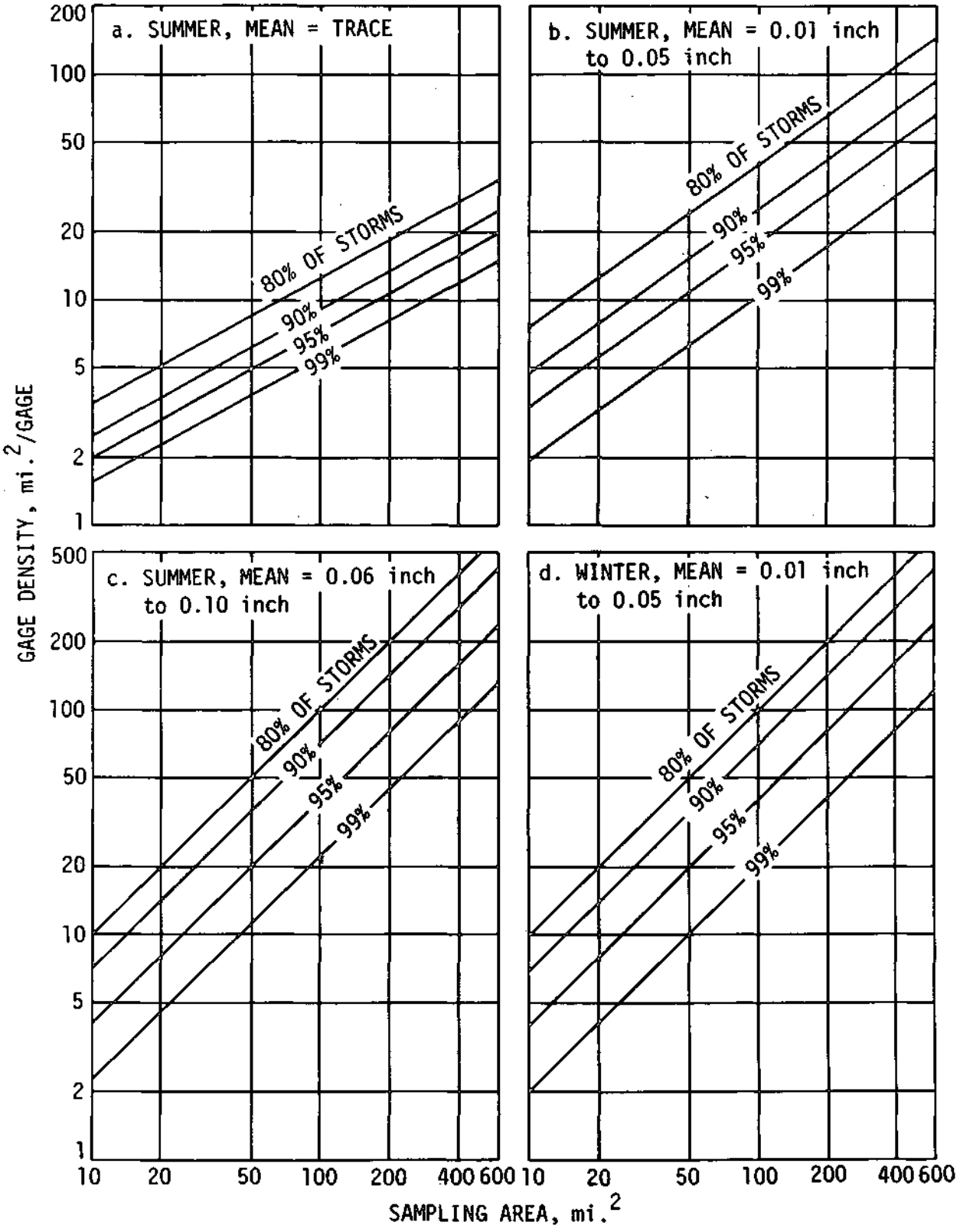

Figure 27. Sampling requirements for precipitation detection.

areal means exceeding 0.05 inch, the summer curves for 0.06-0.10 inch show a required density of only one gage in 90 mi^2. However, this density is still considerably greater than the normal climatic network density which averages approximately one gage per 225 mi^2 in Illinois. The foregoing examples illustrate how sharply the sampling requirements lower as the minimum storm intensity is increased.

The winter curves in Fig. 27 show how much sampling requirements are lowered in the cold season when storms tend to be more widespread and the precipitation much more frequently of the stable type compared with summer. Thus, if one is satisfied with 99% detection of all storms with means exceeding 0.01 inch in winter, the 400 mi^2 density requirement is one gage per 80 mi^2 compared with one gage per 30 mi^2 in summer under the same detection requirement. The winter curves for 0.01 to 0.05 inch are nearly identical with the summer curves for 0.06 to 0.10 inch.

AREAL EXTENT OF STORM PRECIPITATION ON FIXED SAMPLING AREAS

Introduction

Another factor of importance in the determination of measurement requirements on fixed sampling areas is the areal extent of storm precipitation. This is a primary concern when knowledge of the distribution characteristics of light amounts and storms of small areal extent is pertinent. Hydrometeorological studies in Illinois with dense raingage networks have shown that convective storms of small areal extent, such as summer air mass showers, are occasionally not recorded by sampling densities several times greater than those of the normal climatic network.

As part of our investigation of precipitation measurement requirements, a study was made of the areal extent of storm precipitation on fixed sampling areas of 10 to 550 mi^2. This study was accomplished through the use of data from dense networks in Illinois with records ranging from 9 to 12 years in length, as described in the previous section on precipitation detection. The results should be useful to those engaged in weather modification experiments, particularly if warm season, air mass showers are to be seeded and storm precipitation measurements used in verification procedures. The information should be useful also for various climatological purposes.

Analytical Procedures

The precipitation data were grouped according to season and areal mean precipitation. All storms were used in which one or more of the raingages recorded measurable precipitation. It was assumed that the dense network of gages was adequate to detect all storms with measurable precipitation in the

sampling area. Based upon published information on rain cell sizes (Byers and Braham, 1949) and Illinois studies of storm characteristics and sampling requirements (Huff and Neill, 1957), this assumption should not result in substantial errors in the findings. The major possibility of error would be in the underestimation of the number of cases with "trace" averages in summer, and these are the least important category in the study.

After considerable experimentation with the data samples, it was decided to group the data into the class intervals of areal mean precipitation listed below:

Trace	0.16"-0.20"	0.51"-0.75"
0.01"-0.05"	0.21"-0.30"	0.76"-1.00"
0.06"-0.10"	0.31"-0.40"	Over 1.00"
0.11"-0.15"	0.41"-0.50"	

These class intervals are small enough so that the spatial distribution characteristics do not vary significantly with them; at the same time, they usually provide an adequate sample in the most important class intervals to construct a reliable probability curve. For each season and for all seasons combined, the number of storms in each class interval was then tabulated to show the percentage of the area enveloped by precipitation.

From the tabulated data, frequency distribution curves were constructed in which the cumulative percentage of storms was related to the percentage of the area enclosed by precipitation. This was done for each mean precipitation group on each sampling area for each season and all seasons combined. Fig. 28 illustrates the plotting method on the sampling area of 400 mi^2 for several mean precipitation groups in which all seasonal data have been combined to obtain mean annual curves. The log normal distribution shown here provided the best overall fit throughout the numerous data groups.

From the frequency distribution curves for the six sampling areas, curves were constructed to show the areal extent relationship with increasing area in each mean precipitation group. An example of average annual curves for mean precipitation of 0.01 to 0.05 inch is shown in Fig. 29. For a given sampling area, the family of curves shows the relation between the minimum percentage of sampling area enveloped by precipitation and the percentage of all network storms. Thus, Fig. 29 shows that for a sampling area of 100 mi^2, 20% of the storms, on the average, will envelop 100% of the area. Similarly, 50% of the storms will envelop 75% or more of the 100 mi^2, and 95% of the storms will enclose at least 21% of the sampling area.

Results of Analyses

The relationship in the various data groups was found to be closely approximated by the logarithmic fitting illustrated in Fig. 28. From these curves, Tables 51 to 61 have been constructed to summarize conveniently the areal extent relationships for various data groupings.

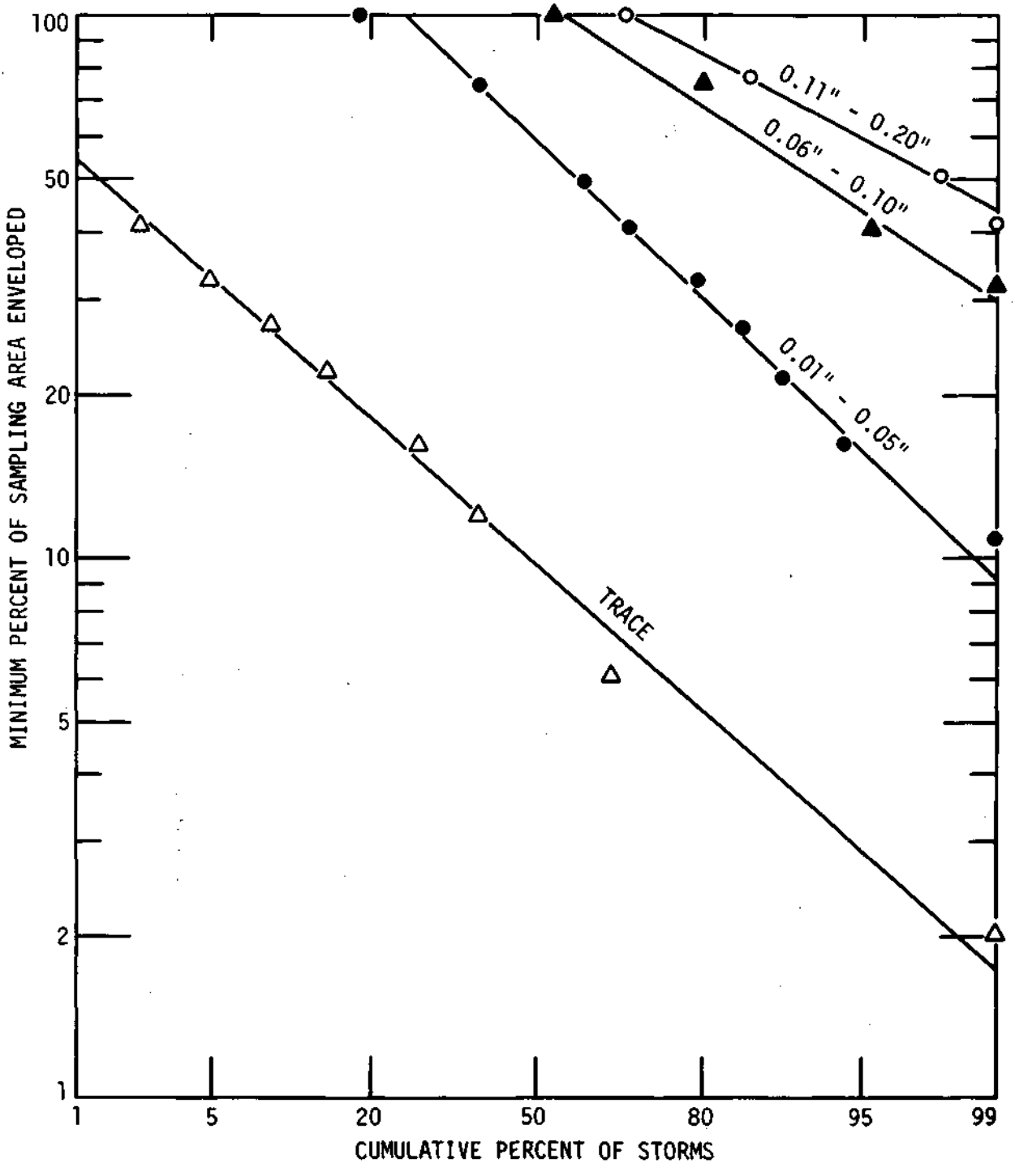

Figure 28. Frequency distribution of storm areal extent on 400 mi^2 network.

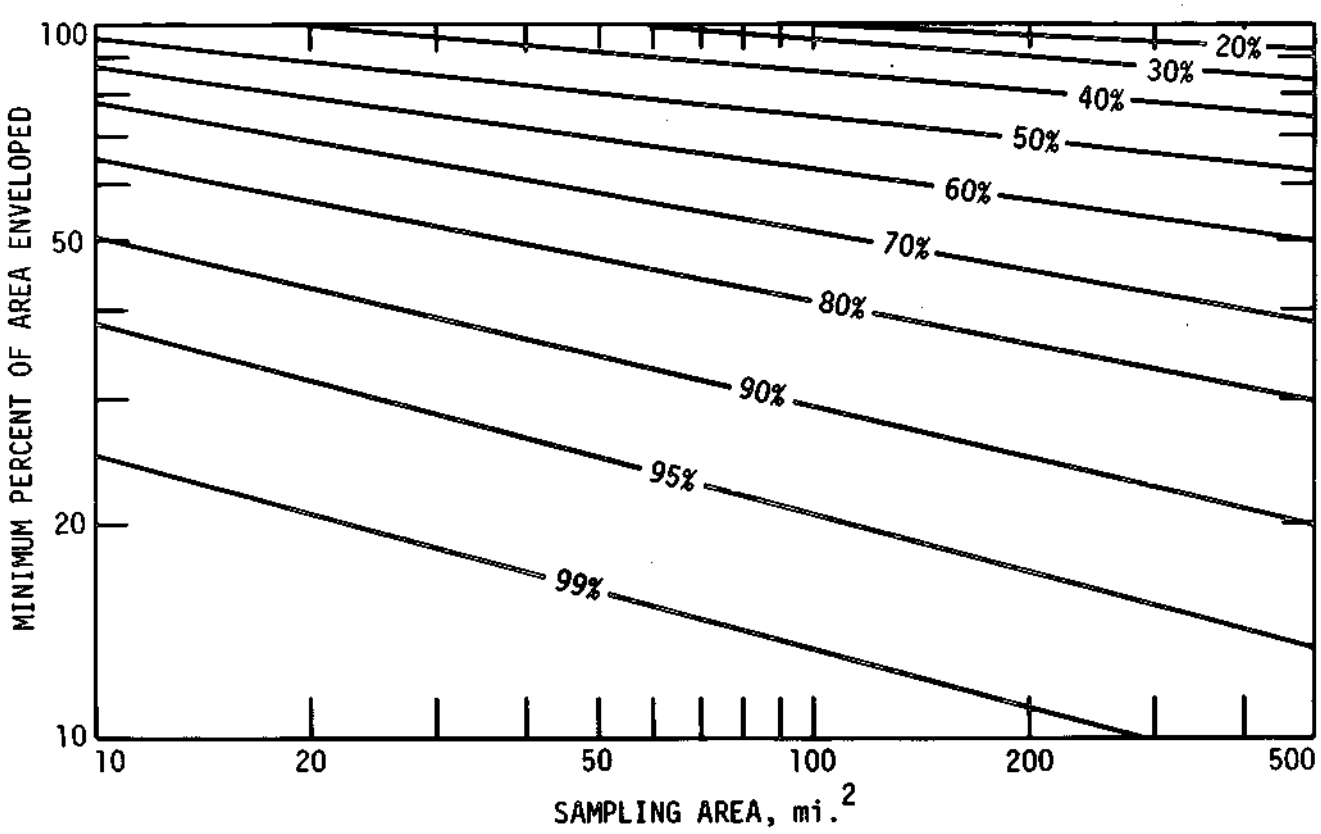

Figure 29. Relation between storm areal extent and size of sampling area for mean precipitation of 0.01 to 0.05 inch.

Tables 51 to 55 show average annual relations based upon the total storm sample for mean precipitation groups through 0.21 to 0.30 inch. For heavier precipitation, the number of storms in which the entire sampling area was not subject to precipitation was too few to construct a reliable frequency distribution. For example, in the range of 0.31 to 0.50 inch there were no storms with less than 100% coverage on the sampling area of 10 mi^2, less than 1% on the 200 mi^2, 9% on the 400 mi^2, and approximately 15% on the 550 mi^2. However, the 15% on the 550 mi^2 includes only 10 storms or less than 1% of the total sample of over 1200 storms.

Tables 56 to 59 show summer relations for mean precipitation groups having sufficient cases with less than 100% coverage, and Tables 60 and 61 present appropriate winter relations. Spring and fall relations have been omitted since their values are between those for summer and winter. Also, traces have been omitted in the summer and winter relations. The summer distributions are very similar to the annual and winter traces with less than 100% areal coverage were too infrequent to derive a relation.

Table 51. Areal extent distribution in all storms with sampling area means of trace.

Percent of storms	Minimum percent of area enveloped for given sampling area (mi^2)					
	10	50	100	200	400	600
10	64	42	35	29	25	22
20	52	33	28	22	18	16
30	41	26	21	17	14	13
40	32	20	17	14	11	10
50	25	16	14	11	9	8
60	22	14	12	9	8	7
70	19	12	10	8	7	6
80	16	10	8	7	6	5
90	14	8	7	6	5	4
95	12	7	6	5	4	3
99	10	6	5	4	3	3

Table 52. Areal extent distribution in all storms with sampling area means of 0.01 to 0.05 inch.

Percent of storms	Minimum percent of area enveloped for given sampling area (mi^2)					
	10	50	100	200	400	600
10				100	100	100
20			100	96	94	91
30		100	96	90	86	83
40	100	92	86	80	76	73
50	96	80	74	69	64	61
60	87	70	62	58	52	48
70	78	59	51	46	40	37
80	65	47	41	36	31	28
90	50	35	29	25	21	19
95	38	25	21	17	14	13
99	25	17	13	11	9	8

Table 53. Areal extent distribution in all storms with sampling area means of 0.06 to 0.10 inch.

Percent of storms	Minimum percent of area enveloped for given sampling area (mi^2)					
	10	50	100	200	400	600
50					100	100
60				100	96	90
70		100	100	92	84	78
80	100	94	85	76	68	63
90	95	73	65	57	52	48
95	81	59	52	46	40	37
99	60	44	39	34	30	28

Table 54. Areal extent distribution in all storms with sampling area means of 0.11 to 0.20 inch.

Percent of storms	Minimum percent of area enveloped for given sampling area (mi^2)					
	10	50	100	200	400	600
60					100	100
70				100	93	87
80			100	92	84	78
90		100	91	82	74	69
95	100	86	78	70	63	60
99	80	60	54	48	42	39

Table 55. Areal extent distribution in all storms with sampling area means of 0.21 to 0.30 inch.

Percent of storms	Minimum percent of area enveloped for given sampling area (mi^2)					
	10	50	100	200	400	600
80					100	100
90			100	100	83	74
95		100	98	83	69	63
99		86	72	59	49	44

Table 56. Areal extent distribution of summer storms with sampling area means of 0.01 to 0.05 inch.

Percent of storms	Minimum percent of area enveloped for given sampling area (mi^2)					
	10	50	100	200	400	600
10		100	95	88	82	79
20		90	82	75	69	66
30	100	78	71	64	58	54
40	90	69	62	55	49	46
50	82	61	53	46	41	38
60	71	52	46	40	35	33
70	57	42	36	32	28	26
80	43	32	28	24	21	20
90	29	22	19	17	15	14
95	20	15	13	11	10	9
99	16	12	10	9	8	7

Table 57. Areal extent distribution of summer storms with sampling area means of 0.06 to 0.10 inch.

Percent of storms	Minimum percent of area enveloped for given sampling area (mi^2)					
	10	50	100	200	400	600
30					100	100
40			100	100	92	88
50		100	97	89	82	78
60		95	86	77	69	66
70	100	82	74	66	59	56
80	93	68	60	53	46	43
90	75	55	48	42	37	34
95	60	44	38	33	29	26
99	48	35	31	27	24	22

Table 58. Areal extent distribution of summer storms with sampling area means of 0.11 to 0.20 inch.

Percent of storms	Minimum percent of area enveloped for given sampling area (mi^2)					
	10	50	100	200	400	600
70			100	100	100	100
80		100	97	89	82	78
90	100	87	80	73	67	64
95	86	67	60	54	49	46
99	63	48	43	38	34	32

Table 59. Areal extent distribution of summer storms with sampling area means of 0.21 to 0.30 inch.

Percent of storms	Minimum percent of area enveloped for given sampling area (mi^2)					
	10	50	100	200	400	600
70					100	100
80				100	89	80
90		100	100	87	73	66
95		99	83	70	59	53
99	100	67	56	46	38	34

Table 60. Areal extent distribution in winter storms with sampling area means of 0.01 to 0.05 inch.

Percent of storms	Minimum percent of area enveloped for given sampling area (mi^2)					
	10	50	100	200	400	600
30				100	100	100
40			100	98	96	94
50	100	100	94	89	85	82
60	96	85	81	76	72	70
70	86	74	69	64	60	58
80	76	62	56	51	46	44
90	60	46	41	37	33	31
95	50	37	33	29	25	23
99	40	28	23	20	17	15

Table 61. Areal extent distribution in winter storms with sampling area means of 0.06 to 0.10 inch.

Percent of storms	Minimum percent of area enveloped for given sampling area (mi^2)					
	10	50	100	200	400	600
70					100	100
80		100	100	100	94	91
90		97	90	84	78	74
95	100	85	77	72	66	63
99	67	56	52	48	45	43

SAMPLING REQUIREMENTS IN THE VERIFICATION OF PRECIPITATION MODIFICATION EXPERIMENTS

This section describes an investigation of the use of storm mean precipitation in the verification of weather modification experiments. Analyses were based upon the 12-year sample of 1344 storms from the East Central Illinois Network. Areal mean and areal maximum precipitation were selected as the verifying parameters.

The primary purpose of this study was to use highly accurate measurements of the natural time and space distribution of storm precipitation to ascertain the efficacy of various statistical designs which have potential applicability in verifying the results of precipitation modification experiments in the Midwest. It was desired also to establish the theoretical frequency distribution(s) that should be used in fitting storm precipitation data in the midwestern type of climate. Frequently, cloud seeding is not conducted on all types of storms, and seeding selectivity is likely to increase as knowledge advances in the science of weather modification. Consequently, it was deemed desirable to evaluate sampling requirements when the precipitation data are stratified according to season, precipitation type, storm type, and precipitation intensity.

Analytical Procedures

Areal mean precipitation was determined for those storms which had measurable amounts recorded at one or more raingages in the network ($\geq$ 0.01). Areal means for the qualifying storms were then stratified into storms with means greater than 0.005 inch (trace), 0.10 inch, 1.00 inch, and $\geq$ 0.01 inch. In addition, the maximum point rainfall was determined for all qualifying storms. These data were then stratified into warm and cold season storms, and into seven synoptic types and three precipitation types. For details on the method of classifying precipitation and synoptic types, the reader is referred to Huff (1967a).

Next, theoretical frequency distributions were fitted to the above data and the distributions used to obtain sample size requirements for five statistical designs using the various types of data. These designs included: (1) random experimental which involves randomization of days over a single target area into seeded and non-seeded days with non-seeded days being the control; (2) random historical in which a random choice is made of days to be seeded over a single target with the historical record as control; (3) continuous historical in which all rain days within a given stratification are seeded, with the historical record as control; (4) cross-over target-control which requires seeding a target chosen at random with another area being the control (random interchange of target and control); and (5) fixed target-control in which all potential rain days are seeded in a fixed target area with a nearby area serving as a fixed control.

In the statistical studies, both the non-classical (sequential) and the classical (non-sequential) analyses were employed. The components of the particular test being used were computed for the non-seeded distributions; then, with assumed changes in the distributional parameters, the sample size was computed through algebraic relations. These values were computed for the log-normal 1- and 2-sample tests and for the Gamma 2-sample tests.

Theoretical Frequency Distributions

The log-normal distribution was fitted to the various data types shown in Table 62. A non-truncated log-normal distribution was used for the samples of mean storm rainfall $\geq$ 0.005 inch, storm mean rainfall in which gage amounts were

Table 62. Probability values for the goodness-of-fit test for the log-normal distribution.

Stratification	Probability level (a) for "goodness-of-fit" Areal mean rainfall for qualifying storms* Means ≥.005	Means >.10	Means >1.00	Gage amounts ≥.01	Maximum point storm rainfall
Warm season storms	<.01	<.01	.04	<.01	<.01
Synoptic type					
Low centers	.36	>.20	>.20	.18	.12
Air mass	.41	.64	>.20	.25	<.01
Cold fronts	.15	.43	>.20	.26	.02
Warm fronts	.04	.23	>.20	.16	.19
Occluded fronts	>.20	>.20	**	>.20	.18
Stationary fronts	.42	.10	.19	.23	<.01
Squall lines	.03	>.20	>.20	<.01	<.01
Precipitation type					
Steady rain	.73	>.20	>.20	.35	.46
Rain showers	.15	.71	>.20	.51	.13
Thunderstorms	<.01	.02	.08	.02	.01
Cold season storms	.04	.76	.59	.01	<.01
Synoptic type					
Low centers	>.20	.73	>.20	.09	.62
Air mass	.15	>.20	**	>.20	>.20
Cold fronts	.04	.09	>.20	.03	.14
Warm fronts	.20	>.20	**	.21	.02
Occluded fronts	.22	>.20	**	.54	.85
Stationary fronts	.75	>.20	>.20	.93	.30
Squall lines	>.20	>.20	>.20	>.20	>.20
Precipitation types					
Steady rain	.08	.44	>.20	.10	.20
Rain showers	<.01	<.01	>.20	<.01	.05
Thunderstorms	.54	.10	>.20	.43	.40

* Storms which had trace amounts for at least one gage in network.

** Sample size too small for computation.

greater than 0.01, and for maximum point rainfall. However, for the stratified samples involving mean storm rainfall greater than 0.10 and 1.00 inch, a truncated distribution was obtained by making the transformation (× - 0.10) and (× - 1.00) on the truncated samples of areal mean rainfall greater than 0.10 and 1.00 inch, respectively. The log-normal mean and variance were then estimated from the transformed samples in each case.

The Kolmogorov-Smirnov goodness-of-fit test was applied when sample sizes were equal to or greater than 40 (Schickedanz et al., 1969). The resulting probability levels (size of the test) are shown in Table 62. When all warm season storms are considered as one sample, a poor fit was obtained for all five types of data. All probabilities were less than 0.01, except for areal mean rainfall greater than 1.00 inch, for which the probability was 0.04. When all cold season storms were grouped together in one sample, a good fit was obtained for means greater than 0.10 and 1.00 inch but poor fits were obtained for the other cases.

At this point, further analysis was restricted to precipitation and synoptic types which are more likely to be seeded during a rain modification experiment. A most likely candidate in the Midwest is the summer air mass storm which tends to be more isolated and slower moving than other synoptic types. This was the type of storm seeded in the Whitetop experiment (Braham, 1966). Among precipitati< types, the thunderstorm is the major source of water during the warm season. Since frontal storms are the major producer of warm season rainfall among the various synoptic types, cold fronts were selected for analysis. During the cold season, low centers and steady rain were selected, since they are major producers of winter precipitation in the Midwest. The average number of storms for each of these types is shown in Table 63, based upon the network sample of storms.

Table 63. Average number of storms expected for selected data types, storm types, and season (based on 12-yr sample).

	Storm type and season				
Storm rainfall	Air mass (warm)	Thunderstorms (warm)	Cold fronts (warm)	Steady rain (cold)	Low center (cold)
Areal mean ≥.005	12.4	27.6	13.0	19.6	26.6
Areal mean >.10	6.1	20.3	7.8	10.5	12.8
Areal mean >1.00	0.3	3.5	1.3	1.1	1.7
Areal mean for gages ≥.01	16.4	28.7	14.7	20.1	29.0
Maximum point rainfall	16.4	28.7	14.7	20.1	29.0

The gamma distribution was fitted to all cases shown in Table 63. A comparison of the gamma and log-normal goodness-of-fit probabilities are shown

in Table 64. For those cases in which the log-normal distribution did not fit (6 out of 25) the gamma distribution provided a good fit for three of these. The three cases were warm season thunderstorms (mean ≥0.005 and maximum rainfall) and warm season cold fronts (probabilities of 0.13, 0.11, and 0.39, respectively).

Altogether, the gamma distribution provided a poor fit for 13 out of 25 cases. This leaves 3 out of 25 cases in which poor fits were obtained for both the log-normal and gamma distributions. These were warm season thunderstorms (areal means ≥0.10, areal means for gages ≥0.01) and warm season air mass storms (maximum point rainfall).

Experimental Design and Tests of Hypothesis

The storm was used as the experimental unit in the various designs. The number of storms required to obtain significance in a rain modification experiment was computed for the various designs and tests. The normal 1-sample and 2-sample tests were used with all of the experimental designs. For purposes of sample size computations, it was assumed that all of the cases in Table 64 were log-normal distributed, although there were 6 out of 20 with probabilities less than 0.05. The following formula was used to obtain the number of observations required for the 2-sample non-sequential test (Davies, 1954):

$$N = \frac{2(\mu_\alpha + \mu_\beta)^2 S^2}{D^2} \qquad (22)$$

where:

μ_α = the normal deviate for α probability level
μ_β = the normal deviate for β probability level
D = the difference in means it is desired to detect
S^2 = the variance

Various increase of δ = 0.05, 0.10, 0.20, 0.40, 0.60, and 0.80 were assumed and applied to the non-transformed precipitation data. The corresponding scale change was affected on the transformed scale by the addition of the logarithm of $(1 + \delta)$. The variances were assumed to be equal, since the variance of the log-normal distribution is unaffected by scale changes in the variate. Equation 22 was then applied with S^2 equal to the variance of the logarithms and D equal to the logarithms of $(1 + \delta)$. For the 1-sample test of random historical design, Equation 22 is used directly to compute sample size. For the 1-sample test of continuous historical design, Equation 22 is divided by 2.0. With the experimental design, both samples must be obtained from the same area. Therefore, Equation 22 must be multiplied by 2.0.

Under the assumption of log-normal precipitation and equal log-normal variance in an area near the network area, the number of storms needed for the cross-over design involving the two areas can then be determined from Equation 23 (Schickedanz et al., 1969):

Table 64. Comparison of gamma and log-normal goodness-of-fit probabilities.

Storm rainfall (in)	Storm type and season: Air mass (warm)		Thunderstorms (warm)		Cold front (warm)		Steady rain (cold)		Low centers (cold)	
	L.N.	G.	L.N.	G.	L.N.	G.	L.N.	G.	L.N.	G.
Areal mean ≥.005	.41	<.01	<.01	.13	.15	<.01	.08	.03	>.20	<.01
Areal mean >.10	.64	.09	.02	<.01	.43	.62	.44	.02	.73	.15
Areal mean >1.00	>.20	>.20	.08	.87	>.20	>.20	>.20	>.20	>.20	>.20
Areal mean for gages >.01	.25	<.01	.02	<.01	.26	<.01	.10	<.01	.09	<.01
Maximum point rainfall	<.01	<.01	<.01	.11	.02	.39	.20	.13	.62	<.01

L.N. - Log-Normal
G. - Gamma

$$C = [(1 - R)S]/2 \quad (23)$$

where:

S = number of observations required for an experimental random design
R = the correlation coefficient between the two areas
C = the number of observations required for the cross-over design

For this study, the correlation coefficient (R) between network storm means in two adjacent areas was assumed to be 0.75. This value was based on a previous study of correlation between adjacent areas discussed elsewhere in this report. The number of storms required for the target-control design can then be computed from Equation 24 (Schickedanz et al., 1969):

$$TC = (1 - R^2)\ S \quad (24)$$

where:

R = correlation coefficient between the two areas
S = the number of observations required for the experimental design
TC = the number of observations required for the target-control design

Equations 22, 23, and 24 were applied to all data groups shown in Table 62 to obtain the number of storms required to obtain significance for the various designs and tests.

The results for a sequential test with the log-normal distribution can be obtained by using the sequential test method of Wald (1947) for the testing of the reduction of a mean from a normal distribution. All that is required is a slight modificaition to allow for the logarithms. To apply this test, one must assume that the historical record is indeed the population for each area. The equations for average sample number were applied to the data from the stratifications in Table 64, and the sample size computed for the random historical and continuous historical designs through use of the 1-sample test.

Sample sizes were also computed for the non-sequential gamma test in those cases in which the log-normal distribution did not fit. The number of observations required for the 2-sample, non-sequential gamma test is given by relations provided by Schickedanz et al., (1969). Using these relations, the number of storms required by the experimental random design was computed.

Sampling Requirements

Fig. 30 shows the number of storms required (detection ability) to obtain significance for a 20% increase in precipitation under assumed seeding effects

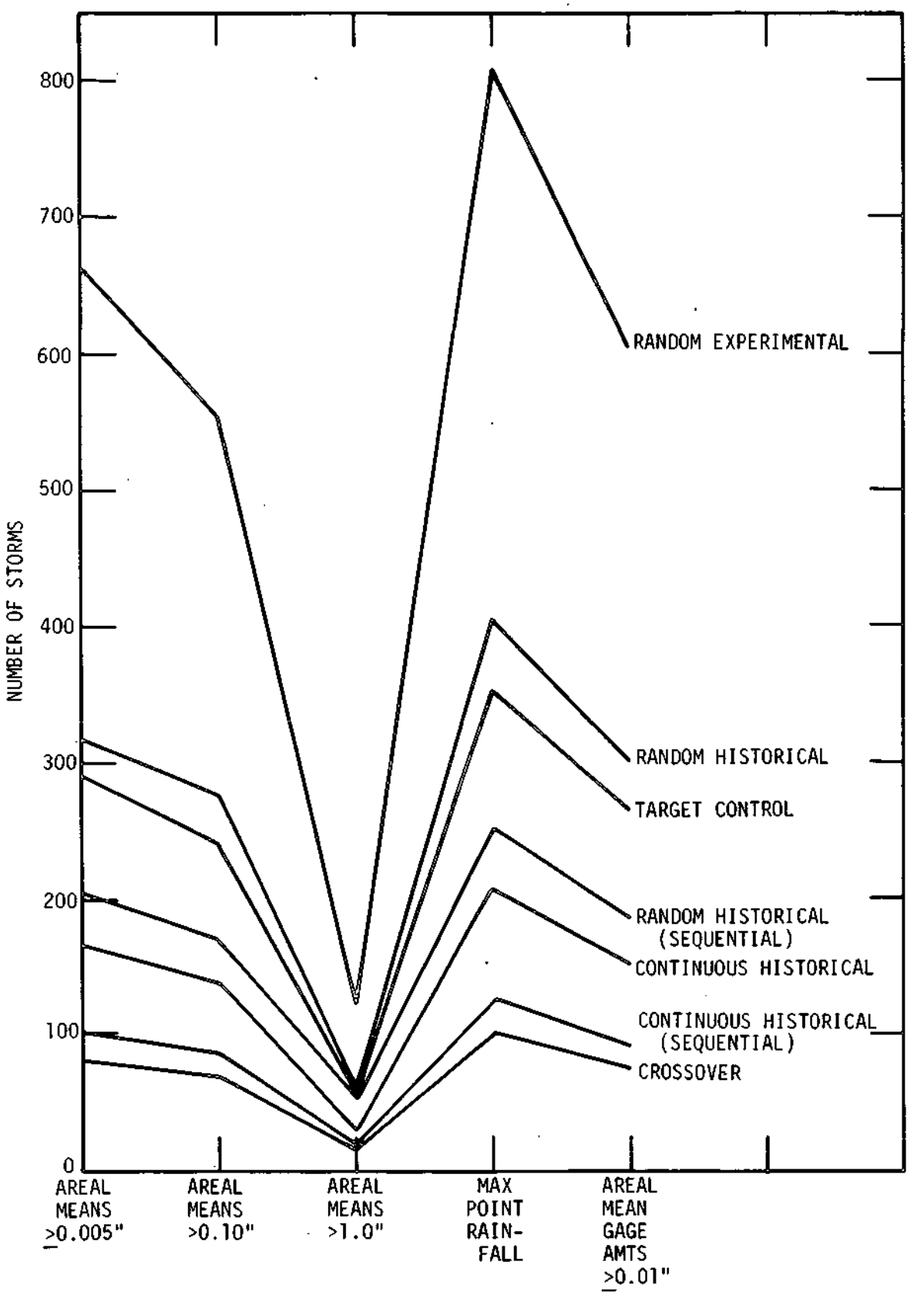

Figure 30. Number of storms required to obtain significance with 20% increase in warm season air mass storms ($\alpha = 0.05$, $\beta = 0.20$).

for various designs and data types for air mass storms. The graph suggests that the stratification of the areal means produced strata in which the storms were more homogeneous than the entire sample. This is reflected in the fact that fewer storms are required to detect a 20% increase with the samples in which means were greater than 0.01 and 1.00 inch than with the sample which included all means greater than 0.005 inch.

Approximately the same number of storms are required when all storms with areal means $\geq$ 0.005 inch are used as when areal means based on gage amounts > 0.01 inch are used. As the design becomes less efficient (requires more storms) the difference between types varies considerably. For example, the difference between maximum rainfall and all storms with means $\geq$ 0.005 inch for the cross-over design is only 18 storms (82 vs 100), whereas for the experimental-random design it is 144 storms (662 vs 806). A most important point brought out in Fig. 30 is that the choice of design in detecting a 20% increase in air mass storms is a very important factor. Although the random-experimental design requires the longest verification time, it should be noted that in the statistical sense, it is the most valid, since no historical data are required and practically no assumptions are violated.

Fig. 30 is a presentation of the detection ability of a particular design in relation to data type. However, the number of storms per year or season varies considerably among data types; therefore, one type of storm may have a high detection ability, and yet require a long time (real time) to obtain significance for a given increase in rainfall. Fig. 31 is a presentation of the number of years required to obtain significance based on the average number of storms per year from Table 63. In real time, the air mass sample of areal means > 1.00 inch requires the longest amount of time to obtain significance for a 20% increase because of the infrequent occurrence of storms of this magnitude. In this real time situation, the mean ($\geq$ 0.005 inch) and maximum rainfall are nearly the same for the cross-over design, but the maximum rainfall becomes a slightly better verifier than the mean as the design becomes less efficient.

At this point, it should be emphasized that the use of maximum rainfall as a verifying parameter is possible through use of a dense network (such as the East Central Illinois used here), which provides a reliable estimate of this parameter. In the normal climatic networks, measurement of the areal maximum would be too inaccurate for use. An excellent correlation between mean and maximum rainfall was obtained on our network of 49 gages in 400 mi^2 as shown in Table 65. Correlation coefficients, which are shown for various synoptic storm types in the warm season, range from a relatively high 0.86 for static fronts to a very high 0.98 for low centers.

Fig. 32 shows the number of storms required for different synoptic and precipitation types. These graphs indicate that differences in sampling requirements between synoptic and precipitation types become more pronounced as the design efficiency decreases. The detection requirements for summer air mass storms vary the most between data types and thunderstorms vary the least. Overall, steady rain in the cold season has the lowest sampling requirements.

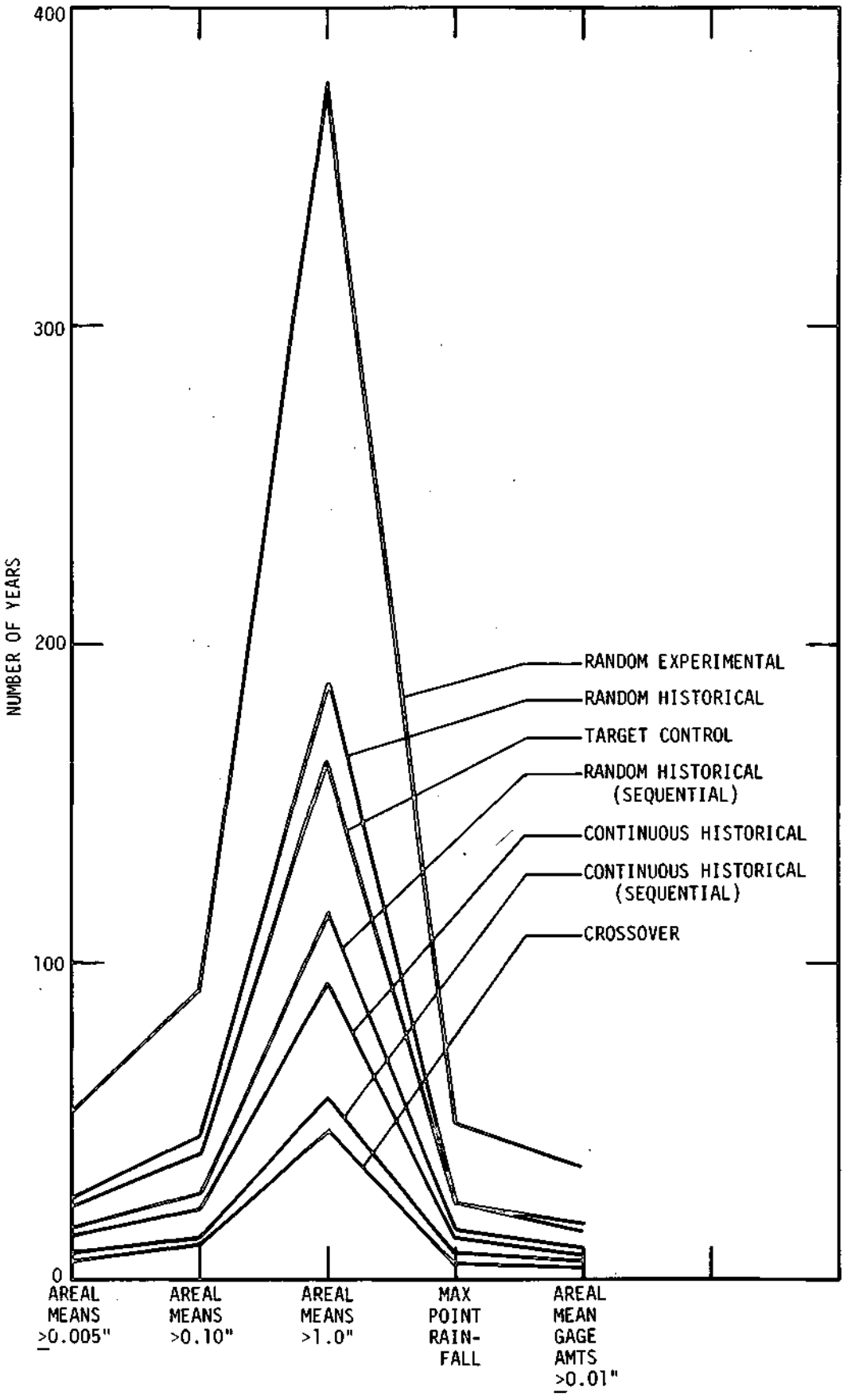

Figure 31. Number of years required to obtain significance with 20% increase in warm season air mass storms ($\alpha = 0.05$, $\beta = 0.50$).

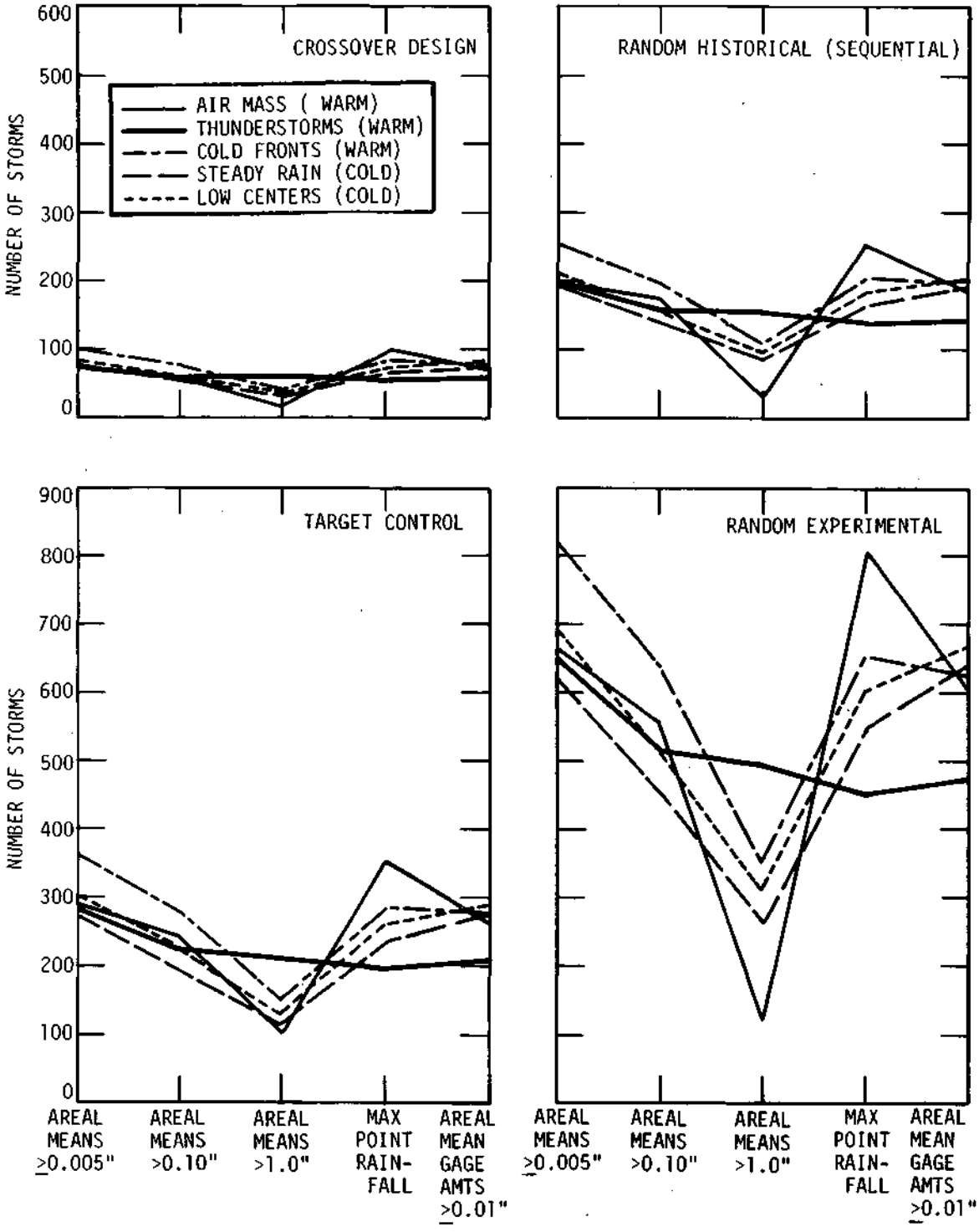

Figure 32. Number of storms required to obtain significance with 20% increase in various precipitation and synoptic types ($\alpha = 0.05$, $\beta = 0.20$).

Table 65. Correlation between mean and maximum precipitation on 49-gage, 400 mi^2 network for several synoptic storm types.

Storm type	Correlation coefficient
Low centers	0.98
Air mass	0.87
Cold fronts	0.93
Warm fronts	0.93
Occluded fronts	0.92
Static fronts	0.86
Squall lines	0.89

Fig. 33 shows the real time requirement for the various synoptic and precipitation types. Whereas the detection capability was variable between data types in Fig. 32, a clear-cut trend emerges in the real time graphs of Fig. 33. For all designs, the air mass storm in summer requires the most time, followed by cold fronts (warm season), steady rain (cold season), low centers (cold season). Thunderstorms (warm season) require the least time because of their much greater frequency (see Table 63).

Fig. 34 shows the number of years required to obtain significance for various increases in areal mean rainfall for different synoptic and precipitation types according to statistical design. It is immediately obvious why there has been controversy in many 5-year weather modification experiments. For the random-experimental design, more than 80% increase in air mass storms is required to obtain significance in a 5-year experiment.

For the case of steady rain and low centers during the cold season, 60% increases would be detectable in a 5-year period using the random-experimental design. An increase of 80% would not be detected in cold front storms and air mass storms using the random-experimental design. For steady rains and low centers, a 20% increase would be detected in 5 years using the cross-over design. A 40% increase would be detected in summer air mass and cold front storms and a 20% increase would be detected within 5 years for warm season thunderstorms with this design. From Fig. 34 it is evident that the larger the seeding effect the less important the choice of design becomes.

The cross-over design requires the smallest number of years to obtain significance. The historical-random design using a sequential test requires less than the target-control design, but for those increases which are detectable in a 5-year experiment the difference between the two is a maximum of 1 year. An important conclusion from this graph is if one desires to detect increases of 40% or less in the mean rainfall within a 5-year experiment, some design other than random-experimental must be used.

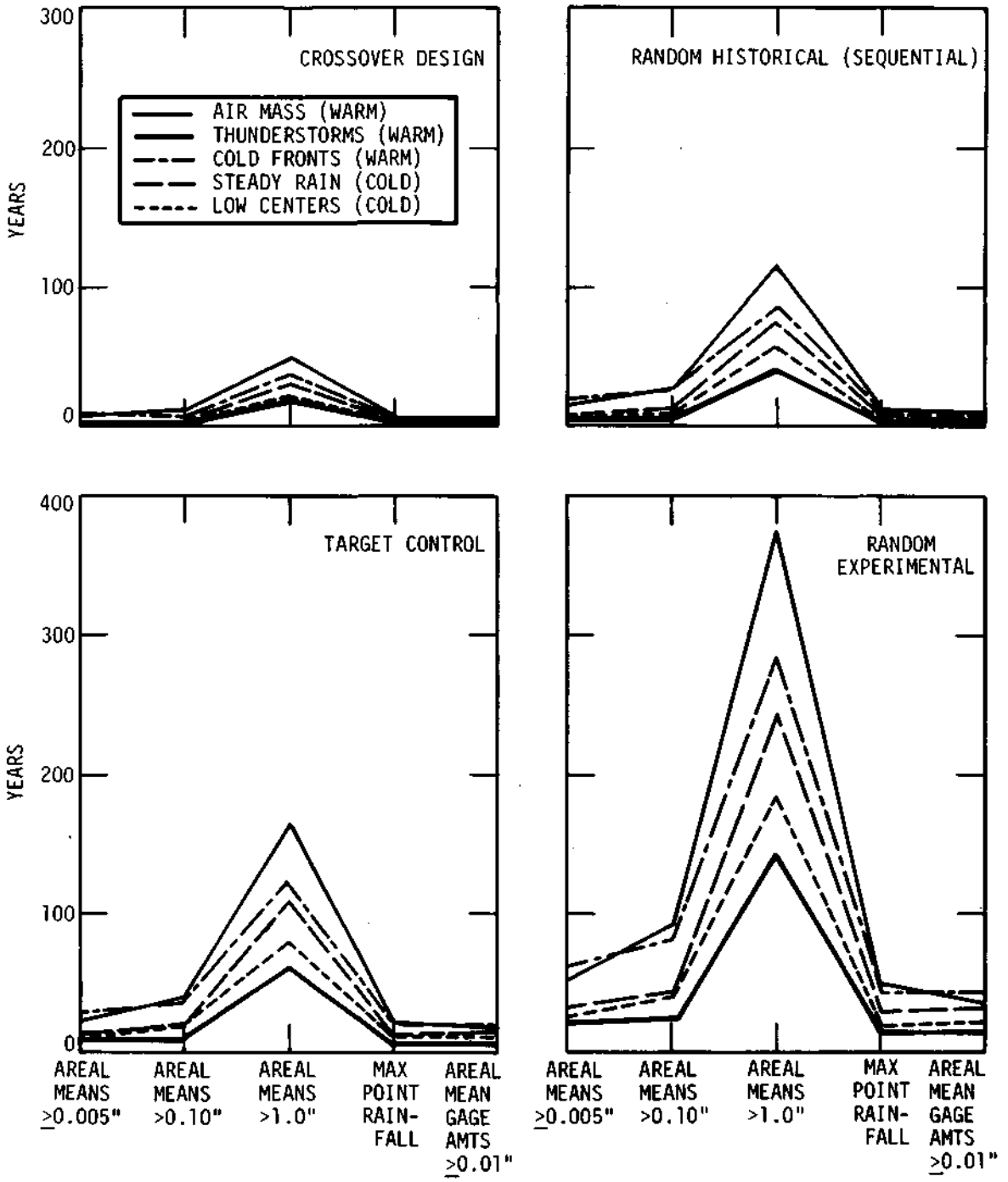

Figure 33. Number of years required to obtain significance with 20% increase in various precipitation and synoptic types ($\alpha = 0.05$, $\beta = 0.50$).

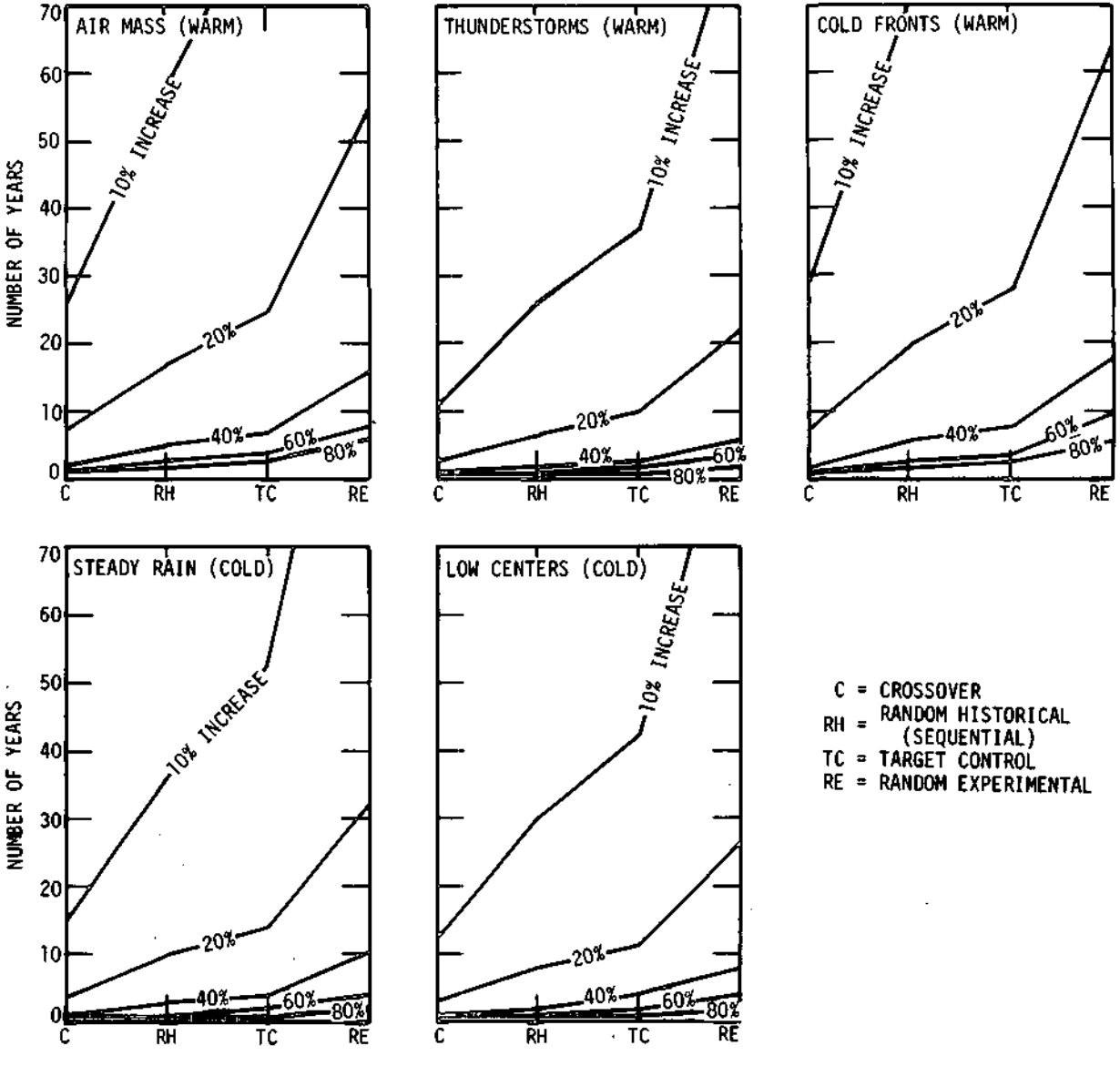

Figure 34. Number of years required to obtain significance for various increases in areal mean rainfall (means ≥ 0.005) according to synoptic type, precipitation type, and experimental design ($\alpha = 0.05$, $\beta = 0.50$).

As indicated earlier, the cross-over requirements are based upon a correlation coefficient of 0.75 between target and control precipitation. This assumes a distance of approximately 30 miles between target and control. As the distance increases, the correlation decreases and sampling length would increase. For example, with a correlation coefficient of 0.50, the sampling time is approximately double that indicated in the preceding discussions.

Under some circumstances, it would be desirable to seed all types of storms during a period of deficient precipitation in Illinois. Table 66 provides estimates of the sampling requirements for three designs during the warm and cold seasons for assumed seeding-induced increases of 20, 40, and 60%. It is assumed that all storms will be seeded and mean rainfall is the verifying parameter. Table 67 shows the same information based upon only those storms with means exceeding 0.10 inch.

Table 66. Number of years required to obtain significance combining all storms in warm and cold seasons ($\alpha = 0.05$, $\beta = 0.50$).

	Years required for given increase (%)					
	Warm season			Cold season		
Sampling design	20	40	60	20	40	60
Random-historical (non-sequential)	8	2	1	6	2	1
Target-control cross-over	2	1	1	2	1	1
Random-experimental	16	5	2	13	4	2

Table 67. Number of years required to obtain significance in warm and cold seasons based upon use of all storms with means > 0.10 inch ($\alpha = 0.05$, $\beta = 0.50$).

	Years required for given increase (%)					
	Warm season			Cold season		
Sampling design	20	40	60	20	40	60
Random-historical (non-sequential)	10	3	2	10	3	2
Target-control cross-over	3	1	1	3	1	1
Random-experimental	21	6	3	20	6	3

At this time, it should be pointed out that the length of sampling period discussed in this section is based upon seeding of all storms within a given stratification. Obviously, this would not normally occur in most seeding experiments. The estimates in the graphs and tables can be readily modified to provide sampling lengths under any estimated seeding efficiency. For example, if an investigator estimates only 50% of the naturally occurring storms will be included in his seeding experiment, then the sampling length is doubled. If only 25% are to be included, the sampling time is four times the number obtained from the graphs.

Fig. 35 depicts the same information as Fig. 34 except maximum rainfall is used as the precipitation measurement rather than mean rainfall. The number of years required are generally similar to those for mean rainfall although the maximum rainfall is a slightly better predictor. This difference is largely due to the fact that the average number of storms for maximum precipitation is slightly greater than for mean rainfall (Table 63). This is because in the mean rainfall sample only storms with areal means $\geq$ 0.005 inch were used.

There were three cases from Table 64 in which the data could be fitted by the gamma distribution and not by the log-normal distribution. For those cases the number of years required by the gamma test was computed and compared with the number of years required by the log-normal test. It was found that the number of years required for the gamma test was approximately the same as that of the log-normal.

Overall Conclusions

1) For the five types of precipitation and synoptic types emphasized in this study, the log-normal distribution provided a better fit than the gamma distribution.

2) The cross-over design requires the least amount of time to obtain significance for a given increase, followed by the continuous historical (sequential), continuous-historical (non-sequential), random-historical (sequential), fixed target-control, and random-historical (non-sequential). The most time is required by the random-experimental design.

3) In terms of years, the difference between continuous-historical (sequential), continuous-historical (non-sequential), random-historical (sequential) and fixed target-control, is, in general, 2 years or less when a seeding increase of 40% or more is present in the data. However, the difference between the cross-over and random-experimental design may be large.

4) The larger the seeding increase becomes, the less important the choice of design and type of data measurement becomes.

5) Mean and maximum rainfall require approximately the same amount of time to obtain significance.

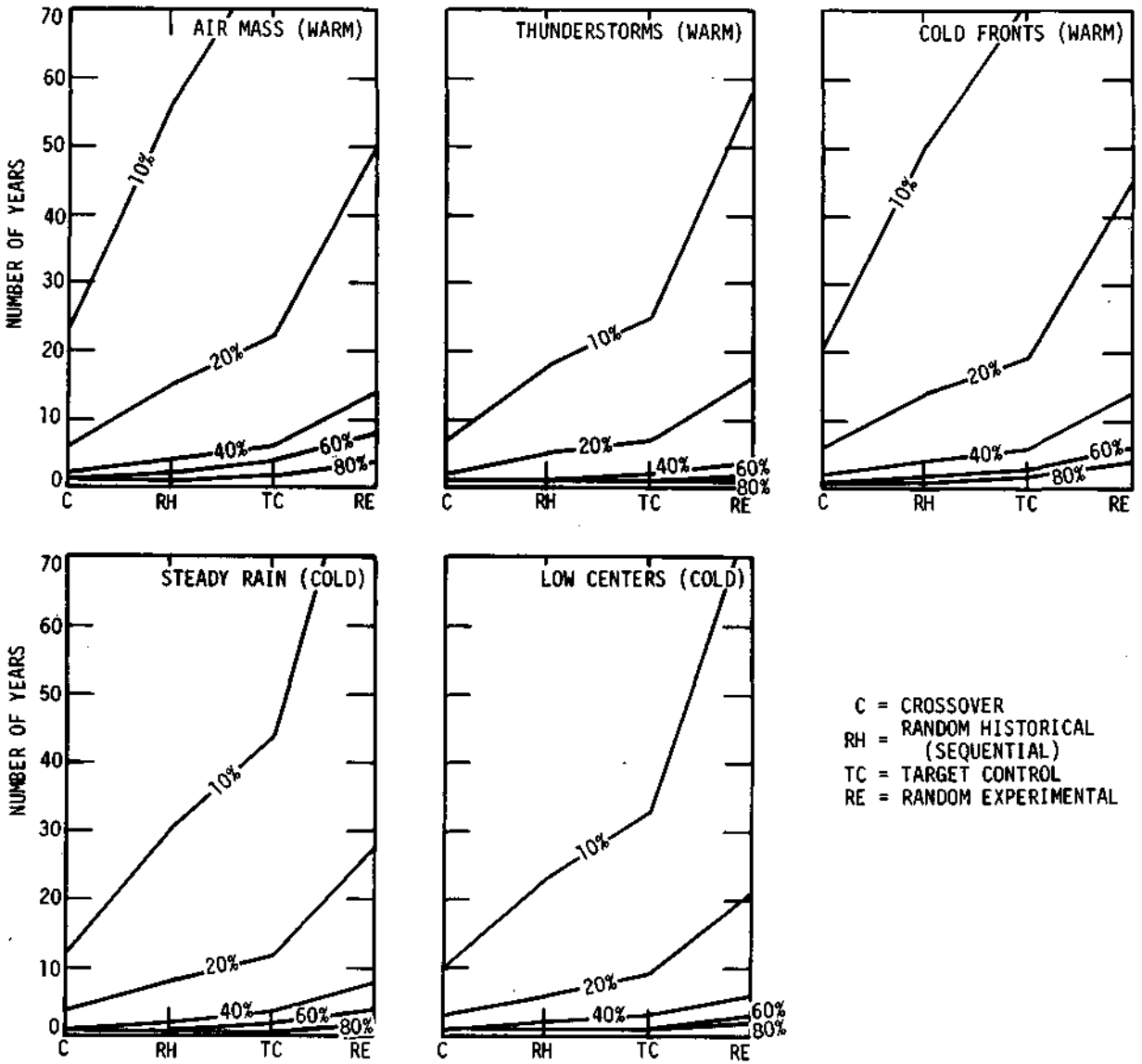

Figure 35. Number of years required to obtain significance for various increases in maximum point rainfall according to synoptic type, precipitation type, and experimental design ($\alpha = 0.05$, $\beta = 0.50$).

6) The stratification of mean areal precipitation into samples of greater than 0.10 and 1.00 inch increases the amount of time to obtain significance.

7) To detect increases ≤ 40% in areal mean storm rainfall, some design other than random-experimental must be used.

USE OF AREA-DEPTH RELATIONS IN THE EVALUATION OF PRECIPITATION MODIFICATION EXPERIMENTS

Introduction

A study of the use of area-depth relations in the design and evaluation of precipitation modification experiments is a logical extension of the study discussed in the previous section in which the use of two parameters, areal mean and maximum point precipitation, were examined. Area-depth curves, frequently used in hydrologic analyses, provide a simple mathematical expression of the spatial distribution of precipitation in a raingaged area. With a recording gage network, a basic requirement for a suitable scientific experiment, a measurement of the time variation in the spatial distribution within a storm can be obtained. The curve provides a measure of the mean and maximum precipitation, rainfall gradient, and skewness of the distribution. The above properties make it potentially useful in weather modification research, in which quantitative assessments of cloud seeding effects upon the spatial and temporal distributions are essential for proper evaluation of benefits. Also, area-depth analyses provide information indirectly on physical changes produced in precipitating cloud systems (Huff, 1968b).

The primary purpose of the study described in this section was to determine whether the three area-depth parameters, mean rainfall, maximum rainfall, and rainfall gradient, can be used together to provide supporting evidence in the verification of rain modification experiments. If so, their use can facilitate verification and improve the reliability of statistical evaluations of seeding results beyond that achieved with analyses of a single parameter, point or areal mean rainfall, which has been used most frequently in past experiments. A 228-storm sample of moderate to heavy rainstorms was used in this feasibility study. This sample was used because area-depth curves were available from an earlier study (Huff, 1968a). In actual modification experiments, storms of lighter intensity would of necessity be included also.

As part of the evaluation of the area-depth technique, studies were made of 1) methods of curve fitting and the suitability of the area-depth transformation (Huff, 1968b) for defining area-depth relations in all types of storms, 2) the degree of correlation between the three area-depth parameters, 3) theoretical frequency distributions applicable to the parameters, and 4) calculation of the number of storms required to obtain significance for various seeding-induced changes in mean rainfall, maximum rainfall and curve slope (rainfall gradient) for various sampling designs and data stratifications that might be used in rain modification experiments.

Data and Analytical Procedures

The area-depth curve is an expression of the average rainfall depth as a function of areal size. The individual average rainfall depths from which the curve is constructed are usually computed from an isohyetal map using the following equation (Light, 1947):

$$\bar{y}_i = \frac{\sum_{i=1}^{n} (\Delta A_i \, Y_i)}{\sum_{i=1}^{n} (\Delta A_i} \qquad i=1, \text{------}n \qquad (25)$$

Where A_i is an increment of area between two successive isohyets, Y_i is the rainfall value mid way between two successive isohyets, n is the number of areas encompassed by a pair of successive isohyets, and $\bar{y}_i$ is the average rainfall depth over a particular areal size. The summation is in descending order of magnitude of precipitation. If the distribution of gages is uniform and the increment of area between two isohyets is proportional to the number of gages enclosed between two successive isohyets, then the values can be obtained for successive increments of area from a ranking of the gage rainfall storm amounts (Huff, 1968a). A regression relation is then obtained between the variables $\bar{y}_i$ and A_i which can be expressed in the form:

$$\bar{y}_i = y_{max} + S \cdot A_i \qquad (26)$$

where $\bar{y}_i$ is the average rainfall depth in inches over a particular increment of area, A_i is the areal size in mi^2 of the increment of area, y_{max} is the regression intercept and is a constant representing the hypothetical maximum point rainfall at the center of the storm, and S is the slope of the regression line and is a constant representing an integrated rainfall gradient. When $\bar{y}_i$ is the value corresponding to the entire area in which the curve has been derived, it is simply the areal mean and will be referred to as $\bar{y}$ in the remainder of this paper.

Huff (1968a) used an 11-year continuous record from the 49 recording raingages on the East Central Illinois Network to derive characteristic area-depth relations in heavy rainstorms on areas of 50, 100, 200, and 400 mi^2. The study was limited to those storms in which the areal mean rainfall exceeded 0.50 inch and/or in which one or more of the gages recorded a rainfall amount equal to or exceeding 1 inch. Since parameters from this sample of storms were already available, these parameters constituted the basic data sample for the area-depth studies. This selection provided 228 storms with durations ranging from 1 to 48 hours; of these storms, 77 were in the cold season (October-April) and 151 were in the warm season (May-September).

Parameters for eight different forms of the area-depth equation were available from the sample thus selected. These forms involved various transformations on the variable $\overline{y}_i$ and A_i. A study of the adequacy of the square-root equation to describe this particular sample of storms showed that all correlation coefficients (i.e., the correlation between average rainfall depth and area) ranged from -0.88 to -1.00 for the square-root relation. Among the various storm durations and areas tested, a few had higher correlation coefficients with other than the square-root transformation, but the maximum difference between the percentage of variation unexplained by the square-root transformation and the other transformations was only 4.8% for the curves derived from the 400-mi^2 area. This was viewed as justification for using the square-root relation exclusively in the subsequent studies.

The 228 storms were first partitioned into warm and cold season storms and then stratified into three precipitation types and seven synoptic conditions. The stratifications are shown in Table 68. Steady rain includes storms with steady rain (R) and storms in which steady rain and rainshowers (R & RW) occurred together. Likewise thunderstorms include storms which were primarily thunderstorms (TRW) and those in which thunderstorms and rainshowers (TRW & RW) occurred together. For details of the precipitation and synoptic typing method, the reader is referred to Huff (1967a).

Major emphasis in this study is placed on the 400-mi^2 area. However, some results on the sample sizes required to obtain statistical significance for the 50-, 100-, and 200-mi^2 areas are included for comparison purposes.

Theoretical Frequency Distributions

The log-normal distribution was fitted to the intercepts (y_{max}) and to the slope parameters (S) of the 228 storms for the 50-, 100-, 200-, and 400-mi^2 areas. The log-normal distribution was also fitted to the areal mean rainfall ($\overline{y}$) in each of the four areas. For purposes of distribution fitting and subsequent statistical analysis the absolute value of the S's was used. The Kolmogorov-Smirnov goodness-of-fit "test was applied when sample sizes were less than 40, and the chi square test was applied when sample sizes were equal to or greater than 40 (Schickedanz et al., 1969). The resulting significance levels (size of the test) are shown in Table 68. In general, the data are well described by the log-normal distribution. For the individual types, cold fronts (warm) and thunderstorms (warm) are the only cases in which the goodness-of-fit probability is less than 0.05. Furthermore, one would expect 1 out of 20 distribution to have a goodness-of-fit probability less than 0.05. For the maximum rainfall data there are 2 out of 16 distributions which have probabilities less than 0.05 or 2 out of 48 (considering all distributions) in the table with probabilities less than 0.05. These factors were viewed as justification for using the log-normal parameters in the subsequent calculations of sample size. Table 69 shows the average number of storms expected per year in each category.

When all of the warm season storms were grouped together, the slope data were still described satisfactorily by the log-normal distribution whereas the maximum and mean data were not. However, when cold season storms were grouped together, all three types of data were described adequately by the log-normal

distribution. Thus, it would appear that the physical makeup of the different types in summer storms may be distinctly dissimilar, whereas in winter storms they are quite similar.

Table 68. Goodness-of-fit significance levels for the log-normal distribution.

	Significance level (a) for goodness-of-fit		
Stratification	Maximum point rainfall y_{max}	Integrated rainfall gradient S	Average rainfall depth $\bar{y}$
Warm season	<.01	.49	<.01
Synoptic type			
Low centers	.20	>.20	>.20
Air mass	>.20	>.20	.08
Cold fronts	.03	.16	.05
Warm fronts	>.20	>.20	>.20
Occluded fronts	>.20	>.20	>.20
Stationary fronts	>.20	>.20	.10
Squall lines	>.20	>.20	>.20
Precipitation types			
Steady rain	>.20	>.20	>.20
Rain showers	>.20	.14	>.20
Thunderstorms	<.01	.88	.09
Cold season	.06	.05	.17
Synoptic type			
Low centers	.08	>.20	>.20
Cold fronts	>.20	>.20	>.20
Warm fronts	.13	>.20	>.20
Precipitation type			
Steady rain	>.20	>.20	>.20
Rain showers	>.20	>.20	>.20
Thunderstorms	>.20	>.20	>.20

Table 69. Average number of storms expected per year of the different precipitation and synoptic types.

Stratification	Average number of storms
Warm season	13.7
Synoptic type	
Low centers	0.8
Air mass	2.9
Cold fronts	3.6
Warm fronts	1.9
Occluded fronts	0.6
Stationary fronts	2.3
Squall lines	1.7
Precipitation type	
Steady rain	0.9
Rain showers	1.4
Thunderstorms	11.4
Cold season	7.0
Synoptic type	
Low centers	2.3
Cold fronts	2.2
Warm fronts	0.8
Precipitation type	
Steady rain	1.5
Rain showers	2.0
Thunderstorms	3.6

Various groupings of synoptic and precipitation types for the warm season were then made in order to increase the number of storms in the various stratifications. Furthermore, seeding of more than one type of storm is likely to occur in either scientific experiments or commercial operations. It is then of interest to know which types are homogeneous enough to be grouped into one sample. For y_{max}, the synoptic types of warm, cold, and stationary fronts can be grouped together to form another sample. For mean rainfall, the low centers could also be grouped with the warm, cold, and stationary fronts to form one sample. For precipitation types, steady rains and rain showers could be grouped together for both Vmax and $\bar{y}$. The slope parameters were similar

enough that all of the warm season parameters could be grouped together (Table 68). The probabilities that the above samples are log-normal were all greater than 0.05.

The relationship between $\overline{y}$ and y_{max} can be approximated by (27)

$$\overline{y} = C_1 + C_2 y_{max} \quad (27)$$

where C_1 and C_2 are the least square estimates of the intercept and slope for the regression of $\overline{y}$ on y_{max}. The relationship between S and y_{max} can be approximated by (28)

$$S = C_3 + C_4 y_{max} \quad (28)$$

where C_3 and C_4 are the least square estimates of the intercept and slope for the regression of S on y_{max}. The constants C_1, C_2, C_3, and C_4 for the summer season as well as their corresponding correlation coefficients (r) are given in Table 70.

Table 70. Regression and correlation coefficients between the area-depth parameters for warm-season synoptic and precipitation types.

Synoptic type	C_1	C_2	r_1	C_3	C_4	r_2
Low centers	.082	.688	.977	.006	-.023	-.899
Air mass	-.398	.727	.956	.029	-.020	-.773
Cold fronts	-.099	.707	.954	-.007	-.022	-.798
Warm fronts	-.244	.799	.958	-.018	-.015	-.646
Occluded fronts	.122	.576	.971	.009	-.030	-.948
Static fronts	-.146	.739	.920	-.017	-.014	-.566
Squall lines	-.379	.802	.943	-.028	-.015	-.573
Precipitation type						
Steady rain	-.181	.835	.944	-.014	-.012	-.491
Rain showers	-.068	.652	.938	-.005	-.026	-.821
Thunderstorms	-.195	.725	.942	-.015	-.020	-.715

C_1, C_3 - intercepts
C_2, C_4 - slopes
r_1, r_2 - correlation coefficients

Experimental Design and Tests of Hypothesis

In the area-depth study the storm was used as the experimental unit in the various designs. The size of sample necessary for the detection of a specified increase in the area-depth parameters due to seeding effects was computed for five experimental designs that might be employed in a weather modification experiment. These designs and the methods of computing sample sizes are the same as those employed in the previous section of this report on sampling requirements for areal mean rainfall.

Results of Analyses

Sample sizes were computed for seven synoptic types and three precipitation types during the warm season and for three synoptic types and three precipitation types during the cold season. However, results are only presented for those cases most likely to be seeded in a weather modification experiment. These are the same as those used in the previous section.

Comparisons of sample sizes required for the various designs in air mass storms are shown in Fig. 36 for the three area-depth parameters on 400 mi^2 and for mean rainfall on 50, 100, and 200 mi^2. The number of storms required for significance for y_{max} and S (400 mi^2) are nearly the same, whereas the number for the average rainfall ($\bar{y}$) is somewhat larger. The increase in sampling time is dramatic as the sampling area decreases from 100 to 50 mi^2. Conversely, there is little change as the area increases from 200 to 400 mi^2. The number of years to obtain significance according to design type is of the same order as found previously for areal mean precipitation when all storm intensities (light, moderate, and heavy) were included (see previous section). The cross-over design requires the least number of storms and the random experimental design requires the most time. The number of years required to obtain significance with air mass storms is presented in Fig. 36 (lower).

A comparison of the number of years to obtain significance for various designs according to weather types is presented in Fig. 37. This figure illustrates that the weather type makes very little difference when using the most efficient design (cross-over), but as the design becomes less efficient the weather type becomes an important factor. For example, 20% seeding increases in all five weather types would be detected in a 5-year period using the cross-over design, but for the random-experimental design, 20% seeding increases would go undetected. Among storm and precipitation types, thunderstorms require the least amount of time to obtain significance, primarily because of their greater frequency of occurrence. The results for air mass storms are an excellent example of the valuable additional information available throught the use of area-depth curves. For these storms, which tend to be isolated and have small areal extent, changes in slope and maximum amounts are easier to detect than the mean. For cold fronts, maximum rainfall and mean rainfall are better predictors than the slope, and again the use of all three parameters would yield useful supporting information in seeding evaluations.

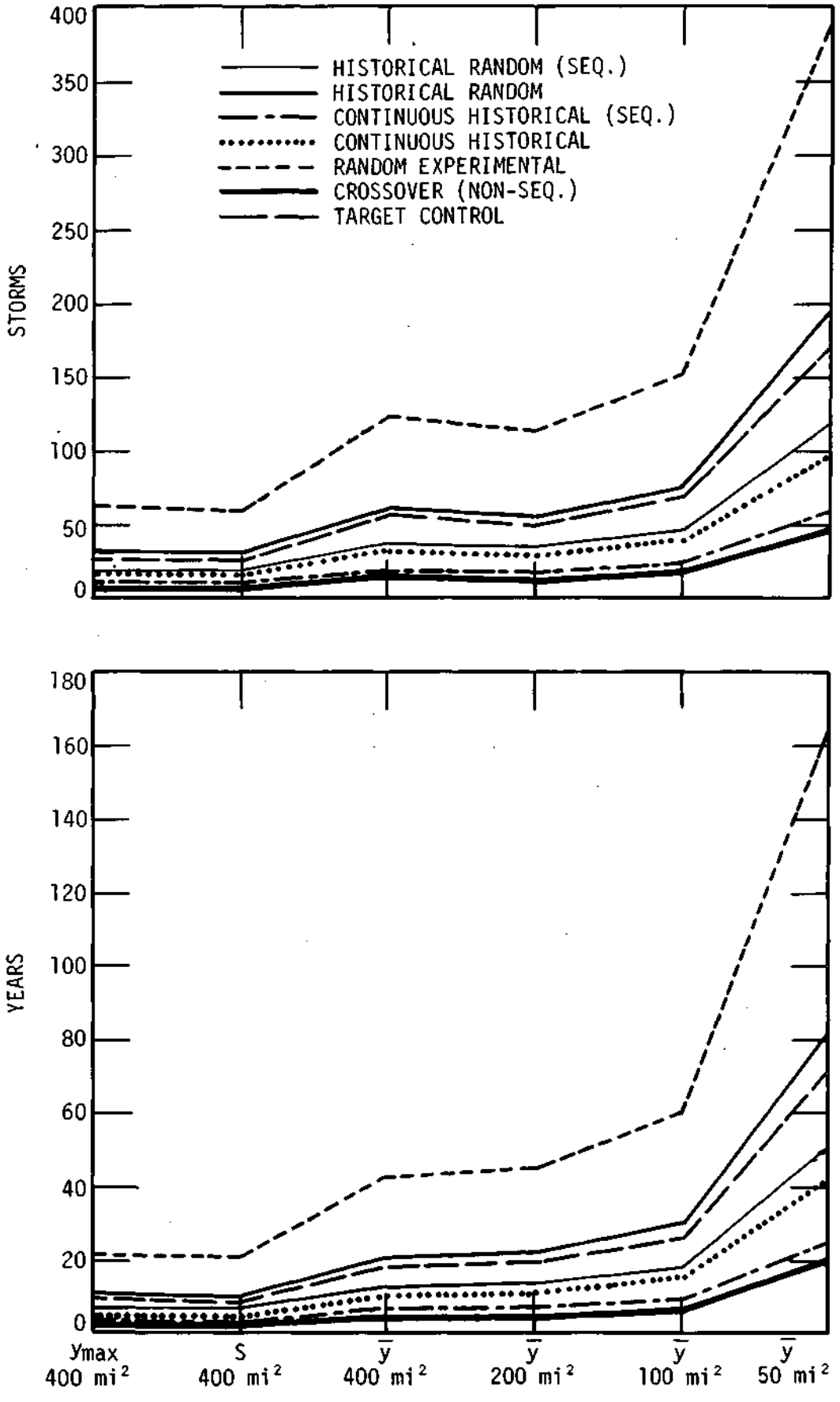

Figure 36. Number of storms and years required to obtain significance for 20% increase in air mass storms for different area-depth parameters (α = 0.05, β = 0.50).

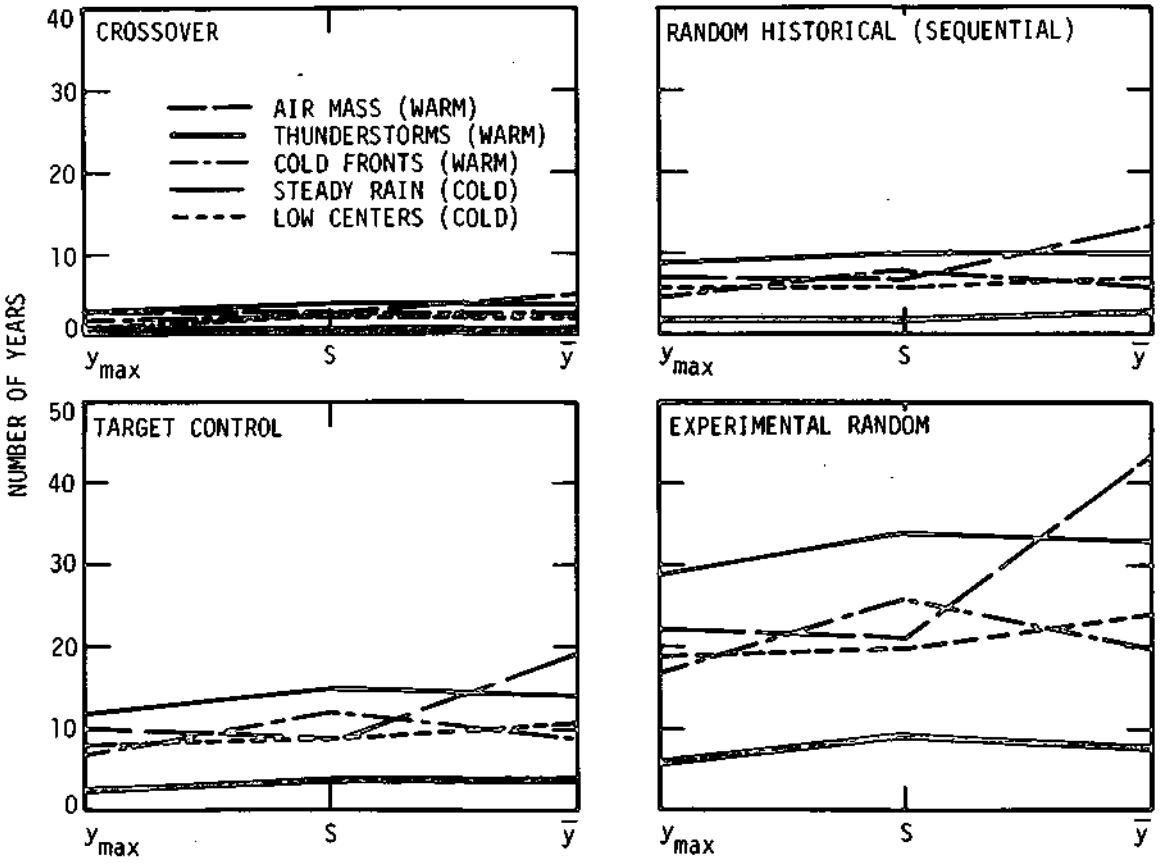

Figure 37. Number of years required to obtain significance for different weather types ($\alpha = 0.05$, $\beta = 0.50$).

Equations 27 and 28 were used to determine the percentage changes in $\bar{y}$ and S related to a 20% change in y_{max} under natural conditions and these changes are shown in Table 71. The table shows that, in general, a 20% change in y_{max} produces smaller changes in $\bar{y}$ and S. This means that not only does y_{max} require smaller sample sizes for a given percentage increase, but that larger increases are more likely to occur in y_{max} than in the other parameters.

Table 71. Percentage increase in $\bar{y}$ and S associated with 20% increase in y_{max} under natural conditions.

	Percentage increase	
Synoptic Type	Average rainfall depth ($\bar{y}$)	Slope S
Cold Fronts	17.7	14.6
Stationary Fronts	18.1	11.3
Warm Fronts	18.8	11.5
Low Centers	15.9	18.6
Air Mass	20.4	11.2
Squall Lines	20.8	9.2
Precipitation Type		
Steady Rain	18.2	11.6
Rain Showers	17.4	15.4
Thunderstorms	18.6	12.8

The number of years required to obtain significance for various increases in maximum rainfall is shown in Fig. 38. Thunderstorms (warm) require the least amount of time to obtain significance mostly because of the large number of storms expected in this category (Table 69). Increases of 60% or more would be detected for all designs and all weather types with a 5-year period. Increases of 40% would be detected in thunderstorms (warm), cold fronts (warm), low centers (cold), for all designs within 5 years, and with the exception of the random experimental design in air mass (warm) and low centers (cold). For thunderstorms, 20% increases would be detected in 5 years with every design except the experimental random, and for this design a 20% increase would be detected in 6 years. For air mass storms, steady rain, and low centers, the 20% change would only be detected using the cross-over design but in the cold front storms, the 20% increase would be detected in both the cross-over and the random historical designs.

Fig. 39 shows the number of years required to obtain significance for various increases in the slope parameter and Fig. 40 shows the number of years for mean rainfall. A comparison of Fig. 39 and Fig. 40 with Fig. 38 reveals

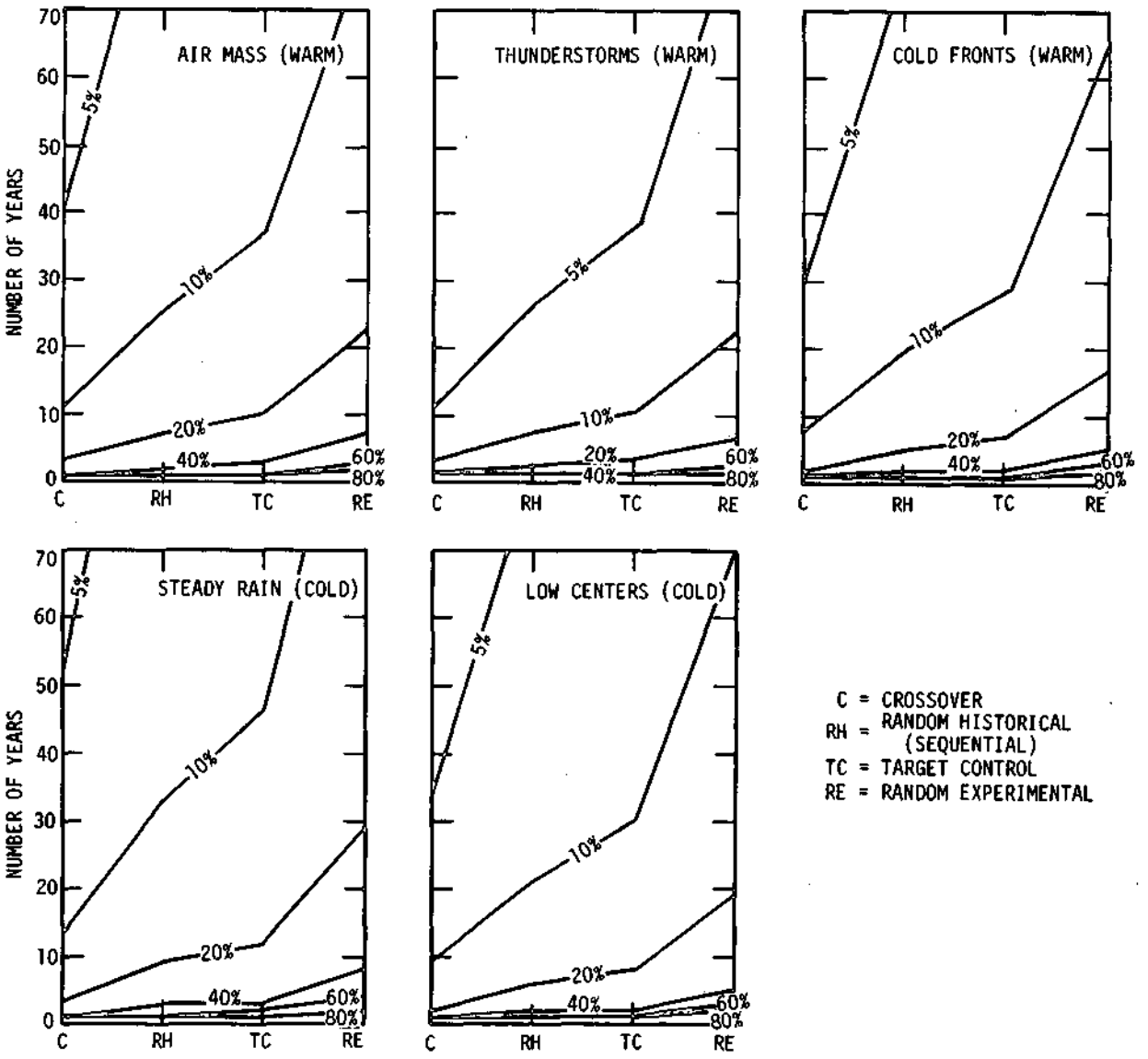

Figure 38. Number of years required to obtain significance for various increases in maximum rainfall according to synoptic type, precipitation type, and experimental design (α =0.05, β =0.50).

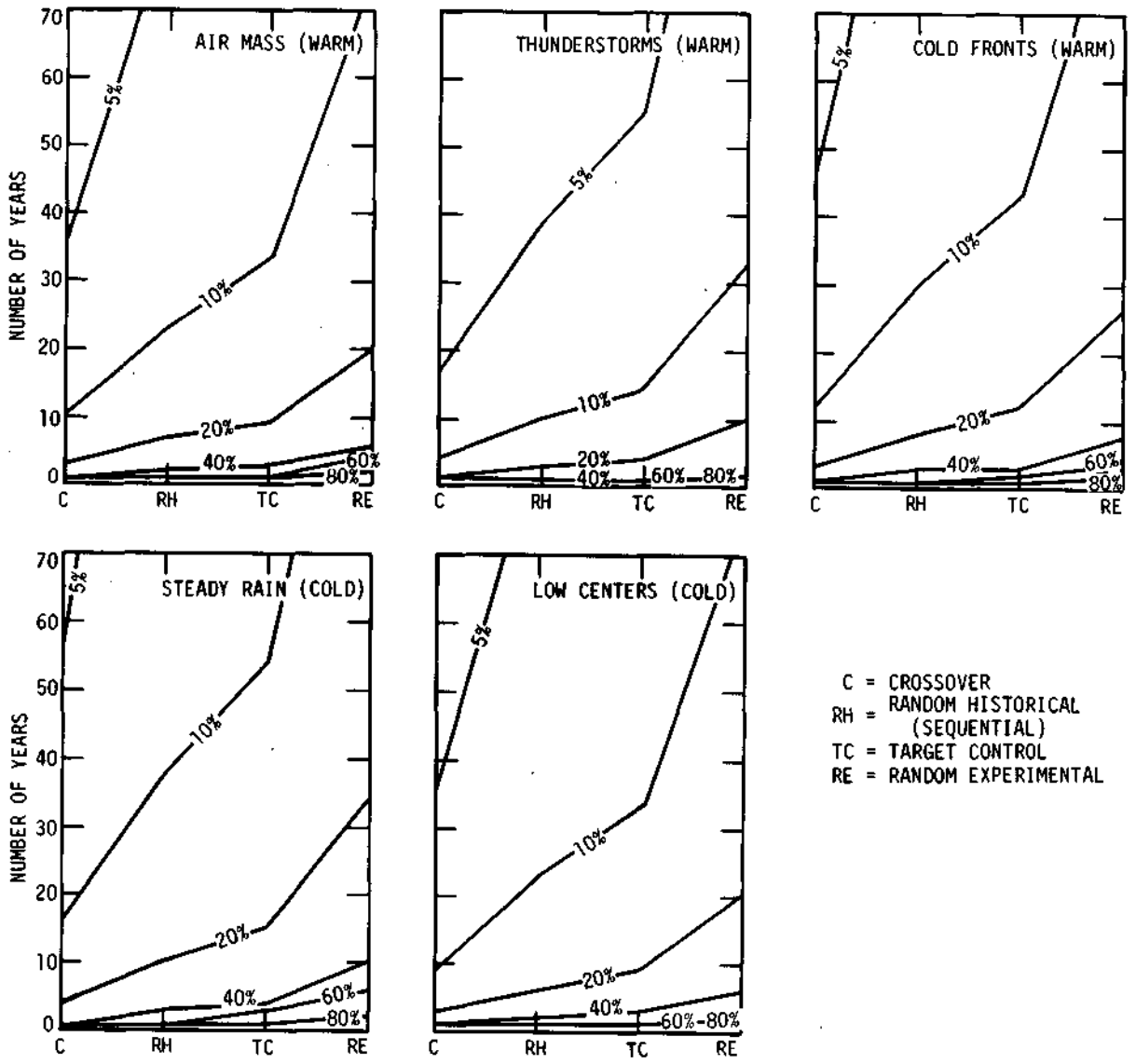

Figure 39. Number of years required to obtain significance for various increases in the slope parameter according to synoptic type, precipitation type, and experimental design ($\alpha = 0.05$, $\beta = 0.50$).

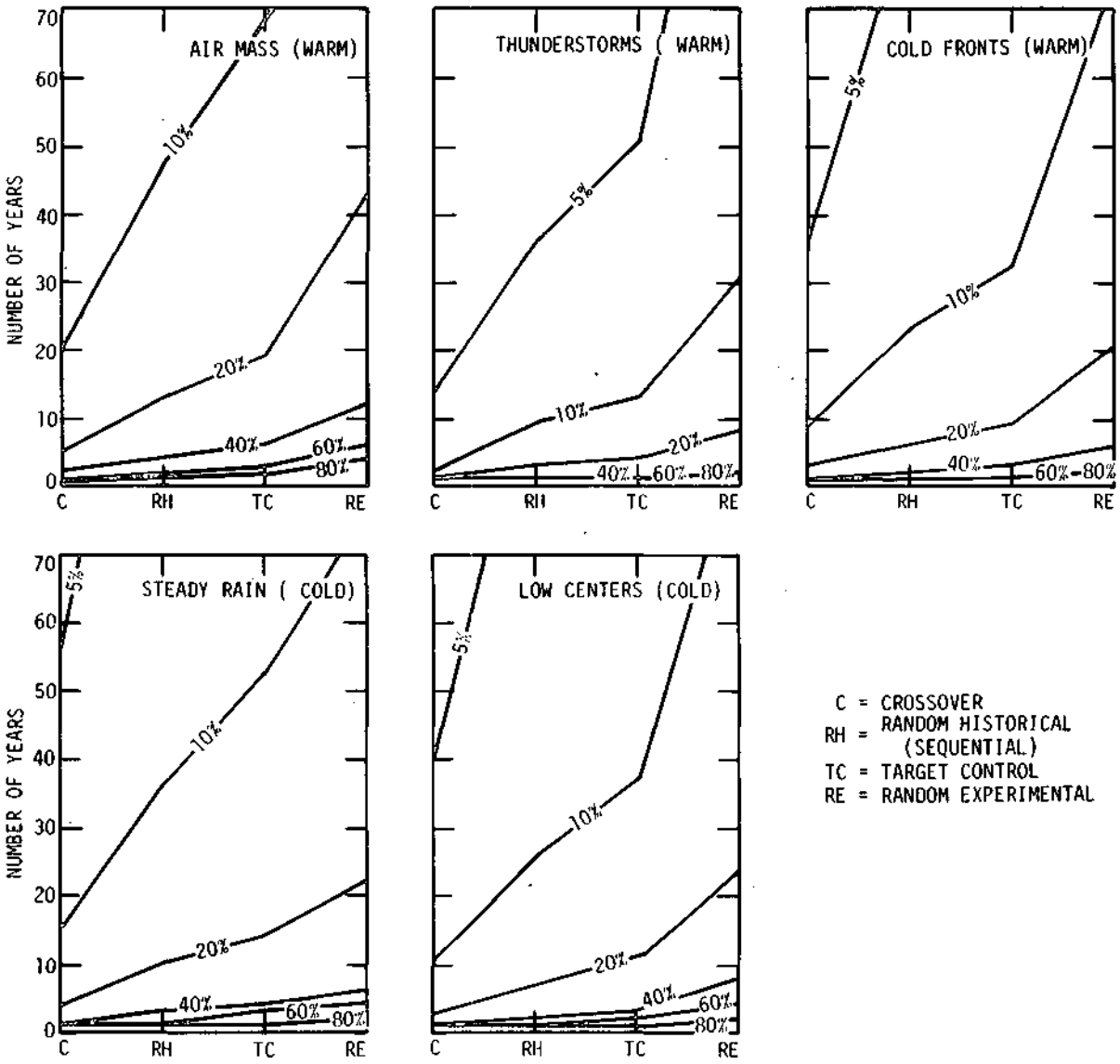

Figure 40. Number of years required to obtain significance for various increases in mean rainfall according to synoptic type, precipitation type, and experimental design ($\alpha = 0.05$, $\beta = 0.50$).

useful information concerning the two area-depth parameters and mean rainfall. For air mass storms, the slope parameter requires the least amount of time to obtain significance, followed by the maximum rainfall and the mean. For thunderstorms, cold fronts, and steady rain, the least amount of time is required with maximum rainfall, followed by the mean and the slope parameter. For low centers, the maximum rainfall requires the least amount of time followed by the slope parameter and the mean. Again, the type of supporting evidence available in using all three parameters is illustrated. The fact that the relation between the detection power of the data types varies according to the weather type that is seeded makes the use of additional parameters even more important.

Fig. 41 shows the number of years required to obtain significance for certain data types when synoptic and precipitation types are combined. By combining the warm, cold, and stationary fronts for maximum rainfall in Fig. 41a, a reduction in sample size over cold fronts alone was obtained (see Fig. 38c). With this frontal combination, 20% seeding increases would be detected with the target-control designs in a 5-year experiment, whereas they would not have been detected with the cold front storms alone.

The combination of warm., cold, and stationary fronts with low centers (Fig. 41) for mean rainfall produced smaller sample sizes than cold fronts alone (Fig. 40). With this combination, 20% seeding increases would be detected with the random historical and target-control designs in a 5-year experiment, whereas they would not be detected with cold front storms alone. The number of years for the random historical design was reduced from 20 to 9.

For cold season storms, all synoptic and precipitation types could be combined which reduces the sample size over the individual weather types.

Optimum Parameters, Designs and Tests

How is one to use the area-depth parameters? The results presented here indicate that the maximum rainfall parameter is the most efficient and the slope parameter is the least efficient for moderate to heavy rainstorms. The maximum rainfall parameter is the most efficient for two reasons. First, it produces smaller sample sizes for the same percentage increase than the other parameters. Secondly, if the natural relation between the parameters remains the same under seeding, then the percentage changes in the maximum rainfall will be larger than in the other parameters (see Table 71). If the relations between the parameters were not the same in the seeded sample, this change could be used 1) as a test of the effectiveness of the seeding, and 2) as an indication of the type of physical changes being produced.

Thus, if in a seeding experiment, one chose to use the mean rainfall parameter for the chief source of verification, then the maximum rainfall parameter would provide extra information at a smaller significance level, and the slope parameter would provide extra information at a larger significance level.

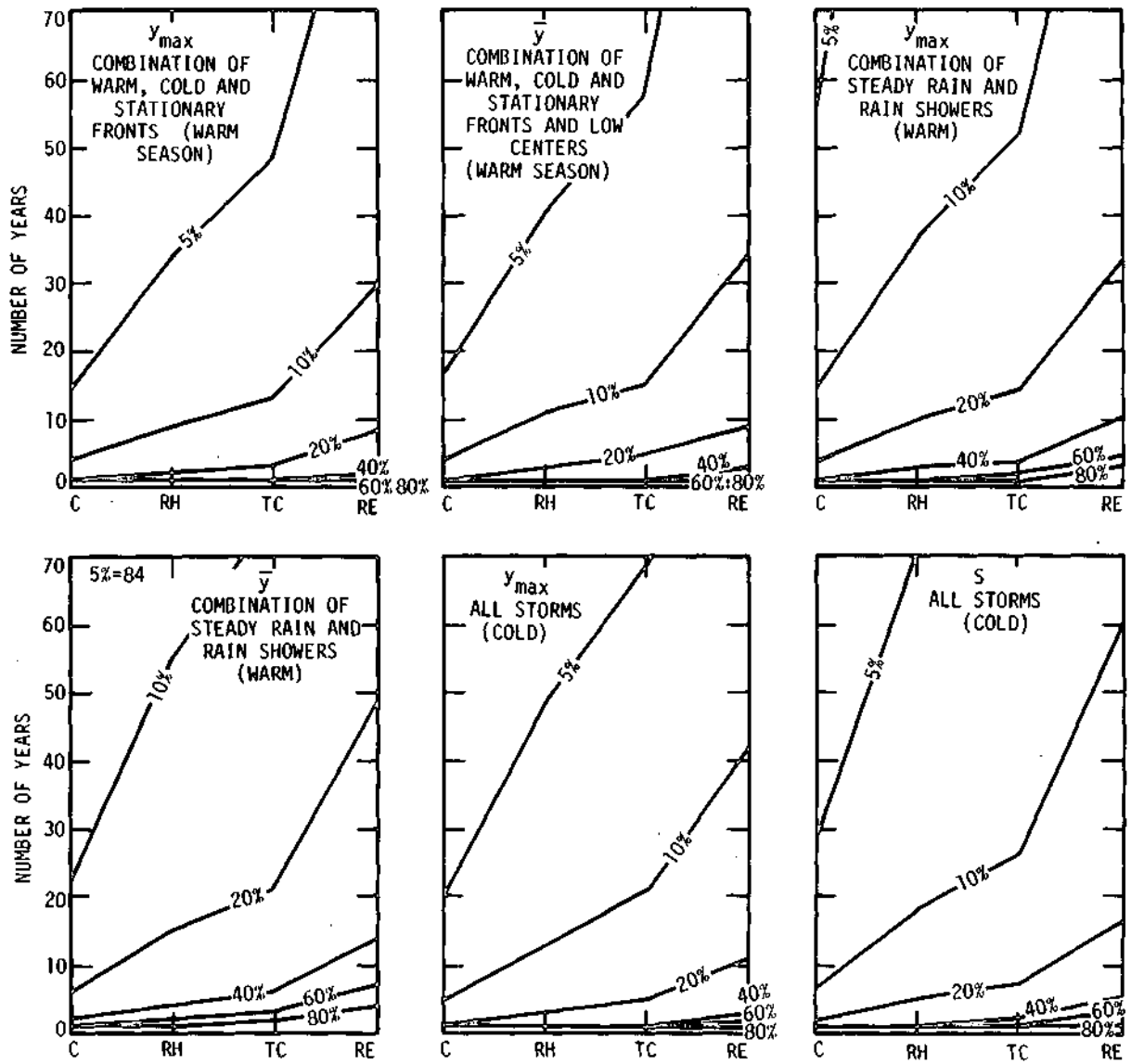

Figure 41. Number of years required to obtain significance for various combinations of synoptic and precipitation types (α = 0.05, β = 0.50).

Overall Conclusions

Although evaluation of the area-depth technique was based upon analyses of moderate to heavy rainstorms, there is reason to believe the method will be applicable throughout the intensity spectrum of storm mean rainfalls. This assumption is lent support by the findings in the previous section in which two of the three area-depth parameters, mean and maximum rainfall, were tested for all intensities of storm rainfall and found to have approximately equal power in detecting seeding-induced precipitation increases. Spatial relative variability and skewness tend to increase with decreasing mean precipitation; therefore, a data transformation other than the square root used in the heavy rainstorm study may be more applicable in light storms. However, an excellent area-depth curve fit can usually be obtained in any type of storm if one is not inflexible in the general equation used for fitting the data (Huff, 1968b).

Other conclusions from results of the area-depth study include:

1) Practically all of the area-depth rainfall stratifications used in this study can be described by the log-normal distribution.

2) There is a high degree of correlation between the mean and maximum rainfall (0.92 or greater in the various stratifications) in the storm sample used in this study.

3) As the size of sampling area decreases the number of years required to obtain significance increases.

4) Maximum rainfall requires less time to obtain significance then mean rainfall for the storm sample used in this study.

5) The relative rank order of the two area-depth parameters and mean rainfall in respect to the power of detection varies according to synoptic type and other factors. Thus, it is very informative to use all three parameters in a verification program to provide additional information.

6) Many of the synoptic and precipitation types can be combined to reduce the amount of time required to obtain significance.

7) The cross-over design requires the least amount of time to obtain significance for a given increase, followed by the continuous historical (sequential), continuous historical (non-sequential), random historical (sequential), fixed target-control, and random historical (non-sequential). The most time is required by the random experimental design.

8) In terms of years, the difference between all designs excluding cross-over and random experimental is two years or less for a 40% seeding increase.

9) The larger the seeding increase becomes, the less important the choice of design becomes.

RAIN CELL CHARACTERISTICS AND THEIR USE IN WEATHER MODIFICATION EXPERIMENTS

Introduction

A limited investigation was made of the characteristics of individual rain cells in warm season storms and how measurements of cell parameters might be utilized as a verification tool in precipitation modification experiments. Recording raingage data from the combined Little Egypt and Shawnee Networks (Fig. 1) were used in the study. Isohyetal analyses were performed to isolate and trace the movement of cells across the network. A rain cell was defined as a closed isohyetal system in the surface rainfall pattern with a definite break in time and space continuity from other isohyetal systems in the sampling network. Only those rain cells which were completely contained in the network during their life history were used in the study. Several examples of rain cells from the storm of June 6-7, 1965, are shown in Fig. 42. Isohyetal patterns, cell movement, and average speed are indicated.

This initial study was restricted to the 3-month period, June-August 1965, because of time and personnel limitations. The isolation and tracking of a cell across the network is very tedious and time-consuming. Careful examination must be made of each significant change in rainfall rate on each raingage chart and these rate changes related to each other to determine the location, movement, and other pertinent characteristics of the cells. Considerable meteorological knowledge and experience in storm isohyetal analyses is required to perform this task well.

With the restriction of complete network enclosure, a total of 335 rain cells on 21 rainy days were obtained for analyses during the 3-month sampling period. This represented 45% of the total number of cells that produced the network rainfall. Because of the shape and orientation of the network and the enclosure restriction, there is a sampling bias toward cells moving in a SW-NE direction. However, this is the most frequent direction of movement of Illinois storms, and maximum sampling of cell life histories for a given size of network is obtained with an orientation such as that used with the Shawnee Network.

Rain Cell Climatology

Although the sampling period was quite short and certain sampling restrictions were imposed in this study, the 21-storm, 335-cell sample should be useful as a first approximation of the climatological characteristics of warm-season rain cells in Illinois. Consequently, a number of sample statistics are provided in the following paragraphs.

Table 72 is a summary of cell occurrences by storm. The number of cells sampled in each storm, the mean storm rainfall and rainfall duration in each storm sampled, and the synoptic storm types are shown. This table shows that a wide range of storm intensities (mean rainfall) and storm durations were

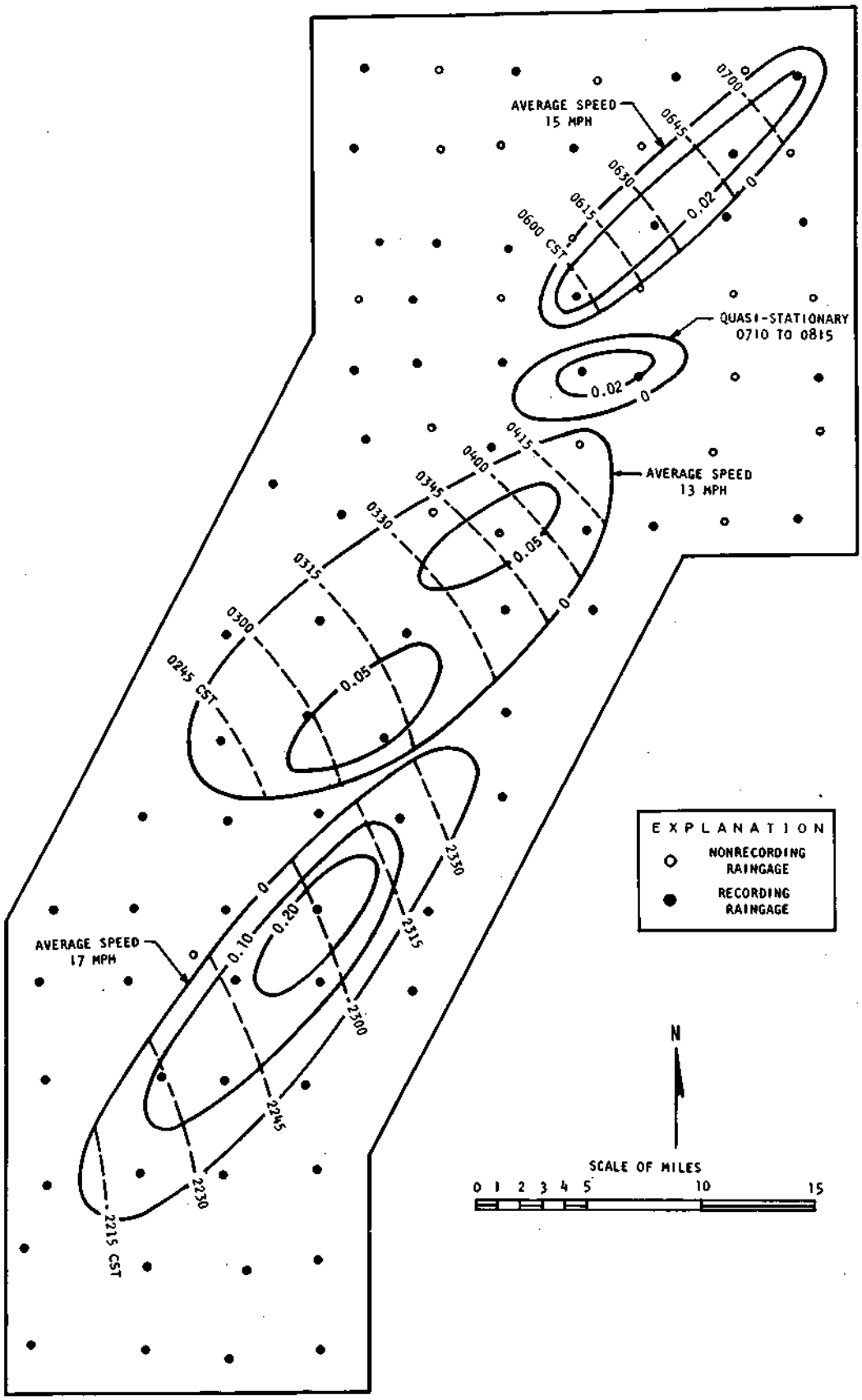

Figure 42. Examples of rain cells on June 6-7, 1965.

sampled in summer 1965; this is a desirable feature from the standpoint of sample representativeness.

Table 72. Rain cell summary for June-August 1965.

Storm date	Number of cells	Network mean rainfall (in)	Storm duration (hrs)	Storm type*
6/21	47	0.84	6.7	S
6/3-4	5	0.72	3.3	S
6/6-7	14	1.42	23.8	C
6/8	11	0.60	2.1	C
6/10	2	0.19	1.7	S
6/23	21	0.36	8.4	C
6/30	13	0.84	3.8	S
7/2	11	1.80	14.2	W
7/9 (AM)	25	0.77	2.7	Q
7/9 (PM)	27	0.65	3.3	C
7/14	9	0.01	0.8	A
7/19	23	0.01	1.8	S
7/31	18	0.09	0.6	C
8/1	16	0.04	0.9	C
8/6	18	0.65	2.1	Q
8/7	4	0.10	1.9	C
8/8	14	0.09	1.2	C
8/18	9	0.73	0.6	C
8/19	9	0.72	6.4	Q
8/24	11	0.14	1.7	A
8/26	3	0.59	3.7	Q
8/31	25	1.15	22.0	C

* S - Stationary front; C - Cold front; W - Warm front; Q - Squall line; A - Air mass.

The cell parameters analyzed included mean, maximum, and minimum rainfall, rainfall duration, total area enveloped by each cell during its life, and the volume of rainfall produced by each cell. Data were pooled from all 335 cells to obtain probability distributions for each parameter. Table 73 shows the median values obtained from this analysis, along with those bounding the upper and lower 5% limits. The primary purpose of this table is to illustrate the wide range in the distribution properties of rain cells under natural conditions.

An illustration of the variation in rain cell characteristics within a specific storm is provided in Table 74. Here, the cell distribution properties, based upon 47 cells, are shown for selected frequencies. Thus, the mean rainfall

in the cell-enveloped areas ranged from 0.46 inch or greater in 5% of the rain cells to a median of 0.12 inch and a 95% envelope value of 0.03 inch. Between the 5% limits, rain durations varied from 18 to 110 minutes, the rain enveloped areas ranged from 18 to 130 mi^2, and cell rainfall volume varied from 33 to 2886 acre feet.

Table 73. Rain cell distribution characteristics in 1965 summer storms.

Cell parameter	Upper 5% limit	Median	Lower 5% limit
Mean rainfall (in)	0.48	0.06	0.01
Maximum rainfall (in)	0.62	0.10	0.02
Minimum rainfall (in)	0.32	0.04	Trace
Rain duration (min)	125	50	15
Area enveloped by rainfall (mi^2)	94	29	7
Rain volume (acre - feet)	1285	110	9

Table 74. Rain cell distribution properties on June 2, 1965.

	Value equalled or exceeded for given parameter			
Percent of cells	Mean rainfall (in)	Rain duration (min)	Rain area (mi^2)	Rain volume (acre-ft)
5	0.46	110	130	2886
10	0.34	100	105	1748
25	0.21	83	73	772
50	0.12	64	48	305
75	0.07	46	32	122
90	0.04	28	22	54
95	0.03	18	18	33

In rain modification experiments, it is often necessary to limit seeding operations to daylight hours when aircraft seeding is involved. Consequently, the diurnal frequency distribution of rain cells would be of major importance in planning experiments involving rain cell seeding. An examination of the time of occurrence showed a maximum frequency of 25% in the 1500-1800 period. In view of diurnal distribution characteristics of Illinois rainfall (discussed elsewhere in this report) this peak period is to be expected in extreme SW Illinois where the Shawnee Network is located. Table 75 shows the percentage distribution by 3-hour periods.

Table 75. Diurnal distribution of rain cell occurrences.

Time (CST)	Percent of cells
00-03	7
03-06	8
06-09	9
09-12	13
12-15	14
15-18	25
18-21	10
21-24	14

Analytical Procedures Used in Evaluating Verification Applicability

The rain cell study provided expressions of the natural differences between temporally related rain cells. These data were then used to determine the required sample size to verify potential rainfall modification experiments that might be based on rain cell data from a pair of similar cells, where one member of the pair is randomly seeded. To more nearly simulate an actual field experiment, certain limiting criteria were defined for selecting rain cells for comparison.

First, any two cells had to have start times occurring within 30 minutes of each other before they were compared. This resulted from a basic assumption that any cells occurring in the sampling area within a 30-minute period were likely to have been derived from separate convective clouds that had similar meteorological characteristics prior to their production of rain. Table 76 shows the number of cell pairs obtained with the above limitations. Each pair was uniquely determined. That is, once a pair was formed, the members of that pair could not be used for further pairing of cells.

Once the cells were paired, the difference between the individual members of each pair was obtained for various rainfall parameters. These parameters were the mean and maximum rainfall values for each cell, the duration of the cell

on the network, its areal extent, and the volume of rainfall produced by it. The maximum value was taken to be the maximum raingage amount in a given cell. The mean was obtained by averaging the gage amounts within the rain cells and the area of each cell was obtained with the use of a planimeter. The duration was determined to be the life history of the cell on the network and the volume was obtained from the mean rainfall and the area enveloped by cell rainfall.

Table 76. Number of rain cell pairs obtained on each storm date.

Date	Number of pairs
6/2	23
6/3	1
6/6-7	6
6/8	4
6/10	0
6/23	7
6/30	5
7/2	5
7/9	24
7/14	3
7/19	11
7/31	9
8/1	8
8/6	8
8/7	2
8/8	7
8/18	4
8/19	2
8/24	4
8/26	1
8/31	9
	143

It is well to note again at this point that the 1-summer sample may not be truly representative of the long-term climatological distribution. Furthermore, only 45% of the rain cells were analyzed because of the restriction for complete containment within the sampling network. This eliminated very large and long-duration cells with other than SW-NE movements. Also, cells moving from a westerly direction were disproportionally sampled because of the relatively narrow width of the network. However, as stated earlier, the information from this study does provide a first approximation of the climatological distribution, and furnishes insight into the use of rain cells in rain modification experiments.

Experimental Design and Empirical Frequency Distributions

In the paired storm design, a pair of clouds are selected with similar characteristics, and one member of the pair is then chosen at random to be seeded. The associated rain cells of the 143 pairs from Table 76 were assumed to have been produced from clouds meeting the paired storm design criteria. One member of each pair was selected at random and designated as seeded. The differences between the various seeded and non-seeded rain cell measurements were then computed and the cumulative ogives for the empirical distributions of differences were formed. These distributions were designated as the natural distributions, that is, the distributions expected if seeding had not occurred. The values of the seeded cells of each pair were then increased 20, 40, 60, and 80% and the respective cumulative ogives were formed (Fig. 43). The differences between the natural and hypothetically seeded curves are assumed to be the effect that seeding would have on the natural differences.

Test of Hypothesis

Because of the dependence between members of pairs, an appropriate test to use is the Wilcoxin matched-pairs signed-ranks test. To derive the number of pairs to obtain significance for assumed increases of 20, 40, 60, and 80%, sample values were generated from the curves of Fig. 43 using a Monte Carlo procedure. As each sample was generated, a tabulation was made of whether significance was obtained for the Wilcoxin matched-pair test. This was continued until a specified number of values had been generated. The process was then repeated, so that a frequency distribution of the number of runs significant at a particular sample size was obtained. The percentage number of significant runs at each sample size is then equivalent to the power of the test.

Results of Statistical Tests

The number of rain cells as well as the number of years to obtain significance for various rain cell measurements are shown in Fig. 44. The sample of pairs used in this study occurred on 20 days during the June-August period. The number of years to obtain significance was obtained by assuming that on an operational basis only one pair would be sampled, or 20 such cases during the 3-month period.

A comparison of the various rain cell measurements reveals that precipitation duration requires the least amount of time to obtain significance, followed by cell area of rainfall, mean rainfall, maximum rainfall, and rain volume. For a 20% increase, duration is the only measurement detectable in a 5-year period. For 60% and 80% increases, all types of rain cell measurements would be detected in a 5-year period. For a 40% increase, all measurements except the maximum rainfall and volume of rainfall would be detected.

It should be noted that many assumptions had to be made to obtain the yearly numbers. For example, the amount of time to obtain significance would be reduced by one-half if two pairs of rain cells could be sampled on each operational day.

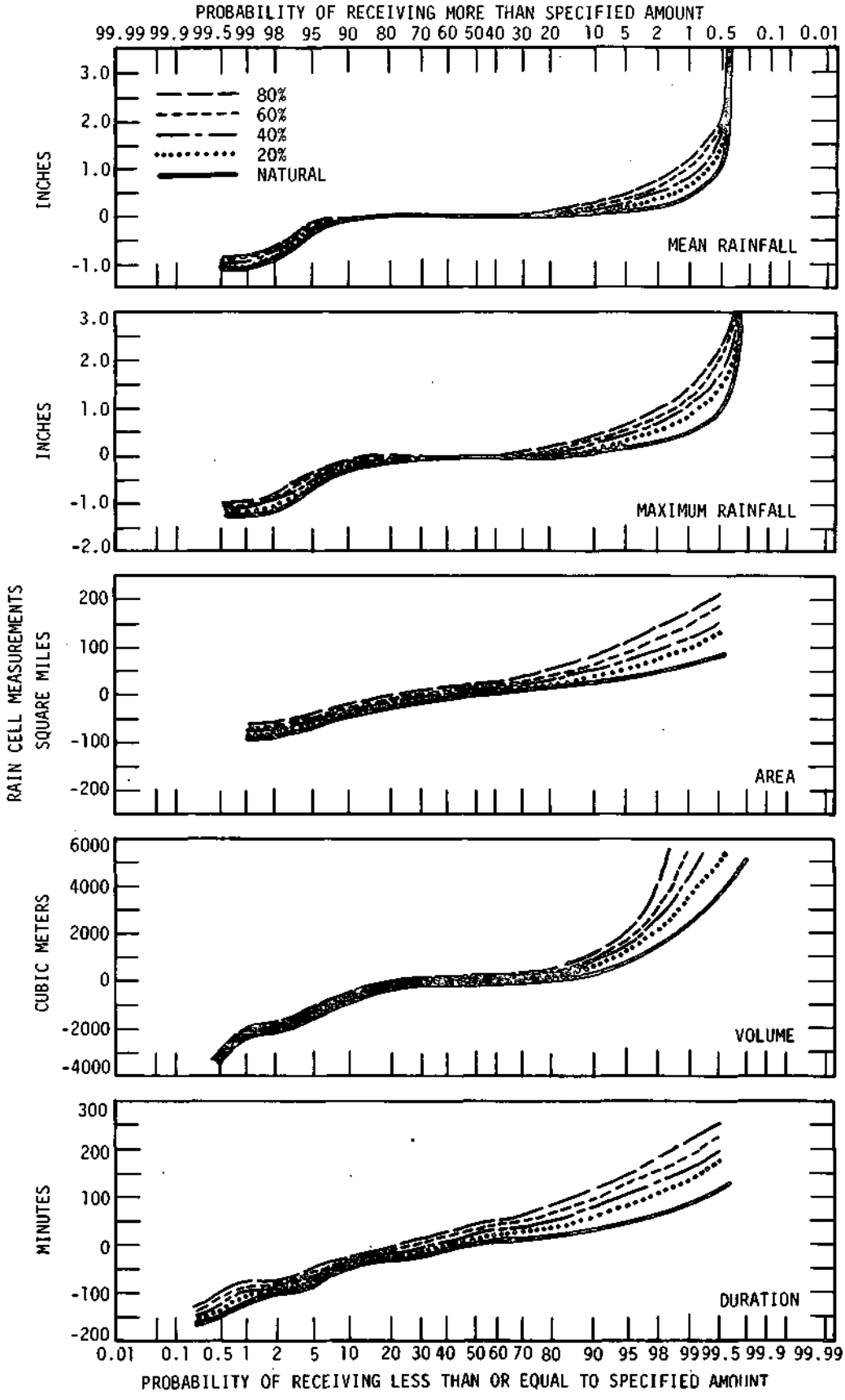

Figure 43. Empirical distributions of differences between rain cell pairs.

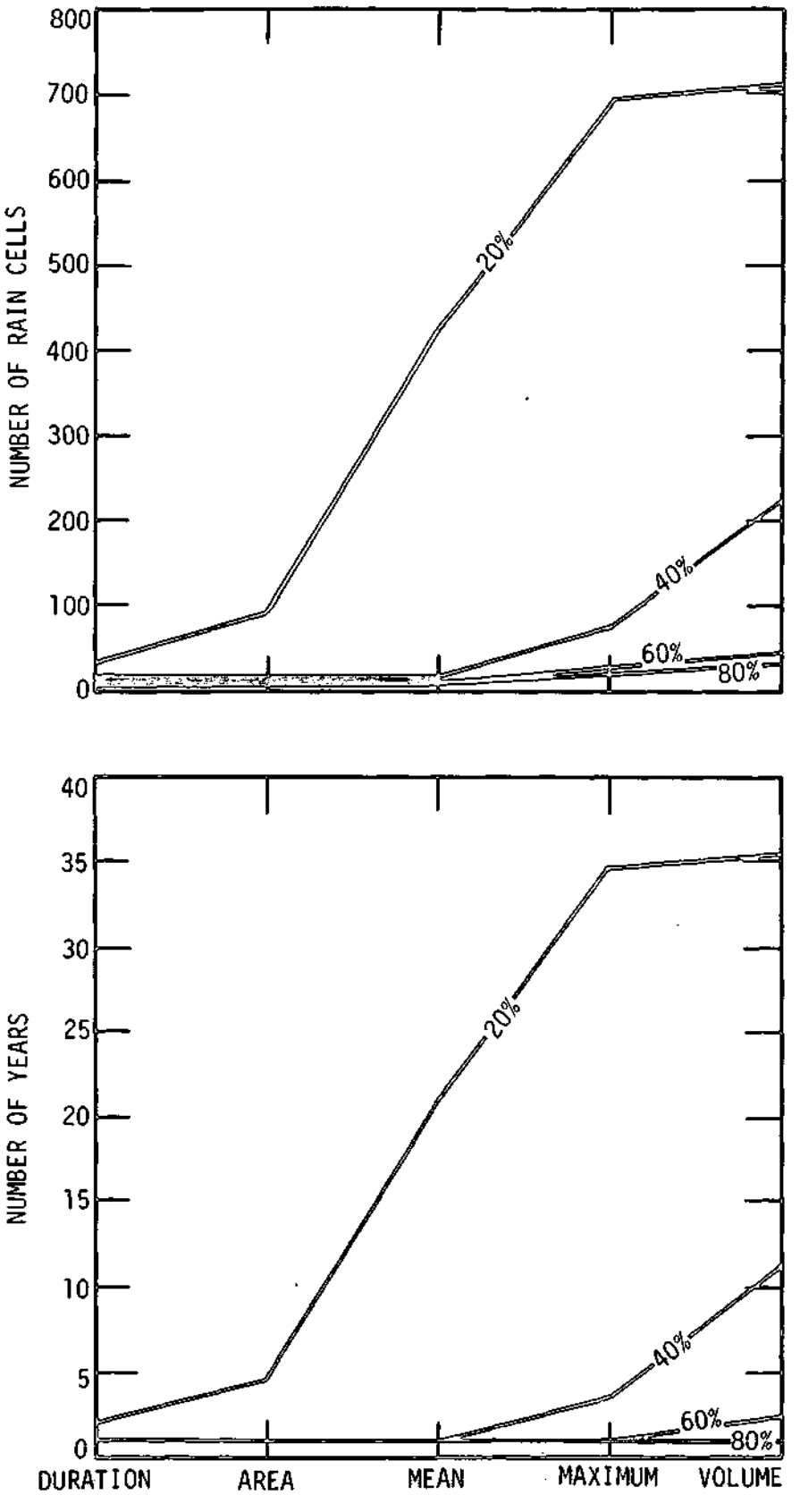

Figure 44. Sample size required to obtain significance for paired rain cells ($\alpha = 0.05$, $\beta = 0.50$).

Overall Conclusions

How applicable are these rain cell measurements to a rain modification experiment? As shown above, duration required the least amount of time to obtain significance. However, this may have been affected significantly by the limiting conditions imposed by the area of the sampling network. That is, the requirement for each rain cell used in the study to remain over the network during its life may have produced a relatively small variation in duration simply because long-duration storms were not sampled. Similarly, storms of very large areal extent could not be sampled. However, mean and maximum rainfall amounts should have been measured adequately by the sampling network. In general, the sample was biased towards shorter duration storms and SW-NE cell movements.

Strictly from a statistical evaluation standpoint, the rain cell comparison method is a potentially powerful evaluation technique. From practical considerations of present scientific knowledge and capabilities, however, its use may be difficult. First, the method assumes the experimenter has the capability to identify accurately and consistently those cloud pairs which have similar characteristics and which will culminate in the production of surface rainfall. Hopefully, this capability may be developed better in the future.

Secondly, a very dense network of recording raingages over hundreds or thousands of square miles would be needed to identify and accurately measure the various precipitation parameters at the surface. It is estimated that a gage density of approximately one per 5 mi^2 would be needed. The surface measurement problem could be partially alleviated through radar measurements; however, it is still not possible to measure rainfall amounts and intensities with acceptable accuracy with radar (despite the occasional glowing report from case studies described in the meteorological literature).

The rain cell comparisons in the Midwest would only be consistently feasible in air mass storms in which isolated convective clouds appear most frequently. There is generally too much clustering and interaction between convective units in frontal storms. Since air mass storms produce only a small portion of the total precipitation, it is pertinent to place major emphasis on frontal storms in evaluating the efficacy of cloud seeding and the potential benefits from modification operations in Illinois and other midwestern areas.

The limited statistical analyses performed in this 1-summer study do provide first approximations of the general range of sample sizes that would be required with the paired storm design. This should provide useful information for those who wish to incorporate this evaluation method into future modification experiments. The rain cell climatology should also be useful for planning purposes.

ESTIMATING NATURAL DISTRIBUTION OF STORM PRECIPITATION IN TARGET AREAS FROM CONTROL AREA DATA

Introduction

Nason and Lopez (1967) have investigated the feasibility of using control area precipitation patterns in storms to predict target patterns in the verification of cloud seeding experiments. This is an application of a technique proposed by Wadsworth (1951). Essentially, this involves fitting a plane or some higher order mathematical surface to the control area precipitation data and extending this surface through the target area. The target predictions are assumed to represent the rainfall pattern expected with no seeding. These values are then compared with measured amounts to determine seeding effects. Nason and Lopez limited their initial investigation to cold season storms in Oklahoma, and indicated favorable results for the technique with this type of storm. Hereafter, this design will be referred to as the control-target extrapolation design.

In our study, further evaluation of the Nason and Lopez approach to cloud seeding evaluation was made through use of data from a dense network of raingages in central Illinois. The investigation included equivalent samples of steady and unstable types of precipitation, since spatial variability differs substantially between these two basic types (Huff and Shipp, 1968). Results of the study provide additional knowledge helpful in assessing the feasibility of verifying seeding effects from comparison of individual storm distributions in target and control areas.

Three types of analysis were performed. In the first, the surface fitting technique was employed. In the second analysis, it was assumed that the best prediction of the precipitation pattern in a target area would be obtained by extension of the adjacent control area isohyetal pattern, taking into account pattern configurations and gradients established in the control isohyetal analysis. The third analysis was restricted to predicting target mean precipitation from a simple averaging of the nearest control area observations, under the assumption that storm mean precipitation remains relatively uniform over distances of a few miles.

Data Used

Two samples of 20 storms each from the East Central Illinois Network of 49 recording raingages in 400 mi^2 (Fig. 2) were used in the study. These were selected from a group of 260 storms analyzed for area-depth relations (Huff, 1968a) in which the network mean exceeded 0.5 inch or point amounts exceeding 1 inch were recorded within the network. Thus, they represent storms of above normal intensity and/or rainfall volume. The first sample consisted of storms in which thunderstorms and/or rainshowers were the prime producers of the network precipitation. The second sample included storms in which steady types of precipitation dominated. The 20-storm sample of unstable precipitation (TRW, RW) was selected so that a proportional number of each synoptic type was

included through random selection from synoptic type groupings of storms. Synoptic types used were cold, warm, stationary, and occluded fronts, air mass storms, low pressure center passages, and prefrontal squall lines (Huff and Shipp, 1968). The steady precipitation sample was restricted to four synoptic storm types that accounted for nearly all of this precipitation type in the 260-storm sample. These included cold, warm, and stationary fronts along with low centers. Network mean precipitation ranged from 0.15 inch to 1.78 inches in the sample of unstable precipitation, and from 0.30 inch to 1.84 inches in the stable group of storms.

Method of Analysis

Initially, the target consisted of 100 mi^2 at the downwind edge of the network, with the rest of the network being the control, as shown in the illustration in Fig. 45. For each storm, the direction of storm cell movement had been obtained previously from analyses of synoptic weather maps and consecutive 30-minute isohyetal maps constructed throughout each storm (Huff, 1967a). The target area was then assigned on this basis. Thus, if the cell movement was W-E, the target was placed at the eastern edge of the network as in Fig. 45; if movement was from the SW, the target was at the northeastern edge of the 400 mi^2. This was done, since it was assumed that assignment of a target area in scientific cloud seeding experiments would be based upon analysis of flow patterns expected during the seeding period. The target-control arrangement shown in Fig. 45 provides a measure of target prediction capability under optimum sampling conditions. Because of the contamination problem, laterally coinciding target and control areas would be difficult to use in field experiments. However, increasing the distance between target and control would tend to increase the target prediction error with the methods employed here.

In the surface fitting method, all gages in the control area of 300 mi^2 were used to construct the surface that was then extended through the target area to obtain the predicted storm precipitation at each sampling point (raingage). The 100 mi^2 target contained 12 raingages, whereas the 300 mi^2 control had 37 raingages.

Two surfaces were used. The first was a simple plane described by equation 29:

$$P = a + b_1 X + b_2 Y \qquad (29)$$

where P is the precipitation at a sampling point (raingage) in the network and the variables X and Y are the coordinates of the sampling point, and a, b_1, and b_2 are least squares regression constants for the plane determined from control data alone. The second surface was a quadratic surface described by the following equation:

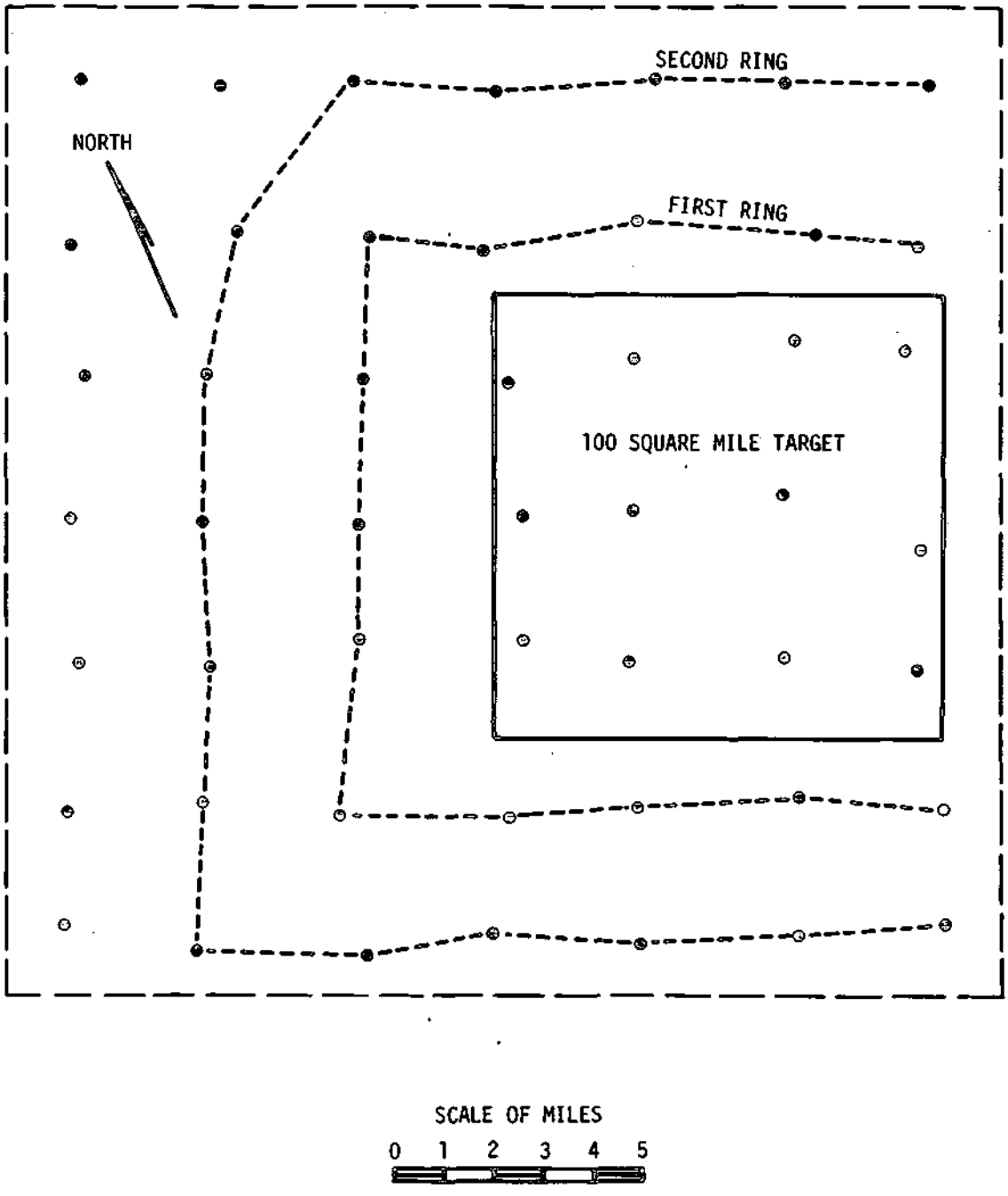

Figure 45. Sampling areas used in target-control estimations.

$$P = a + b_1 X + b_2 Y + b_3 X^2 + b_4 Y^2 + b_5 X Y \quad (30)$$

where P, X, and Y are defined as before and a, b_1, b_2, b_3, b_4, and b_5 are least squares regression constants determined for the quadratic surface from control data alone.

As indicated earlier, the isohyetal pattern in the target areas was obtained through extension of the existing pattern from the control area. With the isohyetal analyses, a target area of 50 mi^2 and a point target were also tested to determine whether the target prediction would improve significantly as the area decreased in size with respect to the adjacent control area. These targets were also selected at the downwind edge of the 400 mi^2 network in the same manner as the 100 mi^2 target. Naturally, some analyst subjectivity was involved, so two experienced analysts were used to make the target estimates. Since only small average differences occurred in the 100 mi^2 target predictions by the two analysts, only one was used for the point and 50 mi^2 analyses.

In determining target mean precipitation from averaging the nearest control gages, the target means were based upon use of (1) the first ring of gages adjacent to the target, and (2) the first two rings combined. The 100 mi^2 rings are shown in Fig. 45. Analyses were made also for targets of 50 mi^2.

Results of Analyses

Table 77 shows a comparison between the prediction errors of target mean precipitation when each of the three methods of estimation was used on the 100 mi^2 target. The percentage errors were obtained by substracting the predicted mean from the 12-gage average of recorded precipitation, dividing by the recorded average, and multiplying by 100. The percentage errors were fitted to a log normal distribution. An example is shown in Fig. 46 for unstable precipitation with the isohyetal extension method. From the log normal curves, the smoothed percentage distributions presented in Table 77 were obtained.

With unstable precipitation, Table 77 indicates that the plane-fitting and isohyetal methods are nearly equal in prediction capability, and both do better than the gage averaging or the quadratic. Use of a single ring of control gages nearest to the target was similar to the use of the quadratic surface and both proved superior to the 2-ring combination in the averaging method. Thus, the prediction error increased as gages more distant from the target were added.

Overall, prediction errors were considerably smaller with stable precipitation. For example, the plane-fitting median was 13% with unstable precipitation compared with 4% for the stable type.

With unstable precipitation and the two best prediction methods, errors equalled or exceeded 30% in 20% of the storms, and approximately 20% in 30% of

the storms. In weather modification experiments in which seeding-induced changes of 10% to 20% must be verified, the prediction capability does not appear to be satisfactory. With steady precipitation in which the prediction error exceeded 20% in only about 10% of the storms, the plane-fitting and isohyetal methods may provide a useful verification procedure.

Table 77. Comparison between three methods of predicting mean precipitation on 100 mi^2 target.

Percent of storms	Error (%) equalled or exceeded for given method				
	Surface fitting		Isohyetal extension	Gage averaging	
	Plane	Quadratic		1-Ring	2-Ring
Unstable precipitation					
10	44	80	53	67	95
20	29	44	29	38	53
30	21	29	19	25	35
40	17	19	14	18	25
50	13	14	10	13	18
60	10	10	7	9	13
70	8	7	5	7	9
80	6	4	3	4	6
90	4	2	2	2	3
Steady precipitation					
10	18	23	19	15	22
20	11	14	13	10	12
30	8	10	10	8	8
40	5	8	8	6	6
50	4	6	6	5	4
60	3	4	5	4	3
70	2	3	4	3	2
80	1	2	3	2	1
90	<1	1	2	1	<1

Other analyses indicated that the prediction errors tend to be largest with air mass storms, followed by static front storms. No substantial difference appeared between warm front, cold front, and low center errors. Additional tests indicated that the prediction error is insignificantly affected by rainfall volume with unstable precipitation, and weakly related with the steady type. This is indicated by correlation coefficients of -0.12 and -0.33, respectively, between mean rainfall and prediction error for the unstable and steady types on the 100 mi^2 target for the isohyetal method. Therefore, no allowance was made for the mean rainfall factor in Table 77, since it is intended only to provide

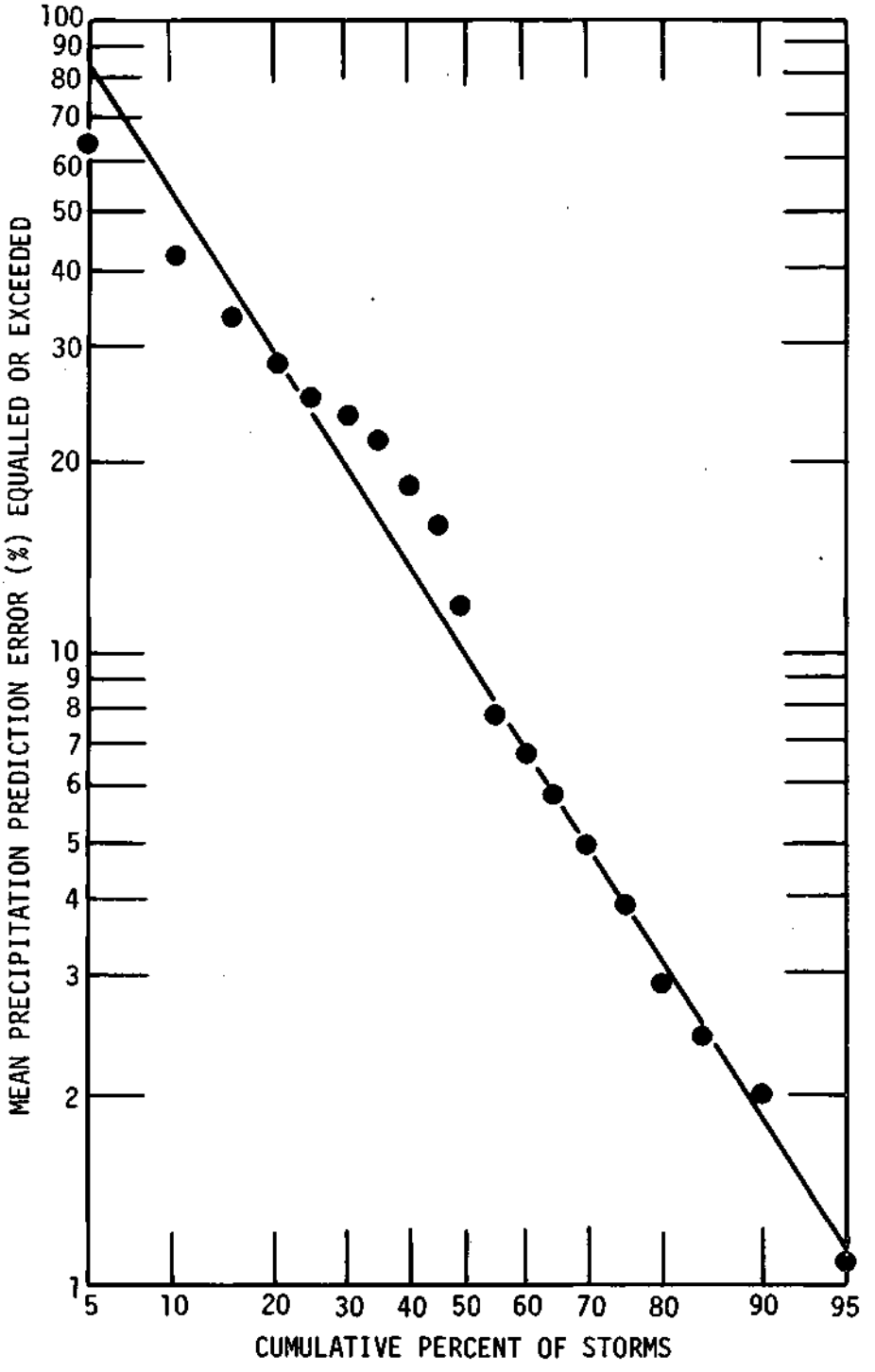

Figure 46. Distribution of prediction errors with isohyetal method.

a first estimate of the size of the prediction error when the control pattern is used to determine the target mean rainfall under natural precipitation conditions.

Using the isohyetal method with steady precipitation, no significant change was found in the prediction error as the target area was reduced from 100 mi^2 to 50 mi^2 and then to a point. However, with unstable precipitation, the error was found to decrease with decreasing size of target, as illustrated in Table 78 for the isohyetal method.

Table 78. Effect of target area on prediction error with unstable precipitation using isohyetal method.

Percent of storms	Error (%) equalled or exceeded 100 mi^2	50 mi^2	Point
10	53	38	27
20	29	22	16
30	19	15	11
40	14	11	8
50	10	8	6
60	7	6	4
70	5	4	3
80	3	3	2
90	2	2	1

On the 100 mi^2 target, an evaluation was made also of how accurately the maximum point rainfall could be predicted from the control isohyetal pattern extension. In the 20 storms with thundershowers and rainshowers, the median percentage difference between the actual and predicted rainfall was 13 and ranged from 1 to 50. Similarly, the 20-storm median for steady precipitation was 7% with a range from 0 to 40%, Comparison of the maximum rainfall prediction errors with those for mean rainfall in Table 77 showed a nearly equivalent prediction accuracy for the two precipitation parameters in these heavy storm samples.

Using the isohyetal method, average differences in inches between predicted and actual point values in the areal target were calculated for each set of storms. These provide a measure of prediction capability of point rainfall in the target from extension of the control isohyetal pattern. The average difference for each storm was then expressed as a percentage of the target mean rainfall to obtain a statistic for comparison between storms. The distribution of these point rainfall percentage errors for the 100 mi^2 target is summarized in Table 79 for each precipitation type. Median differences of

23% and 10%, respectively, are shown for the unstable and steady types, and these differences increase to 72% and 21% at the 90-% level.

Table 79. Average differences (%) between predicted and observed point rainfalls in 100 mi^2 target using isohyetal method.

Percent of storms	Percent differences	
	Unstable	Steady
10	7	5
20	11	6
30	15	7
40	19	9
50	23	10
60	29	12
70	37	14
80	48	17
90	72	21

In a further evaluation of the point rainfall prediction capability within a target area, the root mean square of the 12 differences between the predicted and observed point rainfall was calculated for each storm on the 100 mi^2 target for both stable and unstable types of precipitation with the isohyetal method. Root mean square differences and mean precipitation are shown in Table 80 for selected points along the log-normal distribution curves derived from the data. Both precipitation types were combined for the mean precipitation distribution because of insignificant differences.

Using the surface extension theory developed by Nason and Lopez (1967) an estimate was made of the average length of sequence needed to verify 10% and 20% increases in the actual gage amounts in the target area. The method was only applied to the plane since it had smaller prediction errors than the quadratic surface. The results of the application of the test are shown in Table 81. The table indicates that both percentage increases would be detected well within a 1-year period. Storms were selected from a sample which has an average of 24 storms per year (260 storms in a 11-year period). Nason and Lopez (1967) obtained values of 7.1 and 3.0 for 10% and 20% increases, based on data from the Washita network in Oklahoma. They also applied a fractional power transformation to the data which was not applied in the present study.

Are these numbers realistic? The entire method is dependent upon (1) the extrapolation of a regression equation beyond the range of the original observations, and (2) the use of error formulas for the individual estimate

predicted from a regression equation. Eziekel (1959) states that the estimate of an individual value beyond the range of values represented from a regression equation in the original sample is subject to a hazard beyond the usual error formulas. He also states that the usual error formulas only give accurate values of the probable error of an individual estimate within the range represented by the original sample. Extrapolation of the regression equation or curves beyond that range of values represents an extension into unknown fields, where sudden changes in the nature of relations might conceivably occur. In the present problem, the range of the original observations are those in the control area, and the observation beyond the sample range represent those in the target area.

Table 80. Distribution of root mean square differences and target mean precipitation on 100 mi^2 target using isohyetal method.

Percent of storms	R.M.S. (in) Unstable	Steady	Target mean (in)
10	0.09	0.04	0.25
20	0.12	0.06	0.50
30	0.15	0.08	0.67
40	0.19	0.09	0.82
50	0.22	0.11	0.96
60	0.26	0.14	1.10
70	0.32	0.18	1.25
80	0.40	0.23	1.42
90	0.54	0.32	1.67

Table 81. Average length of storm sequence needed to reach significance using the plane extrapolation method.

Category	10% Increase	20% Increase
All storms	11.0	3.2
Steady rainstorms	13.0	3.2
Unstable rainstorms	16.0	3.2

Table 77 shows the range of predicted values of the mean in the target area. But, an even more important question is whether the errors are similar in the target and control areas? The standard error of estimate (i.e., the standard deviation of the actual values from the predicted values) for storms in the control area was compared with the standard error of estimate for storms in the target area. The average of these errors for steady rainstorms was 0.17 and 0.15, respectively, for the control and target areas, and the average for the unstable rainstorms was 0.25 and 0.21, respectively, for the target and control areas. Thus, for this particular sample, the errors were nearly the same for the target and control areas, but this would not be necessarily true in all cases. In particular, if the target and control areas were farther apart the errors could be considerably different in the two areas.

Another important consideration is how the target and control areas are selected. Nearly optimum conditions were used in this study in which a target area was assumed contiguous to a much larger control area on all except the downwind side of the target. This is an impractical experimental design, since the contiguous control would be subject to possible contamination, and the ability to isolate the target area with respect to wind flow accurately and consistently is doubtful. Also, the 20-storm sample had an abnormal number of storms with heavy rainfall, and such storms have less relative variability, on the average, than storms with light to moderate rainfalls. Thus, the limitations involved in the selection of target and control areas with respect to distance and direction detracts from the small sample sizes obtained when optimum conditions are met.

Overall Conclusions

The plane fitting method may have applicability as an evaluation technique in weather modification experiments. However, target and control areas must be selected so that the target will not be contaminated and at the same time be close enough to the control area to permit a realistic extrapolation of the plane. This problem detracts from the usefulness of the method. Additional research should be conducted to define better the predication capability on the target as its distance increases from the control area.

The prediction error of the target area mean can be large under some circumstances. For example, despite the extremely favorable conditions, reference to the plane-fitting and isohyetal estimates of target mean precipitation in Table 77 for unstable precipitation shows a predication error of 10% or more in 50% of the storms, and this error increased gradually to exceed 44% in 10% of the storms. Unless cloud seeding produces relatively large percentage changes in target precipitation, verification of the seeding effect would be extremely difficult even under these very favorable conditions.

With steady precipitation, Table 77 indicates that the technique may be useful, since the prediction errors are significantly smaller in the 50% of storms with the largest errors, and only exceed 20% in approximately 10% of the storms. However, again it must be stressed that prediction errors would probably be much larger under acceptable target-control operating conditions.

The extension of the procedure to all storms in the spectrum would likely increase the problems considerably. This is because some gage amounts may be zero (especially in unstable precipitation), and the surface of the rainfall pattern will no longer be a smooth surface. The rationale underlying the selection of storms used in this study was that if the method is feasible, it should show favorable results on the heavier storm sample since the rainfall surfaces are relatively smooth. An inkling of the difficulty which might be involved was experienced by one of the authors in an attempt to fit planes to daily rainfall data from USWB stations in five 600 mi^2 areas in Missouri. It was found that the plane would often estimate negative values or distort the confidence intervals in the vicinity of zero gage amounts, so that it was difficult to apply the usual regression error formulas. It does appear that for the method to work effectively on storms, the target area must be small and one must have a dense network of raingages.

For the sample used in this study, the quadratic surface gave larger percentage prediction errors in the target areas than the plane did, although the standard error of estimate in the control area tends to be less than with the plane. Thus, it appears that the greater refinement of the surface in the control area led to larger errors in the target area, because greater restraints were placed upon the surface curving and this made the matching of the target precipitation to the extended control surface more difficult.

The method does show considerable promise for pattern recognition when the surfaces are relatively smooth. Thus, if one is attempting to determine, for example, whether a high in an isohyetal pattern of monthly rainfall data is due to random chance or some other contributing factor, one could conceivably use this method very effectively. The individual months could be treated as storms, the isohyetal high as the target, and the surrounding area as the control. In this way, probabilistic statements could be attached to the high. Research along these lines is highly recommended.

CLIMATOLOGICAL DISTRIBUTION OF AREAL MEAN PRECIPITATION

Under GA-1360, analyses were made of the climatological distribution of precipitation on the East Central Illinois Network when the data were stratified in various ways. This was done to provide background knowledge for use in planning potential weather modification projects which might be undertaken in the state at some future date. In the interest of condensing a mass of statistical data, results of several of these studies have been presented in the form of tables.

Amount-Frequency Relations

In planning a precipitation modification experiment, it would be desirable to have a realistic quantitative estimate of how total areal precipitation is distributed with respect to storm intensity. Information on this distribution is

provided in Tables 82 to 84 for the two seasons, May-September and October-April, and on an annual summation basis. This has been done for areas of 50 and 400 mi^2 to provide a measure of how the distribution varies with increasing sampling area.

In Table 82, the cumulative percent of total precipitation in the 1955-1966 period has been related to storm mean precipitation. For example, on the 50 mi^2 area in May-September, 5% of the total precipitation, on the average, occurs in storms with means of 2.85 inches or more. The storm mean rainfall equalled or exceeded decreases to 0.87 inch at the median level (50%) and to 0.10 inch when 95% of all storms are included. Diffe rences between the 50 and 400 mi areas are relatively small.

Table 82. Relation between mean precipitation and percent of total precipitation in all storms for a given season and given area, ECI, 1955-1966.

Cumulative percent of total precipitation	Mean precipitation (inches) equalled or exceeded for a given season and a given area					
	May-September		October-April		Annual	
	50 mi^2	400 mi^2	50 mi^2	400 mi^2	50 mi^2	400 mi^2
5	2.85	2.78	2.59	2.76	2.61	2.72
10	2.30	2.20	2.03	2.16	2.11	2.18
20	1.71	1.63	1.50	1.58	1.59	1.56
30	1.35	1.30	1.18	1.24	1.26	1.25
40	1.08	1.05	0.95	1.00	1.02	1.02
50	0.87	0.85	0.76	0.80	0.82	0.82
60	0.68	0.68	0.59	0.62	0.65	0.65
70	0.51	0.52	0.44	0.46	0.49	0.49
80	0.35	0.36	0.30	0.31	0.33	0.33
90	0.18	0.21	0.15	0.15	0.18	0.18
95	0.10	0.12	0.08	0.07	0.09	0.09
Number of storms	623	675	656	671	1279	1344

In Tables 83 and 84, cumulative percent of storm occurrences has been related to storm mean precipitation. The relations in Table 83 are based upon use of all storms, whereas those storms in which the areal mean was only a trace have been eliminated in constructing Table 84. Interpretation of these tables is similar to Table 82. Thus, referring to May-September and 50 mi^2 in Table 83, it is seen that 5% of the storms have mean rainfall of 1.35 inches or greater, 50% have means of 0.11 or more, and 5% resulted in only traces. Naturally, when traces are eliminated in Table 84 the values increase at a given cumulative percent of the total occurrences.

Table 83. Distribution of areal mean precipitation in all storms for a given season and given area, ECI, 1955-1966.

Cumulative percent of storm occurrences	Mean precipitation (inches) equalled or exceeded for given season and area					
	May-September		October-April		Annual	
	50 mi^2	400 mi^2	50 mi^2	400 mi^2	50 mi^2	400 mi^2
5	1.35	1.23	1.15	1.18	1.25	1.19
10	0.91	0.85	0.75	0.78	0.83	0.82
20	0.52	0.48	0.40	0.42	0.47	0.48
30	0.31	0.31	0.25	0.25	0.28	0.29
40	0.19	0.18	0.16	0.14	0.17	0.17
50	0.11	0.12	0.09	0.08	0.10	0.10
60	0.06	0.06	0.05	0.04	0.06	0.05
70	0.03	0.03	0.03	0.03	0.03	0.03
80	0.02	0.02	0.02	0.02	0.02	0.02
90	0.01	T	0.01	0.01	0.01	0.01
95	T	T	T	T	T	T
Number of storms	623	675	656	671	1279	1344

Table 84. Distribution of areal mean precipitation in storms for given season and given area (traces eliminated), ECI, 1955-1966.

Cumulative percent of total no. of storms	Mean precipitation (inches) equalled or exceeded for a given season and a given area					
	May-September		October-April		Annual	
	50 mi^2	400 mi^2	50 mi^2	400 mi^2	50 mi^2	400 mi^2
5	1.38	1.42	1.21	1.20	1.31	1.29
10	0.97	1.00	0.81	0.80	0.89	0.91
20	0.56	0.58	0.47	0.47	0.53	0.54
30	0.36	0.37	0.30	0.29	0.34	0.33
40	0.24	0.24	0.18	0.18	0.21	0.21
50	0.15	0.15	0.11	0.11	0.13	0.13
60	0.10	0.09	0.07	0.07	0.08	0.07
70	0.06	0.05	0.05	0.05	0.05	0.05
80	0.04	0.04	0.05	0.04	0.04	0.04
90	0.03	0.03	0.04	0.03	0.03	0.03
95	0.02	0.02	0.03	0.02	0.03	0.02
Number of storms	551	579	596	598	1147	1177

From examination of Tables 82 to 84, it is apparent that a large percentage of the Illinois precipitation occurs in a small percentage of the storms. Quantitative estimates of this relation are provided in Table 85 in which cumulative percent of total precipitation has been related to percent of total storm occurrences. This table shows that, on the average, approximately 50% of the total precipitation is recorded in 11% of the storms in both the warm and cold seasons. Approximately 95% of all precipitation occurs in 50% of the storms.

Table 85. Percentage distribution of total precipitation in storms for a given season and given area, ECI, 1955-1966.

Cumulative percent of total precipitation	Cumulative percent of total storm occurrences for given season and area					
	May-September		October-April		Annual	
	50 mi^2	400 mi^2	50 mi^2	400 mi^2	50 mi^2	400 mi^2
5	0.5	0.4	0.4	0.4	0.5	0.5
10	1	1	1	1	1	1
20	3	3	3	3	3	3
30	5	4	5	4	5	5
40	8	7	7	7	7	7
50	11	10	10	10	10	10
60	15	13	13	14	14	14
70	20	19	19	18	19	19
80	28	27	25	25	27	27
90	41	37	41	40	39	40
95	51	50	52	53	52	51
Number of storms	623	675	656	671	1279	1344

Storm Duration - Synoptic Type - Precipitation Type Relations

Next, an investigation was made of how Illinois precipitation is distributed with respect to storm duration. In Table 86, percent of total precipitation and percent of total storm occurrences have been shown in the warm and cold seasons for selected groups of storm durations on the 400 mi^2 sampling area. In both seasons, storm durations of 3 hours or less are most frequent. During May-September, a greater percentage of the total precipitation occurs in relatively short durations. For example, 43% is indicated for storms of 6 hours or less, whereas only 20% of the October-April precipitation is recorded in storms of this length.

Another evaluation of the relation between storm frequency and storm intensity is presented in Table 87. Here, the percent of total precipitation has been related to percent of total storm occurrences on an annual basis with the precipitation data stratified by storm duration. As expected, a greater percentage of the total precipitation occurs in a small percentage of the storms with short-duration storms than in those of long-duration. For example, 50% of the storms account for 91% of the total precipitation in storms of 3 hours or less, compared with 78% in storms lasting 12 to 24 hours.

Table 86. Average distribution of precipitation on East Central Illinois network grouped by storm duration.

Storm duration (hours)	Percent of total precipitation		Percent of storms	
	May-Sept	Oct-April	May-Sept	Oct-April
≤ 3	22	9	57	35
3.1-6.0	21	11	20	19
6.1-12.0	20	21	12	22
12.1-24.0	23	40	8	19
24.1-48.0	13	16	3	5
> 48.0	1	3	0+	0+

Table 87. Annual relation between storm frequency and precipitation volume for various storm durations.

Cumulative percent of storms	Cumulative percent of total precipitation for given duration (hrs)			
	≤ 3	3.1-6.0	6.1-12.0	12.1-24.0
5	45	25	19	14
10	59	42	34	26
20	74	62	56	44
30	83	75	70	59
40	88	83	79	70
50	91	88	85	78
60	94	92	90	85
70	96	94	93	90
80	97	96	95	94
90	99	98	98	97
95	99+	99	99	99

Tables 88 and 89 show the precipitation distribution when stratified according to synoptic storm types. From these tables, it is apparent that cold fronts are the primary producer of rainfall in the warm season among synoptic types, whereas the passage of major low pressure systems is the major cold season type. Thunderstorms strongly predominate among warm season rainfall types. Frequently, thunderstorms are the major producer of storm rainfall, but are intermingled with rainshowers during lighter rain periods. On the East Central Illinois Network, the combination of thunderstorms and rainshowers accounted for 88% of the May-September rainfall in the 1955-1966 period and were associated with 87% of the storm occurrences. In the cold season, the rainshower-thunderstorm combination were associated with 40% of the storm occurrences, but accounted for 55% of the total seasonal precipitation. Stable-type rains accounted for approximately 30% of the precipitation and storm occurrences in the October-April period. Snow and snow mixed with rain were recorded in 30% of the storms but accounted for only about 14% of the total seasonal precipitation.

Table 88. Average distribution of May-September rainfall on East Central Illinois Network grouped by synoptic storm type.

Synoptic type	Percent of total rainfall	Percent of storms
Cold Front	39	36
Warm Front	14	11
Static Front	21	17
Occluded Front	2	2
Low Centers	7	8
Air Mass	17	26

Table 89. Average distribution of October-April precipitation on East Central Illinois Network grouped by synoptic storm type.

Synoptic type	Percent of total precipitation	Percent of storms
Cold Front	29	28
Warm Front	7	6
Static Front	13	10
Occluded Front	5	7
Low Centers	43	46
Air Mass	3	3

Table 90 defines further the relationship between precipitation and synoptic storm types. In this table, the relation between cumulative percent of storm occurrences and cumulative percent of total precipitation is shown for the major synoptic types on an annual summation basis.

Table 90. Annual relation between storm frequency and precipitation volume for synoptic storm types.

Cumulative percent of storms	Cumulative percent of total precipitation				
	Cold Front	Static Front	Warm Front	Low Center	Air Mass
5	29	29	29	36	38
10	48	48	46	53	59
20	70	70	66	74	78
30	83	83	78	85	88
40	91	91	86	92	94
50	94	94	91	95	96
60	96	96	94	96	97
70	97	97	97	97	98
80	98	98	98	98	98+
90	99	99	99	99	99
95	99+	99+	99+	99+	99+

The characteristics of the precipitation distributions presented in Tables 82 to 90 should be useful to the planner of precipitation modification experiments in Illinois and nearby regions, especially where intentions are to operate in a particular season or selected types of storms.

Wet Day Sequences

Another climatic factor useful in planning precipitation modification experiments is the sequential distribution of wet days that occur naturally. This type of information is especially useful in those experiments where the residual effects of seeding on a target are of concern. Tables 91 and 92 show the distribution of wet day sequences on the East Central Illinois and Little Egypt Networks during 10-year sampling periods for seasonal and annual summations. In these tables, the frequency distribution is provided for sequences of one to five consecutive days and for six days or longer. Both total number of occurrences and percent of total cases are shown for each wet day sequence.

On an annual basis, the differences between the two networks located in the central and southern portions of the state are insignificant. In the

May-September period, there is a trend indicated for more storms lasting three days or longer on the Little Egypt Network in southern Illinois. Thus, there were 22% of the cases with three-day or longer rain periods in the southern Illinois network compared with 16% in central Illinois. This trend reverses in the cold season (October-April) during which 10% of the storms lasted three days or longer in the central part of the state compared with 7% in the south. In both networks and both seasons one-day storm periods predominate.

Table 91. Wet day sequences on Little Egypt Network, 1958-1967.

Number of consecutive days with precipitation	May-September		October-April		Annual	
	Total cases	Percent of total	Total cases	Percent of total	Total cases	Percent of total
1	159	55	314	74	473	66
2	67	23	81	19	148	21
3	35	12	14	3	49	7
4	18	6	8	2	26	4
5	5	2	3	1	8	1
≥ 6	7	2	2	1	9	1

Table 92. Wet day sequences on East Central Illinois Network, 1955-1964.

Number of consecutive days with precipitation	May-September		October-April		Annual	
	Total cases	Percent of total	Total cases	Percent of total	Total cases	Percent of total
1	173	60	257	72	430	67
2	70	24	62	18	132	20
3	24	8	21	6	45	7
4	14	5	12	3	26	4
5	5	2	3	1	8	1+
≥ 6	4	1	1	0+	5	1-

DISTRIBUTION OF POINT PRECIPITATION IN ILLINOIS

Additional climatological statistics for use in planning and evaluating precipitation modification experiments are presented in this section. Results are summarized from analyses of the frequency distribution of point precipitation on a daily and hourly basis in Illinois, based upon records from U. S. Weather Bureau stations. Data from 57 climatological stations with weather records spanning all or most of the 50-year period, 1906-1955, were used in the daily study. Data from 30 stations with recording raingages during the 10-year period, 1948-1957, were used in the hourly analyses. Also, a brief discussion of snowfall climatology is included.

Daily Precipitation Distributions

First, an investigation was made of the frequency distribution of mean annual precipitation according to daily precipitation amounts at each station. Concurrently, an analysis was made of the frequency distribution of days with various daily amounts. Results are summarized in Figs. 47 and 48. Table 93 shows typical station distributions for the northern, central, and southern parts of the state.

Table 93. Average percentage distribution of annual precipitation based on daily precipitation.

	Percent of total precipitation from given daily amount (in)			
Station	0.01-0.10	0.11-0.50	0.51-1.00	> 1.00
Chicago	8	35	28	29
Peoria	5	32	29	34
St. Louis	5	29	28	38
Cairo	4	26	28	42
	Percent of days with given daily amount (in)			
Chicago	48	36	11	5
Peoria	43	37	13	7
St. Louis	41	38	13	8
Cairo	39	36	15	10

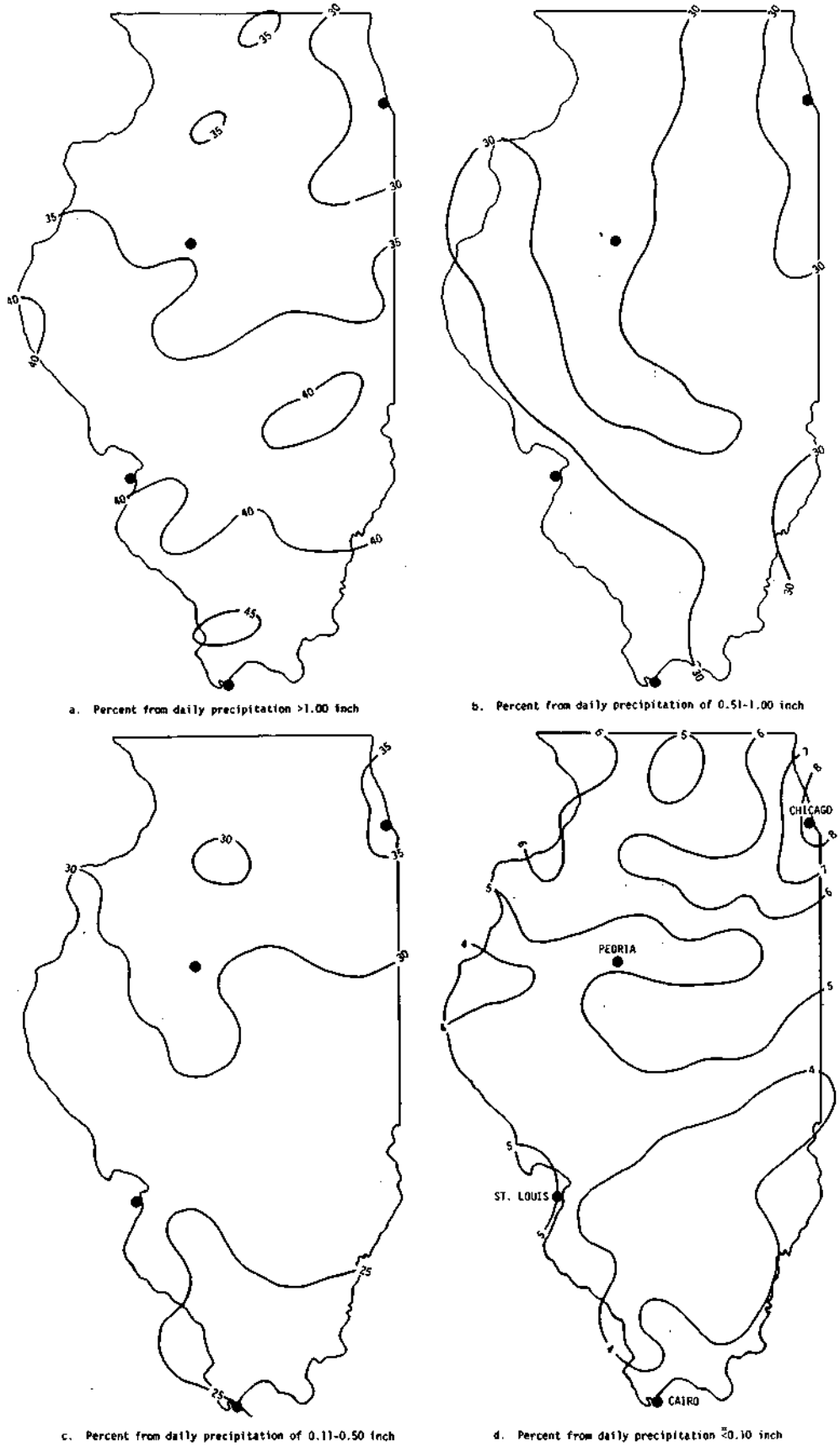

Figure 47. Distribution of average annual precipitation grouped by daily amounts.

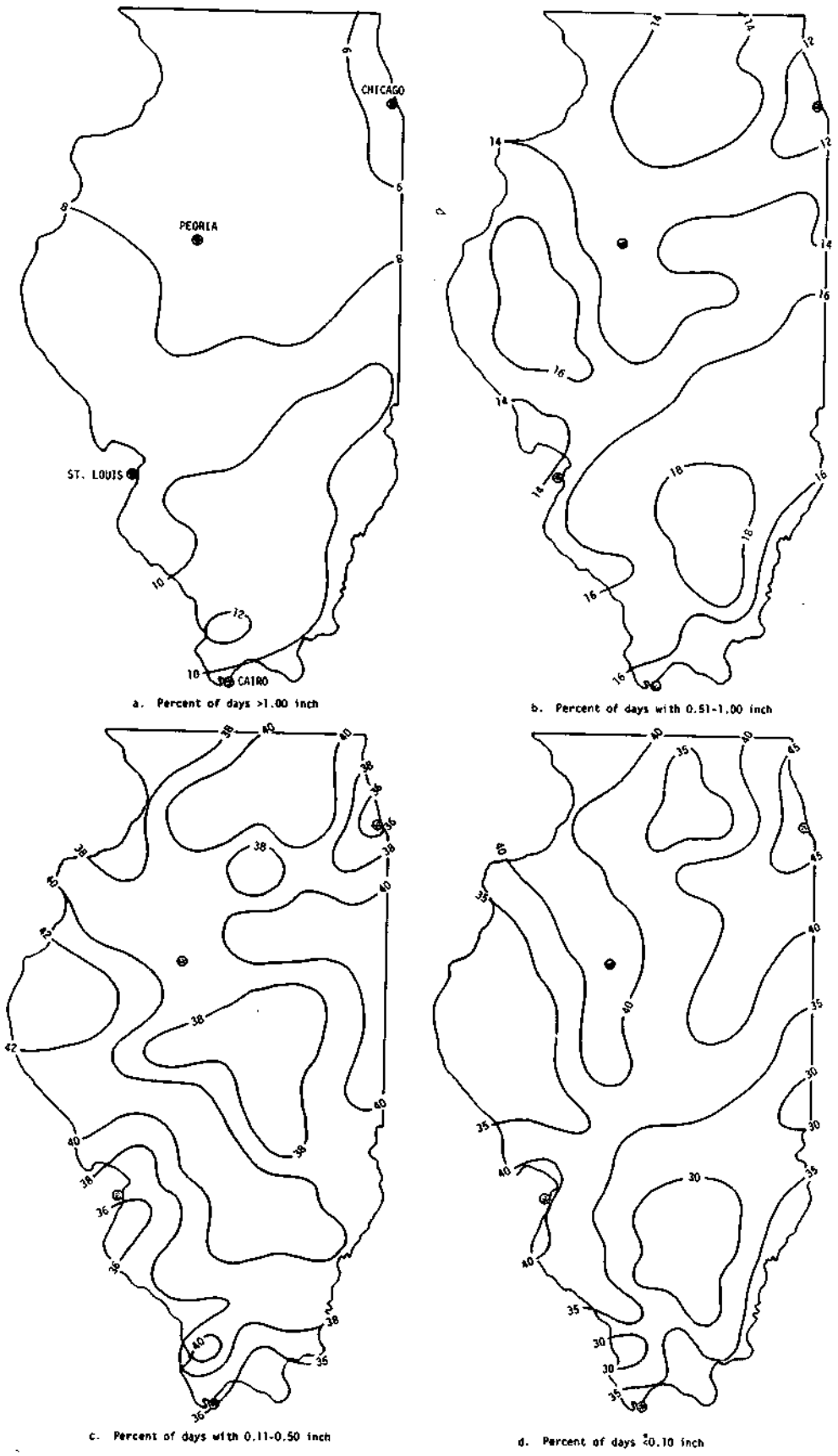

Figure 48. Distribution of average annual precipitation grouped by frequency of daily amounts.

From the maps and tables, it is evident that, whereas daily precipitation falls most frequently into the light class, 0.01-0.10 inch, only a very small amount of the total annual precipitation is accounted for on these days. Thus, if weather modification could either significantly increase the number of these occurrences or increase the rainfall amounts by 10 to 20%, or even 50%, the net result, on the average, would be only a small percentage increase in total precipitation. Climatologically, significant modification of precipitation on those days with amounts from 0.11 to 0.50 inch would appear to be most rewarding, since this group of storms accounts for over one-third of the total annual precipitation and nearly one-third of the annual occurrences. A substantial portion of the annual precipitation results from days with over one inch, but these days are relatively infrequent and the desirability of further increasing precipitation on these days of heavy storms is questionable, even if it were feasible.

The frequency distributions presented to this point are for average conditions. An obvious question concerns the type of precipitation experienced in dry periods. Huff (1969) has discussed results obtained from analyses of the distribution of mean precipitation during average, wet, and dry years in a 12-year network study in Illinois. Further indication of dry-period conditions was obtained from study of two droughts: 1) a widespread severe drought affecting large portions of the state in the 1953-1954 period (Huff and Changnon, 1963); and 2) a localized drought in the corn and soybean belt of east central Illinois during the 1969 growing season.

Fig. 49 illustrates conditions in the 12-month drought, August 1953-July 1954. Isolines show the percent of normal number of days with precipitation of 0.50 inch or more. This drought was most severe in the south central part of the state where the 12-month precipitation was less than 50% of normal, as shown by the cross-hatched area in Fig. 49. Note that the maximum deficiency of heavy precipitation days, those with 0.5 inch or more, nearly coincides with the area experiencing the most severe drought. Near normal to slightly above normal precipitation was recorded in the northern part of the state where the 0.50-inch frequency is normal or slightly higher. The above findings are reasonable and logical, based upon Fig. 47, which show that approximately two-thirds of the annual precipitation in south central Illinois, on the average, occurs on days with precipitation exceeding 0.50 inch. However, only about one-fourth of all precipitation days normally have precipitation of this magnitude.

Fig. 50 shows the percent of normal rainfall in the 3-month period, May-July 1969, in which a severe localized drought occurred in east central Illinois. Most of the state had above normal rainfall during this period. Only about 5% of the state had less than 75% of normal and slightly over 1% experienced the severe drought shown by the 60% isoline in Fig. 50. It would seem reasonable to expect that weather modification might be useful in alleviating such localized deficiencies, whereas in the widespread drought (such as the 1953-1954 case) large-scale atmospheric conditions are likely to prevent much alleviation from cloud seeding.

As in the large-scale 1953-1954 drought, there was a definite deficiency in the number of rainy days with 0.50 inch or more and 1.00 inch or more. Analyses indicated that within the 60% area of Fig. 50, there were an average

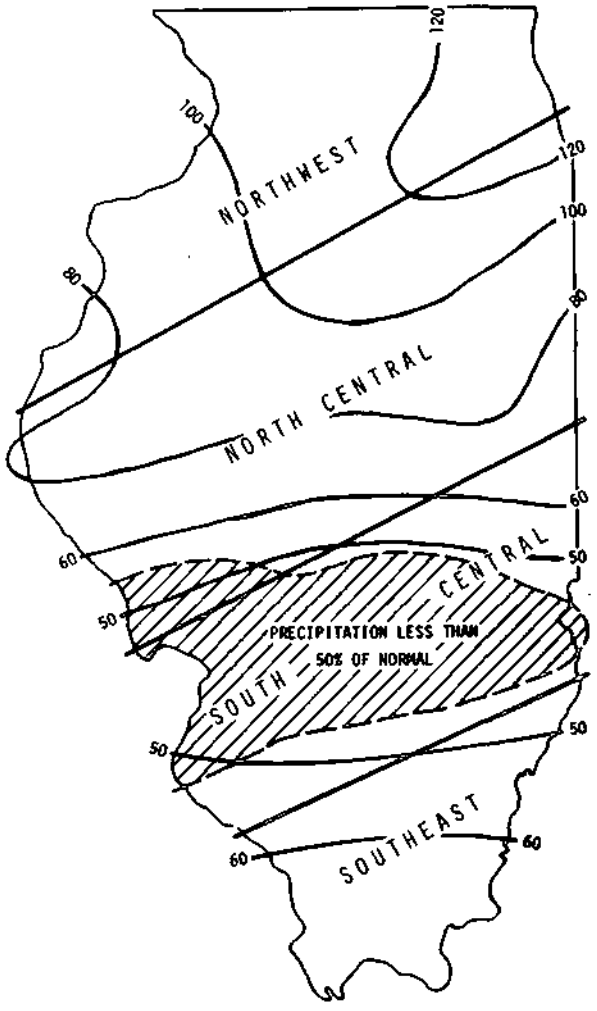

Figure 49. Distribution on 12-month precipitation in a large-scale severe drought.

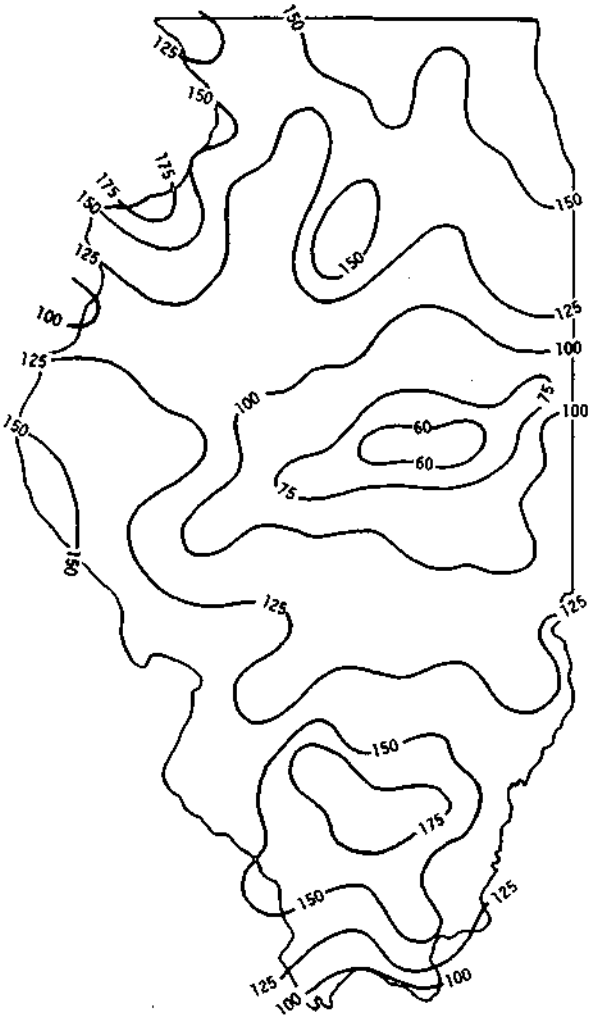

Figure 50. Percent of normal rainfall in a severe localized drought of 3-month duration.

of four days with 0.50-inch or more rainfall, compared with 10-15 days in the areas with above normal rainfall. Similarly, the dry area averaged only one day with rainfall over 1.00 inch, compared with four to eight days in the above normal regions. Based on 165 Illinois stations, the correlation coefficient between May-July 1969 rainfall and number -of days with more than one inch of rainfall was a relatively high 0.79. The correlation coefficient reduced to 0.68 when days with rainfall exceeding 0.50 inch were correlated with the 3-month total.

Hourly Precipitation Distributions

As part of the Illinois climatic studies, 10 years of data from 30 recording raingage stations in and near Illinois were used to determine the frequency distribution of hourly precipitation on a seasonal, annual, and diurnal basis throughout the state. For this study, the state was divided into four sections of similar precipitation climate (Huff and Neill, 1959), and average distributions were developed for each section. Locations of the four sections (northwest, north central, south central, southwest) are shown in Fig. 49.

The annual and seasonal distributions of hourly precipitation are summarized in Table 94. Precipitation modification undertaken in any season would be performed predominately on storms in which hourly amounts are 0.10 inch or less. An appreciable percentage of the hourly amounts exceed 0.25 inch only in summer, when the average is 12 to 13%. The statistics of Table 94 indicate that in Illinois and similar climatic regions seeding operations would usually need to be carried on successfully for several consecutive hours on storm days to achieve substantial increases in total precipitation. Hourly distributions can be easily determined for other areas from U. S. Weather Bureau published data. These can then assist in determining potential benefits from cloud seeding and in planning seeding operations.

The diurnal distribution of hourly precipitation during winter and summer for the four sections of the state is summarized in Tables 95 to 97. Table 95 shows the percentage of the total seasonal precipitation for 3-hour periods in each climatic section. Similarly, Table 96 shows the frequency of occurrence of measurable precipitation by 3-hour periods. Table 97 shows average hourly rates.

Changes in the diurnal distribution are most pronounced between sections during summer, and are most prominant between the Southeast and the two northerly sections (Northwest and North Central).

Snowfall Distribution

The natural distribution of snowfall is of major importance in the planning of precipitation modification experiments during the cold season. For example, intensification of naturally heavy snowstorms would normally

Table 94. Annual and seasonal distribution of hourly precipitation.

Period	Average number of hours per year	Percent of total hours with given hourly amounts (in) 0.01-0.10	0.11-0.25	0.26-0.50	0.51-1.00	Over 1.00
		Northwest Section				
Winter	127	93.4	5.6	0.8	0.1	0.1-
Spring	155	86.2	10.6	2.4	0.7	0.1
Summer	99	71.8	16.4	7.1	3.5	1.2
Fall	87	83.5	12.5	2.8	0.9	0.3
Annual	468	84.6	10.8	3.1	1.1	0.4
		North Central Section				
Winter	135	90.7	7.6	1.2	0.3	0.1-
Spring	151	84.8	11.2	3.0	0.8	0.2
Summer	90	72.1	15.0	8.0	3.7	1.2
Fall	89	84.2	11.4	3.4	0.9	0.1
Annual	465	83.8	11.1	3.5	1.3	0.3
		South Central Section				
Winter	126	84.9	11.7	2.3	0.8	0.3
Spring	137	81.6	13.6	3.5	1.1	0.2
Summer	79	72.4	15.1	7.3	3.9	1.3
Fall	94	78.2	15.6	4.6	1.3	0.3
Annual	436	80.0	13.8	4.1	1.6	0.5
		Southeast Section				
Winter	189	82.3	13.1	3.6	0.8	0.2
Spring	146	77.6	15.5	5.2	1.4	0.3
Summer	83	71.7	15.6	7.8	3.9	1.0
Fall	104	76.2	16.5	5.5	1.5	0.3
Annual	522	78.0	14.9	5.1	1.6	0.4

Table 95. Average diurnal distribution of total precipitation by section and season.

3-Hours ending (CST)	Percent of total precipitation for given section and season			
	North-West	North Central	South Central	South-East
		Winter		
03	11.7	12.9	13.4	14.4
06	13.5	13.5	13.4	15.2
09	12.7	12.3	11.5	11.3
12	13.0	13.8	11.1	10.8
15	10.5	10.1	10.9	9.9
18	13.0	12.6	12.5	10.2
21	11.6	12.1	13.1	12.3
24	14.0	12.7	14.1	15.9
		Summer		
03	13.0	15.6	16.2	10.3
06	17.4	13.4	16.2	11.4
09	15.6	13.3	10.8	14.0
12	7.8	9.2	9.2	11.9
15	9.8	9.8	10.5	16.7
18	11.3	11.9	12.7	15.9
21	12.9	13.5	11.7	9.5
24	12.2	13.3	12.7	10.3

Table 96. Average diurnal distribution of precipitation occurrences by section and season.

3-Hours ending (CST)	Percent of total occurrences for given section and season			
	North-West	North Central	South Central	South-East
		Winter		
03	13.4	13.5	14.5	15.0
06	13.4	13.5	14.1	14.1
09	12.0	13.2	12.0	12.0
12	13.8	13.3	11.8	11.2
15	11.2	11.8	11.2	10.4
18	12.2	11.4	12.0	11.1
21	12.0	11.8	12.3	12.6
24	12.0	11.5	12.1	13.6
		Summer		
03	13.5	14.1	15.3	11.4
06	15.4	12.5	14.7	11.9
09	15.2	14.5	13.3	14.1
12	11.4	12.9	11.7	13.6
15	10.1	11.0	11.7	14.8
18	11.3	11.2	11.7	13.4
21	11.5	11.4	10.4	10.6
24	11.6	12.4	11.2	10.2

Table 97. Diurnal distribution of average hourly rainfall rate by section and season.

3-Hours ending (CST)	Mean rate (in/hr) for given section and season			
	North-West	North Central	South Central	South-East
		Winter		
03	0.035	0.044	0.056	0.065
06	0.042	0.046	0.058	0.074
09	0.043	0.043	0.058	0.064
12	0.038	0.048	0.057	0.064
15	0.038	0.043	0.060	0.065
18	0.043	0.051	0.063	0.063
21	0.039	0.047	0.064	0.066
24	0.047	0.051	0.071	0.080
		Summer		
03	0.116	0.146	0.128	0.102
06	0.135	0.133	0.132	0.108
09	0.122	0.114	0.098	0.111
12	0.092	0.089	0.095	0.090
15	0.110	0.110	0.108	0.128
18	0.120	0.132	0.132	0.135
21	0.134	0.140	0.138	0.102
24	0.126	0.133	0.137	0.121

be an overall disbenefit. Changnon (1969) has indicated that severe winter storms which usually produce heavy snowfall in excess of 6 inches produce more damage in Illinois than any other form of severe weather. In areas where snowfall is the major form of precipitation, however, seeding of snowstorms would be required for substantial seeding-induced precipitation.

Snowfall contributes only a small portion of the annual precipitation in Illinois. Table 98 indicates the average percentage decreases gradually from 8.5 in the Northwest section (see Fig. 49) to 3.0 in the Southeast section. Other Illinois studies have shown that the average number of days with 1-inch or greater snowfalls per year decreases from a high of 13 in the extreme northwestern part of the state to 4 in the extreme south (Changnon, 1969). The average number of 2-day periods with 4 inches or more snowfall decreases from 2-3 per year in the northern part of the state to 1 per year in the south.

Since snowfall is not a major contributor to Illinois precipitation, it should not present a major problem in seeding experiments. The few days with potential for heavy snowfall could probably be avoided in most seeding programs without severely hampering the experiment.

Table 98. Percent of average annual precipitation from snowfall.

Section	Average percentage
Northwest	8.5
North Central	6.1
South Central	4.2
Southeast	3.0

FREQUENCY DISTRIBUTION OF VARIOUS STORM FACTORS

Huff (1967a) used a 261-storm sample (discussed earlier) on the East Central Illinois Network (Fig. 2) to investigate the frequency distribution of various factors that might aid in defining the distribution characteristics of storms of moderate to heavy intensity. Investigation was made of (1) burst characteristics, (2) storm center distributions, (3) time continuity of precipitation in storms, (4) effects of rain type, storm type, and storm duration on the time distribution of precipitation, and (5) storm shapes and orientations.

Frequency of Bursts

A number of analyses were performed to define the rainfall burst characteristics. The first problem was to define a burst, and this definition must necessarily be conditional to a particular interpretation. After considerable probing, definitions were selected to portray most realistically definite changes in rainfall intensity which were associated with significant changes in the atmospheric precipitation process, such as the development of new rain cells over the sampling area, a major change in the rainout characteristics of the existing storm over the network, or arrival of a new storm system. For the purposes of the Illinois study, bursts were separated by (1) a complete cessation of rainfall on the sampling area, (2) a change in successive 30-minute rainfall amounts of 100% or more, provided that these amounts involved 5% or more of the total storm rainfall, and (3) changes in percent of total rainfall from 3, 4, or 5% to less than 1% between successive 30-minute periods. Changes between successive periods ranging from 0.1 to 2% of the storm total were not considered separate bursts.

An evaluation was made of the number of bursts associated with storms stratified by quartile (see section on time distribution models). Combining all storms, those with two, three, or four bursts accounted for 53% of the cases on the 400 mi^2 network. In the first-quartile storms, two or three bursts were found most frequently and accounted for approximately 48% of the occurrences. One to three bursts occurred in 60% of. the second-quartile storms. Three to five bursts were found most commonly with the third-quartile storms and accounted for 52% of the cases. The fourth-quartile storms showed a strong preference for four bursts which were associated with 35% of the storms.

In general, the number of bursts was found to range from 1 to 14 in Illinois storms, and the maximum burst occurred anywhere from the first to eighth burst within the storms. The percentage of the total rainfall occurring in the maximum burst ranged from less than 20% to 100 % on each of the areas investigated.

Next, the effect of total storm duration on the number of bursts was evaluated. It was found that with durations less than 3 hours, single-burst storms predominated, accounting for 52% of the cases. In storm durations ranging from 3 to 12 hours, double-burst storms predominated with 38% of the total cases. Storms with 3 to 5 bursts were found with nearly equal frequency with durations of 12 to 24 hours and accounted for 71% of the cases. With durations exceeding 24 hours, 6-burst storms occurred most often and were found in 30% of the occurrences. Thus, as one would expect, the number of bursts tends to increase with increasing storm duration. Since the heavier areal mean rainfalls tend to occur with the longer rainfall durations, analyses showed the expected trend for the number of bursts to increase with volume of rainfall, on the average.

Maximum Burst Relations

Other information valuable to understanding of the burst characteristics of storms include what percentage of the rain occurs prior to and during the maximum burst and how much of the total storm time has ensued prior to and during

the maximum burst. A large volume of statistics was compiled on these burst characteristics for a point and areas up to 400 mi^2 for each of the quartile storms. In Table 99, results of these bursts analyses have been illustrated for storms based upon the median value of each parameter for a point at the center of the network and for areas of 50 to 400 mi^2 combined, since differences between these areas were small. For each quartile, the cumulative percent of the storm period which had ensued before the start of the maximum burst is shown, along with the cumulative storm time at the end of the burst, the percent of the total storm rainfall prior to the start of the maximum burst, and the percent of the total rainfall in the maximum burst.

Table 99. Median values for maximum storm bursts.

Area, mi^2	Percent of storm time		Percent of total storm rainfall	
	Start of burst	End of burst	Prior to burst	During burst
	First-quartile storms			
Point	0	36	0	71
50-400	0	37	0	77
	Second-quartile storms			
Point	17	67	14	70
50-400	16	62	8	79
	Third-quartile storms			
Point	42	78	24	62
50-400	46	82	25	69
	Fourth-quartile storms			
Point	73	100	43	57
50-400	72	96	39	59

The strong trend indicated earlier for a major portion of the total storm rainfall to occur in the maximum storm burst is apparent in Table 99. The point percentages are somewhat smaller than the areal values, but may be due to sampling vagaries. From the standpoint of duration, the maximum burst time was shortest for the fourth-quartile storms which also had the smallest percentage of total rainfall in the maximum burst.

Storm Center Distributions

The distribution of storm centers and the influence of storm mean rainfall and rainfall duration on the number of centers were investigated. Analyses were made for areas of 50 and 100 mi^2 and durations of 30 minute to 48 hours. Centers as used here refer to either a closed isohyet or, if there were no closed isohyets in the sampling area, the region of heaviest rainfall was considered the storm center.

On the 400-mi^2 area, 1 to 3 centers were the most frequent with all durations. The number of centers varied from 1 to 6. With increasing duration, there was a trend for a greater percentage of the storms to have 4 to 6 centers. The percent of total cases with 1 to 3 centers decreased gradually from 90% with 1-hour storms to 70% with 24-hour rainfalls. Except for very heavy rainfall with areal means of 2 inches or greater, 1 to 3 centers were found most often in the mean rainfall groupings.

Only 1 or 2 storm centers were found on the 50 mi^2 in all cases due to the small area encompassed. For all rainfall durations, single centers dominated with no strong trend for change indicated with increasing duration. Also, no strong trends were observed with varying mean rainfall.

Time Continuity of Precipitation in Storms

An analysis was made to determine what percent of the total storm period experiences rainfall. This revealed an expected trend. The percentage of the total storm period with rainfall somewhere on the sampling area increased with increasing area and decreased with increasing storm duration, as shown by the median values in Table 100.

Table 100. Percent of total storm period with precipitation.

Storm period (hours)	Median percentage for given area (mi^2)				
	Point	50	100	200	400
< 3.0	100	100	100	100	100
3.1-6.0	79	91	100	100	100
6.1-12.0	74	87	88	92	96
12.1-24.0	55	74	81	83	92
> 24.0	42	65	70	76	83

The foregoing discussion and statistics on bursts emphasize the great variability found in their characteristics under various storm conditions. This is typical of almost any rainfall parameter examined in midwestern rainstorms, particularly those of the warm season which produce most of the intense rainfalls.

Relations Between Rain Type, Storm Type, and Time Distributions

Rain type. The distribution of rain type by quartile was examined to determine if any particular type dominated within the four quartiles. Results are summarized in Table 101 in which percentage frequencies are shown for each of seven precipitation types. For storms in which the major burst occurred in the first, second, or third quartile, thunderstorms were the most frequent rain type, particularly in the first-quartile and second-quartile storms. In the fourth-quartile storms, the combination of rainshowers and thunderstorms predominated. These storms tend to last longer than the other quartile storms and, thus, frequently consist of a number of individual storms of varying intensity.

Table 101. Distribution of storms by quartile and rain type on 400 mi^2.

Quartile	R,S*	R	RW	TRW	RW,R	TRW,RW	TRW,A	Number of cases
1	1.2	6.1	12.2	43.9	7.3	13.4	15.8	82
2	2.2	15.4	16.5	42.9	4.4	13.2	5.5	91
3	3.1	15.4	13.8	30.7	3.1	23.1	10.8	65
4	0.0	8.7	13.0	17.4	13.0	34.8	13.0	23
Combined	1.9	11.9	14.3	37.9	5.7	17.6	10.7	261

* R - Continuous rain, S - Snow, RW - Rainshower, TRW - Thunderstorm, A - Hail

Storm type. An examination of synoptic storm types was made to ascertain whether specific types predominated in the various quartile storms. Storms were classified into six basic types and percentage frequencies determined for each type in each quartile. Storm types used were cold front, warm front, stationary front, occluded front, low pressure centers, and air mass storms. Analyses showed no strong trend for a particular type of storm to dominate in a particular quartile. However, a trend was noted for a much larger percentage of the fourth-quartile storms to be associated with combinations of the storm types than occurred with the other quartile types, which might be expected since these storms are longer (see below) giving more chance for several storm types to occur.

Quartile-Duration Relations

As shown in Table 102, a major percentage of the fourth-quartile storms occurred with durations greater than 24 hours, whereas the first-quartile and second-quartile storms occurred most frequently with durations less than 12 hours,

and the third-quartile storms had the greatest number of cases in the duration group of 12 to 24 hours. Combining all storms, 42% fell into the duration grouping of less than 12 hours, 33% in the 12- to 24-hour group, and 25% exceeded 24 hours in duration.

Table 102. Percentage distribution of quartile types.

	Percent of cases for given duration (hr)			
Quartile	≤12	12-24	>24	Quartile frequency (%)
1	45	29	26	32
2	50	33	17	34
3	35	42	23	25
4	22	26	52	9
All storms	42	33	25	100

Storm Shape and Orientation

An investigation of the shape factor in Illinois storms was made with data for areas of 50 to 400 mi^2. Because of their size, storm shapes could not be determined with reliability in many cases on the areas smaller than 400 mi^2.

For rainfall periods of 1 to 12 hours on the 400 mi^2, elliptical patterns were found to predominate, accounting for 51% of the cases. Storms without a closed center that showed an elongated pattern of isohyets outward from a single region of heaviest rainfall near the network border were considered elliptical in addition to the typical closed center storms of elliptical shape. Multicellular patterns, those characterized by several closed isohyets within the network, ranked second with 25% of the cases. Banded patterns, which produce two or more bands of rainfall separated by areas of relatively light rainfall, accounted for 19% of the storms in the 1- to 12-hour group. Indefinite patterns, those too complex or too flat to classify, accounted for the other 5%.

As the rainfall durations increased to 24 hours, the three major patterns (elliptical, multicellular, banded) occurred with nearly equal frequency. Examination of the influence of rainfall volume (storm mean rainfall) on the shape of the pattern revealed a strong domination by elliptical patterns with areal means up to 1.50 inches; in this range, they were found in 59% of the cases. For storms with means in the range from 1.50 to 1.99 inches, there was little difference in the frequencies for each of the three major patterns. With areal means of 2 inches or greater, banded patterns became the most frequent type and accounted for approximately 50% of the cases. Thus, there exists a trend for the storm patterns to become more complex with increasing rainfall duration and rainfall volume. The data were grouped according to storm type also, but no definite differences were noted among the several types.

With the smaller areas, especially 50 mi^2, only a small part of a major storm center or storm zone would extend over the sampling area frequently, so that assignment of a pattern shape was most difficult. When it was possible to assign a shape to the smaller areas, it was found that the elliptical shapes predominated strongly for all storms regardless of mean rainfall or storm duration.

The movement of storms was found to be closely associated with the orientation of the storm patterns. Investigation of the network storm orientations indicated that approximately 45% of the storms moved from the SW or WSW. Complex movements in which individual showers moved from two or more directions during the storm period ranked next with 17% of the cases. Table 103 shows the percentage frequency distribution of the storm pattern orientations. Again, storm type did not appear to influence storm orientations substantially.

Table 103. Percentage frequency of storm pattern orientations.

Direction	Percent
S	1
SSW	11
SW	22
WSW	23
W	12
WNW	5
NW	6
NNW	3
Complex	17

The results in Table 103 are in close agreement with other Illinois studies. An analysis of 106 storms in which mean rainfall exceeded 0.50 inch on the urban network of 10 mi^2 (Fig. 1) during a 10-year period also showed orientations most frequently from the SW and WSW. A study of the large-scale, outstanding flood-producing storms in Illinois (Huff and Semonin, 1960) revealed the most frequent orientation of the storm centers was from WSW through W to WNW. A detailed study of 10 large-scale storms in the period from 1951-1960 in which the 12-hour rainfall exceeded 8 inches at the storm center revealed a median orientation of 270 degrees with an average wind direction in the layer from 5,000 to 20,000 ft of 255 degrees. A study of radar-depicted precipitation lines (Changnon and Huff, 1961) also showed a WSW orientation and movement most frequently.

Two pertinent facts were brought out by the orientation study. First, as the intensity and areal extent of the storms increase, the orientation of the storm core veers from SW-WSW toward W. Secondly, the storm pattern is

oriented, on the average, approximately 15 degrees in a clockwise direction from the average wind flow in the steering layer. This displacement likely results from the recognized trend for new cells to develop on the right flank of the existing storm mass (Newton and Newton, 1959), and the new cell development intensifies with increasing storm strength. The trend for the rotation of the storm pattern in a clockwise direction in large intense storms is believed to result from the greater influence of high-level winds on steering the storms, since the more intense storms tend to build to higher levels. This trend is supported by results of the Changnon-Huff study of radar precipitation lines mentioned above.

Conclusions

The statistics provided in this study provide useful background information on characteristics of storms of moderate to heavy intensity. Unfortunately, time and personnel limitations have not permitted a similar study of light storms. The analyses performed in the study discussed here did not reveal any unique properties of the natural rainfall distribution that substantially lessen the problems encountered in the verification of weather modification experiments.

AN EVALUATION OF DOWNWIND SEEDING EFFECTS FROM THE WHITETOP EXPERIMENT

Introduction

The possibility of downwind seeding effects on rainfall has been suggested by Braham (1965), Brown and Elliot (1968), Brier (1966), Adderley (1968), and Neyman et al. (1969). Indications of both positive and negative seeding effects have been found at distances from 40 to 250 mi downwind of the seeding area. Braham has suggested that the downwind effects result from a stationary wave-like perturbation which spreads outward and downstream with a wave length of 30-50 mi. This downwind wave then creates regions in which dynamic interaction between clouds and their environment may produce further effects on precipitation. Brown and Elliot have suggested that the equivalent of a heat mountain is created in the target area, and convective instability is then released as trailing jump lines emanating from the equivalent heat mountain. They have also suggested that overseeding close to the seeding source may produce cirrus which then drift downwind and seed the underlying cells with large ice particles.

Since indications of downwind effects have been found in some experiments and since working hypotheses have been suggested to explain apparent downwind effects, the present study was initiated to investigate further the possibility of downwind seeding effects through the use of data and analyses not previously employed. The analyses involved primarily the establishment of statistical

probabilities of the existence of downwind increases or decreases in rainfall associated with the 1960-1964 Whitetop seeding project in Missouri. Attention was given also to the problem of natural rainfall variability which interferes with and may lead to spurious conclusions in seeding evaluations when it is not properly understood and incorporated into the verification procedures.

The area surrounding and downwind of the Whitetop experiment was selected for study because of the careful attention given to randomization and because the existence of a negative seeding effect was established in the Whitetop target area (Braham, 1966; Decker and Schickedanz, 1966; Flueck, 1968). Thus, it is logical to test the hypothesis that this decrease may have been extended downwind.

Data and Analytical Procedures

First, average monthly rainfall data from Weather Bureau Cooperative stations for the seeding period, 1960-1961, and for the previous 5-year non-seeding period (1955-1959) were used to investigate the existence of downwind seeding effects. A circular sampling area of 300 mi about the center of the Whitetop target area in southeastern Missouri was studied. Secondly, daily rainfalls for the seeded and non-seeded days from these stations were used to isolate further the differences between rainfall on seeded and non-seeded days.

In the third phase, plume analyses using wind trajectories in the lower 500 mb were performed for the year 1961 to obtain a better estimate of the area which could have been affected on each operational day. This permitted a more detailed study of downwind effects for that year in which previous analyses (Decker and Schickedanz, 1966) indicated a major seeding effect (rainfall decrease) in the Whitetop experimental region.

Next, the study was expanded to incorporate average areal rainfall for each hour on operation days in the 1961 evaluation to facilitate interpretation of results. Finally, hourly rainfall on two dense raingage networks, located approximately 175 and 290 mi downwind from the center of the Whitetop area, were examined 1) for evidence of extensive downwind effects in the 1960-1964 period and 2) to aid in evaluating the degree of natural variability polluting the analytical results.

Except in the dense network analyses, evaluation of downwind effects was dependent upon rainfall measurements from the Weather Bureau climatic network which averages one gage per 300 mi^2 in the study area. Such densities are far from optimum for determining areal mean rainfall on Whitetop operational days; however, these are the only data available. Consequently, this measurement deficiency must be considered in the interpretation of results, especially when isolated departures from the general trend of the findings are noted.

Large-Scale Analysis of Monthly Rainfall Patterns

It is sometimes desirable from technical, economic, and political considerations for cloud seeding effects to extend over a large area, and

to be reflected in the monthly rainfall, especially during the critical growing-season months. If the seeding effect can be found in monthly data, which have numerous factors confounded with the seeding effect, one can then begin to attach economic importance to the seeding operations. Therefore, comparisons were made between the monthly rainfall values of various areas in and surrounding the Whitetop research area. These comparisons were made for the 5-year period prior to the seeding experiment, for the 5-year period during the seeding experiment, and between corresponding areas in the two periods.

The sampling area used is shown in Fig. 51. Circles concentric to the radar site at 50-mile intervals and the location of major cities are shown for convenience in analyses and presentation of results. The Whitetop experimental area, hereafter designated the research circle, is indicated by the 60-mile radius. In order to compare areas of equal size, a grid with 100-mile spacing was superimposed on the sampling area. For each grid area and for the two 5-year periods the areal average monthly rainfall for the summer months was determined. In addition, average monthly percent of normal values were computed for each grid.

The average monthly rainfall values were then computed for the "target" area enclosed by grids 13, 14, 19, 20 (some Whitetop area in each grid) and for the "control" area enclosed by all of the other grids (no Whitetop area in grids). The years 1955-1959 were designated as the non-treatment period and the years 1960-1964 as the treatment period. The 5-year averages for each area and period are shown in Table 104. These averages show that the average monthly rainfall in the Whitetop research circle and the surrounding area (40,000 mi^2) was less than the rest of the grid area shown in Fig. 51 (280,000 mi^2). Long-term normals were used to compute percent of normal values. These are listed in Table 104 and also indicate that the 4-grid area had less rainfall.

The average monthly rainfall values were then computed for the area enclosed by grids 8-10, 13-16, 19-22, and 26-28 (an area generally downwind "target-downwind") and for the area enclosed by grids 1-4, 5-7, 11-12, 17-18, 23-25 and 29-32 ("west-control"). These values are also included in Table 104. During the treatment period the "target-downwind" value was 7% less than the "west-control" and during the non-treatment period it was 1% more.

The large-scale monthly analysis indicated that the average monthly rainfall in summer during the 1960-1964 period was less (93% of normal) in the "target" area than it was in the rest of the large region shown in Fig. 51; this suggests a possible seeding effect within the "target". The average monthly rainfall in the "target-downwind" area, however, was only slightly less than in the "west-control" region (99% vs 101% of normal).

From the information presented in Table 104, it is concluded that there is no strong evidence of <u>downwind</u> seeding effects in the monthly data. However, the downwind effect would need to be quite large to be readily discernible, since both seeded and non-seeded days are included in the monthly totals.

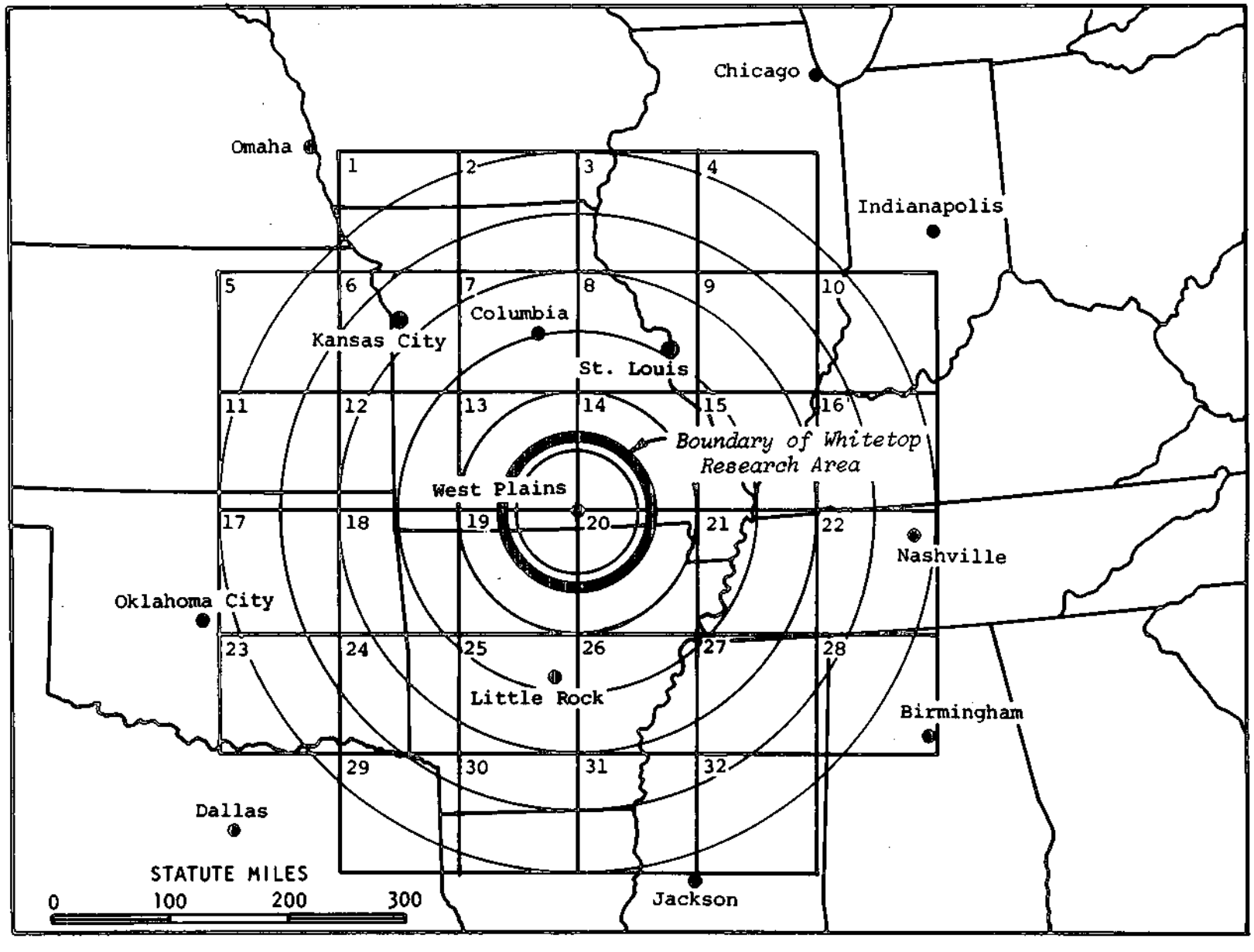

Figure 51. Sampling area used in large-scale monthly analyses.

Table 104. Average monthly rainfall and percent of normal during summer months for treatment and non-treatment periods.

Areas	Treatment period (1960-1964) Amount (in)	Treatment period (1960-1964) Percent of normal	Non-treatment period (1955-1959) Amount (in)	Non-treatment period (1955-1959) Percent of normal
Target	3.53	93	4.10	106
Control	3.83	101	4.00	106
Target-downwind	3.66	99	4.00	108
West control	3.92	101	3.98	103

Equal-Area Analyses of Daily Rainfall Patterns

The procedures followed in the Whitetop experiment provided excellent conditions under which to analyze daily* rainfall in the downwind** areas ranging from North clockwise through South. Because of the randomization procedure, any downwind region has two random samples of seeded and non-seeded days. Thus, valid and meaningful statistical inferences can be drawn concerning the existence of seeding effects provided the sample size is sufficiently large. The sampling areas used in the daily analysis are shown in Fig. 52.

In general, the seeding material should spread laterally and become more diffuse as the distance from the source increases. Areas A, B, and C were selected and oriented so that the seeding material would be more diffuse in those areas farthest from the source, but yet be equal in area to the Whitetop research circle (11,310 mi^2). To perform further analysis in certain downwind areas some were either divided in half or were combined to get areas twice that of the research circle. The areas A_n, B_n, C_n, A_s, B_s, and C_s are one-half the size of the research circle whereas the areas A_t, B_t, and C_t are twice the size of the research circle. Also, the n and s areas were combined to form the areas A_o, B_o, and C_o which are again equal to the area of the research circle.

* The daily rainfall data used here are the 24-hour totals from 0700 to 0700 of the following day.

** The downwind areas are assumed to be those east of the seeding line.

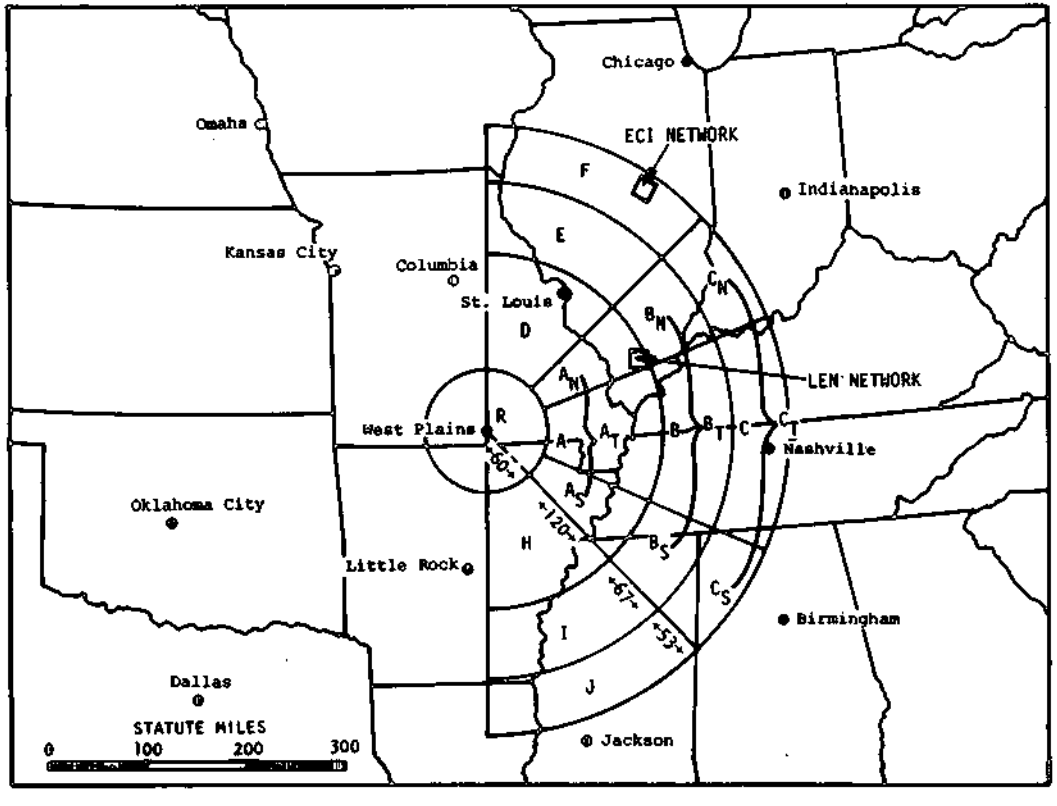

Figure 52. Sampling area used in daily rainfall analyses.

The data from the A_t, B_t, and C_t areas and the various subdivisions of these areas (totaling 15 areas) were analyzed for each year. The non-seeded sample mean was greater than the seeded mean (rainy day averages†) in 6 out of 15 areas in 1960, 14 out of 15 in 1961, 11 out of 13 in 1962, 3 out of 15 in 1963, and 3 out of 15 in 1964. This indicates that, in general, there was a negative tendency in the years 1961 and 1962 and a positive tendency in the years 1960, 1963, and 1964. The non-seeded mean was greater than the seeded mean (operational day averages††) for 3 out of 15 areas in 1960, 14 out of 15 in 1961, 11 out of 15 in 1962, 6 out of 15 in 1963, and 2 out of 15 in 1964. Again the negative tendency appears in the years 1961 and 1962. The means for some of the areas are shown in Fig. 53.

The log-normal distribution was then fitted to the seeded and non-seeded daily rainfall data from all 15 areas. A good fit was obtained for all areas except C_t and B_o on non-seeded days. The probability of the distributions being log-normal was greater than 0.05 for all other areas.

Two statistical tests of hypothesis were then used to test for differences between seeded and non-seeded means of the various areas. The "t" test was used to test the differences between seeded and non-seeded log-normal means on rainy days. The Mann Whitney non-parametic U test was used to test for differences between seeded and non-seeded means on rainy days and the means on operational days. Since recent research indicates that both seeded and non-seeded effects are possible, the null hypothesis (H_o) was chosen to be that the seeded and non-seeded means are equal while the alternative hypothesis (H_a) was chosen to be that the seeded and non-seeded means are different.

For two-tail probabilities the only values significant at the 0.05 level are the test statistics for area C (Prob. = 0.048) in 1964, and for the smaller area C_n (Prob. = 0.01) and B_s (Prob. = 0.02) for 1962. The difference for area C is positive (seeded greater than non-seeded) and is a comparison involving operational day means. The difference for C_n is positive while the difference for B_s is negative (non-seeded greater than seeded) and these are in the rainy day comparisons. These differences could be due to random chance or to seeding. Area C (Fig. 52) extends 247 to 360 miles from West Plains, areas C_n and B_n are more than 180 miles from West Plains, and the 30-mile seeding line is approximately 45 miles upwind of West Plains. Therefore, it is difficult to attribute these differences to seeding. Furthermore, there is no clustering of these areas in time and space, and out of 150 test comparisons (5-year x 15 areas x 2 tests) only 3 had probabilities less than 0.05. It is more likely that these differences occurred by random chance, even though the probability associated with each of the 3 individual comparisons is low. The test statistics and probabilities for some of the areas are shown in Fig. 54.

In Fig. 55, the research circle and the areas A, A_n, and A_t have non-seeded 5-year means for the period 1960-1964 that are greater than the seeded means for

† Based on the total rainfall from 0700 through 0700 the following day. Operational (seed or non-seed) days without rain during this period were excluded.

†† Operational as used here and later includes days with and without rain.

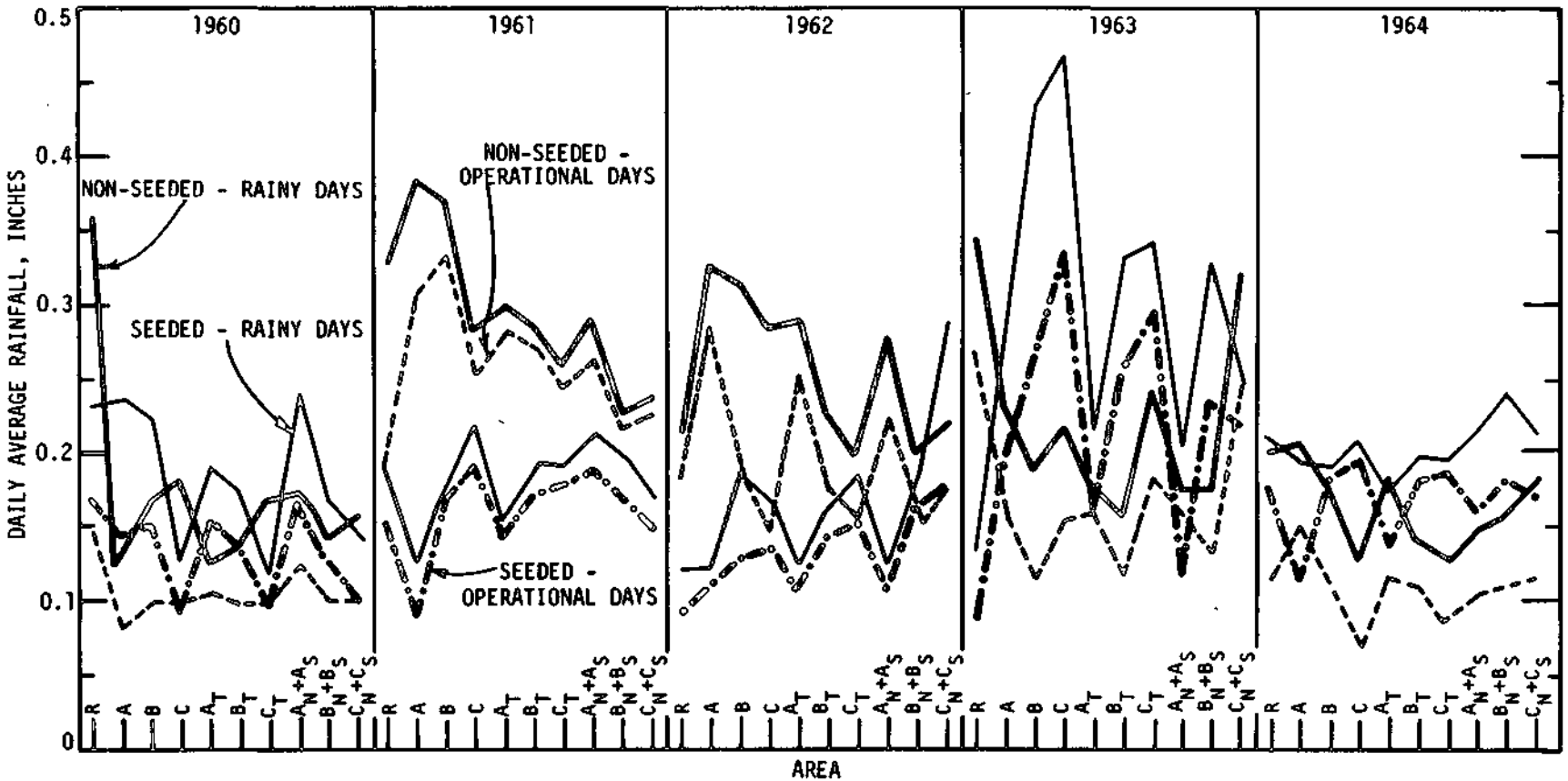

Figure 53. Daily average rainfall for seeded and non-seeded days during individual years.

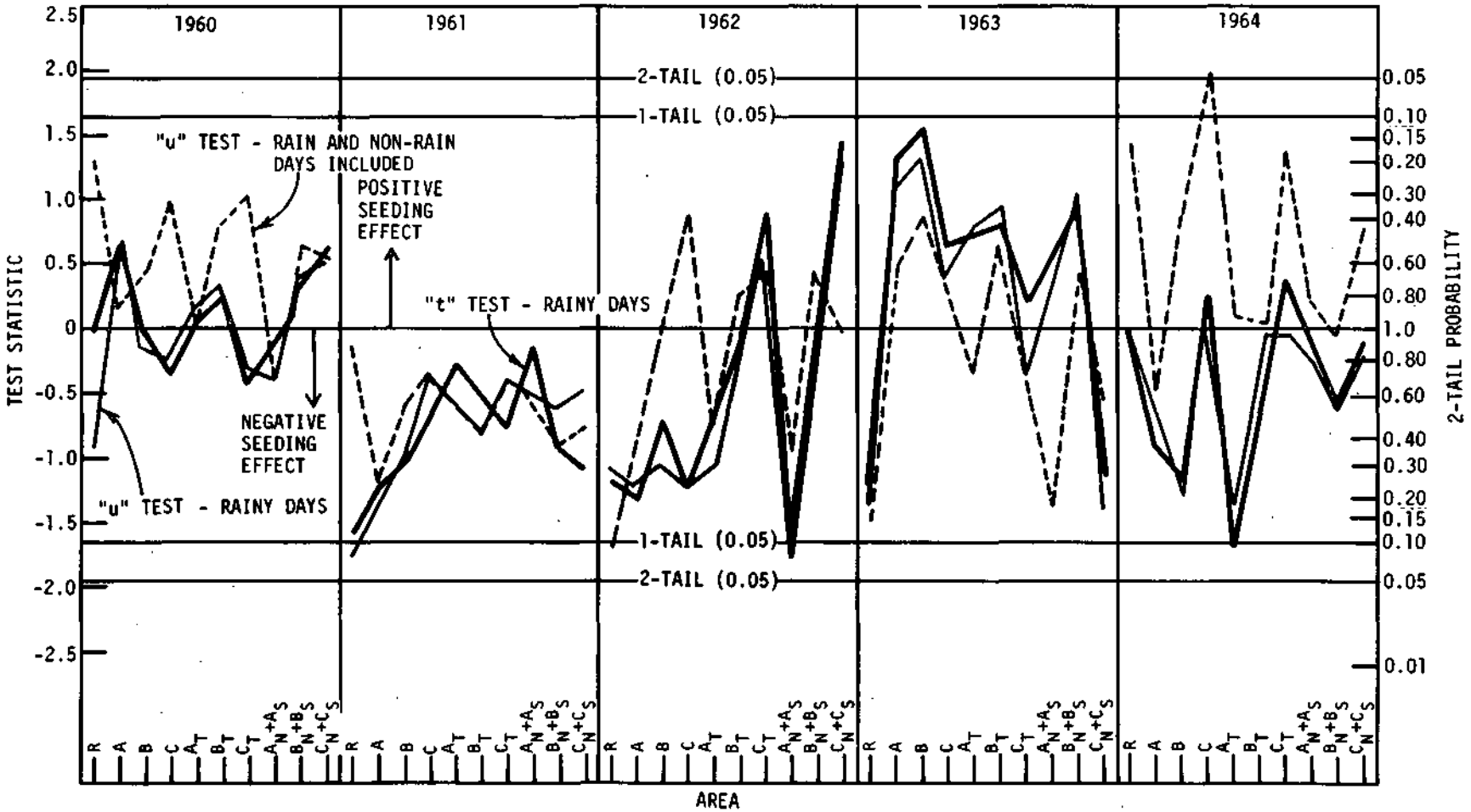

Figure 54. Test of significance for difference between means on seeded and non-seeded days for individual years.

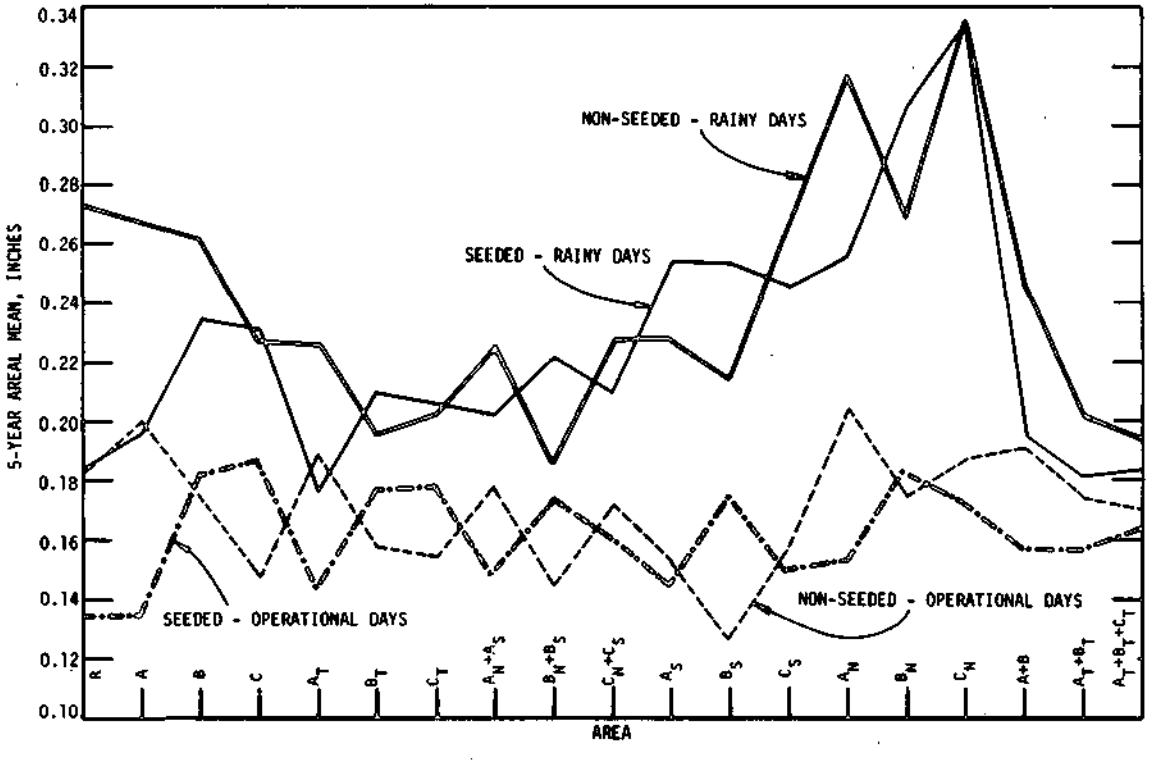

Figure 55. Areal means for research and downwind areas during 1960-1964.

both rainy day and operational day averages. However, Fig. 55 also shows that many of the 5-year areal means are greater on seeded days than on non-seeded days. Thus, there is no clear-cut evidence for downwind effects.

The daily rainfall data for all 5 years were grouped to form seeded and non-seeded 5-year samples for each area shown in Fig. 55. The log-normal distribution was fitted to these data and a good fit was obtained for all areas. The "t" and "U" tests were then applied to test for differences between the seeded and non-seeded samples as was done with the individual years. None of the 15 downwind areas were significant at the 0.05 probability level. Indeed all two-tail probabilities were greater than 0.10. The test statistics and two-tail probabilities are shown in Fig. 56. For the overall 5-year period, the equal-area analysis indicates that none of the seeded and non-seeded differences are significant.

Plume Analyses in the Downwind Area

Wind trajectory analyses were performed using upper air stations and special wind observations taken at West Plains during the Whitetop experiment. Braham (1966) constructed a composite plume based on the most divergent winds from the seeding level to 14,000 ft, whereas Decker and Schickedanz (1966) constructed a plume based on seeding level winds only. These plumes were only constructed for the research circle. However, in this downwind study it was necessary to extend the plume to the edge of the sampling area shown in Fig. 52 to obtain an estimate of its time distribution, location, and areal extent in downwind areas.

Because of the large amount of work required, it was decided to restrict the plume analysis initially to the year 1961. The fact that most of the downwind areas had negative differences made this a desirable choice. Comparison of plume results with those obtained from the equal-area analysis would then determine the desirability of extending the plume analysis to other years. In 1961, the downwind plume analysis was done on 23 days and the plumes were basically defined in 3 different ways. These were composite moving plumes, composite plume envelopes, and flight-level plumes. The composite envelope plumes were then divided into regions 0-100 mi, 100-200 mi, and 200-300 mi for further comparisons. In order to obtain some out-plume control data for comparisons, the composite envelope plume was displaced to positions upwind of the research circle and to positions to the left and right in the downwind direction. Furthermore, because of the possible error involved in determining the limits of the plume in time and space, the plume's boundary was reduced by 0.5 of its width and then increased by 0.5 of its width to form "contracted" and "expanded" plumes.

Composite plumes were obtained by first constructing 700 mb, 500 mb, and seeding-level plumes for each hour through use of mean wind trajectories for these levels. The composite plume was then determined from the maximum extent of the plumes at the three levels. These hourly plumes were extended in space and time until 1) the plumes reached the 300-mile radius shown in Fig. 52 or until 2) 7 a.m. the following day. The composite moving plume for

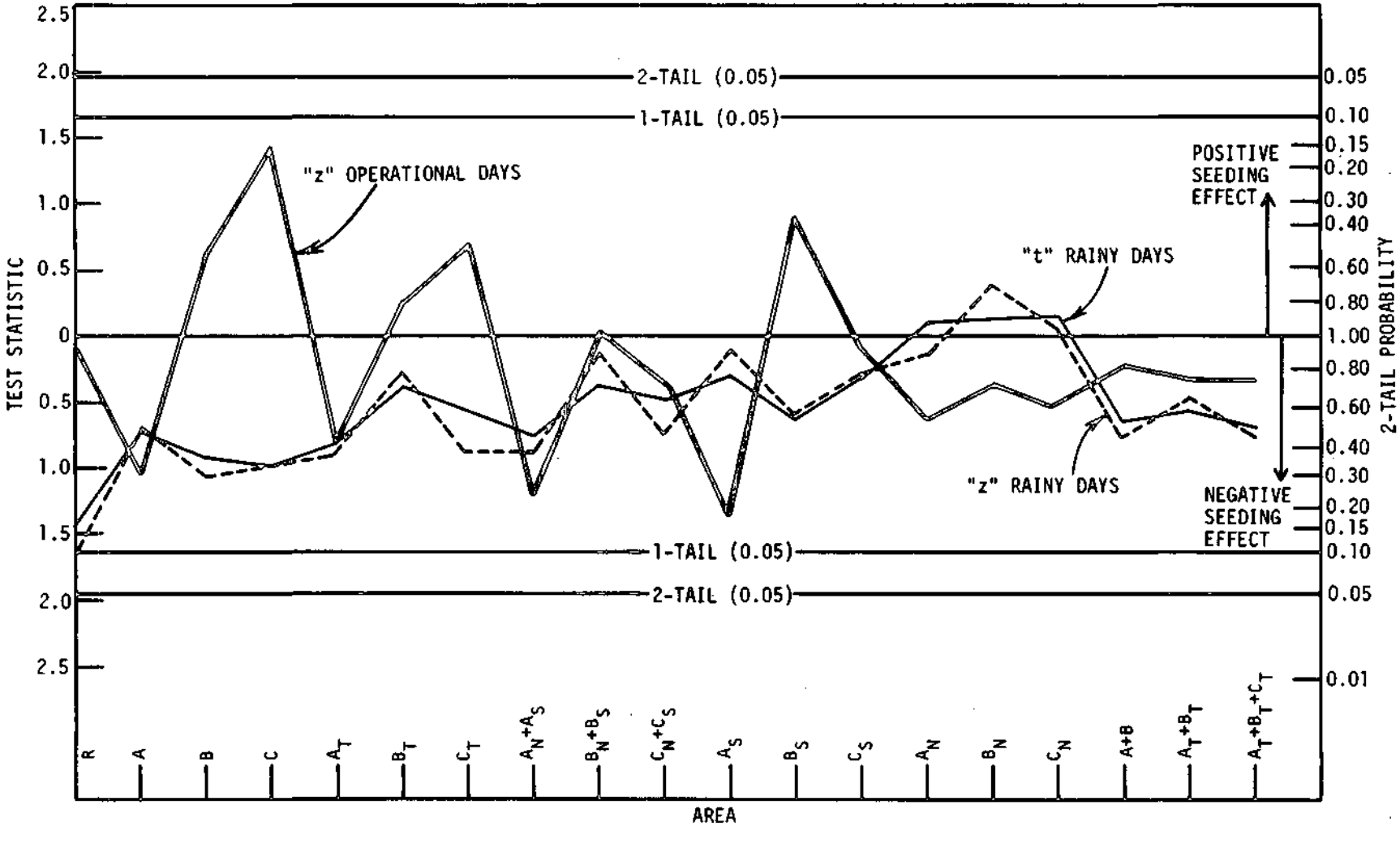

Figure 56. Test of significance for differences between 5-year means on seeded and non-seeded days during 1960-1964.

1200, 1500, 1800, 2100, and 2400 CST on July 20 and for 0300 and 0500 CST on July 22, 1961 are shown in Fig. 57. The composite plume envelope was defined as the total area enveloped by the moving plumes for a 24-hour period or until the time the distance limit of 300 miles was reached.

Because of the scarcity of recording raingages within the hourly plumes it was impractical to obtain average areal rainfall for every hour. Instead, the areal average was determined for the area encompassed by the plume in each 3-hour period until the time limit (0700 the following day) or distance limit (300 miles) was reached. The 3-hour areal means were then averaged to obtain the daily seeded and non-seeded in-plume averages. The log-normal distribution was fitted to the daily averages and a good fit was obtained in all cases. The "t" test was used to test for differences between the log-normal seeded and non-seeded means on all plumes defined above.

The seeded and non-seeded differences were significant at the 0.05 two-tail probability level for the composite envelope plume in the region 100-200 miles downwind. For the contracted plumes, the composite envelope plume had a two-tail probability less than 0.10 for the 0-100 miles region and a two-tail probability less than 0.20 in the 100-200 miles region. All other probabilities were too large to be of any consequence. This suggests possible seeding effects in the region extending 100-200 miles downwind in the year 1961. The two-tail probabilities and their corresponding test statistic for the various plumes are shown in Fig. 58.

Hourly rainfall from the 100-200 mile zone of the A, A_n, A_s, A_o, and A_t areas shown in Fig. 52 was used to check further the result found above. The application of significance tests produced a probability value of 0.08 for the 100-200 mile zone in area A. All other probabilities were greater than 0.20 and of no consequence.

In general, the 1961 plume analysis leads to the same conclusions as the equal-area analysis, and indicates that the equal-area results (practically no significant increases or decreases) are valid. This also indicates that the complicated downwind analysis for the other four years would produce little or no additional information.

Analyses of Dense Raingage Network Data

Data from two dense raingage networks in Illinois were examined (1) for evidence of extensive downwind effects from Whitetop seeding, and (2) to aid in evaluating the natural rainfall variability that may have interfered with and possibly led to erroneous conclusions in the Whitetop seeding evaluations. The Little Egypt Network (LEN) consisted of 49 gages in 550 mi^2 approximately 175 miles ENE of the Whitetop operations center (Fig. 51), and the East Central Illinois Network (ECIN), located about 290 miles NNE, contained 49 gages in 400 mi^2.

Fig. 59 is a portrayal of the diurnal distribution of 3-hourly mean rainfall on seeded and non-seeded operational days for both networks, along with a plot for the remaining non-operational days on ECIN. Some curve smoothing was achieved by using 3-hour moving totals.

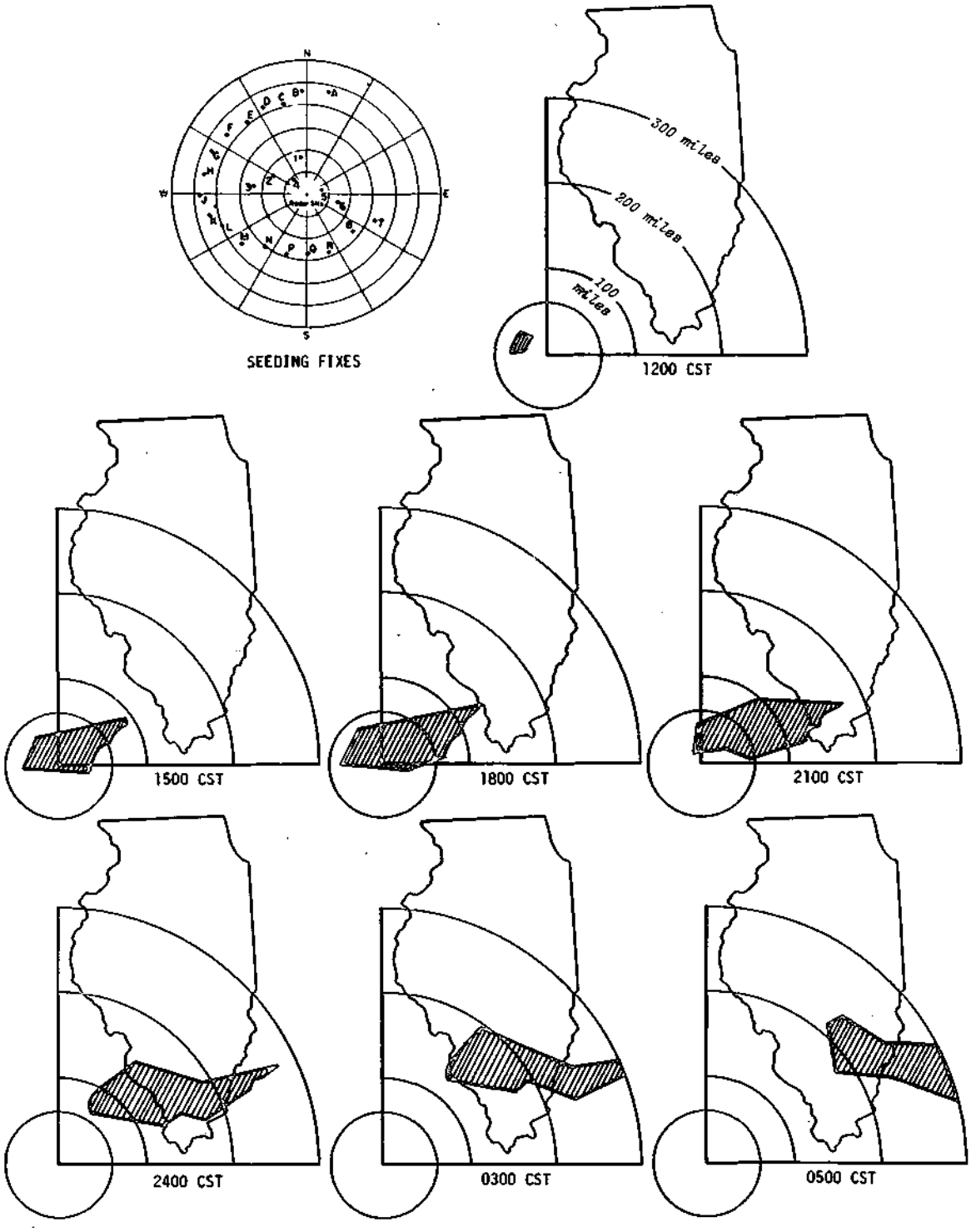

Figure 57. Location of downwind plumes for July 20-21, 1961.

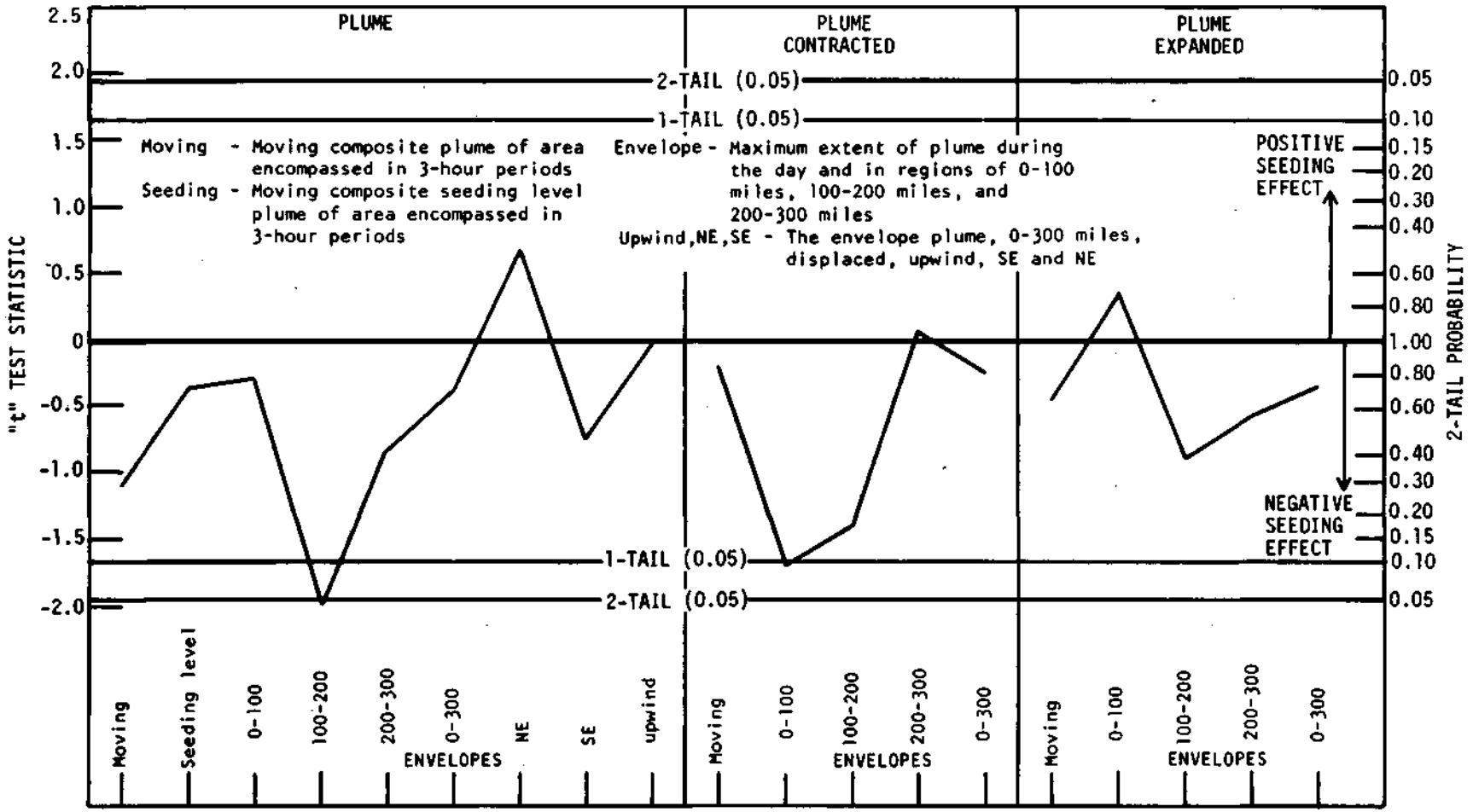

Figure 58. Test of significance for differences between plume areal averages on seeded and non-seeded days in 1961.

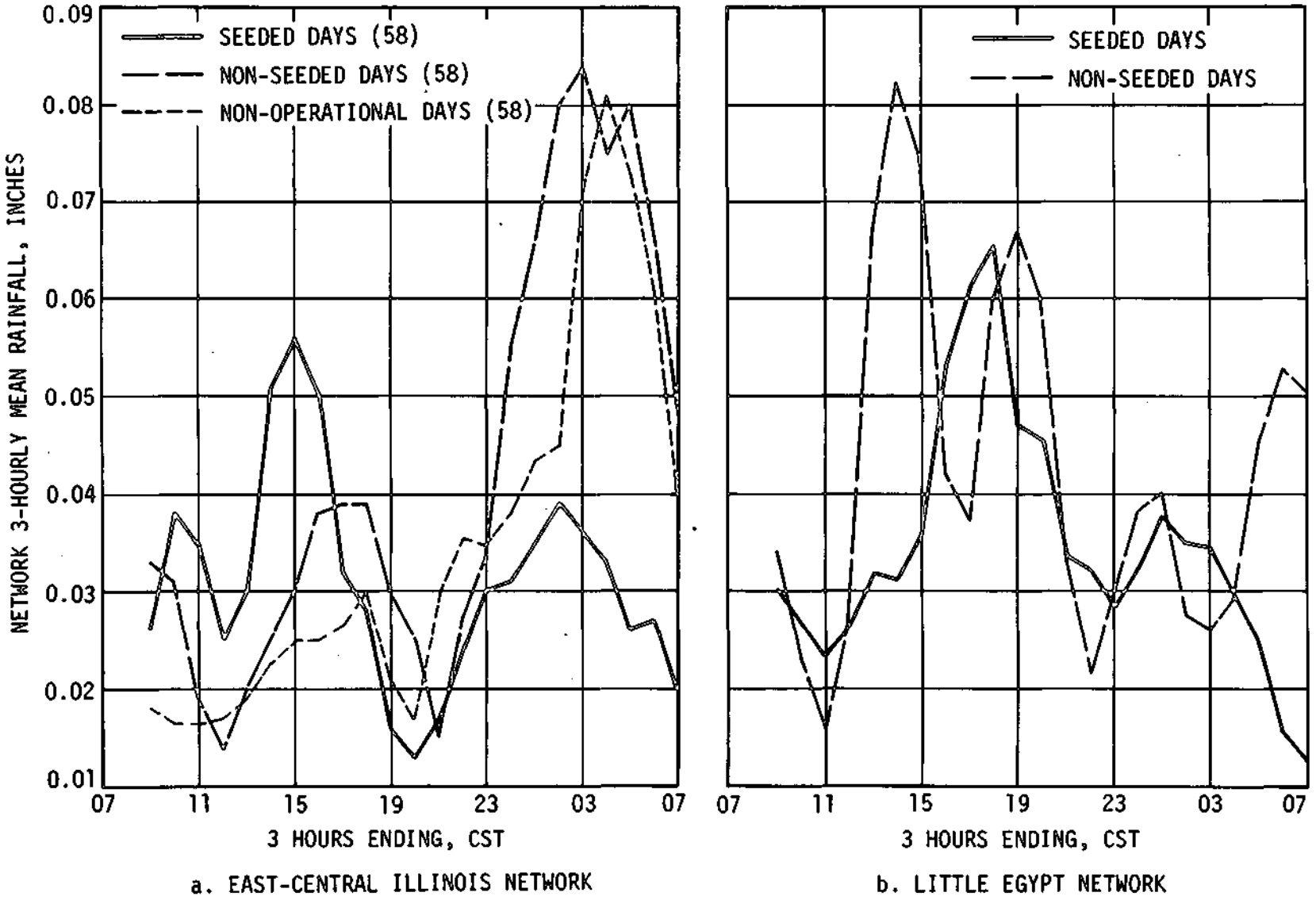

Figure 59. Diurnal distribution of network mean rainfall.

Immediately, attention is drawn to the early morning recognized climatological maximum on the ECI curves. The maxima are strikingly similar for the non-seeded and non-operational curves (no-effect hours), but both show much heavier rainfall than does the curve for seeded days. This is especially interesting since the early morning maximum occurs at a time when Whitetop seeding material or other seeding-induced effects would most likely reach ECI, based on wind speed climatology. Thus, the ECI curves indicate a strong possibility that a relatively large percentage reduction in rainfall occurred nearly 300 mi downwind as a result of Whitetop seeding.

However, the LEN curves show rainfall differences of a similar magnitude in the early afternoon during the 3-4 hours immediately following the starting time of Whitetop seeding. Such a pronounced downwind seeding effect at 175 mi is very unlikely to occur so rapidly or consistently enough to produce this anomaly. Thus, it is concluded that it resulted from natural variability between the two samples drawn from the 1960-1964 rainfall population. The LEN anomaly raises a question as to whether the ECI early morning differences merely reflect a sampling vagary.

Results of the 1961 plume analyses were used to investigate further the probability of the ECI anomaly being natural or seeding-induced. The 1961 analyses for flight level to 500 mb showed that there was a likelihood of a Whitetop plume reaching ECI on only 5 of 37 operational days (14%) and on two of these days no rain occurred on ECI. However, with its closer and more strategic position, LEN could have been reached by plumes on 76% of the 1961 operational days. Consequently, it would be expected that if a seeding effect was present it would be more evident on LEN and should be most prominent between 1500 and 0300 CST, when winds would be most likely to bring Whitetop seeding material, clouds, or seeding-induced mesosystems in to the network. However, the two LEN curves in Fig. 59 are very similar during this period, thus indicating little or no seeding effect.

Assuming that the 1961 plume distributions, in which the calculated areal extent of the plumes was doubled in the network areas to allow for computational error, are reasonably representative of plume movements in the 1960-1964 period, it is very difficult to conclude that downwind seeding effects were the cause of the early morning anomaly shown by the ECI curves. It is more likely a consequence of natural rainfall variability such as produced the early afternoon anomaly on LEN. Huff (1966) has shown that large differences may occur in two samples drawn from the same storm population in a 5-year period because of natural rainfall variability.

The Wilcoxin ranked pairs test was employed in conjunction with the hourly data on LEN and ECI to evaluate the statistical significance of the differences between the hourly averages for seeded and non-seeded days and between the hourly averages for seeded and non-operational days. Results are summarized in Table 105. First, tests were made on a 25-hour period starting at 0600 CST which included hours of potential effect and hours of no effect from the Whitetop seeding. Next, the network time distributions were divided into two parts (based on wind climatology) to include the overall range of hours in which a Whitetop seeding-induced effect may have reached the networks and those hours during which

it was unlikely for any seeding effect to have been present. The no-effect hours were 06-17 on ECI and 06-15 on LEN, whereas the potential effect hours were 17-07 on ECI and 15-07 on LEN.

Assuming that any probability of 0.05 or less is significant, Table 105 shows no indication of downwind seeding effect on LEN, approximately 175 miles downwind of Whitetop. However, highly significant probability values (0.01 or less) were obtained not only for the hours of potential downwind effect on ECI, 290 miles from Whitetop, but for the no-effect period (06-17) in the seeded vs non-operational comparison. Also, a value close to significance (0.06) was obtained in the 25-hour period bracketing effect and no-effect hours in the seeded vs non-seeded comparisons.

Table 105 provides an excellent example of the high degree of statistical significance that may be obtained with differences between two samples drawn from the same rainfall population. One may insist, despite evidence to the contrary presented by the authors, that the highly significant test statistics for 17-07 (effect hours) on ECI were caused by downwind seeding effects. However, there still remains the highly significant 0.01 probability for the no-effect hours in the seeded vs non-operational comparisons on this network.

Table 105. Probabilities for the Wilcoxin paired ranks test statistic for hourly rainfall differences on seeded, non-seeded, and non-operational days on ECI and LEN.

	ECI			LEN
Time (CST)	Seeded vs Non-Seeded	Seeded vs Non-Operational	Time (CST)	Seeded vs Non-Seeded
25-hr (06-07)	0.06	0.47	25-hr (06-07)	0.25
06-17	0.06	0.01	06-15	0.37
17-07	0.006	0.001	15-07	0.41

Overall Summary and Conclusions

1) Detailed plume analyses indicated a statistically significant probability of a seeding effect in an area 100-200 miles downwind during the year 1961; overall, however, the evidence for downwind effects derived from the plume analyses was very weak.

2) There was a tendency for some individual years to have both positive and negative effects in isolated areas of which a few were statistically significant.

However, lack of continuity of the significant differences in time and space imply these were the result of random sampling.

3) The tendency for negative differences (seeded minus non-seeded) was limited mostly to the years 1961 and 1962. Positive differences dominated the other 3 years in downwind areas.

4) No statistically significant seeding effects were present in the downwind areas when data for all 5 years were combined.

5) Detailed hourly analysis of dense raingage network data indicate that large differences in the time distribution of rainfall may occur between seeded and non-seeded days as a result of natural rainfall variability and lead to spurious conclusions if not thoroughly evaluated. Thus, on the ECI network nearly 300 miles downwind a highly significant probability was obtained between seeded and non-seeded cases in the early morning hours following Whitetop operations, and this time period coincided with hours in which seeding material, seeded cloud systems, or other seeding-induced mesosystems would most likely arrive on the network, based on time of travel. However, further analysis, employing results of the 1961 plume analyses, indicated that because of its direction from the seeding source this network would be within the Whitetop downwind plume only infrequently. Furthermore, differences of similar magnitude were obtained on another network (LEN) during hours when downwind seeding effects could not occur because of time-of-travel considerations.

The findings in the downwind study show that one should be very cautious when evaluating seeding results, especially in an area other than that for which the experiment was designed. Also, the problems of sampling density in the experimental area partitioning of the area, and type of data used in evaluation are a real concern. For example, would the partitioning of the Whitetop research circle of 11,310 mi^2 into 28 areas with the size and gage density of the ECI network (400 mi^2) also have produced some extreme differences between seeded and non-seeded days such as found on that network?

Upon consideration of all analyses performed in this research, it is the overall conclusion of the authors that the evidence for downwind effects from the Whitetop experiment is very weak.

A FEASIBILITY STUDY PERTAINING TO THE 'EVALUATION OF POTENTIAL BENEFITS OF WEATHER MODIFICATION ON WATER SUPPLY

Introduction

Major progress has been made in recent years in acquisition of the scientific knowledge and in development of the engineering technology necessary for application of weather modification to increase water supplies. In view of these advances, quantitative evaluation of the potential benefits (and possible damage) of cloud seeding programs under various weather conditions is extremely

pertinent at this time. Although this need has been recognized for some time and considerable debate on the subject has ensued, the literature provides little concrete information upon which to base quantitative estimates. This situation arises from several causes, among which is the lack of previous concentrated effort in this direction, which, in turn, has been discouraged to some extent by the lack of readily available techniques and methods to solve the problem. As part of the NSF-1360 research, a pilot study was made to evaluate the feasibility of undertaking the desired evaluations.

Approach to Problem

Evaluation of water supply potential was restricted in this pilot study to cold-season runoff, since in the Midwest and most of the United States the major contribution is during this season when evapotranspiration is at a minimum. In Illinois, the period from October through April is of primary importance. Step-wise correlation and multiple regression techniques were used to ascertain the optimum relationship between cold-season runoff and various meteorological parameters for two basins selected to provide examples of different climatic conditions, physiography, and geomorphology.

The pilot study has indicated that approximately 85% to 90% of the variance in the precipitation-runoff relation during the cold season can be explained through appropriate selection of weather parameters that determine the runoff characteristics. This has been achieved by including not only the total seasonal precipitation and an antecedent moisture index (the more or less "standard" procedure) but numerous other weather parameters. These additional parameters, although not independent of the total seasonal precipitation in statistical terminology, do exert significant influence on the magnitude of the seasonal runoff, as will be shown later in an example of analyses on an Illinois basin.

Although the best correlator with seasonal runoff is total seasonal precipitation, it is obvious that the nature and magnitude of the seasonal runoff is also dictated to a large extent by how the total precipitation is distributed throughout the season. Through step-wise correlation the various parameters were tested for their importance in defining the seasonal runoff for a given basin. Step-wise regression then established the basin runoff relation by progressively inserting additional variables into the equation, based upon their ability to reduce the standard error of estimate, until all were included. Those which had little effect upon improvement of the regression equation were then discarded, and the potential benefits of precipitation stimulation assessed with this "best-fit" equation.

It is important to pursue the foregoing analytical procedure in cloud seeding evaluation studies, not only to establish the most reliable equation upon which to base the seeding benefit, but to establish those individual weather parameters whose modification can materially affect the runoff under given conditions of climate, physiography, and geomorphology. For example, this pilot study shows that modification of the seasonal snowfall in the Big Muddy basin in southern Illinois would have negligible effect on the cold-season runoff; however, increasing the January precipitation, which climatologically exerts the strongest influence on the winter precipitation in that region, would substantially increase the runoff under certain sequences of cold-season weather events.

The step-wise correlation and regression technique not only provides a means of evaluating seeding potential, but provides information on the relative effects of various precipitation distribution factors on seasonal runoff. Therefore, it can contribute also to better understanding of the rainfall-runoff relation and to better prediction of runoff from precipitation data. The relative effects of the distribution parameters will vary between watersheds with different conditions of climate, physiography, and geomorphology. Therefore, in any future comprehensive studies, basin grouping must be done according to these factors, and possibly others, such as basin size.

Once a basin equation is established, one can then return to the computer and calculate runoff increases that would result under various combinations of the independent variables, assuming various percentage increases in them through cloud seeding. The combinations to be used are determined from a climatological study of the combinations which have occurred under natural conditions during the past. The frequency distribution of these combinations (climatological models) then serve as a valuable tool in the evaluation, providing a logical sequence of weather events to analyze.

Application of Technique

The foregoing description of the analytical technique is illustrated in the following example for Henderson Creek, a basin of 428 square miles in northwestern Illinois with continuous runoff records dating back to 1935. This basin has an average precipitation of 16.20 inches, and an average runoff of 3.95 inches during the October-April period. Snowfall averages 27 inches (approximately 2.7-inch water equivalent) and the winter temperature mean (December-February) is 26.6°F.

In establishing the basin equation, testing was made of the effects of total cold-season precipitation, fall, winter, and spring precipitation totals, individual monthly precipitation, snowfall, number of precipitation days, maximum monthly precipitation during the cold-season, monthly and seasonal temperatures (indexes of ground condition), and September runoff (index of ground saturation at start of season). The step-wise correlation and regression analyses indicated that total seasonal precipitation (P), September runoff (R), seasonal snowfall (S), winter precipitation (W), and maximum monthly precipitation (M) were the most important parameters, and the addition of others did not substantially improve the runoff relationship for this basin. These parameters explained 85% of the variance. The variance explained increased from 62% with total seasonal precipitation alone, to 69% with the addition of September runoff, 75% with inclusion of seasonal snowfall, and 85% with the addition of winter precipitation and maximum monthly precipitation. Addition of 14 additional variables only increased the variance explained to 90%. The basin runoff (Q) in inches is given by:

$$Q = 0.077\, P^{0.44}\, R^{0.29}\, S^{0.49}\, W^{0.49}\, M^{0.57} \qquad (31)$$

Next, a climatological study was made of the occurrence of various combinations of the five variables in the basin region. These provided weather models for which a frequency of occurrence could be assigned. In deriving the climatological models, the data for each climatic element was divided into three groups with approximately equal number of cases. These were designated below normal (B), near normal (N), and above normal (A). A five-element combination was then obtained for each cold season of record. From these five-element models, the frequency distribution of each model was determined. Effects of modifying these models were then calculated by (1) assuming all cold-season precipitation could be increased by certain percentages through cloud seeding, and (2) assuming only certain events, such as snowfall or winter precipitation were amenable to seeding. Seeding under the second assumption may prove to be the most practical, as the science of weather modification becomes better understood. Table 106 shows results of applying a climatological model that is defined by below normal total seasonal precipitation, September runoff, and maximum monthly precipitation and near normal snowfall and winter precipitation.

This model occurs naturally, on the average, once in eight years in the Henderson Creek Basin. Average runoff for the model is 2.29 inches, or 58% of normal (3.95 inches). Results are shown for (1) assumed increases of 10%, 20%, and 30% in P, S, W, and M by cloud seeding and (2) for the seeding applied only to winter precipitation.

A similar study was made for the Upper Big Muddy Basin of 753 mi^2 in southern Illinois. This basin has average precipitation of 22.89 inches and average runoff of 9.15 inches during the cold-season. The mean winter temperature is 35.4°F. Snowfall accounts for only 6% of the cold-season total precipitation. Three variables accounted for 83% of the variance. These were (1) total cold-season precipitation, (2) September precipitation (an antecedent moisture index), and (3) January precipitation. Ranking next in importance but improving the equation predictability only slightly were September runoff (another antecedent moisture index), maximum monthly precipitation in the cold-season, and April precipitation (end of cold-season).

Table 106. Effect of precipitation increases on cold-season runoff on Henderson Creek for a selected weather model.

Condition	Q (inches)	Percent of normal	Q-Increase Inches	Q-Increase Percent
Unmodified	2.29	58	--	--
P, S, W, M increased				
(a) 10%	2.78	70	0.49	21
(b) 20%	3.29	84	1.00	44
(c) 30%	3.85	97	1.56	68
W increased				
(a) 10%	2.44	62	0.15	7
(b) 20%	2.58	65	0.29	13
(c) 30%	2.71	69	0.42	18

Conclusions

Results of this feasibility study indicate the problem is solvable and that it would be desirable to undertake comprehensive regional investigations. Illinois is representative in climate, topography, and food production of the midwestern agricultural region. Previous research and data collection by the Illinois State Water Survey and other state and federal agencies have provided in readily available form the data required for derivation and testing of the evaluation techniques that have been described. Lack of time and funds have prevented the undertaking of a comprehensive study for Illinois under NSF-1360. No provision was made for this study under the foregoing grant.

REFERENCES

Adderley, E. E., 1968: Rainfall Increases Down-Wind From Cloud Seeding Projects in Australia. Proceedings of the First National Conference on Weather Modification, Albany, New York, April 28-May 1, 1968.

Battan, Louis J., and A. Richard Kassander, 1960: Design of a program of randomized seeding of orographic cumuli. Journal of Meteorology, 17, 583-590.

Battan, Louis J., 1966: Silver-Iodide Seeding and Rainfall from Convective Clouds. Journal of Applied Meteorology, 5, 669-683.

Braham, Roscoe R., Jr., 1965: Project Whitetop - A Five Year Randomized Cloud Seeding Study. Paper presented at the 244th National Meeting of the American Meteorological Society on Cloud Physics and Severe Local Storms, Oct. 18-22, 1965, Reno, Nevada.

Braham, Roscoe, Jr., 1966: Project Whitetop: Design of the Experiment. Final Report to NSF, Parts 1 and 2, University of Chicago, 156 pp.

Brier, G. W., 1966: Some Problems in Evaluating Cloud Seeding Effects Over Extensive Areas. Weather Modification Experiments-Proceedings of the Fifth Berkeley Symposium on Mathematical Statistics and Probability, 5, 209-222.

Brown, Keith J., and Robert D. Elliot, 1968: Large Scale Dynamic Effects of Cloud Seeding. Proceedings of the First National Conference on Weather Modification, Albany, New York, April 28-May 1, 1968.

Byers, H. R., and R. R. Braham, Jr., 1949: The Thunderstorm. Report of the Thunderstorm Project, U. S. Dept. of Commerce, Weather Bureau, 95-100.

Changnon, S. A., Jr., 1963: Precipitation in a 550-Square-Mile Area of Southern Illinois. Transactions, Illinois Academy of Science, 56, 165-186.

Changnon, S. A., Jr., 1969: Climatology of Severe Winter Storms in Illinois. Bulletin 53, Illinois State Water Survey, Urbana, 45 pp.

Changnon, S. A., Jr., and F. A. Huff, 1957: Cloud Distribution and Correlation with Precipitation in Illinois, Illinois State Water Survey, Report of Investigation 33, 83 pp.

Changnon, S. A., Jr., and F. A. Huff, 1961: Studies of Radar-Depicted Precipitation Lines. Scientific Report No. 2, Contract No. AF 19(6040-4940, Illinois State Water Survey, Urbana, 63 pp.

Conrad, V., and L. W. Pollak, 1950: Methods in Climatology. Cambridge, Mass., Harvard University Press, 54—55.

Davies, Owen L., 1954: The Design and Analyses of Industrial Experiments. First Edition, Hafner Publishing Co., New York, 636 pp.

Decker, W. L., and P. T. Schickedanz, 1965: The Evaluation of Rainfall Records from a Five Year Cloud Seeding Experiment in Missouri. Proceedings of the Fifth Berkeley Symposium on Mathematical Statistics and Probability, 55-63.

Decker, Wayne L., and Paul T. Schickedanz, 1966: Project Whitetop: A Summary of the Rainfall Analysis. Part IV, Final Report to NSF, University of Missouri, Columbia, Missouri.

Eziekel, M., and Karl A. Fox, 1959: Methods of Correlation and Regression Analyses. John Wiley and Sons, Inc., New York, 3rd Edition, 548 pp.

Flueck, John A., 1968: A Statistical Analysis of Project Whitetop's Precipitation Data. Proceedings of the First National Conference on Weather Modification, Albany, New York, April 28-May 1, 1968.

Gabriel, K. R., 1967: The Israeli Artificial Rainfall Stimulation Experiment. Proceedings, Fifth Berkeley Symposium on Mathematics and Statistical Probability, University of California Press, 5, 91-113.

Hershfield, David M., 1967: Rainfall Input for Hydrologic Models. Proceedings of Geochemistry, Precipitation, Evaporation, Soil-Moisture, Hydrometry, General Assembly of Bern, Sept.-Oct., 177-188.

Huff, F. A., 1966: The Effect of Natural Rainfall Variability in Verification of Rain Modification Experiments. Water Resources Research, 2, 791-801.

Huff, F. A., 1967a: Time Distribution of Rainfall in Heavy Storms. Water Resources Research, 3, 1007-1019.

Huff, F. A., 1967b: Rainfall Gradients in Warm Season Rainfall. Journal of Applied Meteorology, 6, 435-437.

Huff, F. A., 1968a: Spatial Distribution of Heavy Storm Rainfalls in Illinois. Water Resources Research, 4, 47-54.

Huff, F. A., 1968b: Area-Depth Curves -- A Useful Tool in Weather Modification Experiments. Journal of Applied Meteorology, 7, 940-943.

Huff, F. A., 1969: Climatological Assessment of Natural Precipitation Characteristics for Use in Weather Modification. Journal of Applied Meteorology, 8, 401-410.

Huff, F. A., and S. A. Changnon, Jr., 1963: Drought Climatology of Illinois. Bulletin 50, Illinois State Water Survey, Urbana, 68 pp.

Huff, F. A., and J. C. Neill, 1956: Frequency of Point and Areal Mean Rainfall Rates. Trans. Am. Geophys. Union, 37, 679-681.

Huff, F. A., and J. C. Neill, 1957: Rainfall Relations on Small Areas in Illinois. Bulletin 44, Illinois State Water Survey, 43-50.

Huff, F. A., and J. C. Neill, 1959: Frequency Relations for Storm Rainfall in Illinois. Bulletin 46, Illinois State Water Survey, Urbana, 65 pp.

Huff, F. A., and R. G. Semonin, 1960: An Investigation of Flood-Producing Storms in Illinois. Topics in Engineering Meteorology, Meteorological Monograph 4, American Meteorological Society, Boston, Mass.

Huff, F. A., and W. L. Shipp, 1968: Mesoscale Spatial Variability in Midwestern Precipitation. Journal of Applied Meteorology, 7, 886-891.

Huff, F. A., W. L. Shipp, and P. T. Schickedanz, 1969: Evaluation of Precipitation Modification Experiments from Precipitation Rate Measurements. Final Report, INT 14-06-D-6575, U. S. Dept. of Interior, Bureau of Reclamation, Office of Atmospheric Water Resources, 122 pp.

Huff, F. A., and G. E. Stout, 1952: Area-Depth Studies for Thunderstorm Rainfall in Illinois. Trans. Am. Geophys. Union, 33, 495-498.

Light, Phillip, 1947: Hydrologic Aspects of Thunderstorm Rainfall. Hydrometeor. Report No. 5, U. S. Weather Bureau-Corps of Engineers, 260-268.

Linsley, R. K., and M. A. Kohler, 1951: Variations in Storm Rainfall Over Small Areas. Trans. Am. Geophys. Union, 32, 245-250.

MacDonald, Gordon J. F., 1966: Weather and Climate Modification, Problems and Prospects. Final Report of the Panel on Weather and Climate Modification, National Academy of Sciences-National Research Council, Vol. 2, Publication No. 1350, Washington, D. C.

McDonald, J. E., 1956: Variability of Precipitation in an Arid Region: A Survey of Characteristics for Arizona. Institute of Atmospheric Physics, University of Arizona, Tucson, Ariz., p. 2.

McGuinness, J. L., 1963: Accuracy of Estimating Watershed Mean Rainfall. J. Geophys. Res., 68, 4763-4767.

Nason, Charles K., and Manuel E. Lopez, 1967: A Test of Certain Evaluation Designs for Cloud-Seeding. Technical Report B-3662, W. E. Howell, Associates.

Newton, Chester W., and Harriet Rodebush Newton, 1959: Dynamical Interactions between Large Convective Clouds and Environment with Vertical Shear. Journal of Meteorology, 16(5), 483-496.

Neyman, Jerzy, Elizabeth Scott, and Jerome A. Smith, 1969: Areal Spread of the Effect of Cloud Seeding at the Whitetop Experiment. Science, 163, March.

Schickedanz, P. T., S. A. Changnon, and C. G. Lonnquist, 1969: A Statistical Methodology for the Planning and Evaluation of Hail Suppression Experiments in Illinois. Final Report, Part 2, NSF Grant GA-482, Illinois State Water Survey, 140 pp.

U. S. Dept. of Interior, 1968: Project Skywater, 1967 Annual Report, Vol. 1, Summary. Bureau of Reclamation, Office of Atmospheric Water Resources.

Wadsworth, G. P., 1951: A Possible Experimental Design for Testing the Effectiveness of Cloud Seeding. Report for Geophysical Research Directorate, Cambridge Field Station, Mass., Contract AF19(122)-401.

Wald, A., 1947: Sequential Analyses. John Wiley and Sons, Inc., New York, 212 pp.